PB81-242513

Pilot-Scale Development of a Low-NOx Coal-Fired Tangential System

Acurex Corp.
Mountain View, CA

Prepared for

Industrial Environmental Research Lab.
Research Triangle Park, NC

Aug 81

U.S. Department of Commerce
National Technical Information Service
NTIS

IERL-RTP-1233

TECHNICAL REPORT DATA
(Please read Instructions on the reverse before completing)

1. REPORT NO.	2.	3. RECIPIENT'S ACCESSION NO. PB81-242513
4. TITLE AND SUBTITLE Pilot-scale Development of a Low-NOx Coal-fired Tangential System		5. REPORT DATE
		6. PERFORMING ORGANIZATION CODE
7. AUTHOR(S) J.T. Kelly, R.A. Brown, E.K. Chu, J.B. Wightman, R.L. Pam, E.L. Swenson, E.B. Merrick, and C.F. Busch		8. PERFORMING ORGANIZATION REPORT NO.
9. PERFORMING ORGANIZATION NAME AND ADDRESS Acurex Corporation Energy and Environmental Division 485 Clyde Avenue Mountain View, California 94042		10. PROGRAM ELEMENT NO. C9BN1B
		11. CONTRACT/GRANT NO. 68-02-1885
12. SPONSORING AGENCY NAME AND ADDRESS EPA, Office of Research and Development Industrial Environmental Research Laboratory Research Triangle Park, NC 27711		13. TYPE OF REPORT AND PERIOD COVERED Final; 9/78-2/81
		14. SPONSORING AGENCY CODE EPA/600/13

15. SUPPLEMENTARY NOTES IERL-RTP project officer is David G. Lachapelle, Mail Drop 62, 919/541-3444.

16. ABSTRACT

A 293 kWt (1 million Btu/hr) pilot-scale facility was used to develop a low-NOx pulverized-coal-fired tangential system. Conventional tangential system burner and vortex characterization tests defined the major system design requirements for a low-NOx system. Given these requirements, a burner concept was developed which achieves low NOx by directing the fuel and a fraction of the secondary combustion air into the center of the furnace, with the remaining secondary combustion air directed horizontally and parallel to the furnace walls. Such separation of secondary combustion air creates a fuel-rich zone in the center of the furnace where NOx production is minimized. This combustion modification technique has lowered NOx 64%, relative to conventional tangential firing, by injecting 85% of the secondary air along the furnace walls. Under these conditions, NO emissions were 180 ppm corrected to 0% O2. Also at these conditions, CO, UHC, and unburned carbon emissions were less than 40 ppm, 3 ppm, and 2.4%, respectively, comparable to conventional tangentially fired pilot-scale results. Also, the modification places a blanket of air on the furnace walls which reduces wall corrosion and slagging. With the modification, O2 concentrations above the burner level (near the furnace wall) were 12%, nearly three times conventional tangential pilot-scale system wall oxygen concentrations.

17. KEY WORDS AND DOCUMENT ANALYSIS

a. DESCRIPTORS	b. IDENTIFIERS/OPEN ENDED TERMS	c. COSATI Field/Group
Pollution	Pollution Control	13B
Coal	Stationary Sources	21D
Pulverized Fuels	Combustion Modification	
Combustion Control	Tangential Firing	21B
Nitrogen Oxides		07B
Burners		13A

18. DISTRIBUTION STATEMENT Release to Public	19. SECURITY CLASS *(This Report)* Unclassified	21. NO. OF PAGES 239
	20. SECURITY CLASS *(This page)* Unclassified	22. PRICE

EPA Form 2220-1 (9-73)

PB81-242513

IERL-RTP-1233
EPA-600/7-81-137
August 1981

PILOT-SCALE DEVELOPMENT OF A LOW-NO_x COAL-FIRED TANGENTIAL SYSTEM

by

J. T. Kelly, R. A. Brown, E. K. Chu, J. B. Wightman
R. L. Pam, E. L. Swenson, E. B. Merrick and C. F. Busch
Acurex Corporation
Energy & Environmental Division
Mountain View, California 94042

Contract 68-02-1885

Project Officer

David Lachapelle
Industrial Environmental Research Laboratory
Research Triangle Park, North Carolina 27711

INDUSTRIAL ENVIRONMENTAL RESEARCH LABORATORY
OFFICE OF RESEARCH & DEVELOPMENT
U.S. ENVIRONMENTAL PROTECTION AGENCY
RESEARCH TRIANGLE PARK, NORTH CAROLINA 27711

REPRODUCED BY
NATIONAL TECHNICAL
INFORMATION SERVICE
U.S. DEPARTMENT OF COMMERCE
SPRINGFIELD, VA 22161

DISCLAIMER

This report has been reviewed by the Industrial Environmental Research Laboratory (RTP), U.S. Environmental Protection Agency, and approved for publication. Approval does not signify that the contents necessarily reflect the views and policies of the Agency, nor does mention of trade names or commercial products constitute endorsement or recommendation for use.

ABSTRACT

A 293 kW_t (1×10^6 Btu/hr) pilot-scale facility was used to develop a low-NO_x pulverized-coal-fired tangential system. Conventional tangential system burner and vortex characterization tests defined the major system design requirements for a low-NO_x system. Given these requirements, a burner concept was developed which achieves low NO_x by directing the fuel and a fraction of the secondary combustion air into the center of the furnace, with the remaining secondary combustion air directed horizontally and parallel to the furnace walls. The separation of secondary combustion air in this manner creates a fuel-rich zone in the center of the furnace where NO_x production is minimized. This combustion modification technique has lowered NO_x 64 percent, relative to conventional tangential firing, by injecting 85 percent of the secondary air along the furnace walls. Under these conditions, NO emissions were 180 ppm corrected to 0 percent oxygen. In addition, at these conditions, CO, UHC, and unburned carbon emissions were less than 40 ppm, 3ppm and 2.4 percent respectively. These levels are comparable to conventional tangentially fired pilot-scale results. Also, the modification places a blanket of air on the furnace walls which is beneficial from a wall corrosion and slagging point of view. With the modification, oxygen concentrations above the burner level near the furnace wall were 12 percent. This is nearly three times conventional tangential pilot-scale system wall oxygen concentrations. Finally, in some configurations, the modification shows a decrease in NO_x emissions as firebox gas temperature is increased. This characteristic might be beneficially applied in a large-scale system to reduce furnace volume, and thereby capital cost, for a given combustion heat release.

CONTENTS

Abstract iii
Figures v
Tables xiii

1. Introduction 1

   Coal-fired tangential system description 2
   Conventional NO_x control approaches 2
   Pilot-scale development of an advanced NO_x control technique 4

2. Facility 6

   Basic furnace design. 7
   Burners 10
   Instrumentation and data acquisition 10
   Emission monitoring 15

3. Baseline Testing 20

   Comparison of pilot- and full-scale stack emissions under baseline conditions 20
   Comparison of pilot- and full-scale flame and flow patterns under baseline conditions 24

4. Definition of Conventional Tangential System NO_x Formation and Reduction Processes. 34

   Chemical/physical characteristics of fuel 34
   Thermal effects tests 50
   Burner jet and vortex characterization tests. 76
   Circumferential flame-flame interactions 93
   Tangential burner design characterization 100

5. Low-NO_x System Definition 108

   Low-NO_x system concept 108
   Low-NO_x system 1 burner test results 110
   Low-NO_x system 2 141
   System 3 burner testing 180

Preceding page blank

CONTENTS (Concluded)

6. Conclusions and Recommendations 220

    Conclusions 220
    Recommendations 221

References 222

FIGURES

Number Page

1 Tangentially fired system 3

2 Furnace cross section 7

3 Staging-air system 9

4 Coal system schematic 11

5 Coal lance detail 12

6 Corner-fired burner 13

7 Corner burner gas nozzles 14

8 Emission monitoring system 16

9 Hot sampling probe 18

10 NH_3/HCN in flame impinger train 19

11 Tangentially-fired baseline NO emissions 21

12 Front-wall-fired baseline NO emissions 23

13 CO versus theoretical air-to-fuel firing zone 25

14 Percent carbon loss versus theoretical air-to-fuel firing zone 26

15 Water model firebox and burners 28

16 Adjacent jet splitting 30

17 Schematic of quantitative flow and flame pattern data measurement 31

18 Variation of NO with percent excess air 36

19 Variation of NO with stoichiometric ratio 37

20 Variation of doped natural gas NO with SR 39

FIGURES (Continued)

Number Page

21 Char, char plus gas and char plus doped gas NO variations with SR. 41

22 Fuel N conversion for coal and doped natural gas 45

23 Fuel N Conversion for coal, char-plus-doped-gas, and doped natural gas 46

24 Variation of coal-fired NO with NH_3 dopant 49

25 Active furnace wall-cooling tubes. 52

26 Variation of cold-wall gas and firebox temperatures with time 53

27 Placement of main thermocouples in firebox and heat exchange tower 54

28 Effect of heat removal on staged NO. 55

29 Coal NO variation with temperature 57

30 Variation of NO with temperature 58

31 First stage exit and stack NO variation with temperature 60

32 Cold-wall doped gas NO results with SR 61

33 Comparison of cold- and hot-wall doped gas NO results with SR . . 63

34 Effect of NH_3 dopant and SR. 64

35 Cold-wall char and char-plus-doped-gas NO. 65

36 Effect of temperature on coal, char, and char-plus-gas NO. 67

37 Carbon loss results. 68

38 NO results versus percent carbon loss 70

39 Char NO reduction versus temperature 71

40 Effect of adding NH_3 to coal jet 73

41 Effect of adding NH_3 to gas fuel jet 74

FIGURES (Continued)

Number Page

42 Side view of firebox sample port locations and identification numbers 77

43 Concentrations across firebox at sampling location 1-1 78

44 Concentrations across firebox at sampling location 2-1 79

45 Concentrations across firebox at sampling location 3-1 80

46 Concentrations across firebox at sampling location 1-2 81

47 Concentrations across firebox at sampling location 1-1 82

48 Concentrations across firebox at sampling location 2-1 83

49 Concentrations across firebox at sampling location 4-2 84

50 Concentrations across firebox at sampling location 3-1 85

51 Comparison of unstaged and staged firebox NO probing results . . . 87

52 Ceramic NO injectors 90

53 NO dopant remaining following injection at indicated locations 91

54 Flame-flame interaction, 45° configuration 95

55 Flame interaction 96

56 Flame interation, rich/lean 97

57 Flame interaction 98

58 Flame interaction, rich/lean 99

59 Burner configuration NO levels 102

60 Burner configuration effect on NO during staging 104

61 Burner configuration NO level variations with firing rate 106

62 Flame visualization for configuration 4 107

63 Low-NO_x air-on-wall system schematic 109

64 Schematic of Systems 1, 2, and 3 low-NO_x burners 111

FIGURES (Continued)

Number Page

65 Corner burner configurations G, H, I, J, and K 113

66 Corner burner configurations L and M 114

67 Corner burner configurations N and O 115

68 Configurations G, H, I, and J NO versus percent wall air 116

69 Configuration H NO and O_2 firebox concentrations 0.20m above the fuel entry elevation 118

70 Configuration H NO and O_2 concentrations across firebox at 0.45m above the fuel entry elevation 119

71 Configuration I NO and O_2 concentrations across firebox at 0.45m above the fuel entry elevation 121

72 Configurations I, J, and K NO results versus percent wall air . . 122

73 Configuration I NO and O_2 firebox probing results 0.20m above the fuel entry elevation 123

74 Configuration J NO and O_2 firebox probing results 0.20m above the fuel entry elevation 124

75 Configuration K NO and O_2 firebox probing results 0.20m above the fuel entry elevation 125

76 Configuration L NO and O_2 firebox concentrations 0.20m above the fuel entry elevation 127

77 Configurations L, M, N, and O NO concentrations versus percent wall air 128

78 Configuration M NO and O_2 firebox concentrations 0.20m above the fuel entry elevation 129

79 Configuration N NO and O_2 firebox concentrations 0.20m above the fuel entry elevation 130

80 Configuration N NO and O_2 concentrations 0.45m above the fuel entry elevation 131

81 Configuration O NO and O_2 firebox concentrations 0.20m above the fuel entry elevation 132

82 Effect of wall jet inclination angle 134

FIGURES (Continued)

Number Page

83 NO versus gas stream temperature for air-on-wall low-NO_x system. . 135

84 Configurations H through O NO results with percent wall air . . . 137

85 Configuration N staged NO and O_2 firebox concentrations .20m above fuel entry elevation 139

86 Effect of excess air on pilot-scale, full-scale, and air-on-wall system NO emissions 140

87 Configuration H through N staged NO results 142

88 Comparison of system 2 burner configurations 144

89 NO versus excess air for configuration S 146

90 Configuration S NO versus percent secondary combustion air-on-wall 148

91 Staged NO levels for configurations N and S 149

92 NO versus temperature for configurations N and S 150

93 Firebox probing O_2 results for configurations N and S. 152

94 Firebox probing results NO for configurations N and S 153

95 NO versus percent secondary combustion air on wall -- configuration S 154

96 NO variation with fuel tube elevation stoichiometry for configuration S 155

97 NO versus tower gas temperature for configuration S 157

98 Effect of wall jet 2 and 3 velocities on NO levels 158

99 Probing ports versus air port locations for configuration S . . . 159

100 O_2 concentrations across firebox at 0.20m (8 inches) and 0.45m (18 inches) above the fuel tube elevation 160

101 Firebox probing results for configuration S with vertically distributed wall air 161

102 Combustion losses for configuration S 163

FIGURES (Continued)

Number Page

103 NO versus excess air 165

104 NO versus percent secondary combustion air on wall for configuration S and T with vertical wall air 166

105 NO variation with fuel tube elevation stoichiometry for configuration T 168

106 Configuration U, V, and S NO versus percent wall air results (SR_1 = 1.15) 169

107 Configurations U, V, and S NO versus percent wall air results (SR_1 = 0.88) 170

108 Effects of SR_1 on NO emissions for configuration U 171

109 Effects of SR_1 on NO emissions for configuration V 172

110 Coal particle size distribution 174

111 FGR simulation -- NO versus percent N_2 176

112 FGR simulation -- NO versus SR_1 (10 percent NO_2) 177

113 FGR simulation -- NO versus SR_1 (20 percent N_2) 178

114 System 3 burner schematic 182

115 Demonstration burner design 183

116 Systems 1 and 2 and Richmond Power and Light burner designs. . . . 191

117 Comparison of Systems 1, 2, and 3, and full-scale NO results . . . 192

118 NO versus wall angle using variable angle burner blocks without inserts 195

119 Systems 1, 2, and 3 configurations and jet exit areas. 197

120 NO versus wall angle using variable angle burner blocks with inserts 200

121 NO versus wall air for mixed conditions usingvariable angle burner blocks without inserts 204

122 NO versus wall air for mixed conditions using variable angle burner blocks with inserts 205

FIGURES (Concluded)

Number Page

123 NO versus wall air and OFA for mixed conditions using variable angle burner blocks without inserts 207

124 NO versus wall air and OFA for mixed conditions using variable angle burner blocks with inserts 208

125 NO versus annular air for mixed conditions using variable angle burner blocks without inserts 209

126 NO versus annular air for mixed conditions using variable angle burner blocks with inserts 210

127 NO versus center/annular air ratio using variable angle burner blocks with inserts 211

128 Comparison of System 1, 2, and 3 burner NO variation with percent total wall air 213

129 NO versus excess air using variable angle burner blocks with inserts 214

130 NO versus load using variable angle burner blocks with inserts . . 216

131 Coal type effects on NO versus load using System 3 burner with inserts 218

132 Coal type effects on NO versus excess air using a System 3 burner with inserts 219

TABLES

Number Page

1 Analytical Pollutant Measurement Equipment 17

2 Coal Properties 22

3 Qualitative Flow and Flame Pattern Data 32

4 Utah Coal Char and Parent Coal Properties 42

5 Partially Burnt Coal and Char Properties 43

6 Partially Burnt and Parent Coal Properties 72

7 Low Temperature Nitrogenous Species Measurements 75

8 Effect of Yaw Angle on NO. 88

9 Effect of Corner Burner Biasing on NO 93

10 Air-On-Wall Primary Configuration Wall Gas Condition 136

11 System 2 Burners 145

12 Pilot-Scale Combustion Results Comparison. 164

13 System 3 Burner Airflow Splits 186

14 System 3 Burner Results. 187

15 Vortex Parameters for Pilot-Scale Systems 1, 2, and 3, and Full-Scale Demonstration and Conventional Tangential Systems . . 196

SECTION 1

INTRODUCTION

Maintenance of ambient air quality in the United States requires the restriction of NO_x emissions from stationary combustion sources. Presently, tangential coal-fired boilers produce approximately 10 percent of all stationary source NO_x emissions and consume, in kWh, approximately 9 percent of all fuel used in stationary sources (Reference 1). Tangential coal-fired boilers produce 24 percent of NO_x emissions from utility boilers operating on all fuels (Reference 1). In addition, tangential coal-fired boilers produce 35 percent of the NO_x and consume, in kWh, 45 percent of the fuel used in all coal-fired utility boilers (Reference 1). The significant NO_x emissions from these boilers and the expected future increase in the number of these boilers makes them candidates for emission control development both in terms of retrofit and new boiler designs. Demonstrating NO_x reduction technology for these boilers will provide regulatory agencies with additional emissions control options which could be exercised in the future to maintain ambient air quality.

The work described in this report is part of the U.S. Environmental Protection Agency's (EPA's) program to develop and demonstrate advanced emission control technology for utility and industrial boilers and other sources. The primary objective of this work was to develop, in pilot scale, a NO_x control technique for coal-fired tangential systems that would be effective both as a new design and retrofit to existing boilers, yet would not have the limitations of previously tested, globally staged NO_x control approaches (Reference 2). To achieve this goal, the first part of the test program focused on defining the phenomena that control the formation and reduction of NO_x in a conventional coal-fired tangential boiler system. These tests isolated the critical chemical and physical processes controlling NO_x and established the effect of the design parameters on these processes. Utilizing the understanding gained in the first part of the test program, a low-NO_x control technique was developed and tested in the second part of the program. The NO_x control technique, the "Air-on-Wall Low-NO_x System," showed considerable promise to significantly reduce NO_x emissions while maintaining good combustion conditions.

In the following sections, the coal-fired tangential system will be described along with conventional NO_x control strategies applied to tangential and other modes of utility boiler firing. Lastly, advanced NO_x control techniques developed for tangential firing are described.

1.1 COAL-FIRED TANGENTIAL SYSTEM DESCRIPTION

Figure 1 schematically illustrates the flow patterns typically present in tangentially fired furnaces. As shown in the top view, fuel is introduced into the furnace from fuel registers located in the four corners. Above and below the fuel registers are the auxiliary air registers aligned as shown in the sideview schematic of Figure 1. Distribution dampers proportion the air to the individual fuel and air registers; thus, air distribution over the height of the windbox and relative velocity can be varied to change the fuel/air distribution and mixing in the furnace. Also, the fuel and air nozzles can tilt in unison to raise or lower the combustion zone in the furnace to control furnace exit temperature and thus, superheater/reheater heat absorption.

The fuel and air jets issuing from the registers have a nonswirling slow-mix character. Ignition of fuel is provided by impingement of hot, burnt gases from laterally adjacent burners and large-scale internal recirculation of combusted gases. Thus, the ignition and combustion of each corner jet serves to ignite and promote burning in the downstream adjacent jet.

The tangential alignment of the centerlines of the corner jets to the circumference of a circle in the center of the furnace promotes the formation of a large-scale vortex within the furnace as shown in Figure 1. Jet impingement and the vortex motion create eddies that help mix fuel and air. Therefore, precise proportioning of fuel and air at each burner is not required for stable and complete combustion. Locally, fuel-rich or air-rich streams are blended in the vortex region of the furnace allowing complete combustion of the fuel.

Since the fuel/air jets are initially of a slow-mix character, fuel NO_x formation in the rich region of the fuel jets will be reduced below values achieved with rapid-mix swirling jets (Reference 2). Because fuel NO_x represents a significant portion of the total NO_x for coal combustion (Reference 3), reduction of fuel NO_x has a strong impact on the overall NO_x levels. In addition, any NO_x formed can become entrained into downstream adjacent fuel jets. If the NO_x is drawn into a fuel-rich region within the slow-mix jet, it is possible that the NO_x will be converted to molecular nitrogen, as observed in laboratory experiments (Reference 4). Hence, the large bulk recirculation of burnt gases in the vortex and the slow-mix nature of the fuel and air jets should make the tangentially fired system inherently low in NO_x production.

1.2 CONVENTIONAL NO_x CONTROL APPROACHES

During the combustion of pulverized coal in tangential boilers, NO_x is generated from the nitrogen chemically bound in the fuel (fuel NO_x) as well as from the oxidation of atmospheric nitrogen (thermal NO_X). For typical bituminous coals, NO_x emissions from the fuel nitrogen can be a significant fraction of the total (Reference 5). Emissions of NO_x from fuel as well as atmospheric nitrogen have been shown to respond to combustion modification conditions which alter oxygen concentration, temperature, and residence time during combustion (Reference 6).

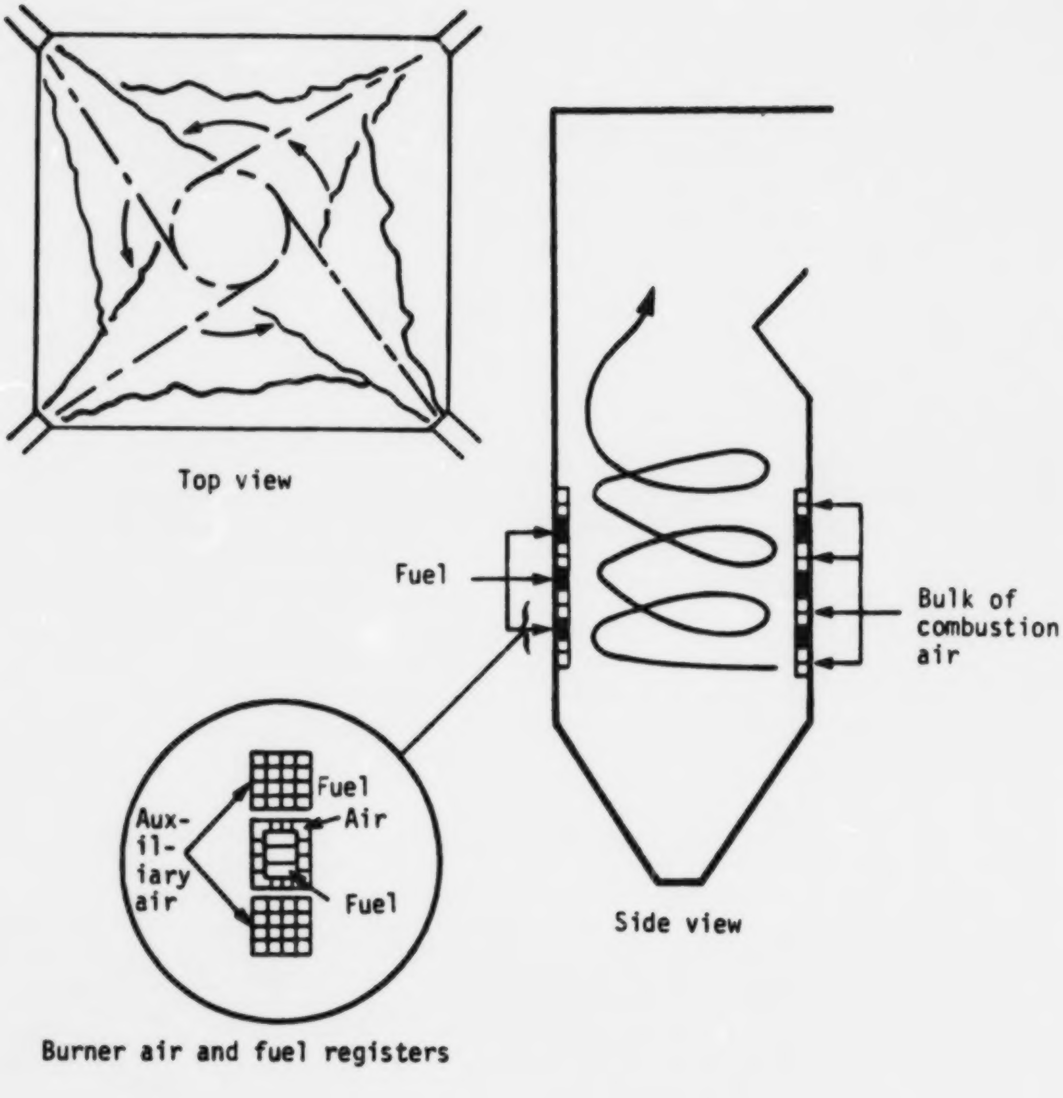
Top view
Fuel
Bulk of combustion air
Aux-il-iary air
Fuel
Air
Fuel
Side view
Burner air and fuel registers

Figure 1. Tangentially fired system.

Reducing oxygen concentration typically leads to lower fuel and thermal NO_x. The level to which NO is reduced is dependent on oxygen concentration as well as residence time at these conditions. Lowering the oxygen concentration surrounding the fuel, either locally by fuel/air stratification or globally by limiting the airflow in the combustion volume, shifts the fuel and atmospheric nitrogen emission reactions from predominantly NO_x formation to a balance between NO_x formation and reduction to molecular nitrogen (Reference 6). In addition, given sufficient residence time at oxygen deficient conditions, previously formed NO_x can be reduced to molecular nitrogen by homogeneous (Reference 7) and heterogeneous (Reference 8) catalyzed and noncatalyzed reactions.

Lowering peak temperature under excess air conditions decreases thermal NO_x formation (Reference 9). However, under highly fuel-rich staged combustion conditions, lowering first-stage temperature can increase NO_x (Reference 9). This is due to less fuel nitrogen being volatilized in the first stage and carrying over into the oxygen-rich second stage where the potential for NO_x formation is high (Reference 9).

Even though imperfectly understood, these basic relationships between system parameters and NO_x emissions have been employed to reduce NO_x emissions from tangential, as well as other types of utility boilers (Reference 10). For example, combustion volumes have been increased to decrease temperature and lower thermal NO_x. Also, overfire air concepts, where oxygen concentration in the lower furnace volume is limited, have been used to decrease both fuel and thermal NO_x. Applying these and related techniques has led to moderate decreases in NO_x emissions. Significant reductions in NO_x by overfire air type concepts require operation of the entire firebox under extremely fuel-rich conditions, which is undesirable from the point of view of wall corrosion and slagging.

1.3 PILOT-SCALE DEVELOPMENT OF AN ADVANCED NO_x CONTROL TECHNIQUE

Further significant reductions in NO_x from tangentially fired boilers under acceptable combustion conditions require a better understanding of the combustion processes that control NO_x formation/reduction. Therefore, this study was separated into two phases. The objective of the first phase was to develop an understanding of the processes controlling NO_x formation/reduction in pulverized-coal-fired tangential boilers.

The testing used to gain an understanding of the dominant processes controlling NO_x was performed in a pilot-scale furnace which closely simulates full-scale system emissions and combustion performance. The facility was designed to model full-scale system firing intensity, overall residence time, and furnace exit gas temperature. Also, burners and their placement in the firebox are patterned after full-scale tangential systems. Under baseline conditions, NO, CO, and carbon loss emissions from the pilot-scale facility were comparable to full-scale system levels. In addition, similarities were found for: (1) ignition standoff and character, (2) flame spreading angles from the burners, (3) apparent jet centerline angle from the corners, and (4) vortex size. These similarities between the pilot-

and full-scale facilities ensured that low-NO_x techniques developed in this program were applicable to full-scale systems.

Tests to provide understanding of NO_x formation and reduction processes in tangentially fired systems covered all the important processes expected to influence NO_x in tangentially fired systems including: (1) fuel chemical/physical characteristics, (2) thermal environment, (3) importance of near burner, burner jet/vortex interaction, and vortex zone on NO (see Figure 1 for zone definitions), (4) NO flame processing, (5) flame-flame interaction, (6) early burner mixing, and (7) overall firebox mixing. Results of these tests showed that: (1) distance of ignition point from burner face, (2) concentration of oxygen in the fuel jet/vortex interaction zone, (3) maintenance of a collimated fuel jet into the vortex, (4) lower firebox mixing, and (5) operation of a portion of the char burnout zone (vortex core) oxygen deficient were important to NO_x control.

Using the results of these tests, an advanced low-NO_x combustion modification technique was developed and demonstrated in pilot scale during the second phase of the program. The technique, called the "Air-on-Wall Low-NO_x System," differs from normal tangential boiler practice only in directing a fraction of the auxiliary combustion air horizontally along the furnace wall rather than into the center of the furnace (see Figure 1). This causes the center of the furnace to operate fuel rich where NO_x formation is minimized. In addition, the walls of the furnace are maintained in an oxidizing environment, which is beneficial to furnace wall corrosion and slagging. This concept, which can be used to retrofit existing tangential systems or applied to new designs, significantly lowers NO_x (roughly 60 percent) under acceptable combustion conditions.

The following sections discuss the facility, process definition tests, and low-NO_x concept tests employed in the development of the "Air-on-Wall Low-NO_x" coal-fired tangential system.

SECTION 2

FACILITY

The EPA pilot-scale multiburner combustion facility at Acurex was designed to simulate front-wall, opposed, and tangentially fired utility boiler combustion and emission performance. A close simulation of full-scale conditions in this facility allows the development of NO_x control techniques under conditions approximating actual boiler practice. In this program, the multiburner facility was used in the tangential firing mode to efficiently develop NO_x control technology without the difficulties associated with large-scale testing.

This section describes the multiburner facility firebox, burners, and support systems including instrumentation, data acquisition, and emission measurement equipment.

2.1 BASIC FURNACE DESIGN

The basic furnace and heat exchange sections used in support of this program are shown in Figure 2. The basic firebox was designed to simulate the combustion aerodynamics of either a front-wall, opposed, or tangentially fired utility boiler. Horizontal extension sections can be added to the firebox to simulate a package boiler. In this program, tangential firing was employed in almost all testing.

A variable geometry heat exchange section allows for a variable quench rate or increased combustion volume by removal of heat exchange surface.

The heat exchange surface consists of 24 U-tube drawer assemblies which can be inserted in "windows" in the heat exchange sections. The heat exchange sections are refractory-lined so that they may become part of the combustion volume when the heat exchange surface is removed and the windows are plugged.

The facility was also designed for investigating staging as a NO_x control technique. Stage-air injection ports were provided at numerous locations over the length of the heat exchange section. Thus, the first-stage residence time could be varied by changing the stage-air injection location. Similarly, the second-stage residence time (time from stage-air injection to quenching of the exhaust gases) can be varied by placement of the heat exchanger surface.

1. Combustion chamber .99m (39") wide
2. Ignition and flame safeguard
3. Observation ports
4. Ashpit
5. In flame probing ports
6. C.E.-type corner fired burners
7. 2033K (3200°F) refractory
8. Heat exchange sections
9. Drawer assemblies
10. Staged injection ports

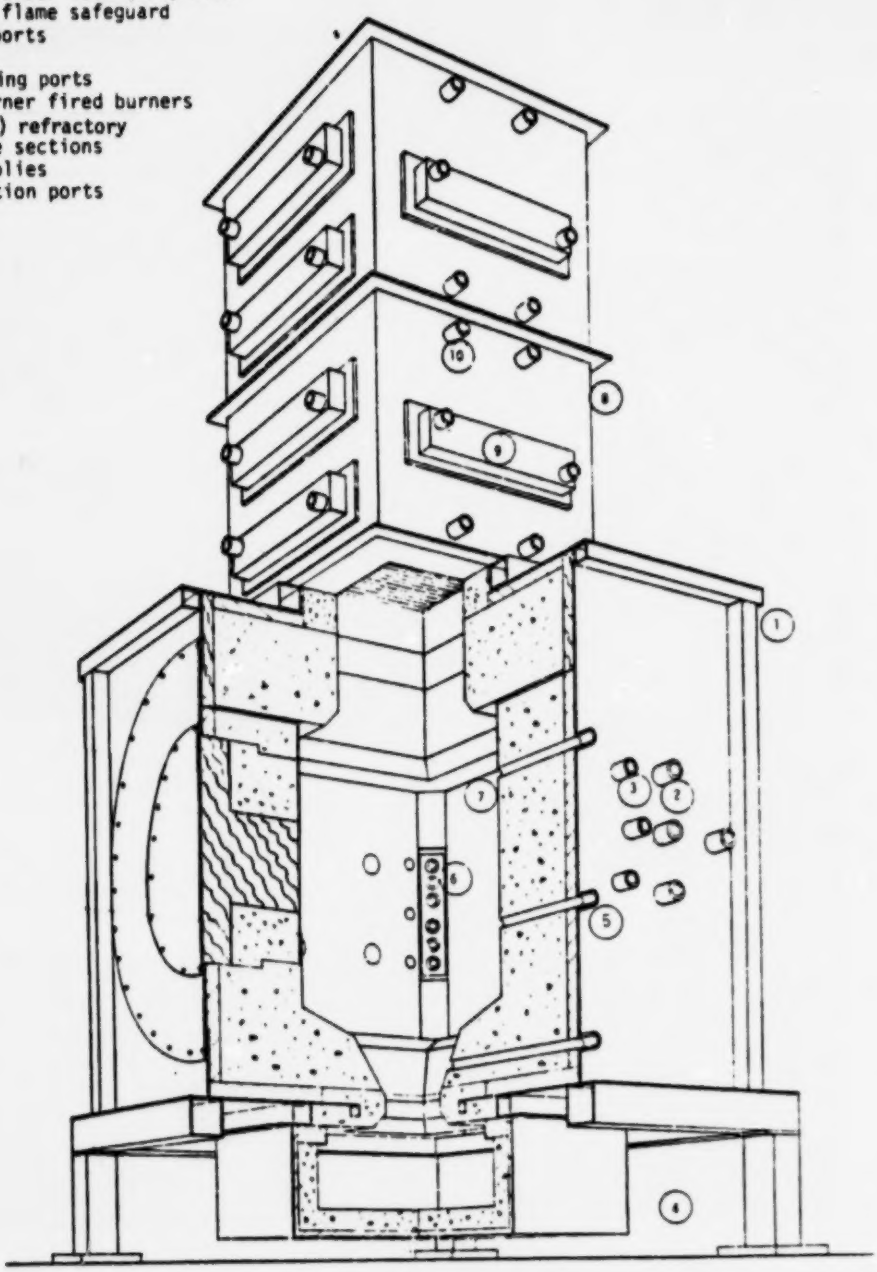

Figure 2. Furnace cross section.

The main firebox is a refractory-lined chamber, 1.35 m^3 (47.7 ft^3) in volume. As shown in Figure 2, numerous sampling and viewports are located around the periphery of the main firebox.

With this firebox design, volumetric heat release rates and residence times are matched between pilot- and full-scale facilities. Also, realistic full-scale furnace exit gas temperatures are achieved by low heat loss firebox refractory linings. The refractory operates at much higher temperatures than full-scale, water-cooled furnace walls. Hot walls are needed in this facility to model furnace exit gas temperature. This is because the surface area to volume ratio in a pilot-scale facility is much greater than a full-scale facility. With cold furnace walls in the pilot-scale facility, excessive heat would be lost from the gases resulting in firebox exit gas temperatures much below full-scale practice.

Heat is extracted from the flue gases by a closed-loop Dowtherm G® heat exchange system using the drawer assemblies previously mentioned. The heat is then dissipated to the atmosphere through two Dowtherm-to-air heat exchangers. A wide range of loads may be absorbed by bypassing flow around the Dowtherm-to-air heat exchangers. Temperature of the Dowtherm or tube wall may also be controlled from 65.6°C (150°F) to 232°C (450°F) by this valving system.

Combustion air is provided by a 0.38 m^3/s (800 scfm), 55 kPa (8 psig) centrifugal blower for the primary (coal transport air), secondary, and stage air. The secondary air may be heated and controlled to a maximum temperature of 427°C (800°F) through a duct-type electrical heater. Heated staged air is supplied from the same heater, but the temperature can be varied by addition of cold air downstream of the heater.

Secondary air is supplied to two manifolds on either side of the furnace with 8 outlets on each side for a maximum of 16 outlets. The controlled airflow from each outlet is measured by a standard flange tap orifice. Natural gas, compressed air, and oil manifolds are attached to the secondary air manifold assembly, each with 5 outlets on each side of the furnace.

A 10.16-cm (4-inch) diameter U-shaped manifold supplies the staged air to the heat exchange tower from a vertical manifold as shown in Figure 3. This vertical manifold allows the U-manifold to be positioned at four levels to access the staging air ports in the heat exchange tower.

Staged air is introduced through four opposed jets of high velocity (greater than 30.5 meter/second (100 feet/second) at 15 percent staged air), which rapidly mixes staged air and combustion products without any backmixing into the main combustion chamber. Since no stage air enters the main combustion chamber, stage separation was excellent for this system. Therefore, staging results for this system represent a very effective application of this technique relative to common full-scale boiler practice.

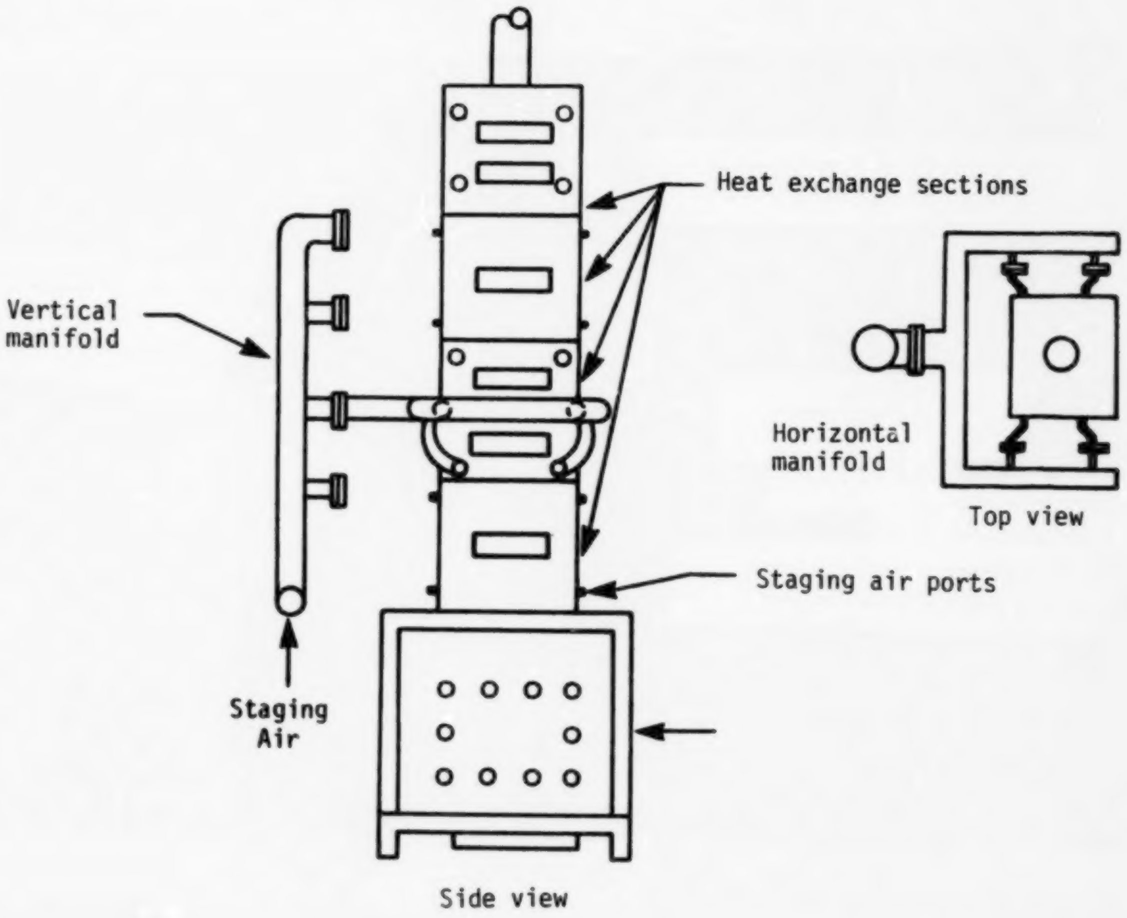
Heat exchange sections
Vertical manifold
Horizontal manifold
Top view
Staging air ports
Staging Air
Side view

Figure 3. Staging-air system.

Cooling water for the burners and firebox structure cooling is provided from a manifold at the base of the furnace. The water is supplied from a recirculating evaporative cooling tower system.

Coal is delivered to the furnace through four copper tubes from a fluidized bed. The coal system is schematicized is shown in Figure 4. Pulverized coal is dumped into a large hopper using a commerical bagdump. The coal is fed intermittently from the hopper to a pressurized Acrison screw feeder. The screw feeder, in turn, transfers the coal at a uniform rate to the fluidized bed. The coal feed rate to each line from the fluidized bed is metered by controlling the pressure drop across an orifice in a lance immersed in the fluidized bed (see Figure 5). The primary airflow to each line is individually controlled and measured.

After passing through the furnace heat exchange section, the flue gases enter the stack where the gaseous emission sample is taken. The flue gas is then ducted through the roof to the particulate sampling station, across the roof and down into a baghouse for particulate removal. An induced draft fan and damper downstream of the baghouse allow control of the furnace draft pressure from -5.1 cm (-2 inches) to 5.1 cm (2 inches) H_2O.

2.2 BURNERS

The corner-fired burners used in the baseline testing are patterned after the Combustion Engineering (CE) tangentially fired burners in terms of geometric scaling of major areas and percentages of airflow. However, while the CE burners are rectangular, the pilot-scale burners use three concentric circular air/fuel/air inlets, as shown in Figure 6. The circular cross-sections were used for ease of fabrication and modification. Deviations of performance from full-scale because of this geometrical difference should not be significant. The distribution of air and fuel in the vertical plane, as well as relative air velocities between ports, remains at the same levels as in the CE units. Matching burner and firebox geometry and, thereby, relative velocities yields similar mixing between pilot- and full-scale facilities under turbulent flow. Four burners of 110 kW_t capacity (375,000 Btu/hr), one in each corner, were used for a total of 440 kW_t (1.5×10^6 Btu/hr) capacity. The burners also have the capability of $\pm 30^\circ$ tilt, $\pm 10^\circ$ yaw, and have interchangeable air sleeves and fuel nozzles.

For most tests, burner yaw was set 6° from the diagonal to give the same tangential circle firing relationship as in some full-scale CE units. Tilt was set at 0° for all testing.

For system heatup purposes, six axially aligned holes were used to feed gas into the secondary airflow, as shown in Figure 7. After system heatup and upon coal feed initiation, the gas flow was terminated.

2.3 INSTRUMENTATION AND DATA ACQUISITION

The facility is fully instrumented for temperature and pressure measurements. Each subsystem has temperature and pressure measurements for monitoring the status of the system as well as for input for flow measurements.

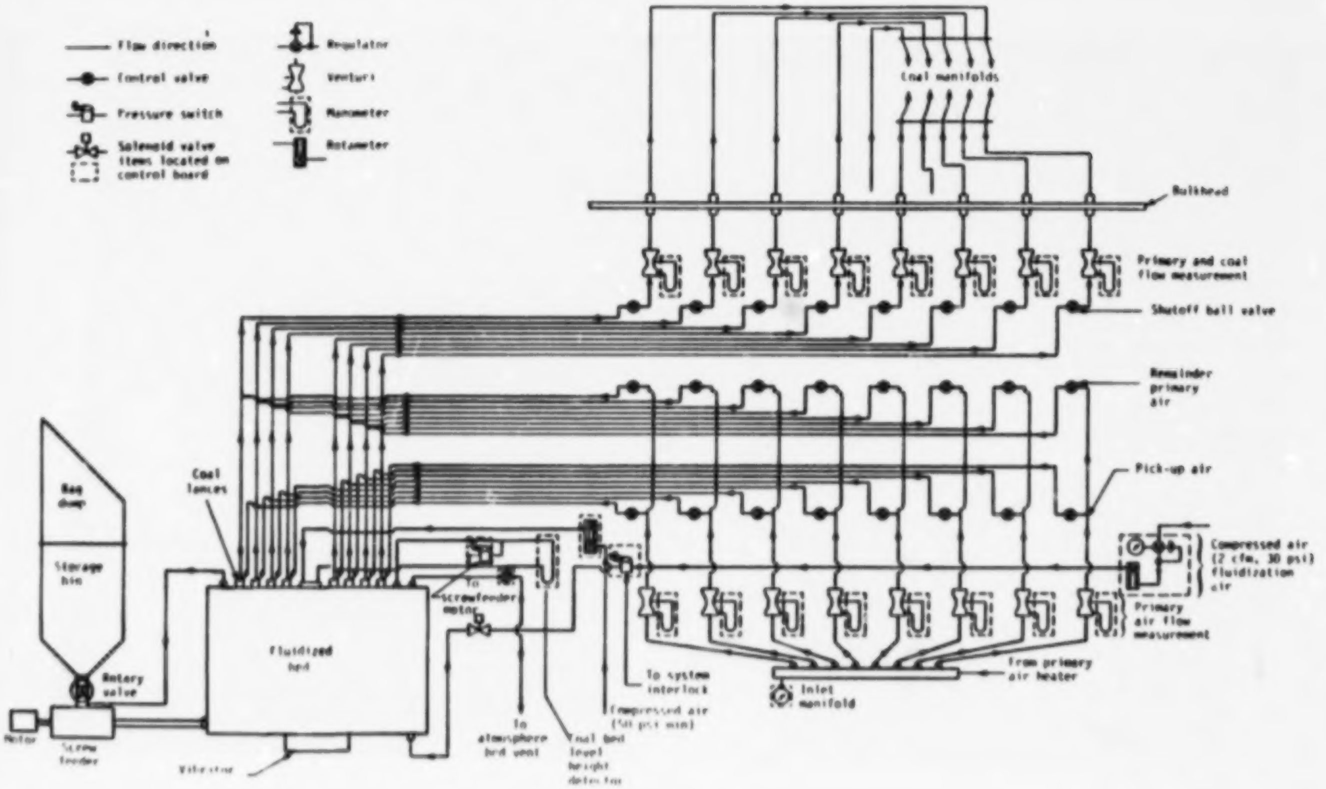
Flow direction
Control valve
Pressure switch
Solenoid valve
Items located on control board
Regulator
Venturi
Manometer
Rotameter
Coal manifolds
Bulkhead
Primary and coal flow measurement
Shutoff ball valve
Remainder primary air
Pick-up air
Compressed air (2 cfm, 30 psi) fluidization air
Primary air flow measurement
From primary air heater
Inlet manifold
To system interlock
Compressed air (50 psi min)
Coal bed level height detector
To atmosphere bed vent
To screwfeeder motor
Fluidized bed
Coal lances
Bag dump
Storage bin
Rotary valve
Motor
Screw feeder
Vibrator

Figure 4. Coal system schematic.

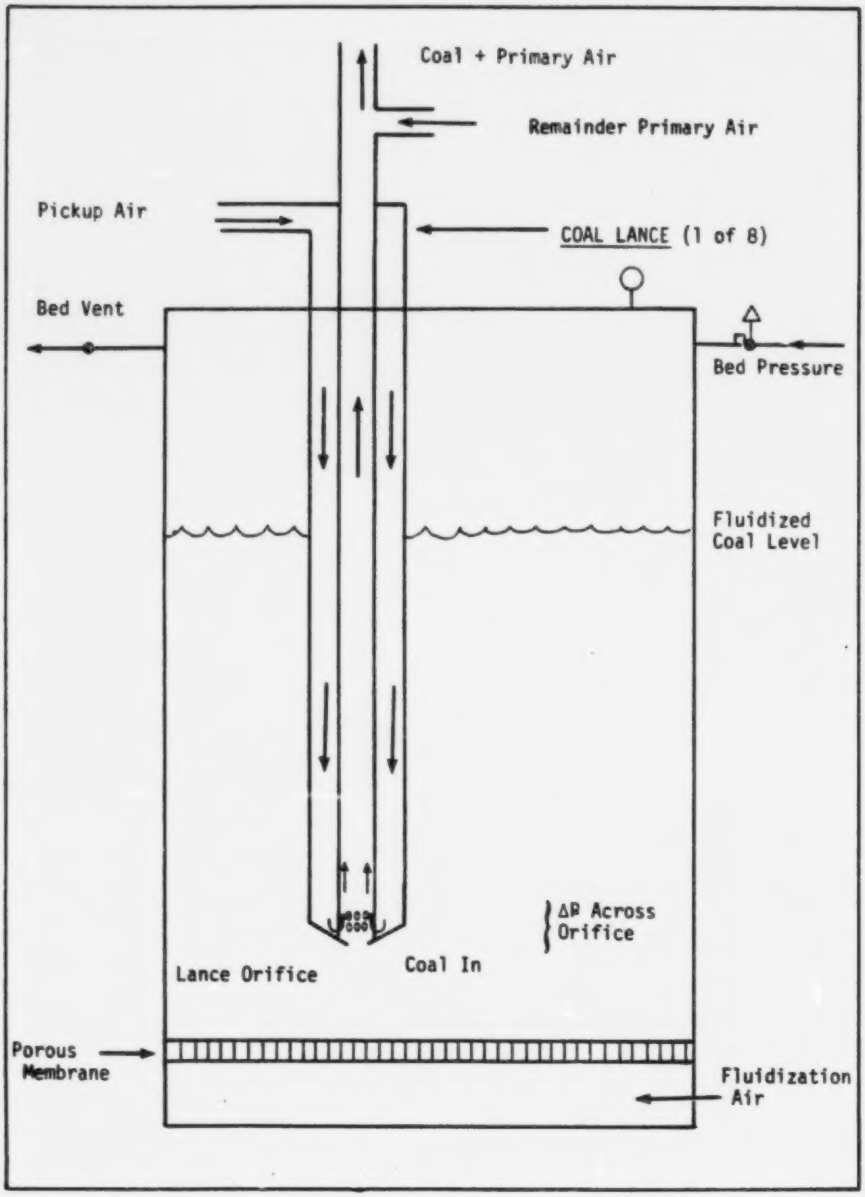
Coal + Primary Air
Remainder Primary Air
Pickup Air
COAL LANCE (1 of 8)
Bed Vent
Bed Pressure
Fluidized Coal Level
ΔP Across Orifice
Lance Orifice
Coal In
Porous Membrane
Fluidization Air

Figure 5. Coal lance detail.

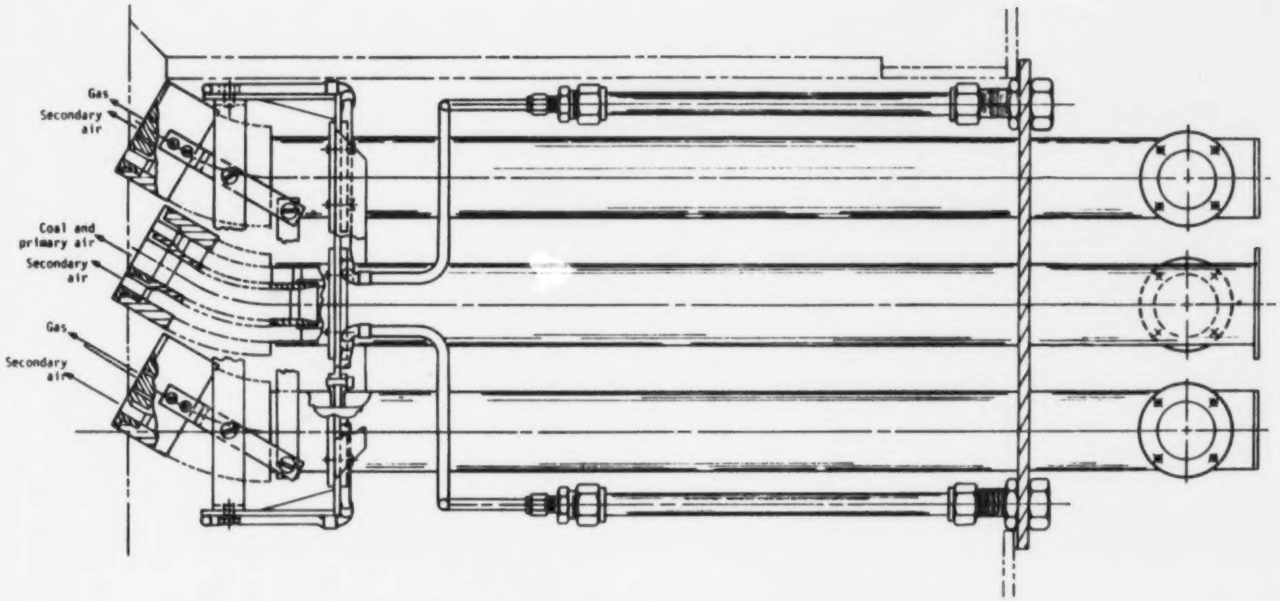
Gas
Secondary air
Coal and primary air
Secondary air
Gas
Secondary air

Figure 6. Corner-fired burner.

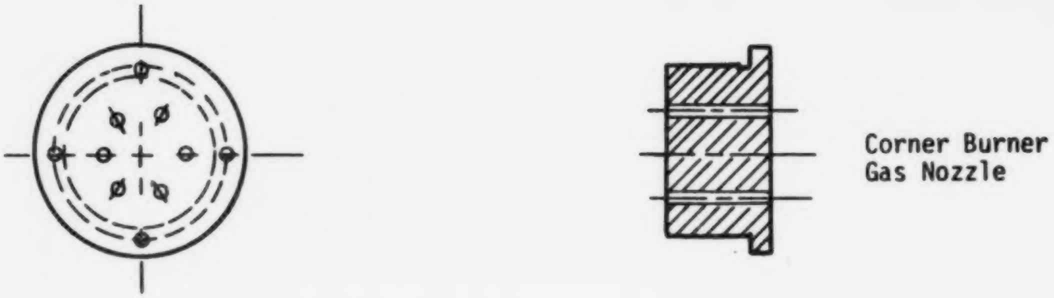

Corner Burner
Gas Nozzle

Nozzles are located in the centers of the auxillary air jets, above and below the coal feed tube.

Figure 7. Corner burner gas nozzles.

Flow measurements in the air system are accomplished using sharp-edged orifice sets. The pressure drop across each orifice is read out on a manometer. The pressure at the orifice is monitored with a diaphragm gauge. Orifice temperatures, as well as all other thermocouple measurements, are monitored by a minicomputer data acquisition system. The millivolt signals are sent to the computer where they are interpreted and displayed as temperatures every 30 seconds on a CRT screen in the furnace control room. This same data acquisition system is used to monitor the emission data, as well as to calculate and record the various flowrates.

The gas flowrate is determined using a rotameter and the Dowtherm flow is monitored with a Barton flow indicator based on an orifice P measurement. The coal flowrate is set approximately using the screw feeder controller, but is normally back-calculated from the airflow and O_2 measurements.

Critical cooling water flows are monitored with flow switches tied to the flame safeguard system. If any of these flows are lost, the flow switches trip the fuel solenoid valves and the furnace is shut down. Other safeguard switches include overtemperature switches on the flue gas into the baghouse, the Dowtherm exit temperature, and Dowtherm minimum flowrate.

Firebox temperatures are roughly measured using a ceramic-sheathed unshielded platinum-platinum/rhodium thermocouple. Although these measurements have considerable radiation error, they give an indication of the approximate temperature level and the relative temperature changes.

The furnace draft is monitored by a magnehelic gauge both in the firebox and at the point in the stack where the emissions are sampled. During a test, the firebox and stack are maintained at positive pressure to ensure that air is not leaking into the system. When a port is to be opened, the furnace is temporarily placed under negative pressure using the damper control on the induced draft fan.

The pressure measurement between the firebox and the stack also indicates when the heat exchanger tubes are fouled and soot blowing is required. A similar pressure drop measurement is made across the baghouse to indicate when baghouse pulse cleaning is required.

2.4 EMISSION MONITORING

As mentioned in the previous section, emission samples are continuously drawn from the stack just downstream of the heat exchanger section but prior to the baghouse. The temperature of the exhaust gases at this point is from 149°C (300°F) to 316°C (600°F) with the temperature usually held to the lower limit.

A schematic of the gaseous emission monitoring system is shown in Figure 8. A sample is pulled through a heated filter where the bulk of the particulates are removed. From the heated filter, the sample flows through a heated Teflon line to an oven. Additional filtration is performed in the oven and the sample divided three ways. Calibration or zero gas may also be added at this point. From the heated oven, the three sample lines pass through a

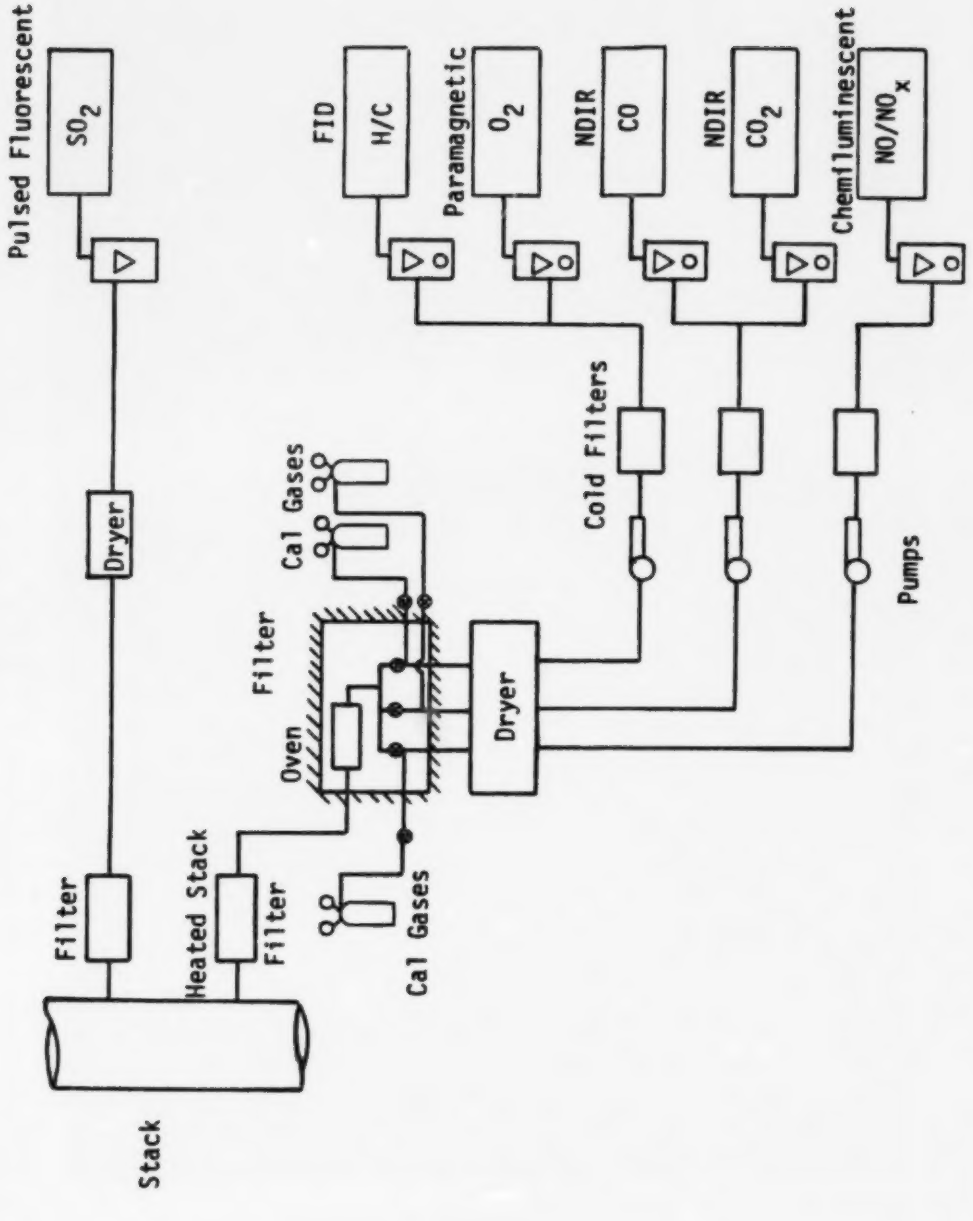
Stack
Filter
Heated Stack
Filter
Dryer
Pulsed Fluorescent
SO$_2$
Cal Gases
Oven
Filter
Cal Gases
Dryer
Pumps
Cold Filters
FID
H/C
Paramagnetic
O$_2$
NDIR
CO
NDIR
CO$_2$
Chemiluminescent
NO/NO$_x$

Figure 8. Emission monitoring system.

refrigerant dryer where the sample is condensed to a dew point of 2°C (35°F). From the dryer, each sample gas passes through a pump and another filter prior to entering the instruments. Table 1 lists the instruments and principle of operation for each of the gaseous emissions measured. These include O_2, CO, CO_2, NO, NO_x, THC, and SO_2. The SO_2 unit uses a separate heated filter, sample line, and condenser.

Sampling in the hot (1094°C (2000°F)) combustion gases for NO, NH_3, HCN, and particulate was performed during some of the tests. This sampling was accomplished using the water-cooled spray quench probe shown in Figure 9. Sufficient water is sprayed into the tip to rapidly quench the reactions and unburned hot coal particles. This slurry of char, water, and gaseous sample is drawn by a vacuum pump to a dropout pot. Here, the gases are routed to the emission system and the water and char slurry are separated.

This probe is also used to measure NH_3 and HCN concentrations in the firebox and before the heat exchangers, using the impinger sampling train shown in Figure 10. The solutions are then analyzed for NH_3 and CN using Orion Company specific ion electrodes. NH_3 is measured by ion electrode no. 950022 and CN is measured by ion electrode no. 94-06A reference electrode 90-02-00. The readout occurs on an Altex digital pH meter no. 3560.

TABLE 1. ANALYTICAL POLLUTANT MEASUREMENT EQUIPMENT

NO/NO_x	Intertech Model 32C chemiluminescence analyzer
O_2	Intertech Model Magnos 5T paramagnetic O_2 analyzer
CO	Intertech Model URAS 2T NDIR CO analyzer
CO_2	Intertech Model URAS 2T NDIR CO_2 analyzer
U/HC	Intertech Model FID0008 FID N/C analyzer
SO_2	TECO Model 40 Pulsed Fluorescent analyzer

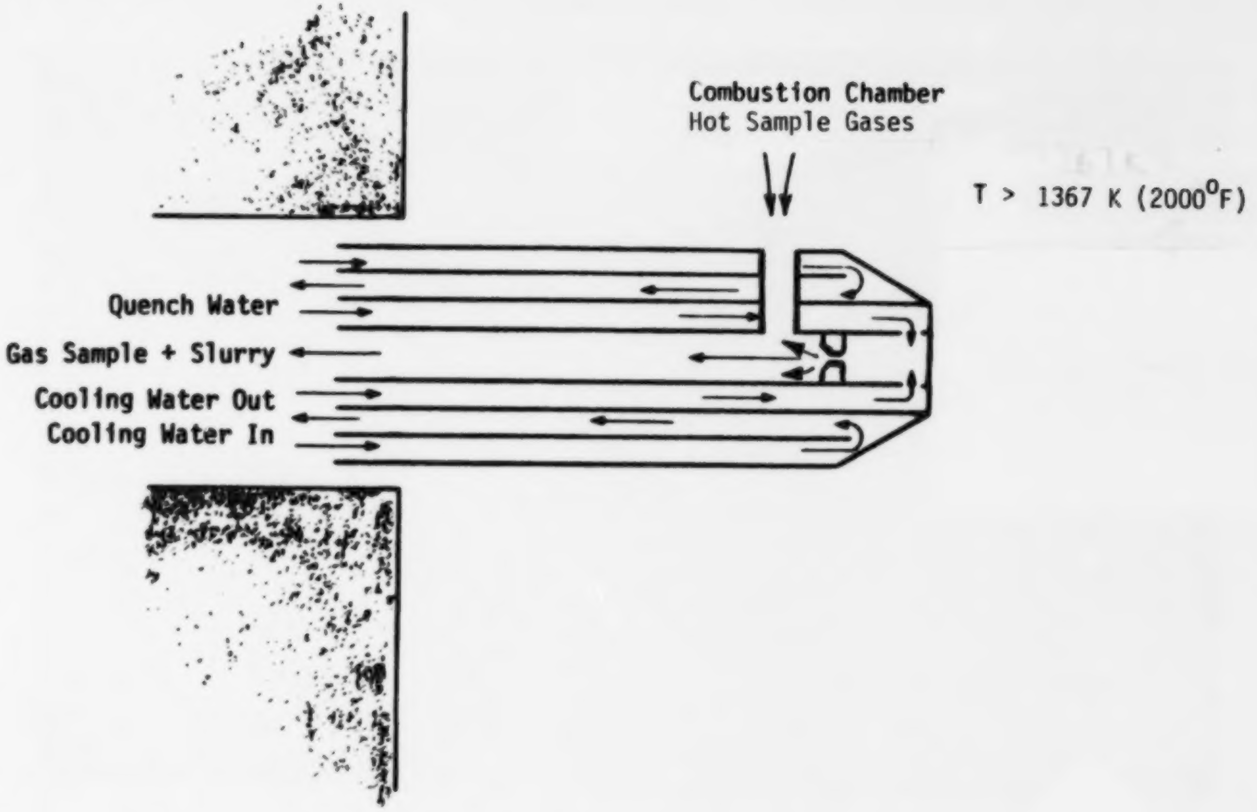
Combustion Chamber
Hot Sample Gases
T > 1367 K (2000°F)
Quench Water
Gas Sample + Slurry
Cooling Water Out
Cooling Water In

Figure 9. Hot sampling probe.

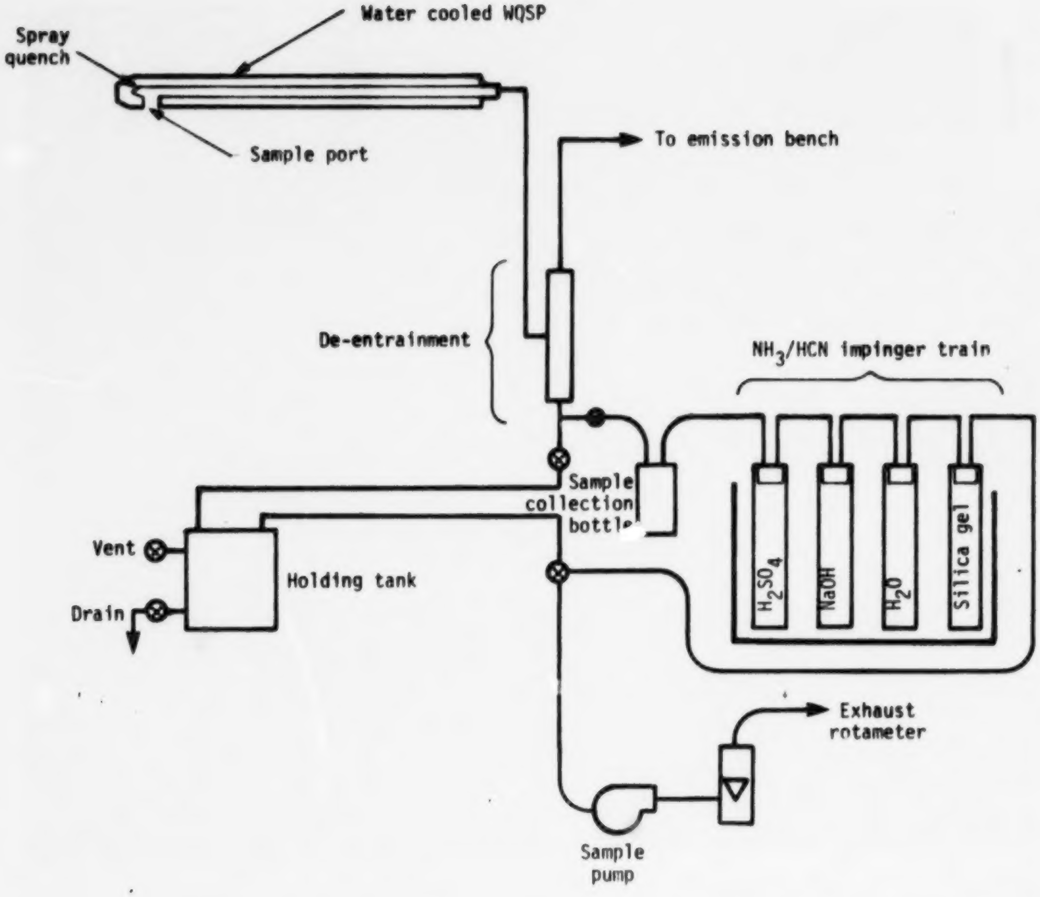
Water cooled WQSP
Spray quench
Sample port
To emission bench
De-entrainment
NH_3/HCN impinger train
Sample collection bottle
Vent
Drain
Holding tank
H_2SO_4
NaOH
H_2O
Silica gel
Exhaust rotameter
Sample pump

Figure 10. NH_3/HCN in-flame impinger train.

SECTION 3

BASELINE TESTING

For the pilot-scale low-NO_x system results to be useful for full-scale application, it must be clearly demonstrated that the combustion environment inside the pilot-scale system is representative of full-scale system environments. This must be shown for at least baseline combustion conditions typical of full-scale practice. The purpose of this task was to demonstrate that realistic combustion environments are produced in the pilot-scale facility. This was accomplished through comparisons of pilot-scale and corresponding full-scale NO, CO, and carbon loss stack emissions, and flame and firebox flow patterns under typical field conditions.

3.1 COMPARISON OF PILOT- AND FULL-SCALE STACK EMISSIONS UNDER BASELINE CONDITIONS

Figure 11 compares the NO emission levels achieved by the pilot-scale facility at various excess air levels on several coal types to full-scale utility boiler levels (References 11 and 12). These results were achieved for the characteristic operating parameters listed. Burner parameters and yaw for these tests are set at values typical of full-scale systems. Properties of the coals used are given in Table 2.

The full-scale results were achieved with eastern bituminous coal, and comparison with the Western Kentucky and Pittsburgh No. 8 coal pilot-scale results is most relevant. The pilot-scale burners were patterned after the Barry No. 2 unit of Alabama Power Company, and agreement between the Western Kentucky coal pilot- and full-scale results is excellent. In general, pilot-scale results correspond well with the full-scale results, considering the variability of full-scale system results with design, operation, and fuel type. Matching the NO trend with excess air is encouraging in that this may be an indication of the matching of mixing processes between full- and pilot-scale systems.

As shown in Figure 12, front-wall-fired results, achieved in this same facility, also matched full-scale data. These results showed a higher rate of emission increase with excess air indicating a more premixed nature for this type of firing versus tangential firing. The good agreement between pilot- and full-scale tangential and front-wall-fired NO_x indicates that the pilot-scale test facility can simulate these widely differing combustion methods over the excess air range of interest.

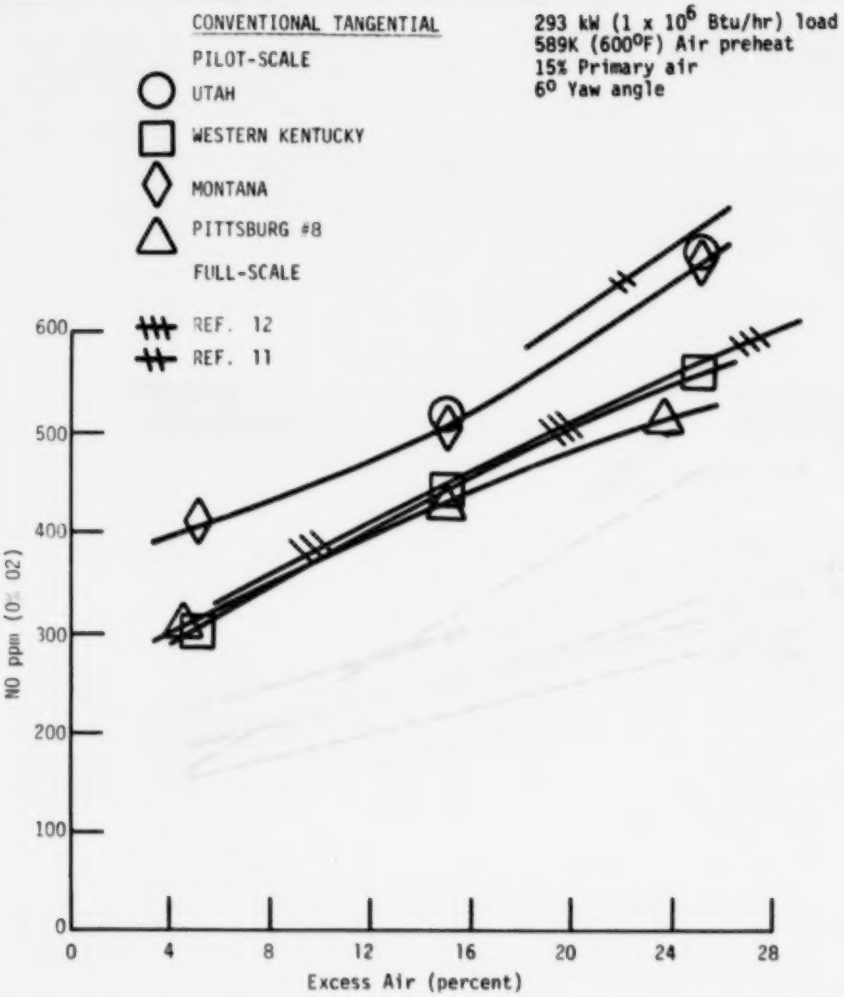

Figure 11. Tangentially fired baseline NO emissions.

TABLE 2. COAL PROPERTIES

Coal	Utah	Pittsburgh #8	Western Kentucky	Montana-Powder River Region
Ultimate Analysis (percent dry)				
C	69.91	77.2	73.0	67.2
H	5.15	5.2	5.0	4.4
N	1.5	1.19	1.40	1.10
S	0.98	2.6	3.1	0.9
O	12.46	5.9	9.3	14.0
Ash	10.0	7.9	8.2	11.7
Heating Value, J/kg (Btu/lb, Wet)	2.757×10^7 (11,842)	3.18×10^7 (13,700)	2.882×10^7 (12,450)	2.068×10^7 (8,900)
Proximate Analysis (percent wet)				
Volatile	40.6	37.0	36.1	30.5
Fixed Carbon	44.4	54.0	51.2	39.0
Moisture	5.6	1.2	4.8	21.2
Ash	9.4	7.8	7.8	9.2

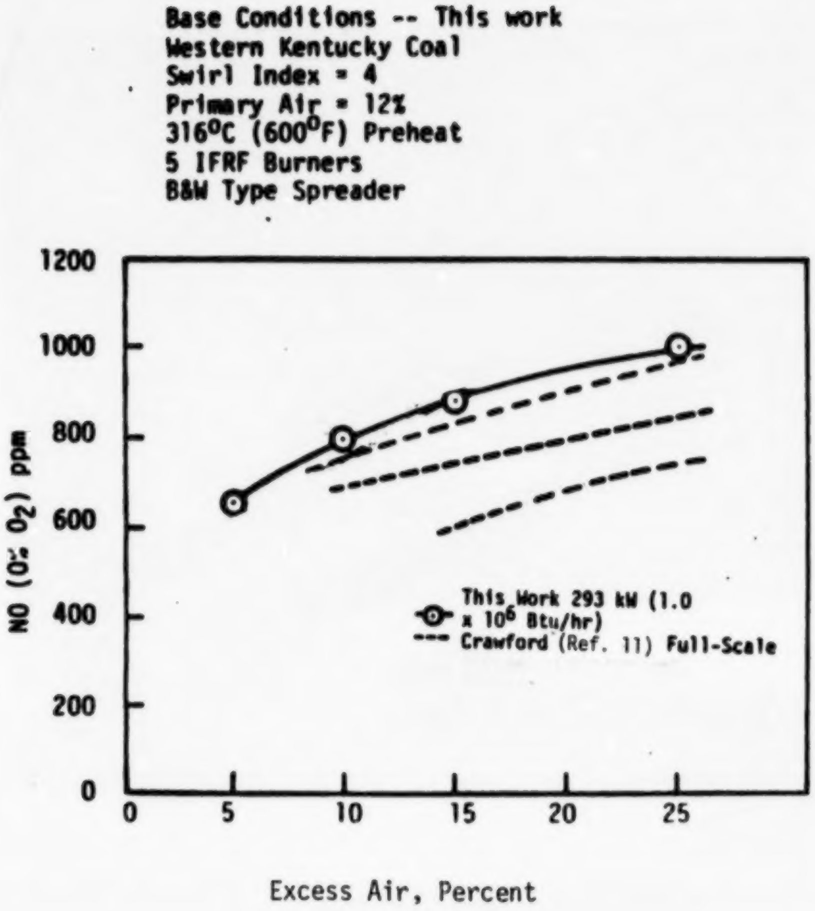

Figure 12. Front-wall-fired baseline NO emissions.

CO, UHC, and carbon loss emissions measured during baseline testing indicate that complete combustion is occurring in the pilot-scale facility. Figures 13 and 14 compare pilot- and full-scale tangentially fired CO and carbon loss emissions respectively over a range of excess air. The full-scale data were obtained in the Barry No. 2 unit (Reference 12) which the pilot-scale system design was patterned after. Above 10 percent excess air, the CO and carbon loss pilot- and full-scale results agree. Below 10 percent excess air, the full-scale results rapidly increase while the pilot-scale results remain low. The difference in CO and carbon loss might be due to the difference in wall conditions between the two systems.

To obtain proper exit gas temperature, the pilot-scale facility has much hotter walls than full-scale systems, (1,589°K versus 700°K, (2,400°F versus 800°F)). Therefore, in the full-scale system, particles and flames that contact the walls can be quenched. If excess air and oxygen concentrations are low, these quenched particles may never fully "reignite" to high temperature. The result will be increased carbon loss and CO emissions, as observed in Figures 13 and 14.

Even though agreement of CO and carbon loss at low excess air levels is not good, the good agreement at excess air levels of interest to full-scale practice, 10 percent and greater, is supporting evidence that the pilot-scale facility is simulating full-scale system combustion environments.

The good comparison achieved between pilot- and full-scale NO results, the complete combustion of the fuel in the pilot-scale facility, and the good correspondence between CO and carbon loss emissions at excess air levels above 10 percent are encouraging evidence that the pilot-scale facility can simulate full-scale NO_x and burnout results.

3.2 COMPARISON OF PILOT- AND FULL-SCALE FLAME AND FLOW PATTERNS UNDER BASELINE CONDITIONS

To fully confirm the simulation capability of the pilot-scale system, a comparison of detailed firebox properties between the pilot- and full-scale systems, as well as a comparison of stack emissions, is required. At present, insufficient full-scale firebox data are available to make this comparison. However, as discussed in section 1, fuel/air contact through mixing plays an important role in NO_x formation, and a comparison of flow patterns and firebox mixing of the two systems could supply additional information needed to assess the simulation capability of the pilot-scale furnace.

The objective of this task was to assess the capability of the pilot-scale furnace to simulate a coal-fired tangential system through comparisons of pilot- and full-scale flame and flow patterns. Another objective was to obtain a better definition of flow patterns and mixing in both full- and pilot-scale facilities, and thereby, a better understanding of NO_x formation and reduction.

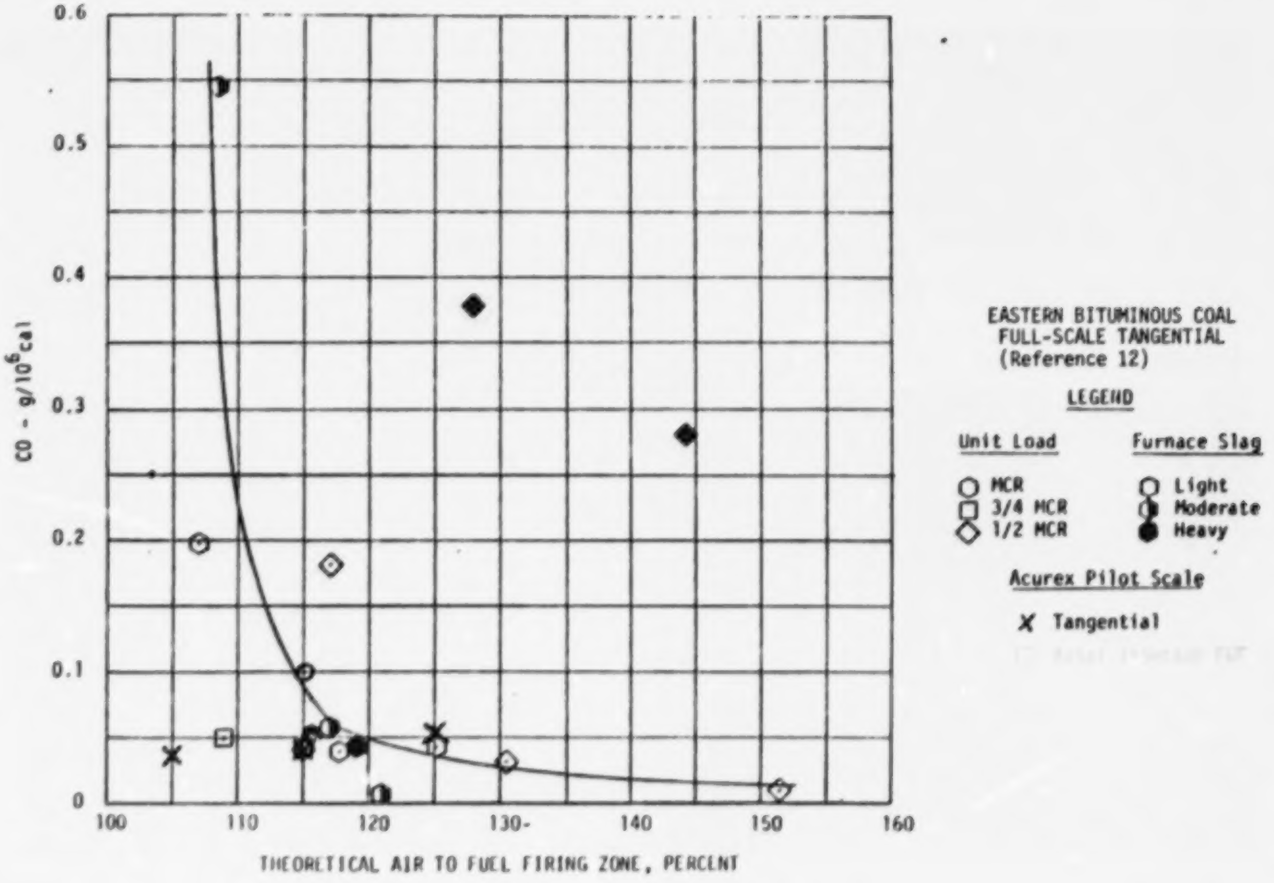

Figure 13. CO versus theoretical air-to-fuel firing zone.

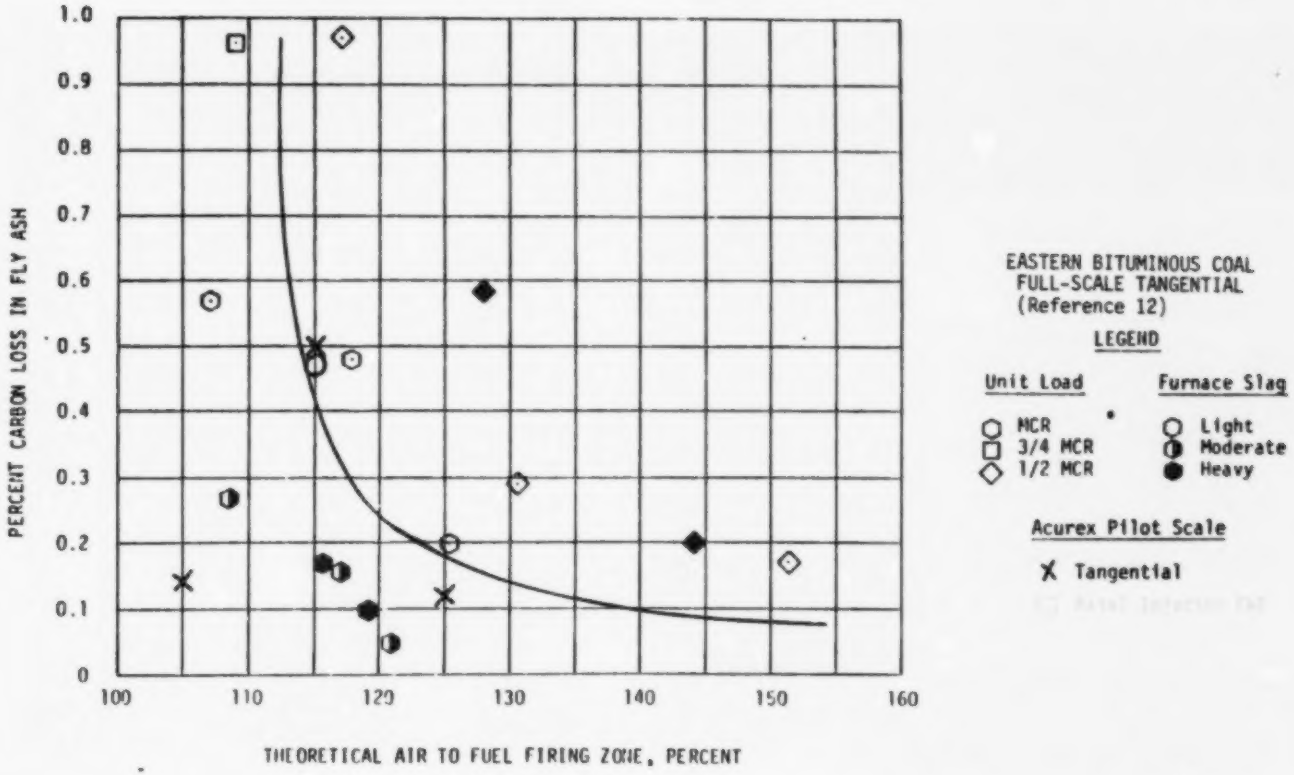

Figure 14. Percent carbon loss versus theoretical air-to-fuel firing zone.

3.2.1 Flame and Flow Pattern Visualization

To define the flow patterns and mixing in the pilot-scale furnace, a cold flow water model was built to simulate the pilot-scale furnace. Dye was injected into the fuel and air ports of the model and the flow patterns were filmed. The films of the cold model were compared with photographs of the pilot furnace firebox flame and flow patterns and with films provided by Combustion Engineering Company (CE) of a full-scale tangential facility in operation.

3.2.1.1 Cold Flow Model

There were a number of reasons why a cold flow model was chosen to provide data for this task. The model would serve as a bench-scale test apparatus which is simple and relatively inexpensive to build and modify as needed. The model would also provide the flow visualization needed for this task, where the actual furnace can only provide visualization from one view at best. In addition, good correspondence has been shown (References 13, 14, and 15) between cold flow models and actual combustion systems.

Among established modeling similarity criteria (References 16 and 17), the criteria considered most important for mixing and flow patterns were geometric and dynamic similarity. The model was built of plexiglass with the geometry of the EPA furnace at one-third scale. For dynamic similarity, the velocity was scaled directly to match the jet-to-jet interaction time of the pilot-scale furnace. Reynolds numbers of hot and cold systems were high, giving turbulent flow. Under these conditions, the Reynolds numbers do not have to match for dynamic similarity.

Water was chosen as the flow medium rather than air because the system and equipment required for turbulent flow are more compact for water than for air. To further assure dynamic similarity, the air and fuel nozzles of the model were distorted to account for the density change of the flow in the hot system. The nozzles were enlarged by the density ratio, following the modified Thring-Newby similarity criteria (Reference 15), to assure similar momentum in the cold flow model where no temperature, therefore no density, changes occur. Also tested was a nozzle configuration where only the secondary air ports were distorted by the Thring-Newby criteria and the fuel and primary air ports were directly scaled. This scaled fuel port configuration was expected to provide a better model of near-burner flow and mixing. The Thring-Newby criteria distorted fuel port configuration was expected to provide a better far-field flow and mixing modeling. Unfortunately, the system is neither near or far field dominated and therefore both processes must be modeled. This suggests that a modeling between directly scaled and Thring-Newby distorted ports might be the best approach. However, the selection of this type of criteria is not clear and was not pursued in the task.

Figure 15 presents the water model firebox and burner configuration. As in the pilot-scale facility, round air ports are used rather than rectangular air ports typical of full-scale facilities.

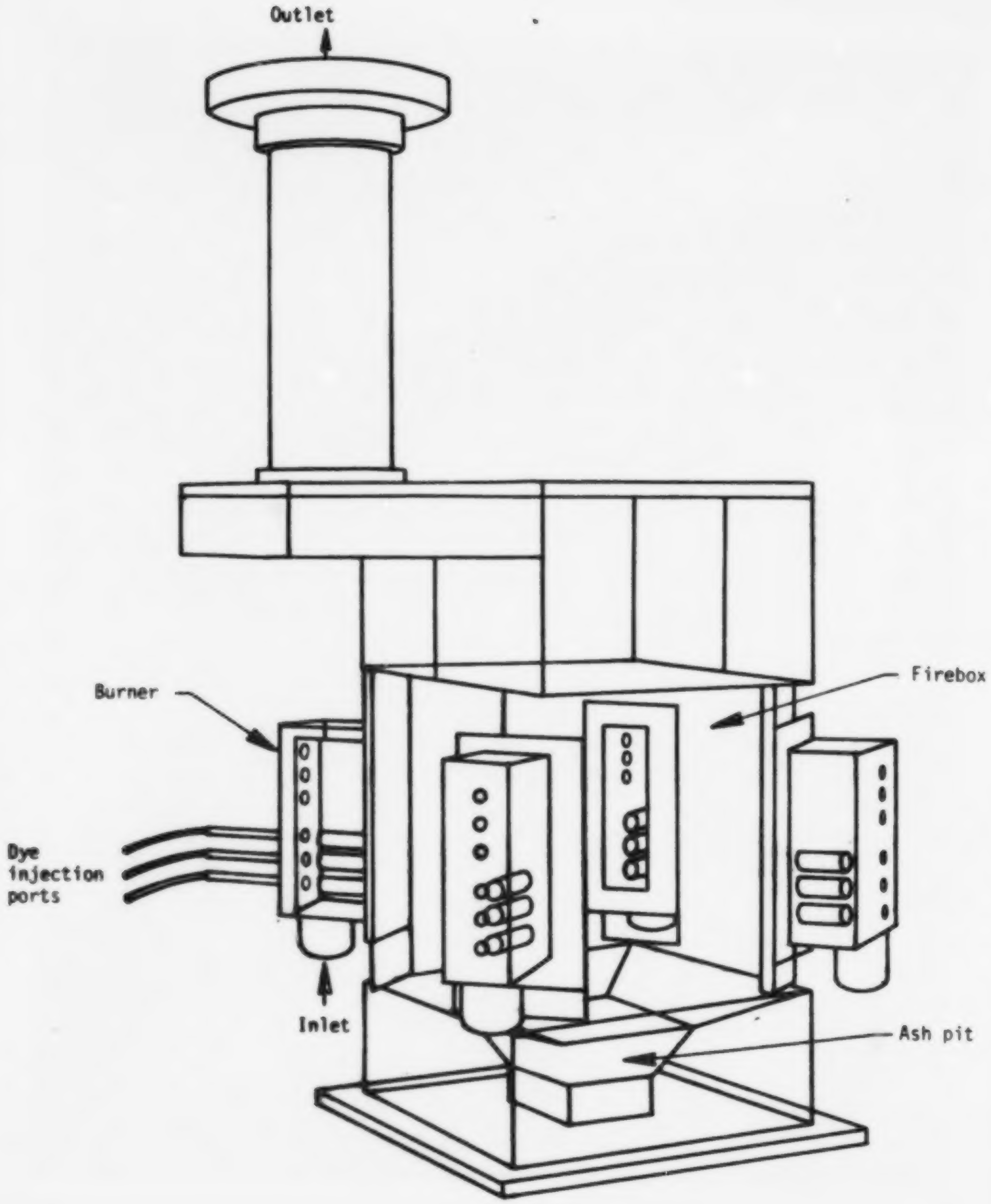
Outlet
Burner
Firebox
Dye injection ports
Inlet
Ash pit

Figure 15. Water model firebox and burners.

Since the velocity in the model was designed to match the jet-to-jet interactions of the pilot-scale furnace, the flowrate was too high to visualize the flow patterns without the aid of a high-speed camera. Dye was injected into the four fuel ports simultaneously and the flame-like patterns filmed from the top for vortex and jet-to-jet interaction data. For jet spread and additional jet interaction data, side views were filmed with dye injected into only the fuel port, then the fuel and secondary air ports. The top and side views were filmed with both Thring-Newby and the scaled fuel port configurations. The film sequences provided qualitative data, while quantitative data were obtained from single frames taken from the films.

3.2.1.2 Pilot-Scale Facility

Photographs of the pilot-scale facility vortex, viewed from below, provided part of the comparison data needed for this simulation study. To photograph the vortex, the ashpit was removed from the pilot-scale furnace, a mirror placed beneath the firebox, and flame and flow patterns photographed. The flame patterns were larger than the available field of view, but the photographs still captured enough vortex and jet interaction data for comparison.

3.2.1.3 Full-Scale Facility

The full-scale facility data were derived from a single frame taken from a CE film (Reference 18). For the CE film, a camera was placed high above the fuel injection ports of the combustion chamber of a full-scale tangential system, providing a top view of the flame patterns.

3.2.2 Results

Both qualitative and quantitative data were obtained from the cold model films and the hot system photographs. Qualitatively, in both cold model and pilot-scale facility photographs, the flow patterns clearly showed a vortex similar to full-scale systems. From the side, the scaled port configuration in the water model showed splitting of the jet on interaction with the adjacent jet as shown in Figure 16. This splitting was also seen in the pilot-scale facility photographs.

Other qualitative data included the relative size and shape of the vortex. The hot systems appeared similar with both having large vortices with jets laying close to the combustion chamber wall. The cold flow model had two different patterns, depending on the nozzle configuration. With the scaled fuel ports, the vortex was smaller with the higher velocity jets pointing more toward the firebox center. With the Thring-Newby distorted fuel ports, the vortex was very large and the slower jets were directed along the wall. In the cold model, somewhere between the Thring-Newby ports and the scaled ports appeared to best simulate the actual hot systems.

Quantitative measurements for this study were jet spread, jet centerline angle, and vortex size. A sketch of each type of measurement is shown in Figure 17. Jet spread is a measure, in degrees, of the size of the mixing zone of the jet. Jet centerline angle quantifies how far from the

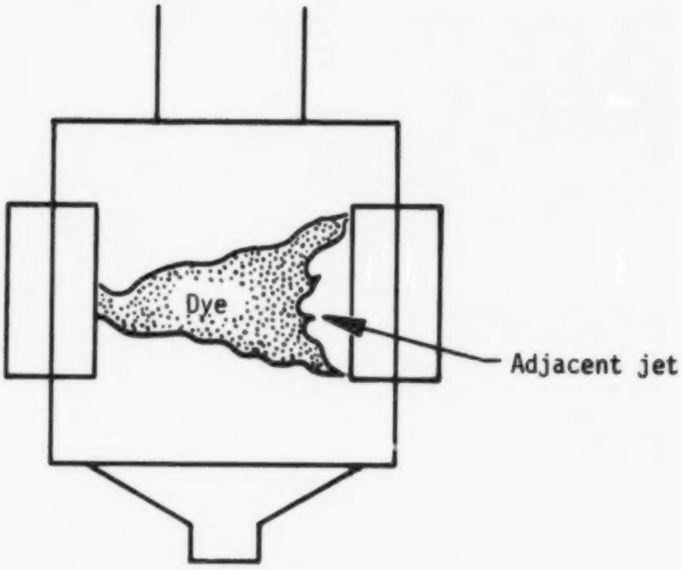
Dye
Adjacent jet

Pilot-scale model
Scaled ports
(side view)

Figure 16. Adjacent jet splitting.

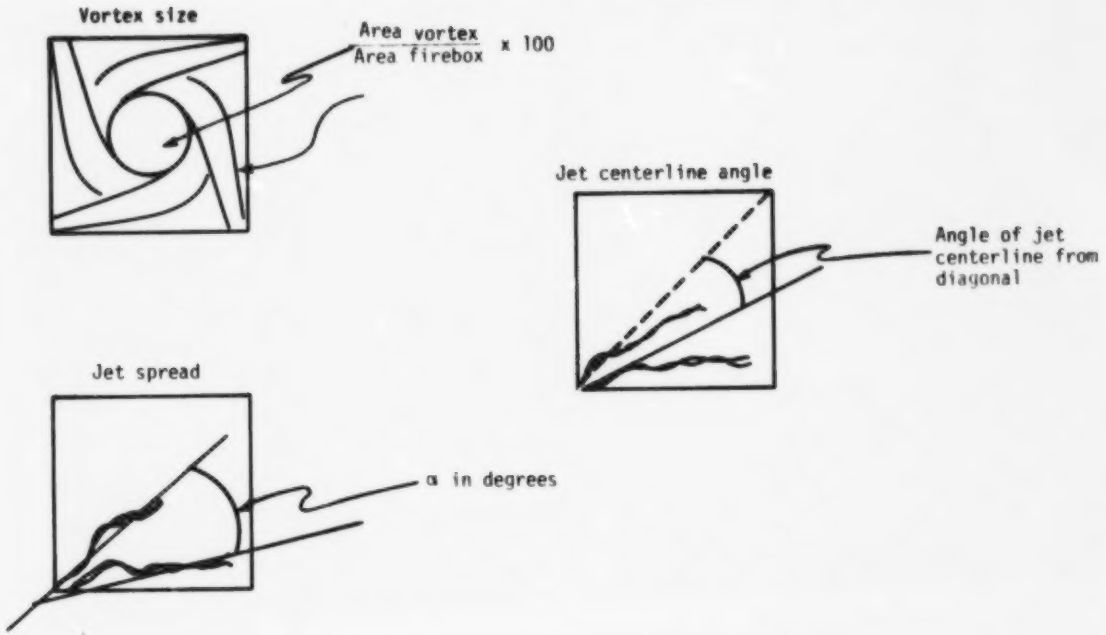

Vortex size
$\frac{\text{Area vortex}}{\text{Area firebox}} \times 100$
Jet centerline angle
Angle of jet centerline from diagonal
Jet spread
α in degrees

Figure 17. Schematic of quantitative flow and flame pattern data measurement.

firebox diagonal is the centerline of the jet. This is a measure of jet bending by vortex interaction. Vortex size is a measure, in percent, of the area of the inner circle of the vortex to the area of the firebox. Results from each of the hot systems and from the two different port configurations of the cold model are shown in Table 3.

As shown in Table 3, jet spread in all systems was similar, at about 20° to 25°. Port configuration in the cold model had no effect on jet spread. The similarity in jet spread indicates that both the cold model, in either port configuration, and the pilot-scale facility are accurate simulations of jet spread and mixing related to jet spreading in a full-scale facility.

The jet centerline angle of the pilot-scale facility was very similar to that of the full-scale facility, 20° and 23°, respectively. This similarity is another indication that the pilot-scale facility simulates the full-scale facility. For the water model, however, the port configuration had a large effect on jet centerline angle. The scaled port configuration caused a small vortex, as described earlier, with a centerline angle of only 9°. The Thring-Newby port jets, however, had an angle of 33° from the firebox diagonal. Here again, as indicated by the qualitative data, an interpolation between the two port sizes would probably best simulate the hot facilities.

A comparison of the vortex size presents further evidence that the EPA furnace flow patterns and mixing match that of the full-scale facility. Vortex size as a percentage of total firebox area was 10 percent for the pilot-scale and 9.3 percent for the full-scale facility. The water model data show again that the best simulation is a port size somewhere between the scaled port and the Thring-Newby port.

TABLE 3. QUALITATIVE FLOW AND FLAME PATTERN DATA

	Jet spread (degrees)	Jet centerline angle (degrees)	Vortex size (% of box)
Water Model			
1. Pilot -- scaled ports	25	9	3.5
2. Pilot -- Thring-Newby ports	24	33	15.0
Hot Systems			
3. Pilot-scale facility	19	20	10.0
4. Full-scale facility	25	23	9.3

In addition to the above, other observations were made which help in the understanding of tangential system NO_x emission and combustion performance. The jet spreading from the side view of the cold model indicated that initial spreading of the fuel jet is like a turbulent free jet, which has a diffusion flame character (Reference 19). As a diffusion flame, the jet initially experiences slow mixing and, therefore, probably lower NO_x. The splitting of adjacent jets by the burner fuel and air jets was also seen from the side of the water model, as shown in Figure 16. The pilot system results showed stagnation zones on the front of, and recirculation zones on the back side of, the fuel jet created by the cross-flow of the hot gases from the adjacent jets. These zones promote ignition, which occurs approximately 3 to 5 burner diameters from the burner face. This ignition standoff distance is characteristic of observations in full-scale systems.

Top views also revealed relatively unpenetrated regions in the firebox center and along the walls. The center represents a hot zone that helps stabilize the system but might increase NO_x. The walls, however, cool the gases in the unpenetrated wall region, decreasing thermal NO_x. The strongly mixed center of the vortex and the relatively aerodynamically quiescent wall region character of the tangentially fired system is of interest to low NO_x system development. Whatever fuel/air stratifications are developed in the initial mixing zone of a burner will eventually be destroyed by strong vortex mixing away from the wall. Therefore, if fuel and air are to remain separated for a sufficient length of time to reduce NO_x, some of the air should be placed in the relatively quiescent wall region and the rest of the air and fuel in the center of the furnace.

In conclusion, this study revealed that the pilot-scale facility simulates a full-scale facility closely in terms of flow patterns and mixing, which are important factors in NO_x formation. In addition, the water model provided good visualization and, therefore, better understanding of the effects of flow patterns and mixing on NO_x formation in a tangentially fired system.

SECTION 4

DEFINITION OF CONVENTIONAL TANGENTIAL SYSTEM NO_x FORMATION AND REDUCTION PROCESSES

The objective of this phase of the study was to develop a better understanding of processes controlling NO_x formation during combustion of pulverized coal in tangentially fired furnaces. Based on the results of this phase of the program, low-NO_x retrofit or new design concepts were then recommended for testing in the second phase of this study.

As described in Section 1, tangentially fired furnaces are complex systems with many of the design parameters potentially influencing NO_x formation. In addition to furnace design parameters, fuel characteristics also play a role in NO_x formation. Because of the complexity of the system, the initial testing focused on a gross definition of the processes on NO_x formation. Based on these initial tests, a second series of tests was identified to more closely define the influence of system design parameters on NO_x formation. The results of these definition tests were then used to define low-NO_x systems for testing in the second phase of this study.

The NO_x formation testing used to identify (1) fuel chemical and physical characteristics important to NO_x formation and reduction, (2) the effect of design variables on these processes and (3) the potential of these processes to control NO_x will now be discussed.

4.1 CHEMICAL/PHYSICAL CHARACTERISTICS OF FUEL

The objective of these tests was to define the relative importance of fuel chemical and physical processes on NO_x formation in tangentially fired systems. By determining the dominant NO_x formation processes, control strategies could then be directed at those processes which have the greatest potential for NO_x control.

These tests took place under conventional tangentially fired configurations, as described in Section 3. Stack gas and, in some cases, particulate emissions, were monitored continuously during these tests. Both staged and unstaged tests were run with coal, char, gas, and doped gas fuels. Constant mixing conditions were maintained for all fuels tested to separate the fuel characteristic effects. This was achieved by a fixed secondary air geometry and proper adjustments to the fuel delivery tube area to give the correct initial fuel/air mixing for the different fuels tested.

With unstaged conditions, the NO_x formation is dominated by local fuel/air contacting in the mixing zone near the burner face (Reference 9).

With staged combustion, the initial fuel/air contacting is not as important, and the NO_x emissions are more strongly influenced by the NO_x decay processes in the first stage and NO_x formation at the staged air addition point (Reference 9). By testing both staged and unstaged cases, NO_x processes could be established for both mixing dominated and chemical reaction dominated cases. Also, it was anticipated that some form of local or global staging would be required for NO_x control, and, therefore, it was appropriate to test staged combustion.

4.1.1 Baseline Utah Coal Tests

The purpose of these tests was to show that Utah coal, selected as the primary fuel type for this study, had a NO formation behavior not atypical of the many bituminous coals used in utility boilers.

Unstaged and staged Utah coal tests were run under the same conditions as Western Kentucky, Pittsburgh No. 8 and Montana coals, extensively tested in a previous program phase (Reference 9). Table 2 gives the coal properties. The Western Kentucky and Pittsburgh No. 8 coals are high-sulfur eastern bituminous coals. The Montana coal is a low-sulfur subbituminous coal and the Utah coal is a low-sulfur western bituminous coal.

Figure 18 shows the NO emissions for Utah coal as a function of excess air compared to the other coal results. All coals yield the same increasing trend of NO with excess air. The western coals, both the Utah and Montana, yield significantly higher NO than the eastern Western Kentucky and Pittsburgh No. 8 coals. As explained earlier, these NO levels correspond to typical full-scale system levels.

Figure 19 shows the variation of NO under staged combustion conditions as a function of first-stage stoichiometry for the Utah, Montana, and Western Kentucky coals. Utah coal results were obtained for both 300°K and 589°K (80°F and 500°F) air preheat. All other coals were tested at 589°K (600°F) air preheat.

In staged combustion, as the stoichiometry of the lower firebox is decreased, the NO formed in the early combustion processes is reduced to molecular nitrogen and possibly NH_3 and HCN (Reference 7). At the staged air addition point, depending on first stage stoichiometry and temperature, the NH_3 and HCN might convert to NO, react with NO to form molecular nitrogen, or be reduced to molecular nitrogen by some other path. In addition, fuel nitrogen contained in the char can be oxidized to NO in the oxygen rich second stage. The first stage NO decay and the second stage NO formation processes govern the amount of stack NO produced and yield the characteristic dip in the stack NO results. It should be noted that the NO reductions achieved by staging in these tests are superior to those found in full-scale systems. This is because of the 25 percent longer first stage residence time and good first- and second-stage separation in the pilot-scale test facility. Therefore, the staging test results presented herein represent the maximum potential NO benefit achieved by staging. The excess air level in the stack at all first stage stoichiometries was 15 percent.

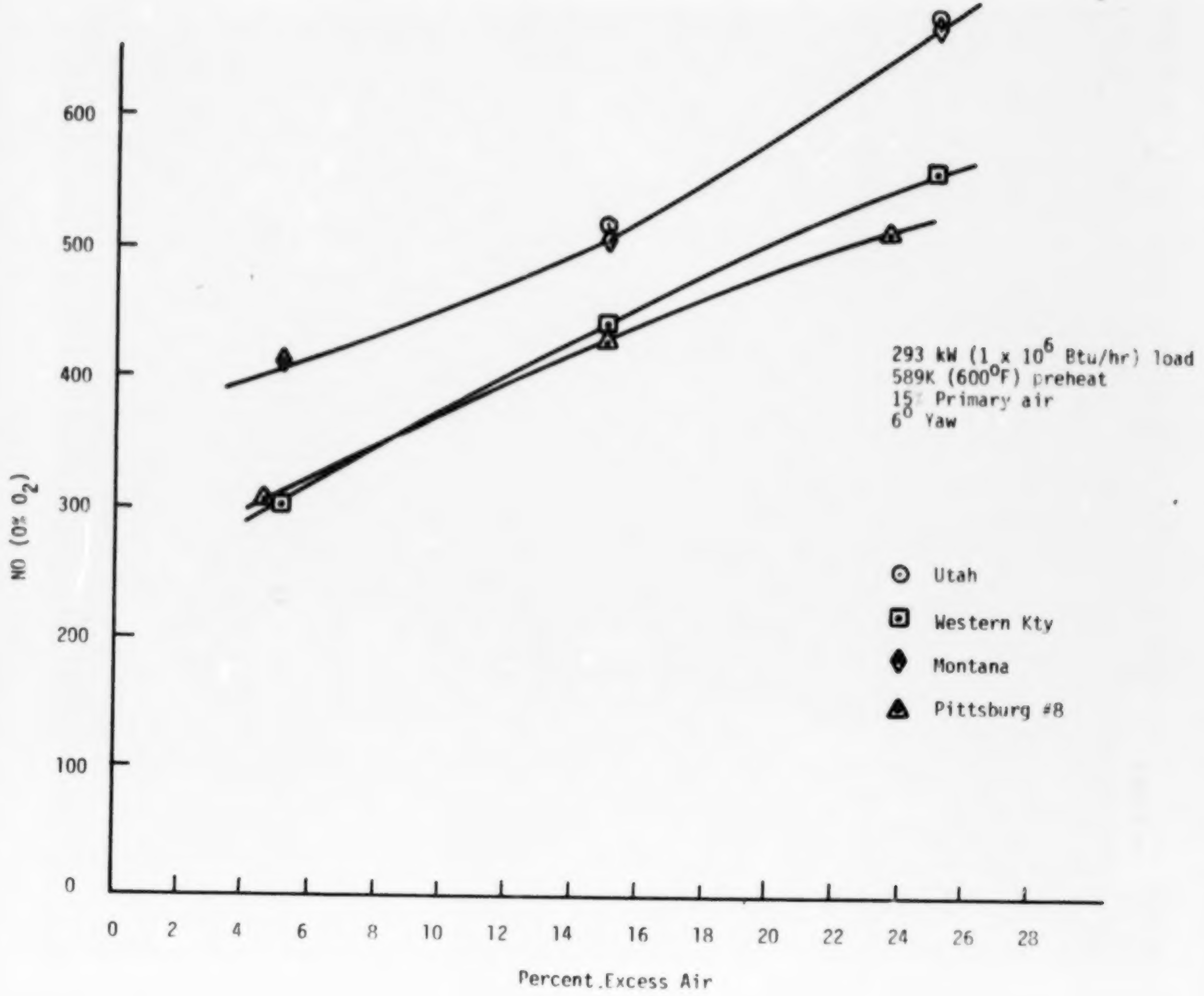

Figure 18. Variation of NO with percent excess air.

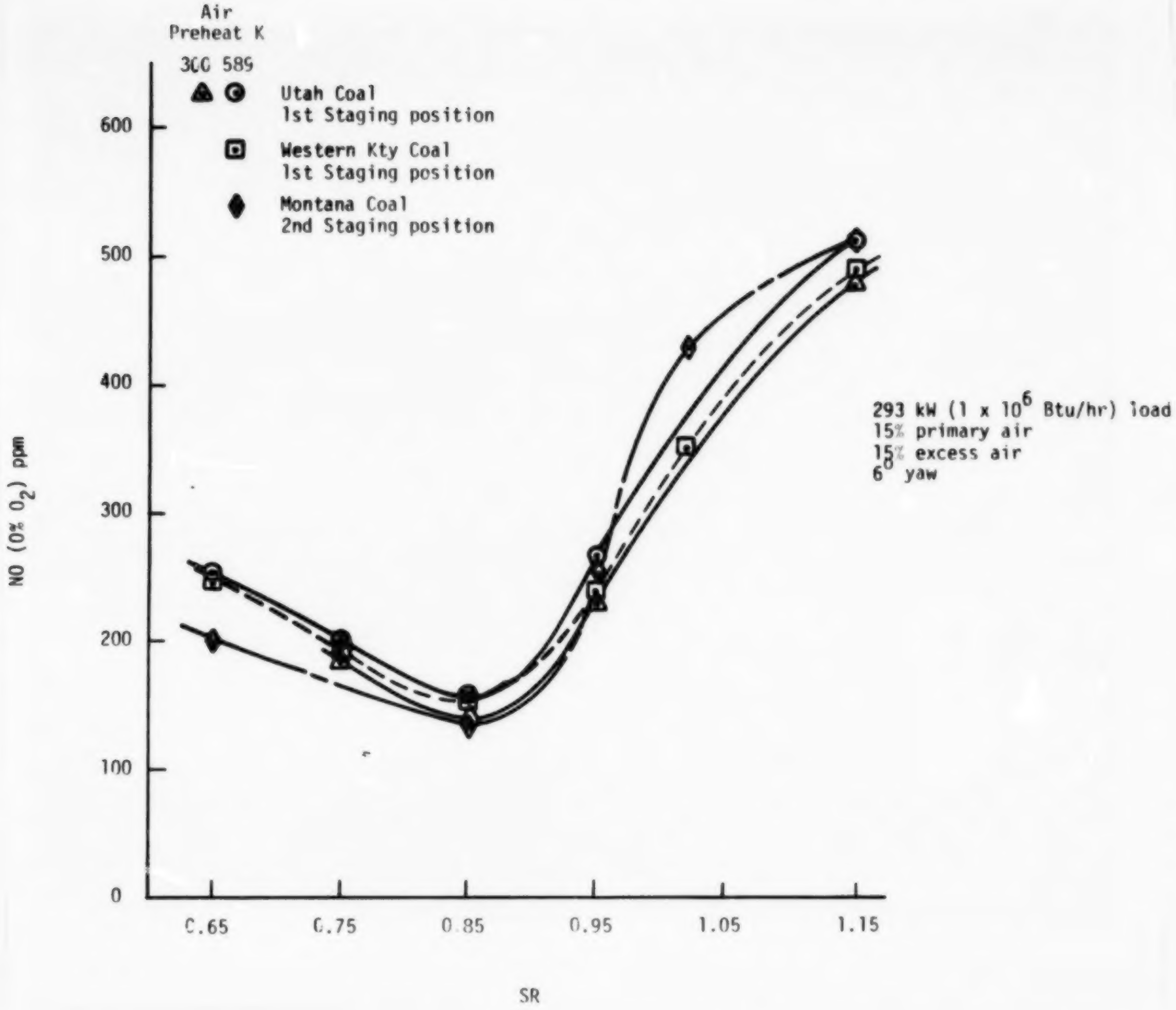

Figure 19. Variation of NO with stoichrometric ratio (SR).

As in the excess air tests shown in Figure 18, the western coals have higher NO emissions for stoichiometries greater than one. At stoichiometries less than 0.85, the NO differences between the Utah and eastern bituminous coals become small. Under these same conditions, the Montana coal has the lowest NO emissions.

As explained in a prior report (Reference 9), the higher NO for the western coals might be a result of the lower sulfur content of these coals. As shown by Wendt (Reference 20), the presence of sulfur enhances NO under fuel-rich conditions and depresses NO under fuel-lean conditions. This behavior is consistent with the comparison between the low-sulfur Montana coal and other coals tested. This is not as strongly supported by the Utah coal comparison with the eastern coals. Of course, coal nitrogen and oxygen content (Reference 5) and the ease with which fuel nitrogen is evolved from the coal (Reference 21) can influence NO formation. Either of these effects can lead to NO formation, due to intimate contact of fuel nitrogen and oxygen in the early stages of combustion. The difference in these effects between the coals tested can easily lead to the NO differences noted in Figures 18 and 19.

In summary, comparison of the NO results from Utah and coals previously tested shows that Utah coal has a behavior similar to the other bituminous and subbituminous coals under both excess air and staged combustion conditions. Therefore, low-NO_x concepts proven on Utah coal should also be applicable, in some form, to other coals.

4.1.2 Gas, Doped Gas, and Char Tests

The purpose of these tests was to define the relative importance of fuel chemical and physical processes on NO formation in a coal-fired tangential system.

Presently, there is only a limited amount of information on how fuel nitrogen, atmospheric nitrogen, volatile nitrogen, and char nitrogen contribute to the overall NO levels in tangentially fired systems. In addition, the influences of the fuel/air mixing, coal particle heating, and volatile evolution rates on NO formation in tangential systems are not fully known. In these tests, natural gas, doped natural gas, and char fuels, either by themselves or in combination, were used to simulate the volatile and char components of the coal fuel. By examining the performance of these constituents alone, and in combination, the influence of the previously mentioned processes on NO could be estimated. Low-NO_x control techniques could then be applied to the dominant processes to achieve the maximum NO reduction with the least amount of effort.

Figure 20 depicts the staged and unstaged gas and doped gas results for a range of first-stage stoichiometries. Detailed conditions for these tests are the same as the coal tests described in section 4.1.1 and are presented in Figure 20. The doped gas results represent a rough simulation of an instantly and completely devolatilized coal fuel. Weight percent nitrogen, sulfur, and oxygen contents of the fully doped natural gas were matched to the Utah coal/primary air composition case. To simulate the N, S, and O components

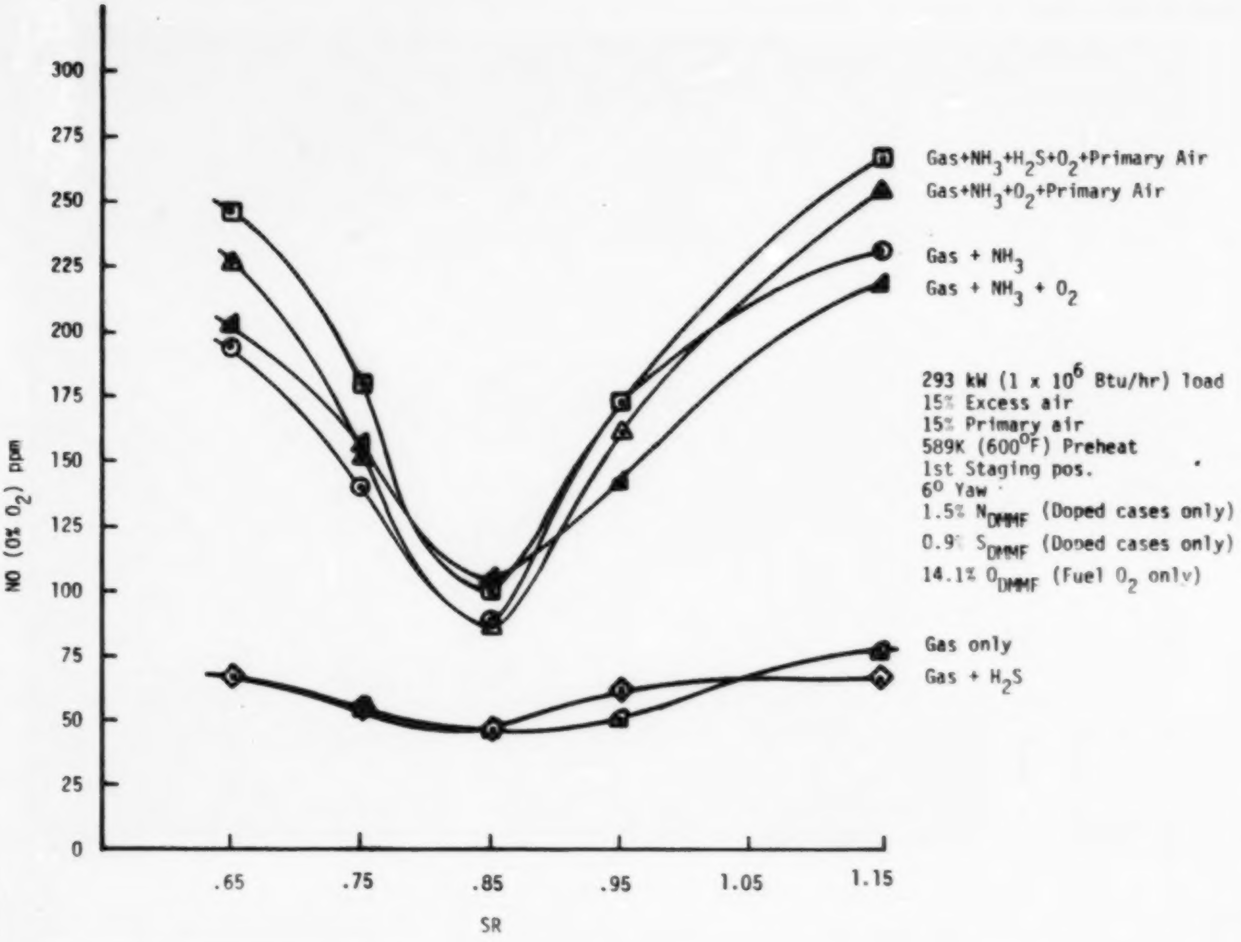

Figure 20. Variation of doped natural gas NO with SR.

of the coal fuel, NH_3, H_2S, and air dopants were respectively added to the natural gas fuel jet. Both NO and SO_2 dopants were also tested and gave comparable results (to within 20 ppm NO). However, NH_3 and H_2S were used for the bulk of the testing, since the hydrogen bonding of these dopants was believed a better simulator of the coal fuel components than the oxygen bonding of the NO and SO_2 dopants. Of course, the carbon to hydrogen ratio of the simulated volatiles is not correct.

Care was taken in the design of the fuel jet to ensure that the initial fuel/air velocities and consequent mixing rate were matched between the coal and doped gas cases. For the cases with and without primary air different size fuel tubes were used to match velocity ratios.

By using the doped gas as a simulator of the coal volatiles in these tests, the effect of volatile fuel fraction components on NO could be obtained in the absence of any heterogeneous reactions and volatile evolution processes.

As Figure 20 shows, the gas-only and gas-plus-H_2S NO levels are much lower and flatter with first-stage stoichiometry than the doped gas cases with NH_3. Since the gas only case does not contain any fuel nitrogen, these results can be taken as a measure of the thermal NO_x formation for the system. This represents about one-quarter of the total NO produced by the fully-doped gas case under unstaged combustion conditions. This thermal NO_x fraction is low compared to full-scale practice, which is typically estimated at about 50 percent (Reference 5). However, the results support that thermal NO is not the major component of total NO, and that it is not strongly influenced by staging in this type of system.

The NH_3-doped cases show that the major contributor to total NO comes from the fuel nitrogen component. The levels and shape of the NH_3-doped gas NO curve with stoichiometric ratio can be explained on the basis of standard homogeneous gas phase kinetics (Reference 22). At the unstaged and staged conditions, the effect of H_2S, O_2, and primary air on NO is much smaller than the effect of NH_3. The fuel N,S and O,N interactions in these cases are not significant. The major effect on NO is fuel N, followed by O and then S. The N,O and N,S effects lead to differences of less than 10 percent in NO on an individual basis.

The fuel N,S interaction effect on NO is not as significant as was found by Wendt in his doped diffusion flame studies (Reference 20). However, Wendt used much higher concentrations of sulfur to produce the observed differences. For the fuel S concentration employed in this study, the effect is not large.

Primary air has roughly a 25 percent maximum NO increase effect in these tests. This appears reasonable based on comparisons of doped premixed and diffusion flame laboratory results (Reference 23).

Staged and unstaged char, char-plus-gas, and char-plus-doped gas NO test results are presented in Figure 21. The char used in these tests was prepared from the parent Utah coal by the Peabody Coal Company char process.

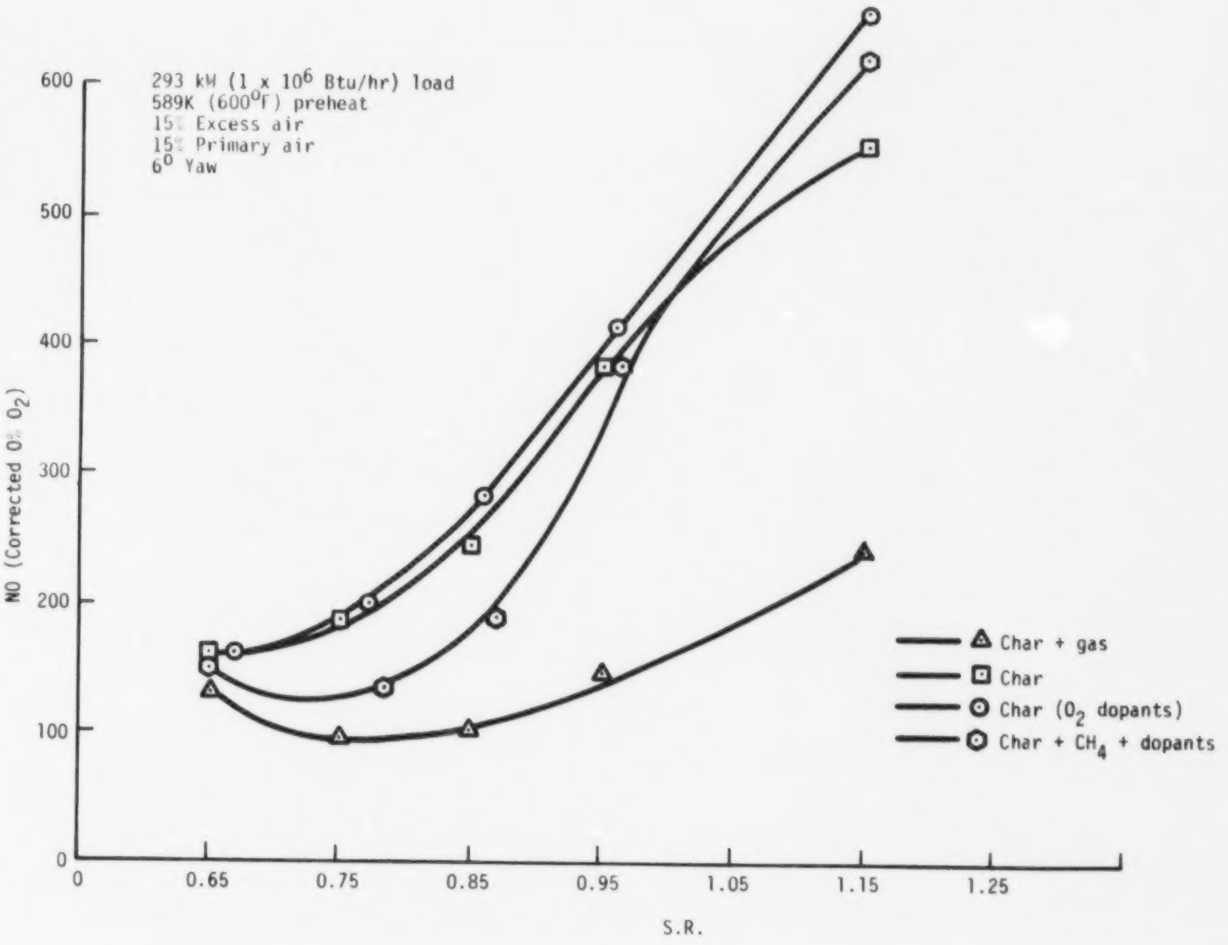

Figure 21. Char, char plus gas and char plus doped gas NO variations with SR.

The composition of the char relative to the parent coal and some relevant char formation processes are given in Table 4.

The char-plus-doped gas results represent a full simulation of the volatile and char fractions of the coal fuel. Gas fuel fractions used in these cases were equal to the ASTM volatiles content of the coal as given in Table 4. Total weight percents of nitrogen, sulfur, and oxygen were equivalent to the coal fuel. As in the doped gas case, the fuel tube was sized to give initial mixing similar to the coal case. The detailed test conditions were the same as the coal baseline tests. These conditions are presented in Figure 21. In all cases, 15 percent of the combustion air was used to transport the char into the furnace.

The results in Figure 21 show that the char-plus-oxygen dopant case gives the highest NO for all first-stage stoichiometries and the char-plus-gas

TABLE 4. UTAH COAL CHAR AND PARENT COAL PROPERTIES

	Utah Coal	Char
Carbon	69.91	78.3
Hydrogen	5.15	1.44
Sulfur	0.98	1.13
Nitrogen	1.5	1.20
Oxygen	12.46	0.83
Heating Value		
Joules/kg	2.9168×10^7	2.7632×10^7
(Btu/lbm dry)	(12,540)	(11,880)
Moisture	5.6	0.72
Volatile	40.6	6.3
Ash	10.0	17.1
Peabody Coal Company		
20 min @ 1283°K (1850°F)		
60 min in refractory shaft-cooldown		

case gives the lowest NO. Both the char and the char-plus-O_2 dopant cases monotomically decrease with first-stage stoichiometry. The char-plus-gas and char-plus-doped gas cases both have a characteristic NO minima similar to that observed for the coal and doped gas cases. At extreme staged combustion conditions, NO results for all cases are roughly equivalent. Table 5 gives properties of a particulate sample taken in the firebox above the burner level for both coal and char combustion. The similarity of percent nitrogen, carbon/nitrogen ratio, and percent volatiles shows that the difference between the char and coal results must be due to the early burning processes. Observations of the flames in the firebox showed that the char, by itself, had a larger flame standoff distance than the coal or char-plus-gas case. The char-only case therefore had more air mixing with the fuel prior to ignition. This more premixed nature of the char-only combustion could have led to the higher NO levels (Reference 3), as observed in Figure 21. This is also supported by the char-plus-O_2 dopant case which is even more premixed than the char-only case and shows an even higher NO level.

With the char-plus-gas case, the gas ignites rapidly and shields the char from O_2 thereby limiting char NO formation. The low NO levels for this

TABLE 5. PARTIALLY BURNT COAL AND CHAR PROPERTIES

	Percent		
	Base coal	Partially burnt coal	Partially burnt char
Volatiles	39.0	14.0	14.0
Nitrogen	1.5	0.98	0.99
Nitrogen/Carbon	0.019	0.012	0.012

293 kW (1 x 10^6 Btu/hr) load

589^0K (600^0F) air preheat

15 percent excess air

15 percent primary air

6^0 yaw

case under lean conditions are also due to the reduced amount of fuel nitrogen for the gas-plus-char fuel compared to the char-only case. Correction of the NO levels for the dilution effect of the low-NO gas combustion products would raise the NO levels by roughly 25 percent. This NO level would still be lower than the char-plus-doped gas results under unstaged conditions.

Since, in coal combustion, volatile combustion alters the amount and time at which oxygen reaches the char, char-only combustion is not a good indication of char NO_x formation. A better determination of coal combustion char NO_x is given by gas-plus-char combustion. In this case, the gas simulates the oxygen consumption by the volatiles. However, this simulation is not perfect since the gas does not evolve slowly from the solids, like coal volatiles, and gas-only combustion contributes to NO_x, though the contribution is small. In general, char NO_x cannot be easily separated from volatile NO_x. The volatile combustion sets up conditions in which the char combustion and NO_x formation take place. Therefore, coal char NO_x determined by char-only combustion must be carefully interpreted before applying the results to coal combustion.

4.1.3 Comparison of Coal, Doped Gas, and Doped-Gas-Plus-Char Tests

Through the comparison of coal, doped gas, and doped-gas-plus-char NO results, the significance of volatile evolution and the presence of the solid was determined.

Figure 22 compares the doped gas to coal results on a percent conversion basis. Since the air requirement for natural gas combustion is greater than that for coal combustion, an equal weight percent of N dopant totally converted to NO during natural gas combustion would yield lower NO levels than the same weight percent N in coal combustion. Utilizing percent conversions corrects for this difference in concentration.

Comparison of the doped gas and coal results in Figure 22 shows that, under lean conditions, where mixing is important, the coal results are higher than the doped gas. At a SR of between 0.95 and 0.85, all cases agree to within 1 percent conversion. At SR's less than 0.75, the coal results are lower than the doped gas results.

It may be speculated that, under unstaged conditions, the coal diffusion flame will initially burn in an abundance of oxygen. This is because the fuel is evolving from the coal into the primary air jet, which contains 15 percent of the total combustion air. Under these conditions, the fuel nitrogen evolved from the coal will be rapidly oxidized to NO. For doped gas combustion, the fuel nitrogen does not evolve slowly from a solid; therefore the initial reaction of the fuel-bound nitrogen occurs in an environment which has less available oxygen and the initial NO_x formed is lower than in the coal case. This hypothesis is also supported by the doped gas-with-oxygen case, shown in Figure 21, which gives NO levels intermediate to the coal and NH_3 doped gas cases. The doped gas-with-oxygen case has more O_2 available to the fuel than the doped gas, but less than the coal. Therefore, the intermediate NO levels for this case seem reasonable. These results imply that the more oxygen available to the fuel in the early burning zone, the higher the NO.

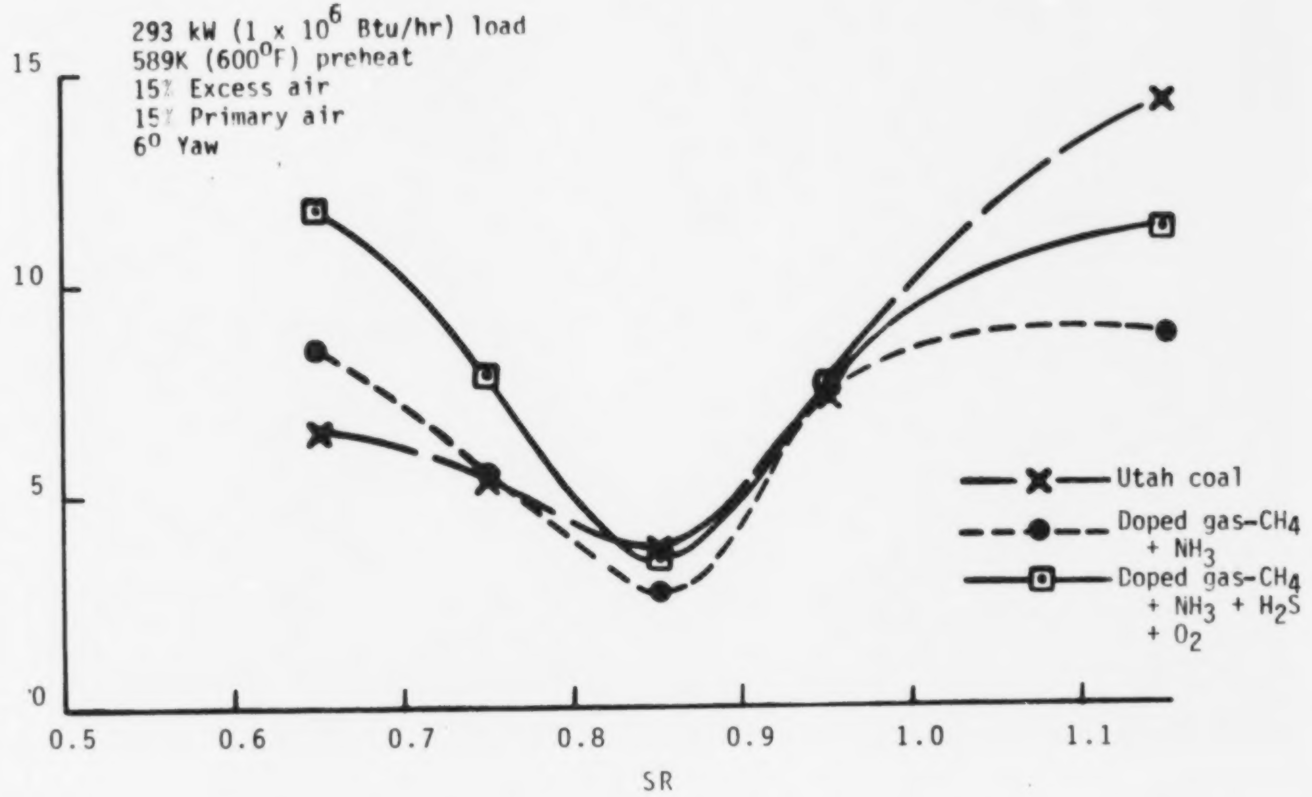

Figure 22. Fuel N conversion for coal and doped natural gas.

Under fuel-rich staged conditions, the effects of mixing become less important and the chemical effects of NO decay in the fuel-rich first stage and second-stage NO formation dominate the NO results. The coal NO results are equal to or lower than the doped gas results under rich conditions. It might be speculated that for coal combustion, the fuel components evolved during the volatile evolution process and the presence of the solids might be leading to the lower NO levels. As described earlier, the increase in NO as SR decreases below an SR of 0.8 is due to the formation of NH_3 and HCN type species in the first stage, which eventually get fractionally converted to NO in the second stage. In the case with coal, the presence of the hot solid particles might reduce these species to molecular nitrogen, or the coal-bound nitrogen might generate less NH_3 and HCN in the evolution process from the coal compared to doped gas, thereby leading to lower stack NO levels.

Some coal tests have shown that the rate at which the fuel nitrogen evolves relative to fuel components determines stack NO levels (Reference 21). For unstaged conditions, a coal in which the fuel nitrogen was delayed from volatilizing relative to the fuel would be beneficial to NO formation. This is because the oxygen mixing into the fuel jet would be consumed by the fuel components, leaving a greater percentage of the fuel nitrogen unoxidized. However, under staged combustion conditions, the delayed fuel nitrogen evolution from the coal would limit the time available for NO decay in the fuel-rich first stage. This could result in less effective NO control by staging. The high and low fuel nitrogen conversion for unstaged and staged Utah coal combustion respectively suggests that this fuel might have an easily volatilized fuel nitrogen component.

In summary, compared to doped gas, coal gives higher conversion of fuel-bound nitrogen under unstaged conditions, comparable results for moderate staging, and less conversion under extreme staging. These results show that coal NO formation is responsive to staged combustion, even at very low SR. Comparison of the doped gas and coal results shows this is due to the coal's detailed structure rather than to its elemental composition.

Figure 23 compares, on a percent conversion basis, the doped gas, doped-gas-plus-char, and coal results. All of these fuels have the same weight percent N, S, and O content. Under lean conditions, char-plus-doped gas has the maximum, coal the intermediate, and doped gas the lowest percent conversion. Under moderate staging, all of the results are comparable to within 1 percent conversion. Under extreme staging, the char produces the lowest conversion, and the doped gas the highest conversion.

As we progress from doped gas to doped-gas-plus-char to coal, the reaction rate of the fuel versus the rate of combustion air mixing decreases. In the case of gas, the fuel is immediately available, and burning and reaction are very rapid. With gas and char, the gas fraction is immediately available for reaction, but the char must be heated and ignited, and oxygen must diffuse to the char particle surface. In the case of coal, the coal particle must be heated before any fuel is available to the oxygen. Therefore, under lean conditions, significant O_2 will mix into the coal fuel jet prior to ignition, so combustion will be more premixed in this case than

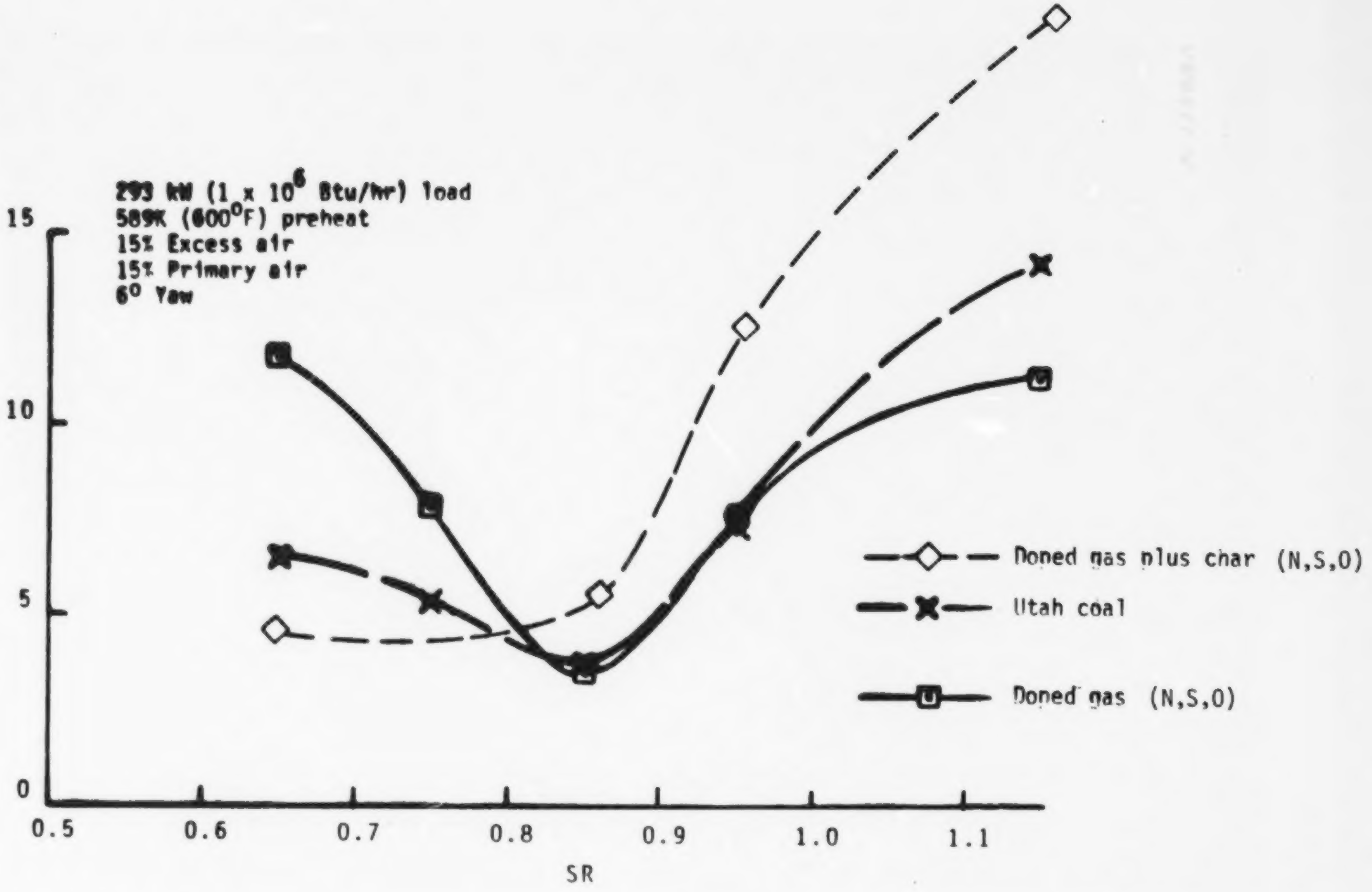

Figure 23. Fuel N conversion for coal, char-plus-doped-gas, and doped natural gas.

with doped gas. Premixing can lead to the observed higher NO for the coal and doped-gas-plus-char cases during unstaged combustion.

As the first-stage stoichiometric ratio decreases, the mixing or premixing processes become less important (Reference 9) and the NO results become dominated by the chemical reactions controlling the decay of NO. Under the extreme staging conditions, the char might be either preventing the formation or reducing NH_3 and HCN species. As previously shown (Reference 22), these species are NO precursors and are responsible for the increase in NO observed under extreme staged combustion conditions. If these are limited by the presence of the solids then the NO would be reduced for coal and doped-gas-plus-char combustion relative to the doped gas case.

The ability of the solids to reduce NH_3 type species was supported to some extent by tests in which NH_3 was added to the coal fuel jet. Figure 24 shows that adding a significant amount of NH_3 to the fuel jet results in a negligible change in NO for staged combustion and only a small increase for unstaged conditions. The same experiment with doped natural gas fuel showed an increase in NO for both staged and unstaged conditions.

These results indicate that NH_3 is prevented from forming NO in coal flames, possibly due to the presence of the char particles. This is especially true in staged combustion. This might be the reason why the NO under extreme staged conditions is lower for the coal and char cases.

The case of intermediate staging where the coal, doped gas, and doped-gas-plus-char results are comparable probably represents a balancing of the detrimental effect of premixing against the beneficial effect of the presence of the solid.

In summary the doped gas, doped-gas-plus-char and coal fuels, all with identical N, S and O fuel weight percents, gave significantly different NO levels under unstaged and extreme staged combustion conditions. The fuels with solids gave lower NO under extreme staged conditions, and higher NO under unstaged combustion conditions. At moderate staging conditions all NO results agree.

These tests showed that the weight percent of N, S, and O elements in the fuel do not alone determine the NO levels. Fuel structure, which impacts the volatiles evolution rate and char formation, and possibly the detailed species structures evolved from the coal, might be more important to NO formation than weight percent of N, S, and O elements in the coal.

These tests showed that the coal volatiles evolution process is important to NO formation. For the tangentially fired system, the simulated "instantly devolatilized" doped gas fuel had lower NO levels than the coal under unstaged combustion conditions. The coal fuel, which required time for volatiles evolution, had more oxygen mixed with the fuel prior to ignition and thereby higher NO levels. Another example of the detrimental effect of premixing was the char-plus-oxygen-doping NO results, which had the highest NO of all the cases tested. Flame observation for this case showed a significant degree of flame standoff from the burner face and therefore significant

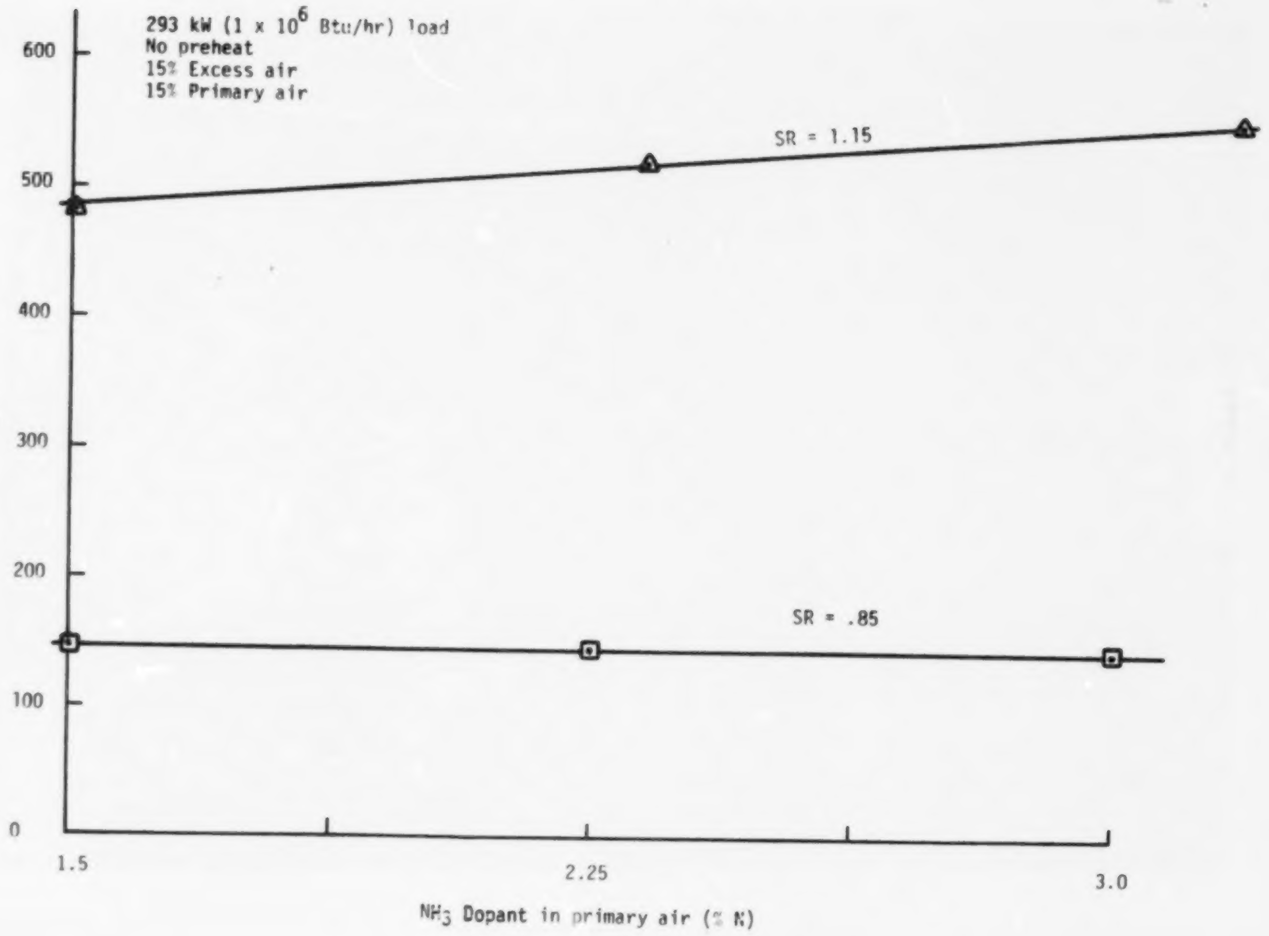

Figure 24. Variation of coal-fired NO with NH_3 dopant.

premixing prior to ignition. For the slow-mix diffusion flame conditions of the tangentially fired system, minimizing premixing of the fuel and air is beneficial to NO formation.

Under extreme staged conditions, the conversion rate of the coal and char-plus-doped gas fuels was smaller than the doped gas case. Tests of coal fuel doped with NH_3 showed that the potential for the NH_3 to form NO is reduced for the case with solids present compared to the doped gas case. Since under extreme staging conditions the concentrations of the NO precursors, NH_3, and HCN, are significant in the first stage, the presence of the solid might help limit NO formation through reduction of these precursors. As shown, the coal fuel is much more responsive to NO control under extreme staged conditions than is the doped gas.

Test results showed that char NO formation is sensitive to fuel/air premixing. As in coal combustion, initial fuel/air contacting influences char NO_x formation. Since coal volatile combustion influences the amount of oxygen reaching the char formed from the coal, char-only combustion is not a good simulation of coal char NO_x formation. A closer, but not perfect simulation, would be the char-plus-gas combustion case. Results of these tests showed that char NO_x formation is less than volatile NO_x formation.

The N content of the fuel is a significant contributor to NO with the fuel N,S and fuel N,O interactions playing only a minor role in NO formation. In the tangentially fired system, the major fraction of the NO comes from the fuel-bound nitrogen with thermal NO_x playing a secondary role.

4.2 THERMAL EFFECTS TESTS

The purpose of these tests was to define the influence of temperature on staged and unstaged NO emissions from coal-fired tangential systems.

Prior staged and unstaged coal-fired tangential system tests had shown that NO emissions were not strongly influenced by modest temperature variations (Reference 9). The changes in NO with temperature in these tests could be primarily associated with changes in thermal NO formation (Reference 9). Testing at Babcock and Wilcox showed that substantial reductions in temperature could significantly reduce NO formation (Reference 24) for a staged, front-wall-fired burner system. The tests performed in this task explored the benefit of significant temperature reductions on NO formation in tangentially fired systems. As in the normal temperature condition tests, coal, gas, doped gas, gas-plus-char, and doped-gas-plus-char were tested. Through the use of these fuels, thermal, volatile, and char NO_x components were approximately modeled under low-temperature combustion conditions.

4.2.1 Low-Temperature Coal NO_x Formation

The purpose of these tests was to determine the benefit of significantly lower combustion temperatures on NO formation in coal-fired tangential systems.

In the tests performed by Johnson, active first-stage cooling and/or significant flue gas recirculation were used to reduce second-stage flame temperatures to the range 1089 K (1500°F) to 1478 K (2200°F) (Reference 24). To achieve a similar range of temperatures in the tangentially fired pilot-scale tests, water-cooled tubes were placed along all four furnace walls in a serpentine fashion as shown in Figure 25. These tubes remove roughly 40 percent of the heat release uniformly around the periphery of the firebox. This heat removal is in addition to the roughly 30 percent typical heat removal in the radiant section of the furnace. This active cooling heat removal rate is the maximum achievable with clean tube surfaces. During coal combustion, as the cooling tubes build up ash deposits the heat removal decreases and firebox gas temperatures rise. This is shown in Figure 26, where gas and wall temperatures rise over a period of 9 hours due to cooling tube ash deposition during coal combustion. The locations of the bare thermocouples used to measure the temperatures presented in Figure 26 are given in Figure 27. It is estimated that the bare thermocouples in the gas stream read a few hundred degrees below the actual gas temperature, due to radiative heat loss to the cooler furnace walls. However, even though in error on an absolute basis, these temperature measurements are useful for indicating relative changes of gas temperatures in the firebox. The wall temperature thermocouple was embedded 0.025m (1 in.) from the inside firebox surface.

Referring to Figure 26, both staged and unstaged conditions were tested over the 9-hour test period. Some temperatures are sensitive to flame patterns and staging, such as T_{24}, which is in the firebox. Firebox wall and heat exchange tower temperatures are less influenced by flame results and show a consistent increase of average temperature with time.

Through the use of this active cooling and the slow degradation of the cooling rate with time due to deposition, temperature regimes similar to Johnson's were tested. Staged and unstaged test results at low temperatures and several SR's are shown in Figure 28. The NO results for these cold conditions are much lower than the hot results presented in Figure 19. The sequence in which these data were taken is indicated on the figure along with the general test conditions. As testing proceeded, the amount of heat removal extracted by the cooling tubes in the first stage decreased. Therefore, each data point should have an increase of NO over the prior point, due to increasing gas temperature. This change is in addition to the effect of SR changes. Conditions 6 and 7 represent hotter conditions than 1 and 2, due to the change in heat removal as indicated on the figure. Comparison of conditions 1 and 2 with 6 and 7 shows that, for unstaged conditions, NO increases significantly as temperature increases. Also, the shape of the NO curve with SR under cold conditions is similar to the hot NO results but appears to vary less with SR at high heat removal and thereby very low temperatures.

From Figure 28, a SR of 0.85 is optimal for NO_x reduction. Therefore, this condition was selected to define the effect of staged combustion NO_x formation at several firebox temperatures. The unstaged condition was also selected for extensive testing over a range of temperatures. NO_x formation for SR's between 0.85 and 1.15 was expected to

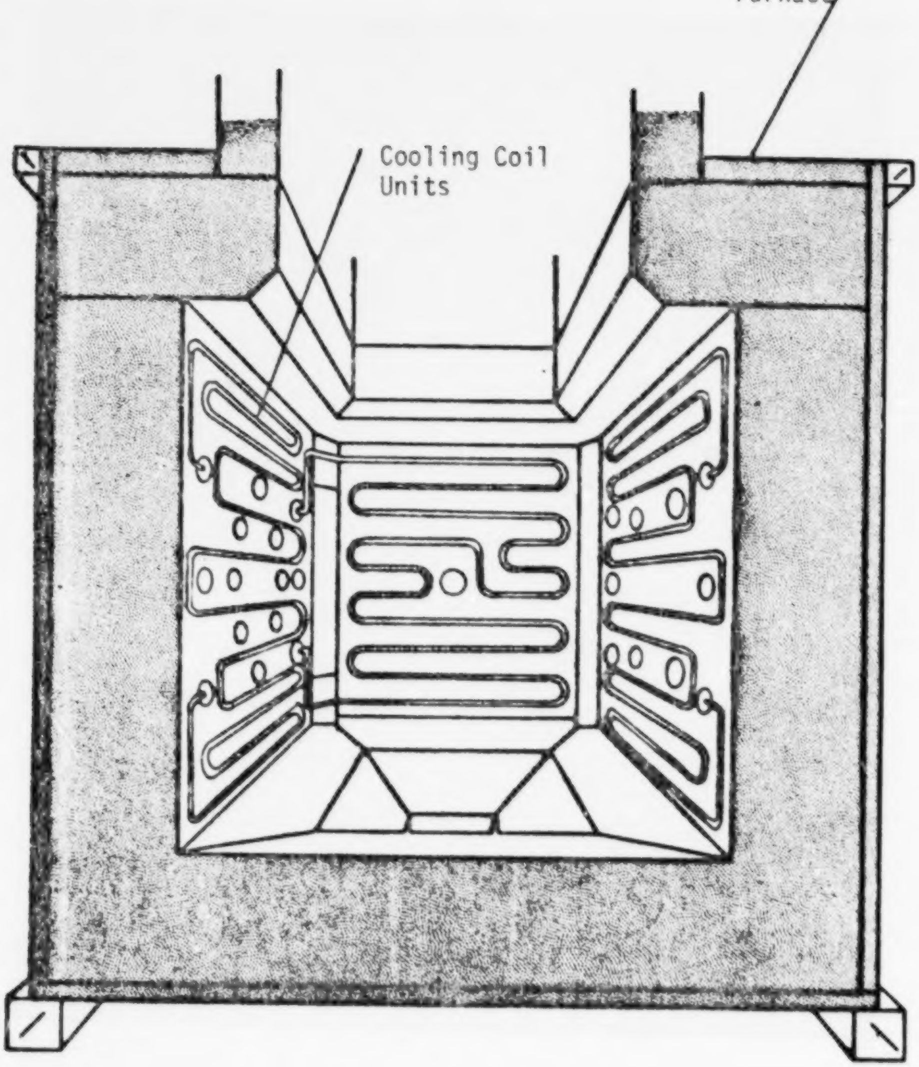
Furnace
Cooling Coil Units

Figure 25. Active furnace wall-cooling tubes.

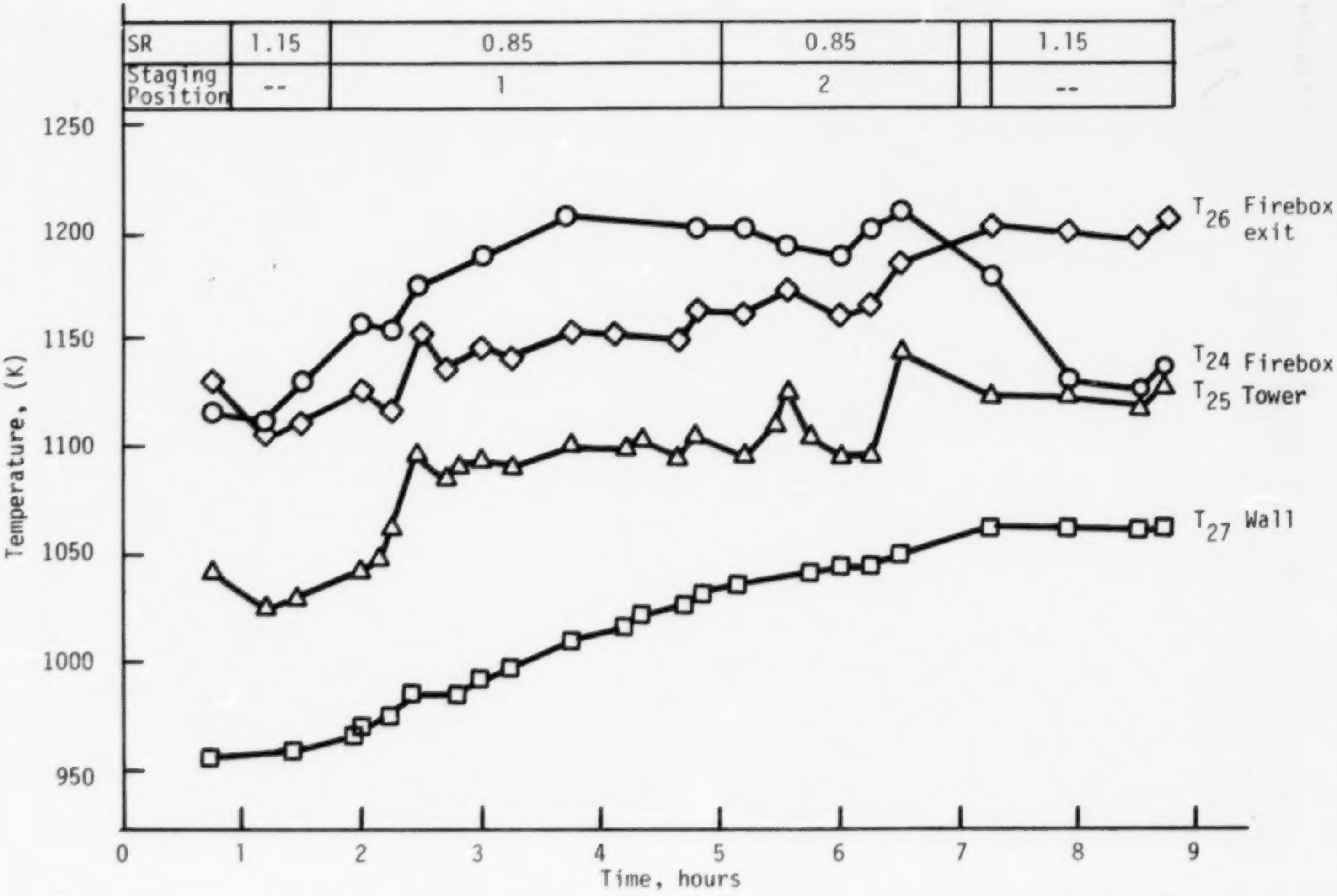

Figure 26. Variation of cold-wall gas and firebox temperatures with time.

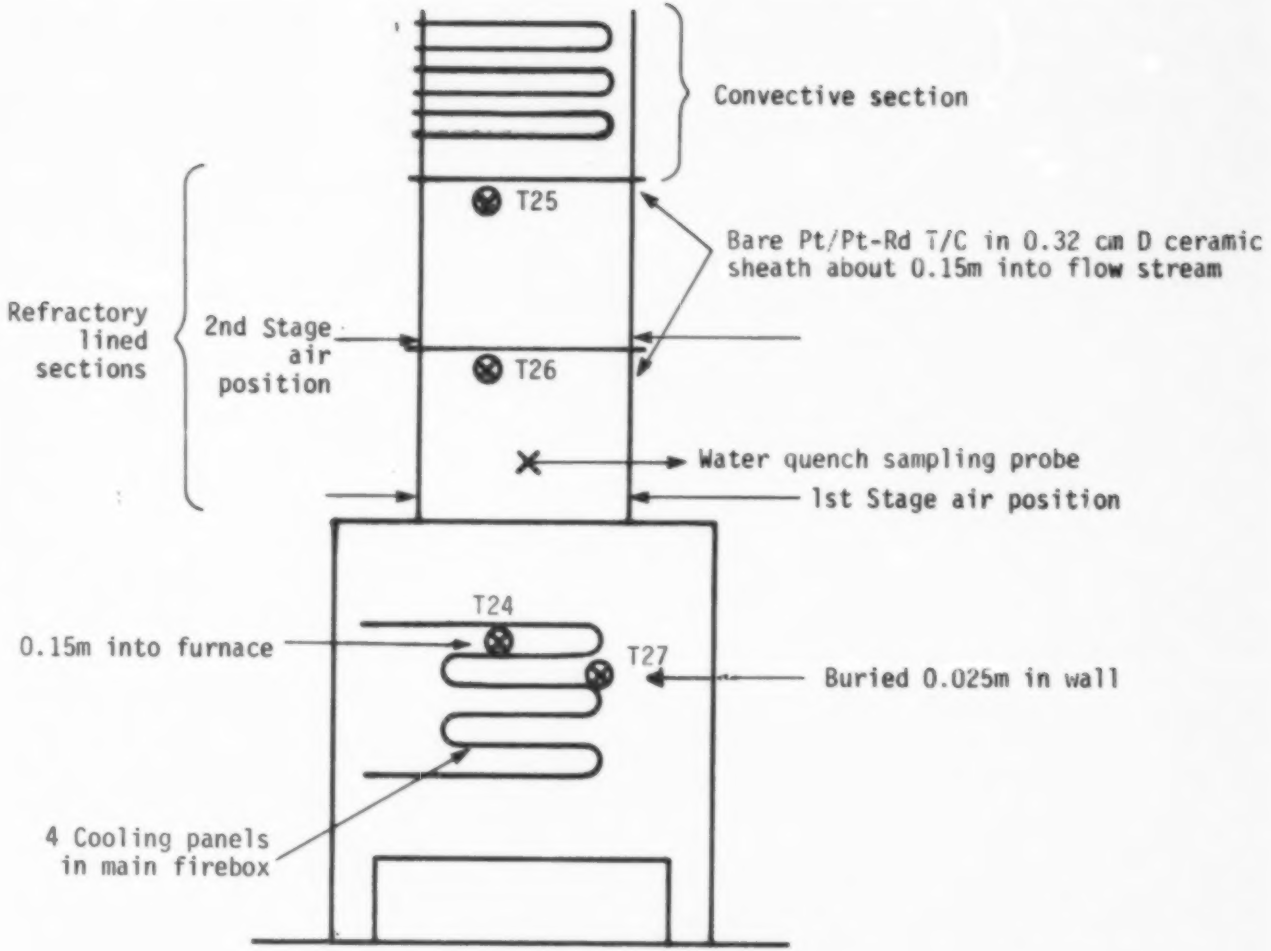
Convective section
T25
Bare Pt/Pt-Rd T/C in 0.32 cm D ceramic sheath about 0.15m into flow stream
Refractory lined sections
2nd Stage air position
T26
Water quench sampling probe
1st Stage air position
T24
0.15m into furnace
T27
Buried 0.025m in wall
4 Cooling panels in main firebox

Figure 27. Placement of main thermocouples in firebox and heat exchange tower.

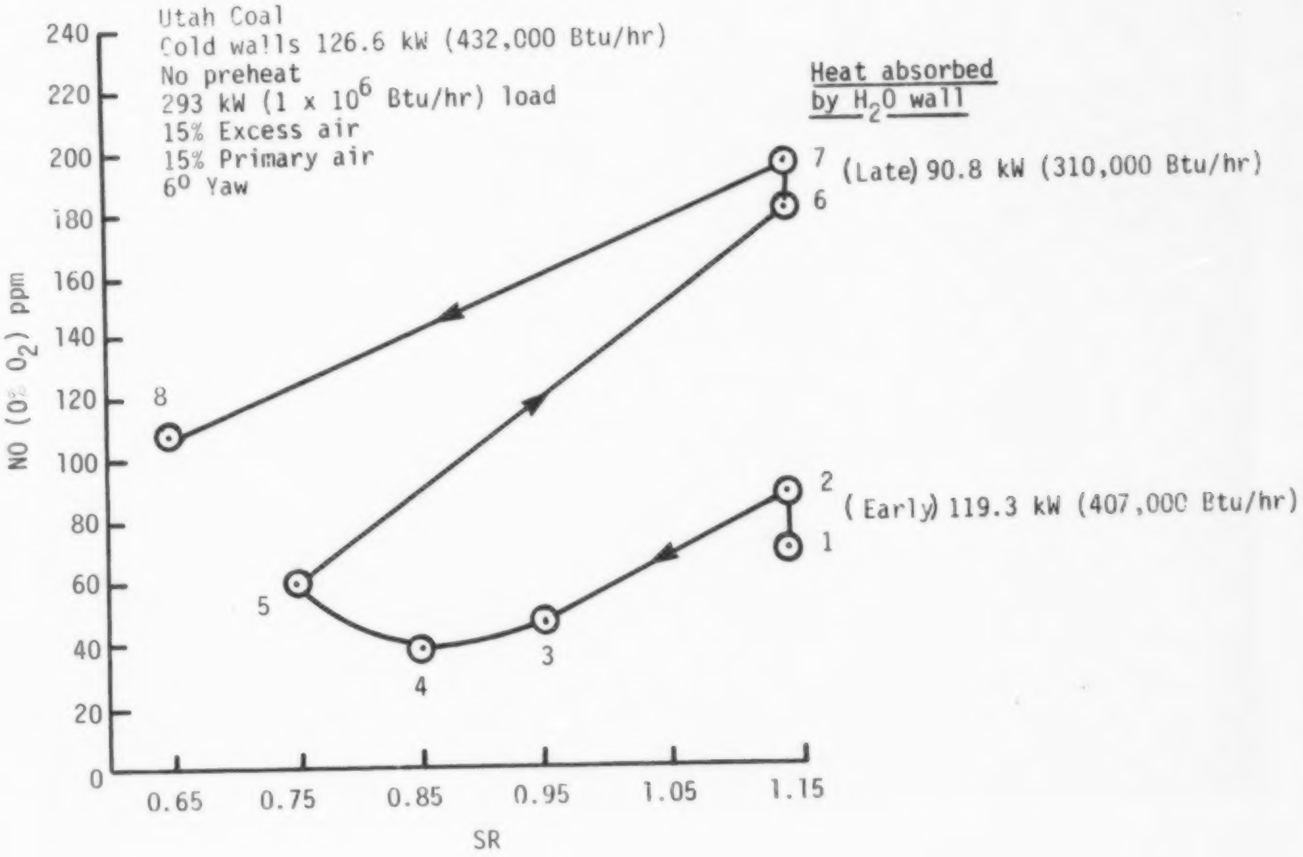

Figure 28. Effect of heat removal on staged NO.

fall between these two conditions. Figure 29 gives the 0.85 and 1.15 SR NO results as a function of first-stage wall temperature, T_{27}. As can be seen from the data, the active cooling results covered only a limited range of low temperatures, separated by a gap until the nonactively cooled results, reported in the last section, are reached. Because of the limited temperature variation data under the nonactively cooled conditions, the variation of NO with temperature under these conditions was not determined. Prior testing experience on different coals in this same system indicates that the variation of NO in this region with temperature is not significant and can be mainly associated with thermal NO_x (Reference 9).

From Figure 29 it is clear that there is a significant decrease of NO as wall temperature is reduced below 1089 K (1500°F) for the unstaged coal case. Extremely low levels of NO are achieved at around 950 K (1250°F) wall temperature. This corresponds to firebox exit and heat exchanger tower gas temperatures of approximately 1117 K (1550°F) and 1033 K (1400°F), respectively.

The staged results at a SR of 0.85 reach similar NO levels at these low temperatures. The correspondence of the SR of 0.85 and 1.15 results at a wall temperature of 950 K (1250°F) suggests that the NO versus SR curve is essentially flat at this temperature. At higher temperatures, the staged NO results are much lower than the unstaged results and are less sensitive to temperature. As can be seen in Figure 29, a straight line of small slope seems to represent the staged data over the complete temperature range.

In Figure 30, the SR of 0.85 and 1.15 NO results presented in Figure 29 are plotted as NO versus the inverse of tower gas temperature, T_{26}. Also included on this plot are the equilibrium NO curve, and Johnson's data (Reference 24) taken with Pittsburgh coal. Normal boiler combustion conditions are denoted by a temperature range on the side of the figure. The SR of 0.85 curve appears to be well defined by a straight line parallel to the Johnson results. All results seem to be strongly influenced by temperature. The linear behavior of these results on this plot yields an activation energy form for the NO process which has an energy of approximately 12 kilocalories/gm. Johnson's results, also obtained with a fuel-rich first stage, have a similar activation energy.

The displacement of the SR of 0.85 and Johnson's curve is probably due more to temperature definition than actual superiority of the tangentially fired results over the front-wall-fired results. To correlate his data, Johnson used a second-stage "flame front" temperature obtained by radially traversing the second-stage gases. The present data are correlated on a fully mixed gas temperature downstream of the staged air addition point. This temperature definition probably does not correspond to Johnson's temperature definition.

First- and second-stage mixing between present and Johnson's results was considerably different. The present results had a slow-mix first stage and rapid-mix second stage. Johnson's results had a rapid-mix first stage and a slow-mix second stage. The similarities in behavior with temperature of these results suggest that, at low temperature, the NO process is not

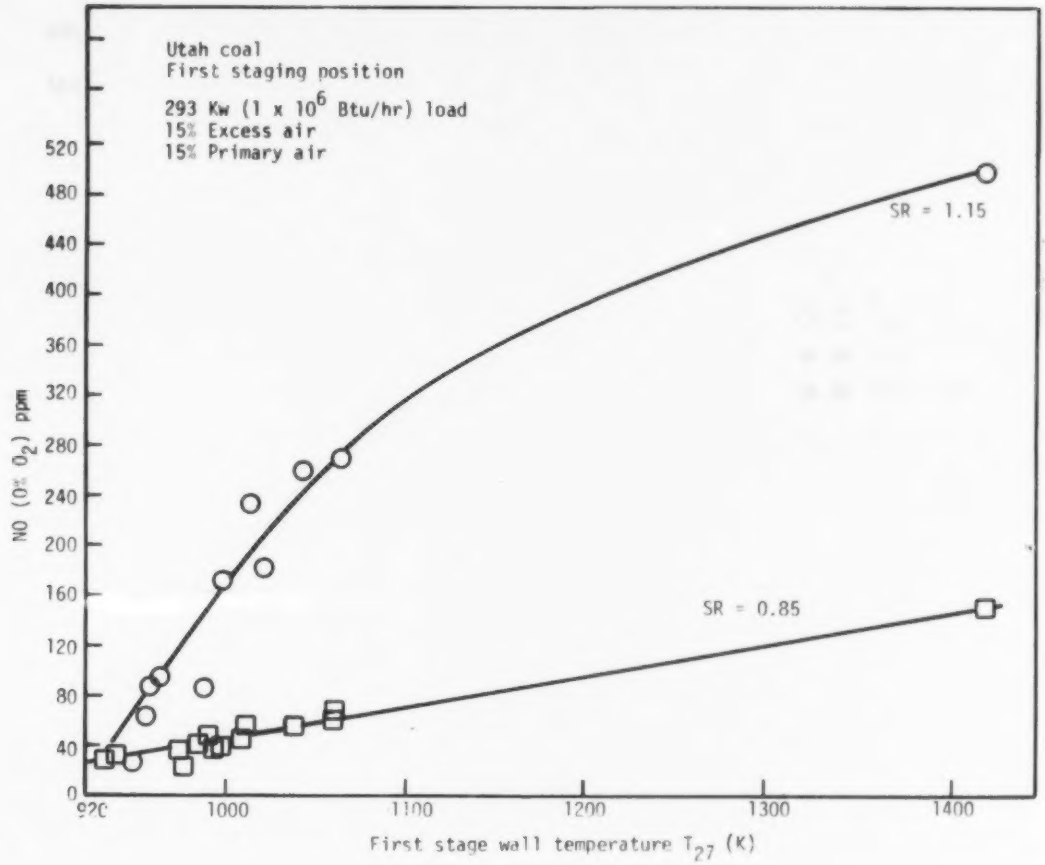

Figure 29. Coal NO variation with temperature.

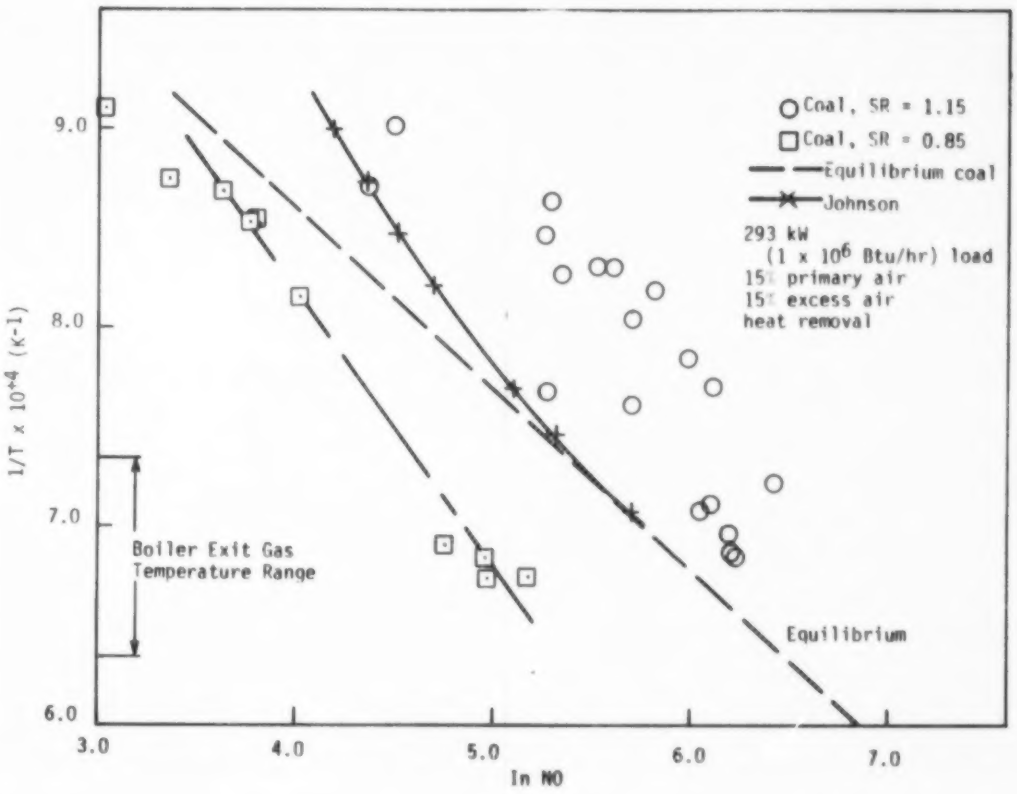

Figure 30. Variation of NO with temperature.

dominated by either first- or second-stage mixing. This hypothesis is consistent with normal temperature condition results found in earlier testing (Reference 9).

Johnson has suggested that the low-NO phenomena might be related to an equilibration of combustion products in the second-stage flame front (Reference 24). The correspondence of his results and the equilibrium line over a limited temperature regime supports this hypothesis to some extent. However, the tangentially fired results fall either below or above the equilibrium line, depending on whether the first stage SR is either 0.85 or 1.15. The influence of the tangentially fired results on first-stage SR suggests that the process is not a true equilibrium process, which would be fully independent of first-stage conditions.

As shown, at extremely low temperatures, NO levels become insensitive to SR. At these conditions, the SR of 0.85 and 1.15 results are converging on the equilibrium results. For these conditions, equilibrium might be occurring. However, insufficient data are available to confirm the existence of equilibration at these extreme conditions.

In addition to measuring the stack gas and particulate concentrations, firebox exit conditions were measured in some cases with the water quench sampling probe for both staged (SR = 0.85) and unstaged (SR = 1.15) conditions. Figure 31 shows both firebox exit and stack NO levels as a function of firebox wall temperature. These results show that under staged conditions there is a significant reduction of NO in the second stage under cold conditions. As temperature rises, the reduction of NO in the second stage decreases. The change in firebox exit NO with temperature is not as significant as the change in stack NO with temperature. Therefore, second-stage NO reduction is the dominant factor in low NO at low temperatures.

As seen in Figure 31, unstaged firebox exit and stack NO levels increase more rapidly with temperature than the staged results. Also, firebox exit and stack NO results for the unstaged results are fairly close together over the full temperature range tested. Therefore, whatever NO limiting process is occurring for the unstaged case must be occurring in the first, as well as the second stage.

4.2.2 Low Temperature Gas, Doped Gas, and Char NO_x Formation

The purpose of these tests was to define the relative importance of fuel chemical and physical processes on NO formation under low-temperature combustion conditions. By utilizing gas, doped gas, and char, alone and in combination, the effect of low-temperature combustion conditions on thermal, fuel nitrogen, volatile, and char NO could be approximated.

Figure 32 gives the gas and doped gas NO results for a range of SR's at low temperature. General test conditions, as given on Figure 32, correspond with the normal temperature gas and doped gas tests reported in Section 4.1.2. Wall temperatures for this case were between 932 K (1217°F) and 957 K (1263°F). These temperatures are more than 556 K (1000°F) cooler than the normal combustion conditions reported in section 4.1.2. As shown in Figure 32,

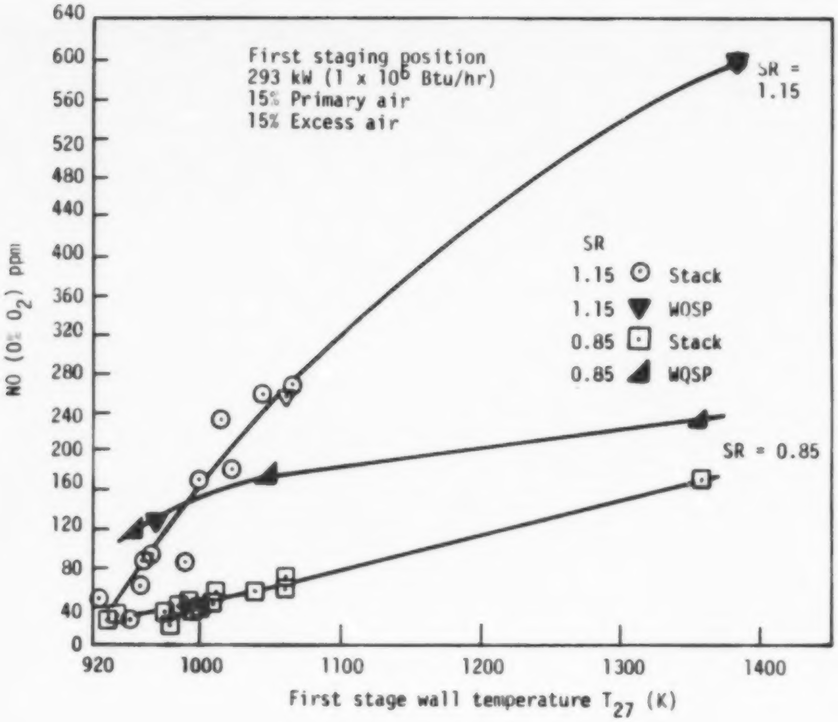

Figure 31. First stage exit and stack NO variation with temperature.

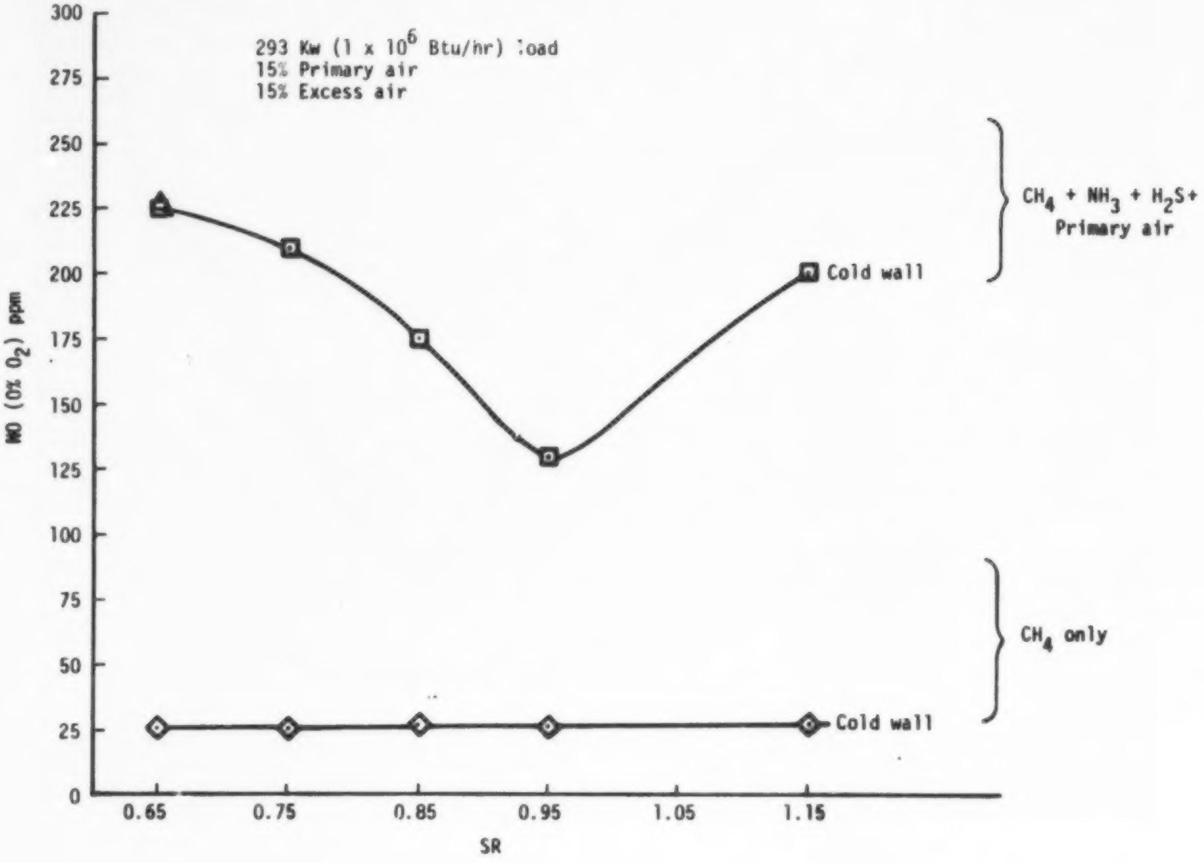

Figure 32. Cold-wall doped gas staged NO results.

gas-only NO results do not vary with SR and are just under 25 ppm. These very low NO levels should represent the thermal component of NO formation under these conditions.

At low temperatures, thermal NO is suppressed and the major portion of the NO produced may be "Prompt NO." This NO is formed in the oxygen deficient core of the fuel jet by attack of hydrocarbon fragments on molecular nitrogen. The resulting nitrogenous compounds generated in this process are eventually fractionally oxidized to NO. Prompt NO may represent the lower limit of NO formation for this system on gas.

The low-temperature doped gas NO results have a similar shape to the normal doped gas results. As in the normal condition case, fuel nitrogen, combined with other dopants, dominates NO formation. Even though the shapes of the NO curves are the same for the normal and low-temperature cases, significant differences in absolute NO levels exist. These differences are clearly shown in Figure 33, where the normal and low-temperature NO results are compared. At an SR of 1.15, under unstaged conditions, the low-temperature NO results are lower than the normal temperature NO results by roughly 50 ppm. This difference is roughly equivalent to the difference between the low and normal temperature gas only case. Therefore, it may be speculated that the difference in the doped gas cases might be reductions in thermal NO under low-temperature conditions.

Another interesting difference between the low and normal temperature cases is the higher minimum NO and the shift in minimum NO to higher SR for the low-temperature case. As discussed earlier, the dip in the NO curve with decreasing SR is due to NO decay in the first stage. Under low-temperature conditions the decay processes are slowed considerably, with the result that the minimum NO is higher and shifted toward higher SR.

As in some of the coal cases, the water quench sampling probe was used to measure NO, NH_3 and HCN concentrations at the firebox exit. The NO results at the firebox exit are compared to stack levels in Figure 34. In contrast to the coal results presented in section 4.2.1, the low-temperature gas results show that NO is formed in the second stage for both staged and unstaged conditions. In the coal tests, significant NO reduction occurred in the second stage for staged conditions and remained relatively unchanged for unstaged combustion conditions. Comparing absolute levels of coal (Figure 21) and doped gas NO levels (Figure 32) at low temperatures shows that the coal results are significantly lower than the gas results under staged and unstaged conditions. These differences in results, in comparing normal to low temperature doped gas and coal behavior, indicate that the NO mechanisms between the fuels are quite different.

Figure 35 gives the doped char and doped gas-plus-char NO results for a range of SR's under low-temperature conditions. Both stack and firebox exit conditions are given on the figure. The doped char tests consisted of doping the char with NH_3 and H_2S to the extent needed to bring the weight percent nitrogen and sulfur up to the coal levels. The general test conditions are the same as for the doped gas case and are given on the figure.

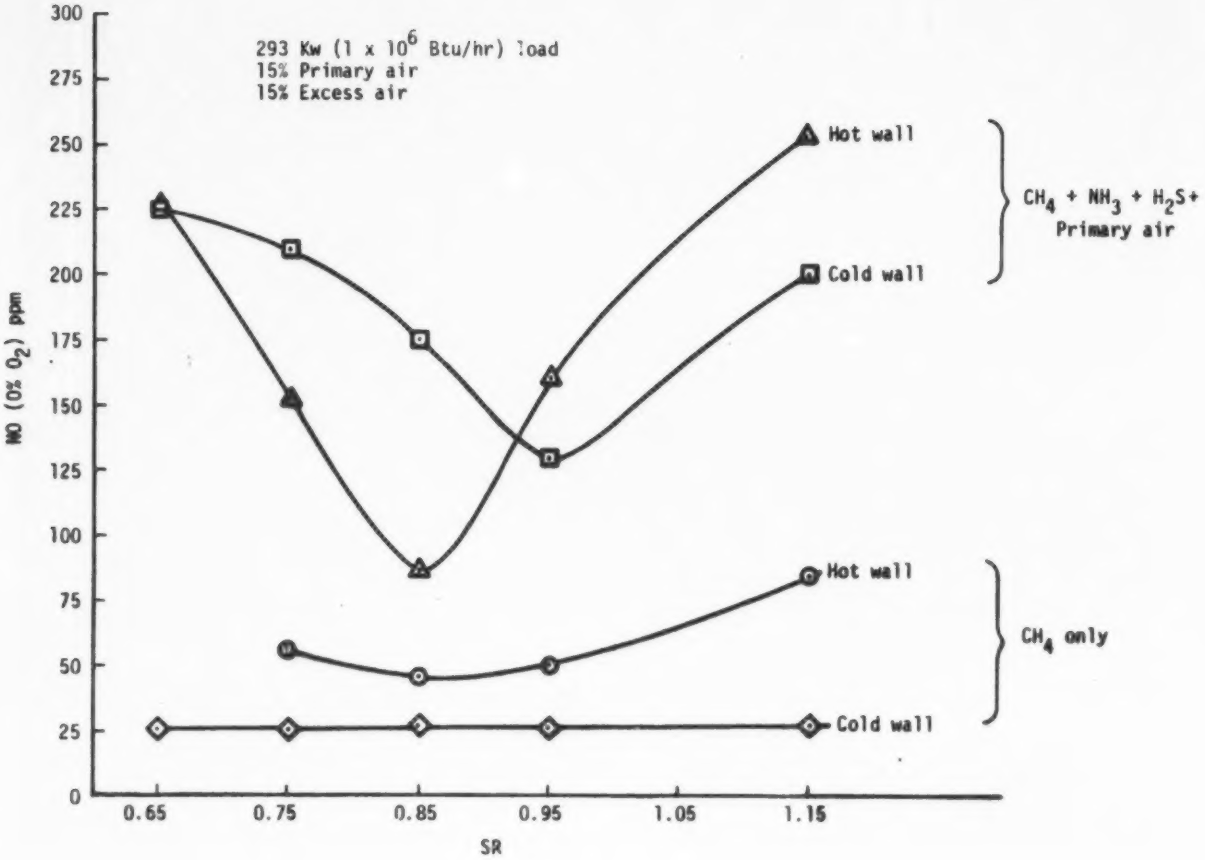

Figure 33. Comparison of cold- and hot-wall doped gas NO results with SR.

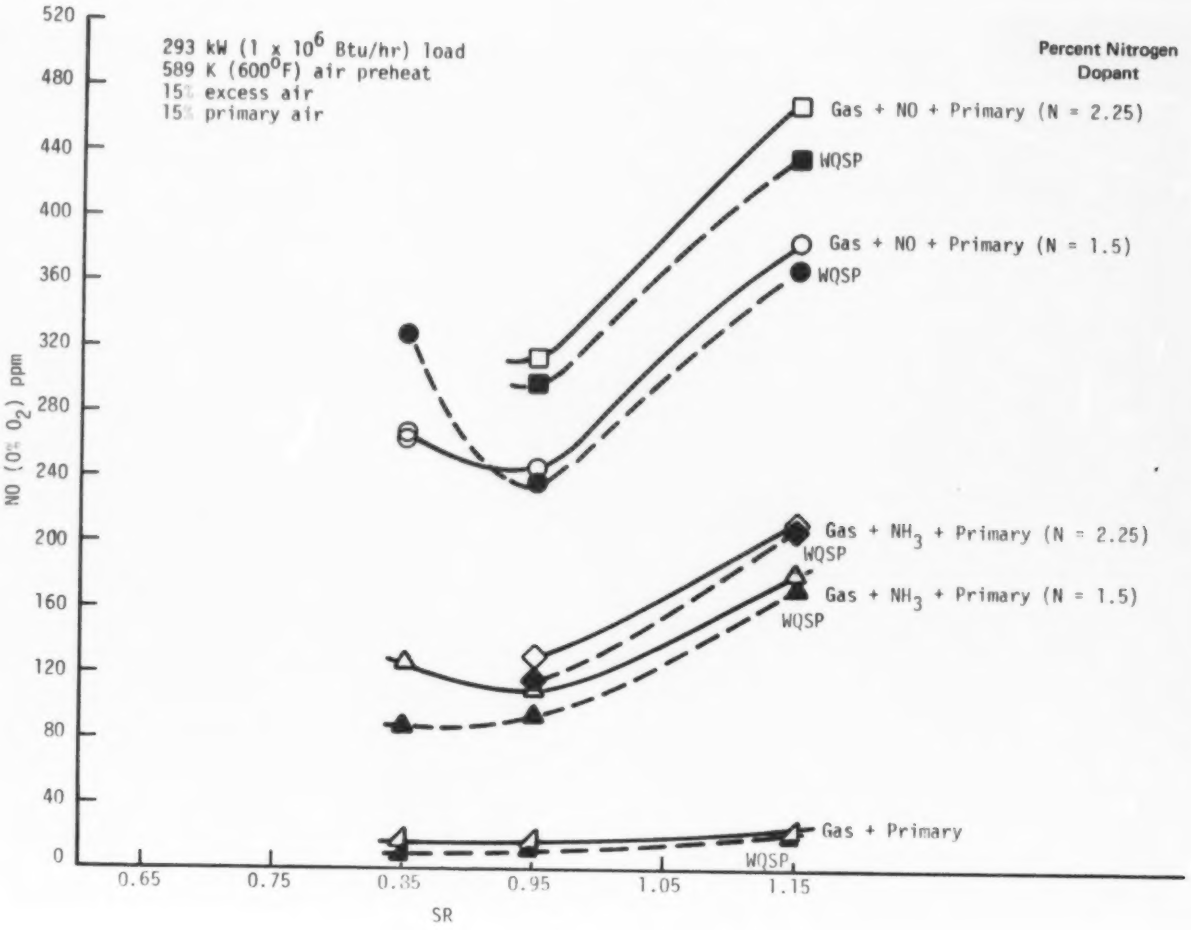

Figure 34. Effect of NH_3 dopant and SR.

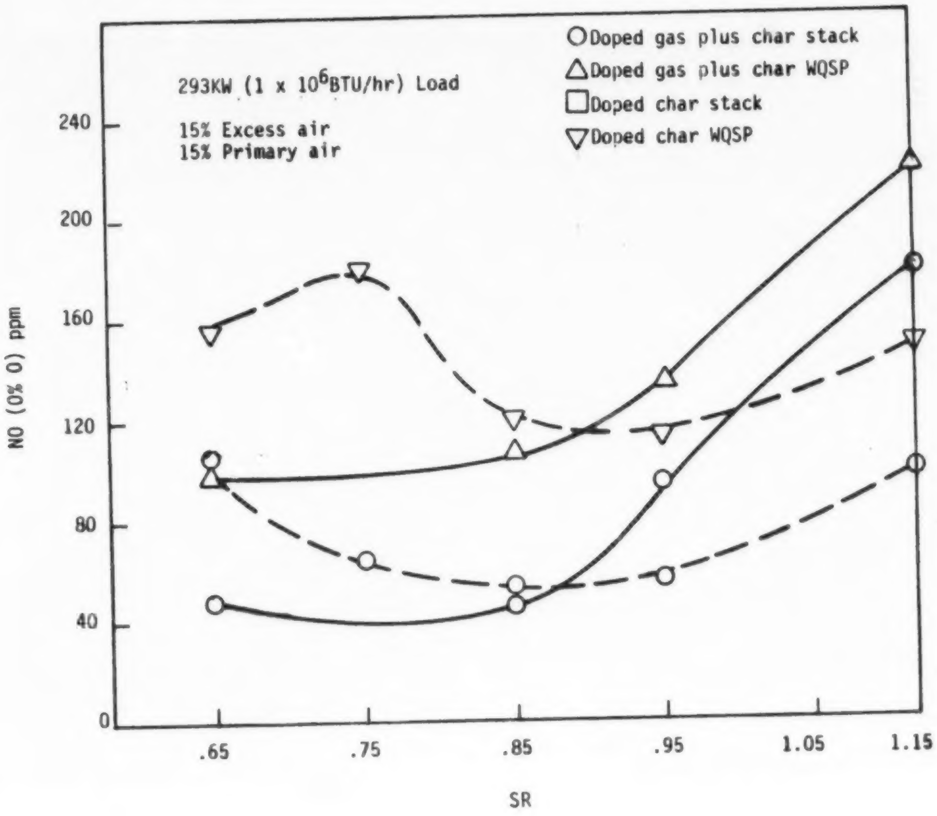

Figure 35. Cold-wall char and char-plus-doped-gas NO.

Wall temperatures for all of these low-temperature cases varied between 1095 K (1511°F) and 1064 K (1456°F). Absolute levels of NO from char with or without doped gas are very low, particularly for the staged combustion conditions. Char-plus-doped-gas gives lower NO than char alone at low SR and higher NO at high SR. Comparing the first-stage exit to stack NO levels, significant NO reduction in the second stage is experienced for both char-plus doped-gas and char alone. Both cases roughly achieve the same decrease in NO through the second stage, with the difference in stack NO due mainly to the difference in first-stage processes.

The very low levels of NO achieved by the char tests at low temperature are similar to the coal results. Also, as in coal combustion at low temperature, a significant amount of char exited the system unburnt. Considerable char deposits were found in the baghouse and ashpit upon system shutdown following the char tests. Quantitative carbon loss measurements were not made due to lack of available test time at low temperatures.

4.2.3 Comparison of Coal, Gas, Doped Gas, and Char NO Results at Low Temperature

Comparisons of the NO results in Figures 28, 32, and 35 show that, under low temperatures, coal and char, with or without doped gas, have very low NO levels compared to doped gas. This is clearly shown in Figure 36 where the char and coal NO results correspond, particularly the staged results. The doped gas NO results are much higher than the coal and char at low temperatures and lower at high temperatures. At low temperatures the mechanisms dominating NO are potentially different from the high temperature NO mechanisms.

The reduced levels of NO observed under low-temperature conditions for coal could be a result of homogeneous and heterogeneous NO reduction processes acting separately or in combination. As shown in section 4.1.3, combustion of the volatiles contributes most significantly to NO production. Through either direct oxidation to NO or generation of NH_3 and HCN species, which eventually get oxidized to NO, volatile combustion is the dominant NO formation process. Char and thermal NO production is less significant than volatile combustion NO. Acting along with NO production are NO reduction processes. NO can be reduced by reactions with hydrocarbon fuel fragments (Reference 25), NH_3 type species (Reference 26), and either direct reduction (Reference 27) or catalyzed reduction (Reference 28) on hot carbon surfaces. The balance between these production and reduction processes yields the overall NO level observed in the stack.

Data taken during these tests shed some light about which potential processes are strongly contributing to the lower coal NO emission levels at low temperatures.

Corresponding to the very low NO levels at reduced temperatures is the increase in carbon loss during coal combustion, as indicated in Figure 37. Carbon loss was measured from particulate samples taken immediately in front of the convective heat exchangers. As seen in Figure 37, up to 15 percent carbon loss was observed for staged combustion conditions at extremely low

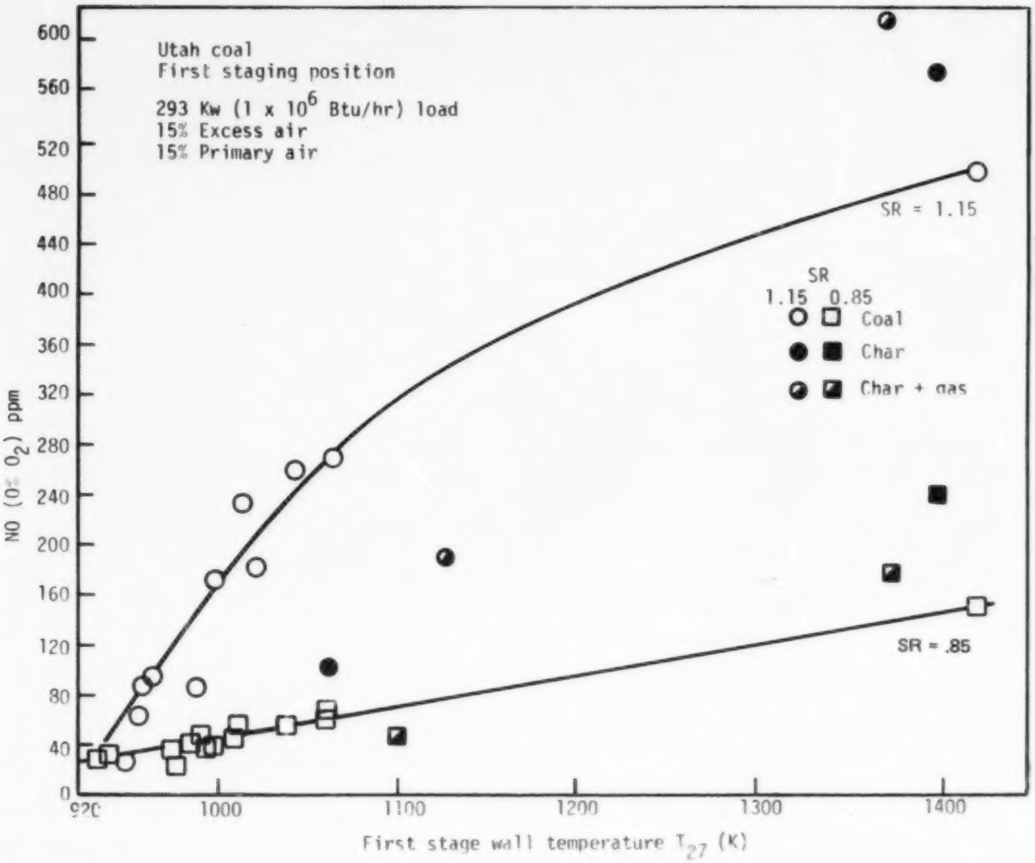

Figure 36. Effect of temperature on coal, char, and char-plus-gas NO.

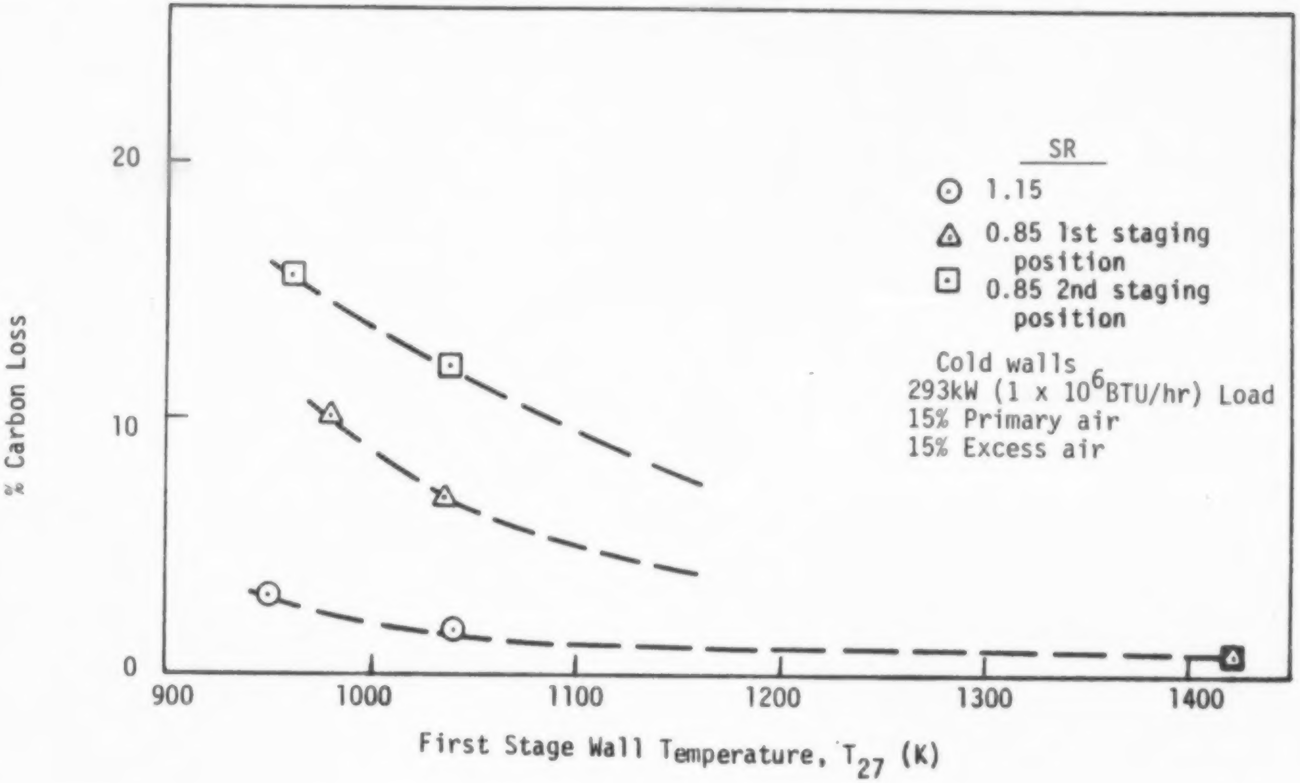

Figure 37. Carbon loss results.

temperatures. This occurred for the second staging position conditions. The first staging position conditions had a longer residence time under excess oxygen conditions and therefore better carbon burnup. Under the fuel-lean SR of 1.15 conditions, the maximum carbon loss measured was 3 percent. These high carbon-loss levels are in contrast to the less than 1 percent carbon loss under normal combustion conditions.

Since flue gas oxygen concentration was maintained constant for all temperatures, the firing rate was 293 kW (1×10^6 Btu/hr) independent of carbon loss for all cases. Therefore, as carbon loss increased, the percent of carbon present for a fixed firing rate increased.

As shown previously, carbon can reduce NO through either direct reaction (Reference 27) or by catalysis of CO and NO reduction reactions (Reference 28). The significant amount of carbon present under cold combustion conditions could have caused significant NO reduction in the system. Figure 38 gives the staged and unstaged low-temperature NO results as a function of the percent carbon loss. A close correlation between the different cases is not found for this limited amount of data. This indicates that other processes are influencing NO as well as the amount of carbon present. However, it is possible that the presence of considerable amounts of carbon can influence NO levels.

Figure 39 presents a theoretical estimate of the NO reduction potential of either soot or char carbon. Based on data in Reference 27, NO reduction by char increases as temperature rises. However, as given in Reference 29, the rate of char burnup increases even more strongly with temperature. Therefore, the best overall NO reduction by char occurs at low temperatures, as shown in Figure 39, where the char reduction is less rapid but the total surface area of carbon is large. This type of behavior can produce the NO results given in Figure 36.

Char and char-plus-doped gas combustion, in which a significant amount of solid carbon is present throughout the entire system, also exhibited low-NO levels and significant second-stage NO reduction. Char combustion gave the lowest NO levels under lean conditions and is the case which has the largest amount of solid carbon present. Doped gas combustion gave much higher NO results and showed an increase rather than a reduction in NO in the second stage under staged combustion. Comparison of these results shows that the presence of the solids is limiting NO emissions either by limiting production of NO or by reducing any NO that is formed.

Further insight into the role of particle processes is provided by comparing the normal and low-temperature in-firebox particulate sample analysis to the unburned coal's analysis in Table 6. The low-temperature particle sample analysis is the average of 14 samples taken in the stack and at the firebox exit for both staged and unstaged conditions. The deviation of this average sample from the mean is small, which justifies comparing the average to the unburned coal. These results show that, at low temperature, the particulates have weight percent nitrogen contents similar to the parent coal with less volatiles and a somewhat lower nitrogen-to-carbon ratio. Under normal combustion conditions, the weight percent nitrogen is reduced from the

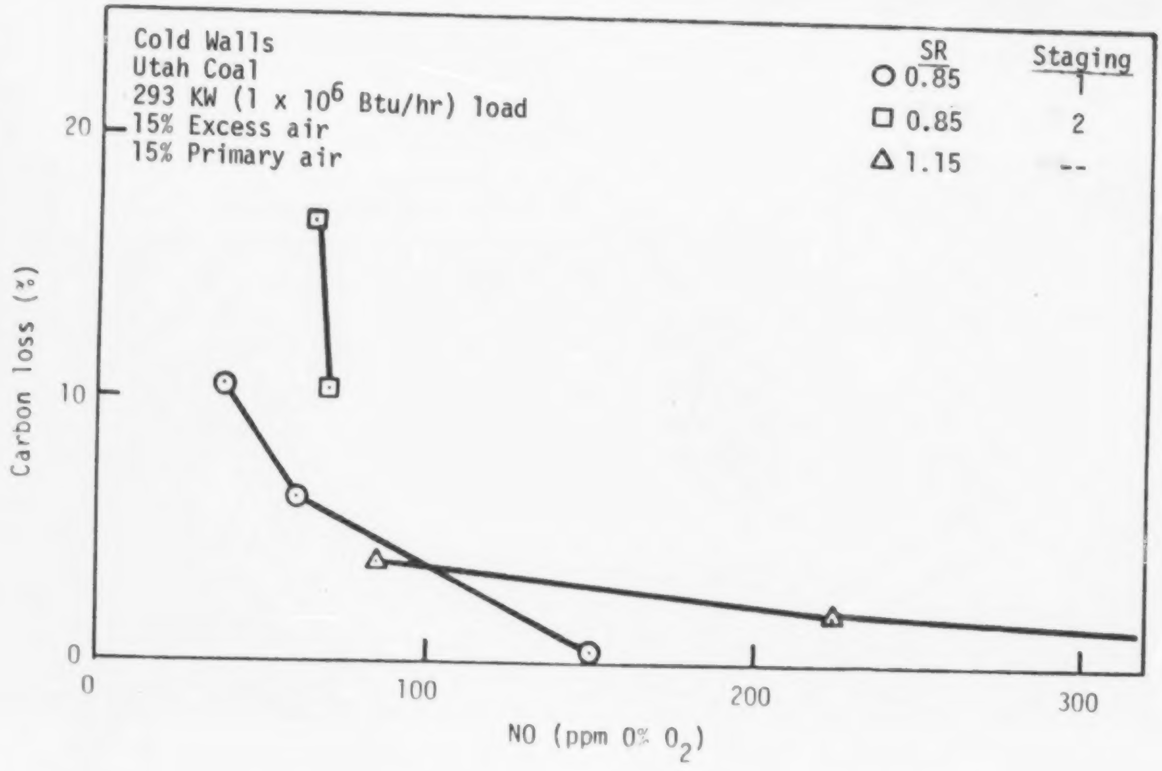

Figure 38. NO results versus percent carbon loss.

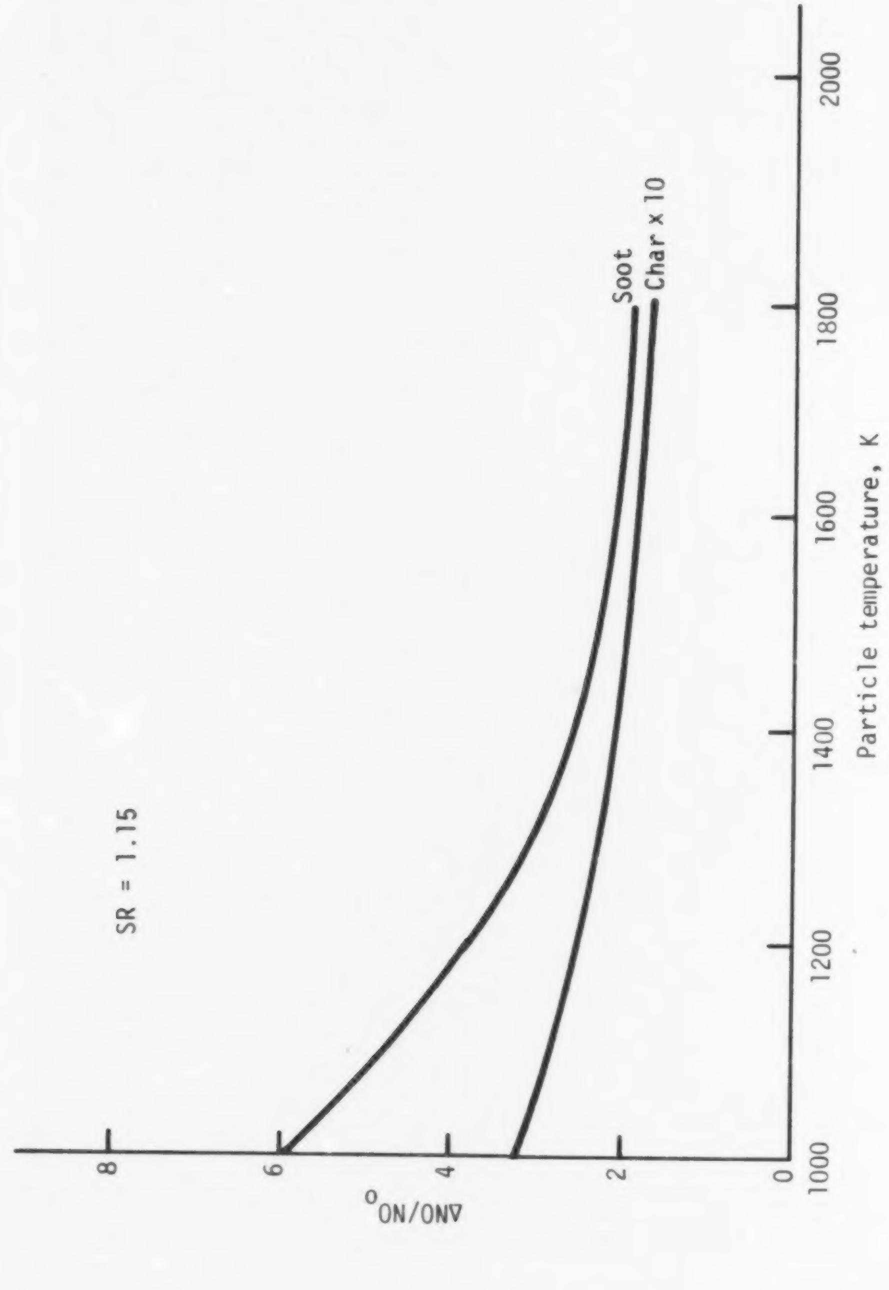

Figure 39. Char NO reduction versus temperature.

TABLE 6. PARTIALLY BURNT AND PARENT COAL PROPERTIES

	Percent		
	Base coal	Low-temperature partially burnt coal	High-temperature partially burnt coal
Volatiles	39	17	17
Nitrogen	1.5	1.44	0.99
Nitrogen/Carbon	0.019	0.015	0.012

parent and low-temperature condition cases and the nitrogen-to-carbon ratio is lower. This difference is especially significant since the normal temperature particulate samples were taken at a lower elevation in the firebox than the low-temperature samples and thus represent an earlier time particulate composition. These results suggest that, under cold conditions, the nitrogen bound to the fuel does not evolve as rapidly or as fully as the normal temperature case. As discussed earlier, volatile NO formation dominates NO production. Under low-temperature conditions, the reduction in fuel nitrogen volatilization lowers the volatile NO production and thereby possibly lowers NO. In addition, any NO formed can be potentially reduced by direct or catalyzed reaction with the significant amount of carbon present.

A further demonstration on the difference between coal and doped gas is provided by comparing Figures 40 and 41. These figures give the change in NO produced by adding significant NH_3 dopant to the coal and doped gas jet respectively. As in the normal temperature results, doping a coal jet with NH_3 produces negligible NO changes under staged conditions and moderate changes under unstaged conditions. NH_3 doping of the doped gas fuel shows an increase in NO for both staged and unstaged conditions. Apparently, the presence of the solids limits the amount of NH_3 which is converted to NO under staged combustion conditions. This could be another reason the coal NO results are lower than the doped gas results.

It appears clear that the presence of solid particles in coal and char combustion contributes significantly to the reduction in NO at low temperatures. The role of the gas phase processes is less clear.

As described, hydrocarbons in the combustion gases can reduce NO. However, reduction is only effective under fuel-rich conditions (Reference 25). Since both coal and char results have low levels of NO under fuel-lean as well as fuel-rich conditions, hydrocarbon NO reduction is probably not dominating NO formation.

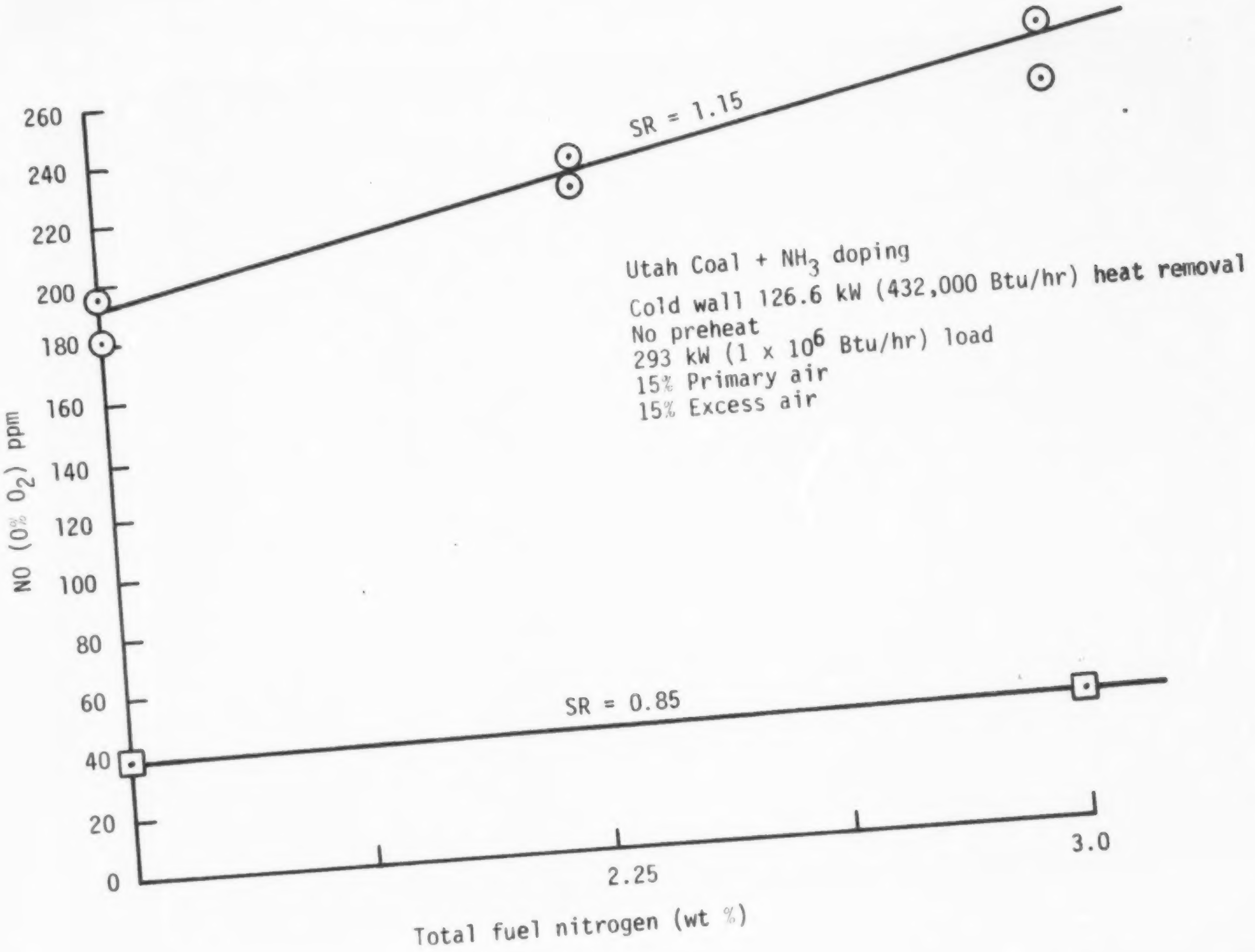

Figure 40. Effect of adding NH_3 to coal jet.

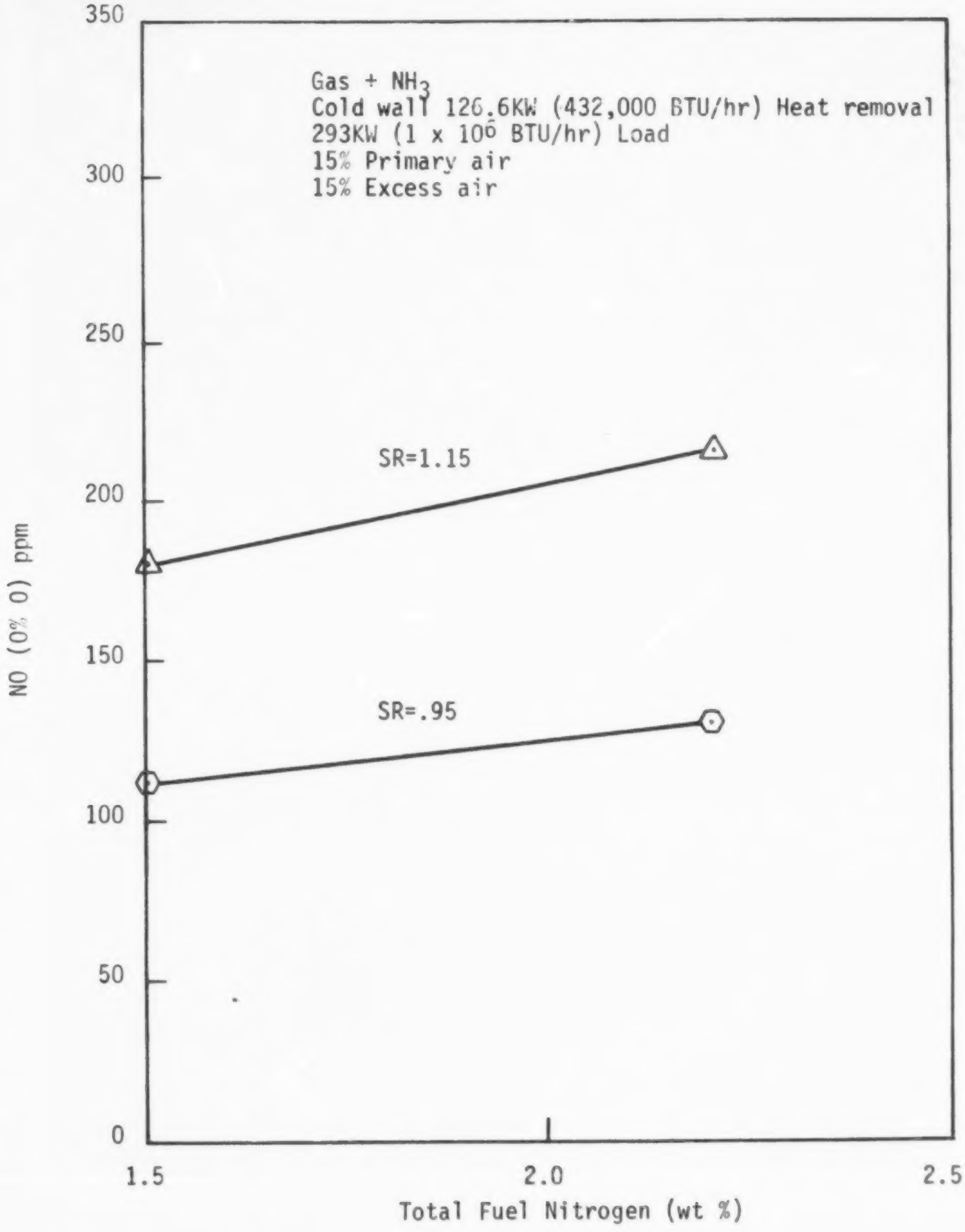

Figure 41. Effect of adding NH_3 to gas fuel jet.

Reduction by NH_3 might be possible under both fuel-rich and fuel-lean conditions (Reference 26). Table 7 gives the NH_3 and HCN first-stage exit and stack concentrations for coal and doped gas results. As can be seen in this table, the concentrations of NH_3 for coal combustion are low and somewhat higher than the gas results. Because they are low, it is expected that NH_3 would not play a significant role in NO reduction. This is further supported by the fact that very significant second-stage reductions in NO are found for coal whereas no reductions are observed for gas.

In summary, under low-temperature conditions, coal and char can have NO levels in the range of 50 ppm (at 0 percent O_2). Under staged combustion conditions, significant NO reduction takes place in the second stage to yield very low NO levels. For unstaged conditions, the NO limiting process occurs in the first stage. Up to 15 and 3 percent carbon carryover is obtained for the low-temperature staged and unstaged results, respectively. These levels are excessive compared to normal temperature carbon losses of less than 1 percent.

Through comparison of coal, char, and doped gas test results, particle processes seem to play an important role in limiting NO at low-temperature combustion conditions. This is supported by: (1) particle analysis tests which showed a reduction in fuel nitrogen evolution from the coal at low temperatures, (2) NO correlation with carbon loss and a theoretical estimate of NO/char reduction potential with temperature, and (3) reduced NH_3 (a NO precursor species) dopant conversion to NO in coal combustion.

TABLE 7. LOW TEMPERATURE NITROGENOUS SPECIES MEASUREMENTS

		Utah coal				Doped gas	
		WQSP-1st stage exit (ppm)		Stack (ppm)		WQSP-1st stage exit (ppm)	
SR	Staging position	NH_3	HCN	NH_3	HCN	NH_3	HCN
0.85	1st	2-8	20-300	3.2	1.7		
0.85	2nd	19-37	45-500[a]	3.0	1.5		
1.15		23-24	20-40	2.1	5.1		
0.95	2nd					3.3	35

[a]Estimated based on impinger catch

Lastly, thermal NO at low temperatures is below 25 ppm (0 percent O_2), and can probably be associated with "Prompt NO" produced in the fuel jet.

4.3 BURNER JET AND VORTEX CHARACTERIZATION TESTS

The objective of these tests was to define regions in tangentially fired systems where the primary NO_x formation/reduction processes are occurring. In particular, the tests determined the relative importance of near burner mixing, burner jet/vortex interaction, and vortex zones to NO_x formation/reduction. These zones were described in section 1.

To define important NO_x zones during conventional tangential firing, in-flame gas and solid samples were taken in the firebox with a water-quenched sampling probe. Once important firebox zones were defined, NO was then injected into these zones to determine the NO_x reduction potential of these zones. Finally, burner yaw angles and biasing were varied to determine the influence of these major design variables on NO_x. The following sections describe the testing procedures and the results in detail.

4.3.1 In-Flame Probing

During these tests, the facility was operated at baseline conditions identical to those employed for the tests presented in Figures 18 and 19. Using the water-quenched sampling probe described in Section 2, in-flame gas and solid samples were taken at a variety of firebox locations to determine the relative importance of near burner mixing, burner jet/vortex interaction, and vortex zones on NO_x processes. A limited number of sampling locations above, at, and below the fuel entry elevation were chosen to characterize these zones. Figure 42 shows a side view of the arrangement of sampling ports relative to the burner centerline and burner faces. The intent of these tests was not to fully map the entire flow field and define rates of NO formation. Rather, the objective of the tests was to define the major NO_x zone, (general rich and lean zones), identify significant asymmetries, and establish the trajectory of the burner jets. These results help define the NO_x character of tangentially fired systems.

Figures 43 through 45 present as-measured gas concentrations across the firebox for 15 percent excess air conditions and low burner yaw (below 3^o). The rest of the operating conditions are listed on the figures. Figures 46 through 50 present the gaseous concentration data for similar conditions at a burner yaw angle of roughly 6^o. Both sets of figures, while exhibiting different overall concentration levels, have similar trends. These results show that near the burner face and at the fuel entry elevation (Figures 43 and 47), NO is lower than exit levels on the wall side of the jet, is minimum in the center of the fuel jet where the fuel is relatively unburnt, and peaks on the vortex core side of the jet.* The peak NO levels, similar to firebox exit values, correspond in location with hot ignition zones observed during testing. These zones are created by the interaction and mixing of the fuel

---

*Furnace side as opposed to the wall side.

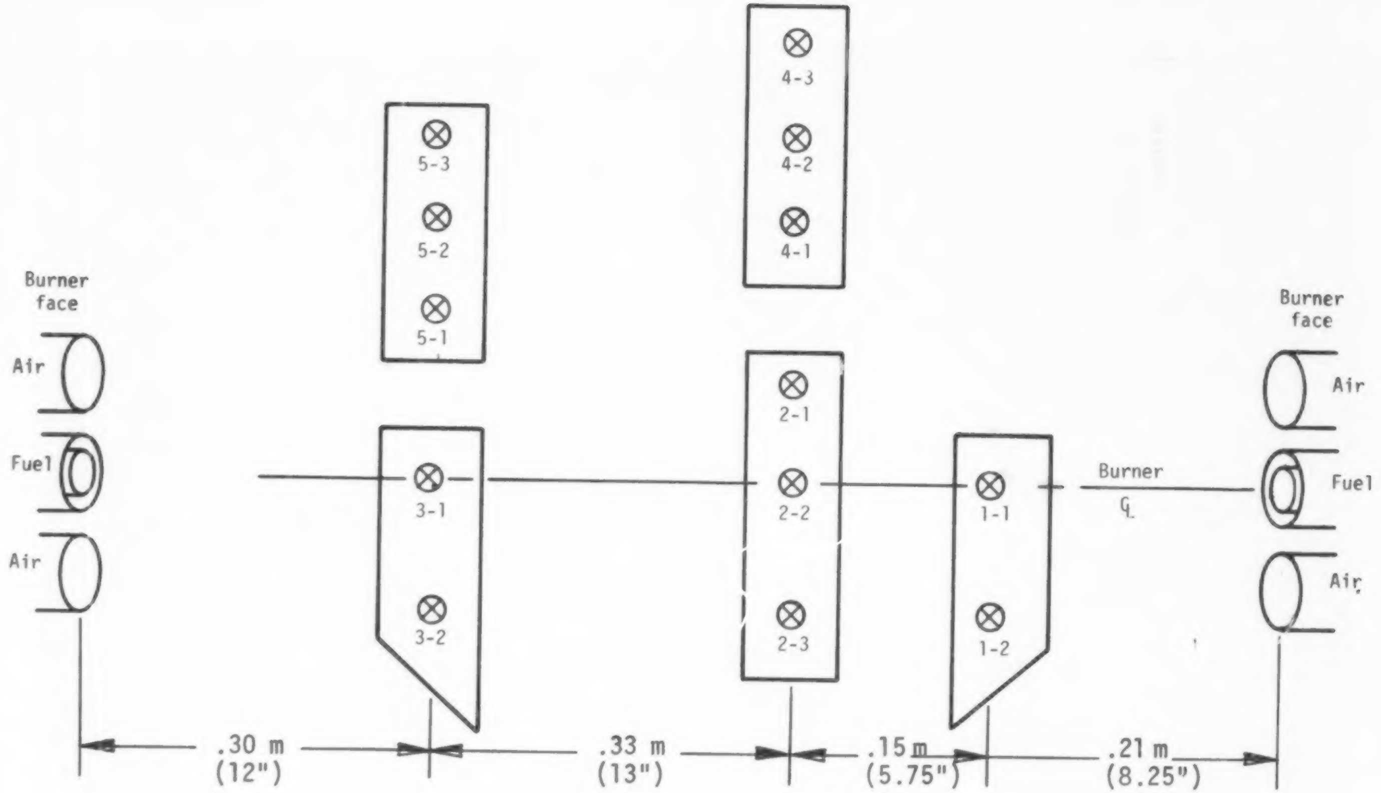
Burner
face
Air
Fuel
Air
5-3
5-2
5-1
3-1
3-2
4-3
4-2
4-1
2-1
2-2
2-3
1-1
1-2
Burner
℄
Burner
face
Air
Fuel
Air
.30 m
(12")
.33 m
(13")
.15 m
(5.75")
.21 m
(8.25")

Figure 42. Side view of firebox sample port locations and identification numbers.

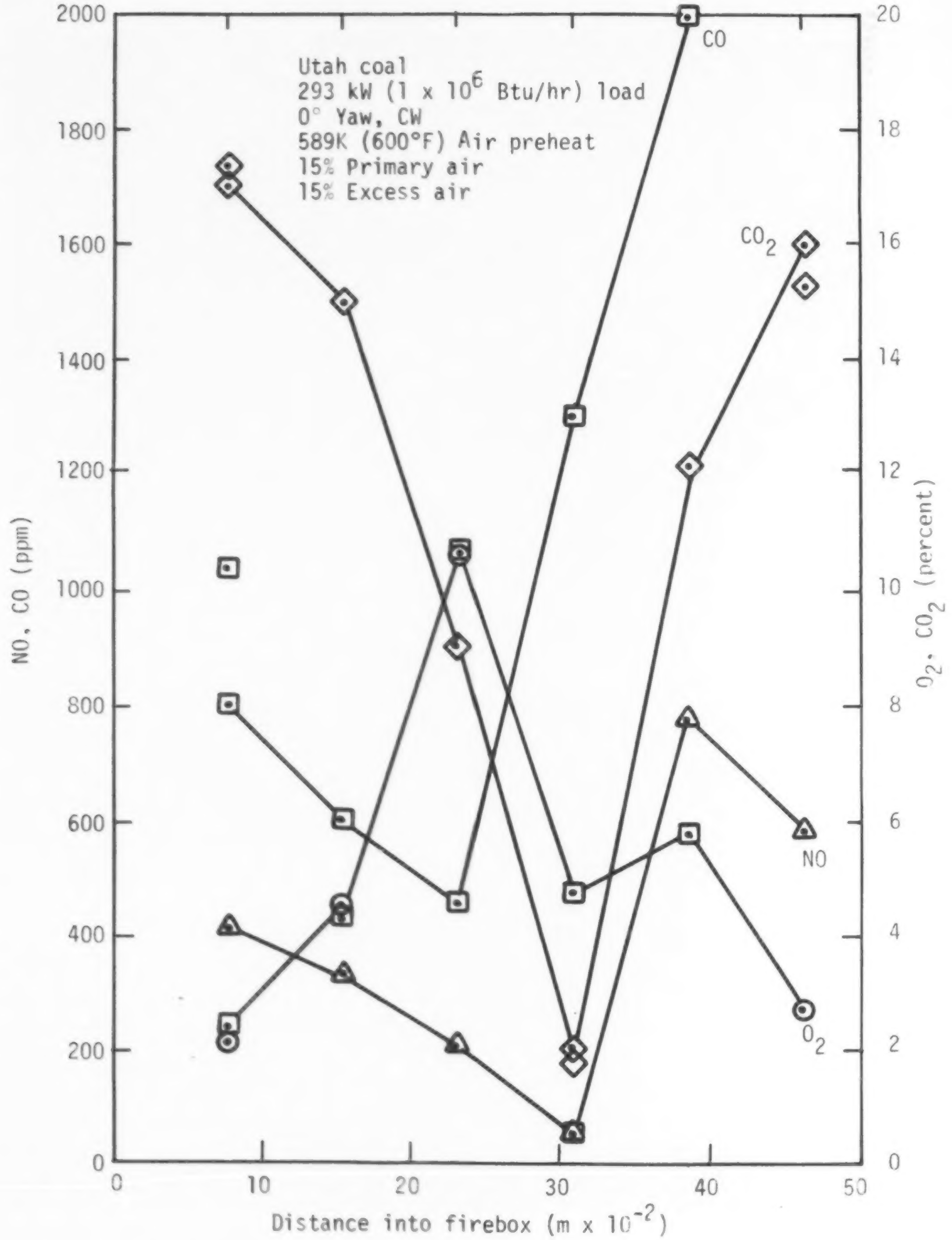

Figure 43. Concentrations across firebox at sampling location 1-1.

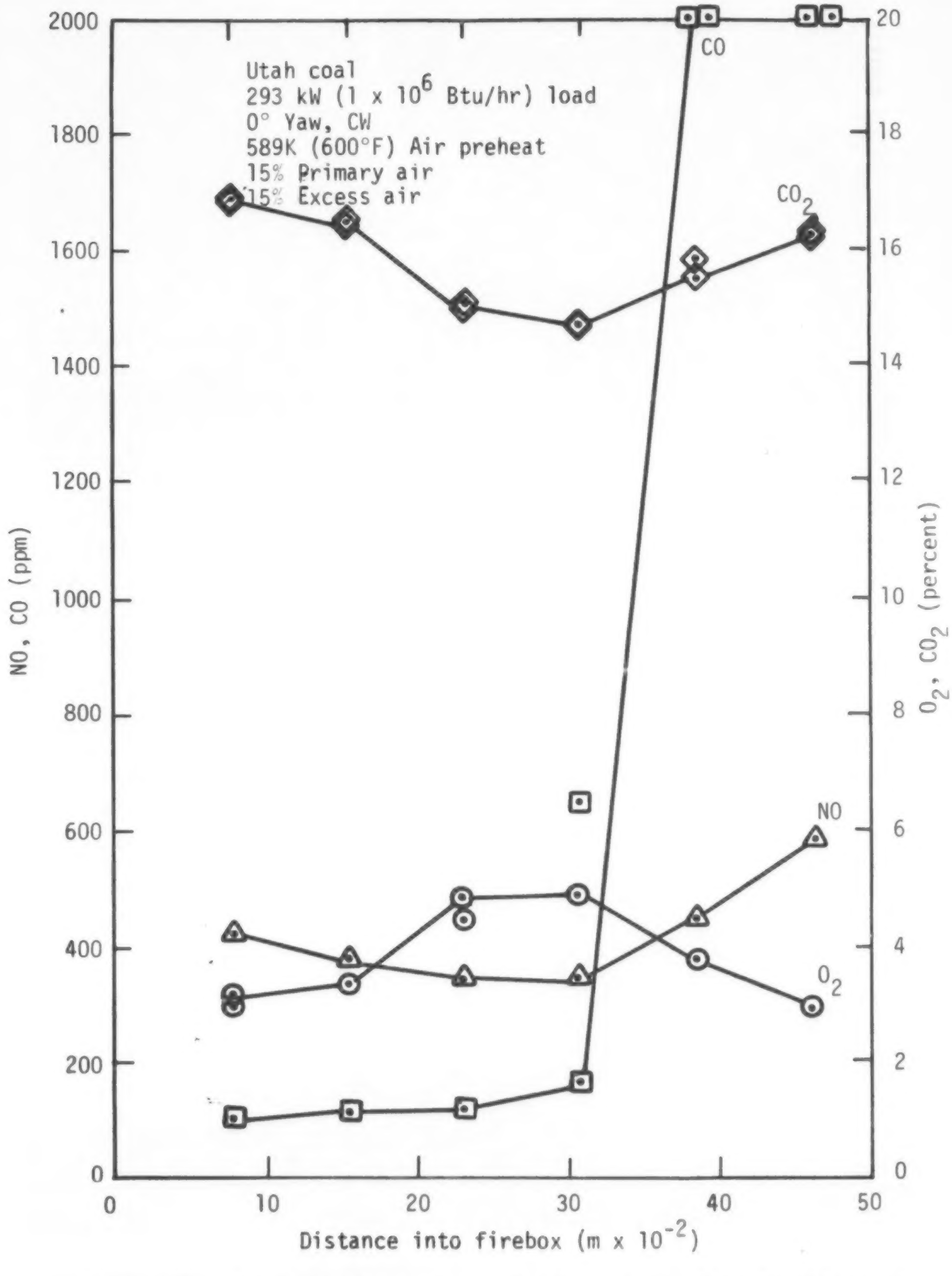

Figure 44. Concentrations across firebox at sampling location 2-1.

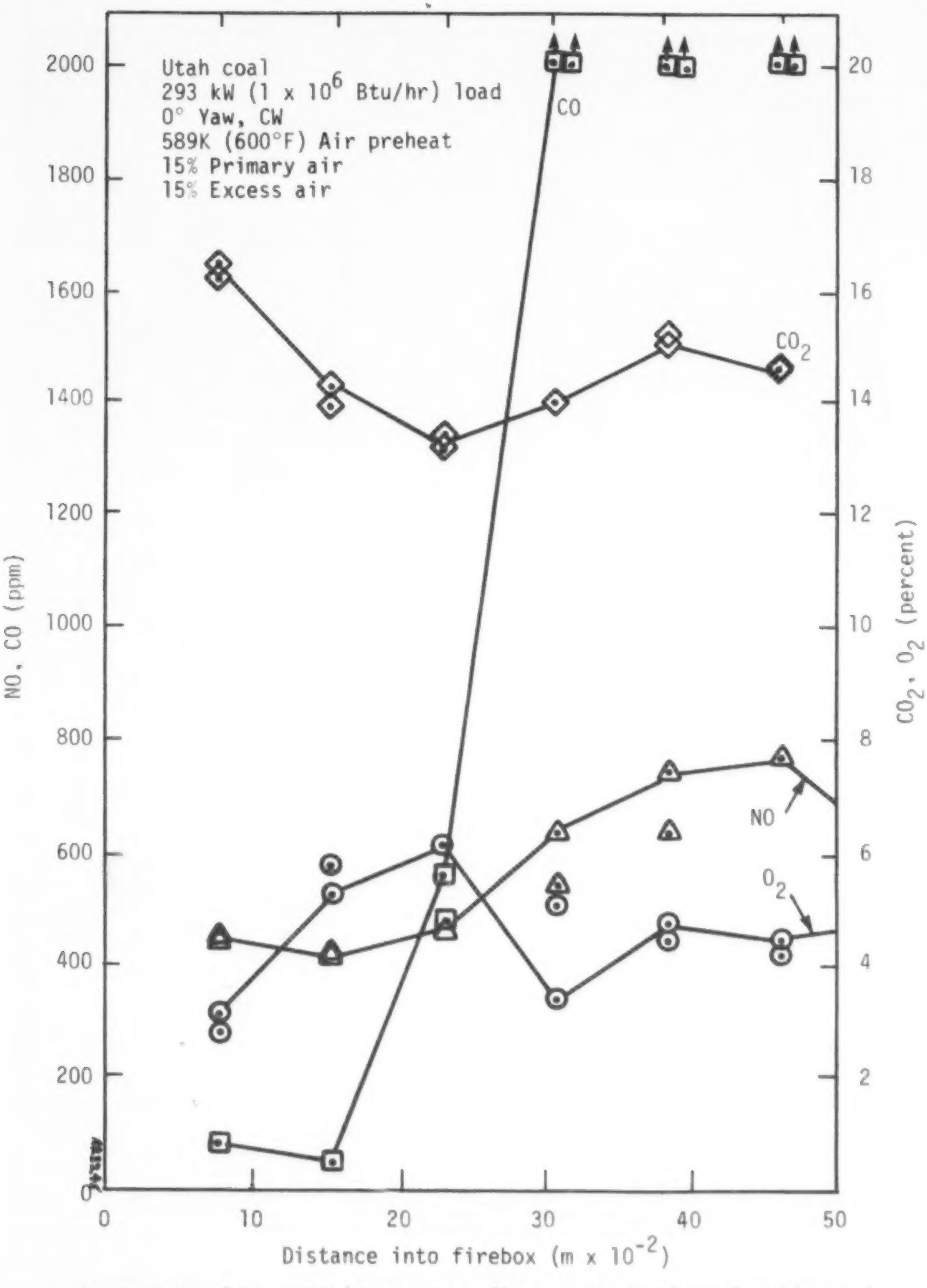

Figure 45. Concentrations across firebox at sampling location 3-1.

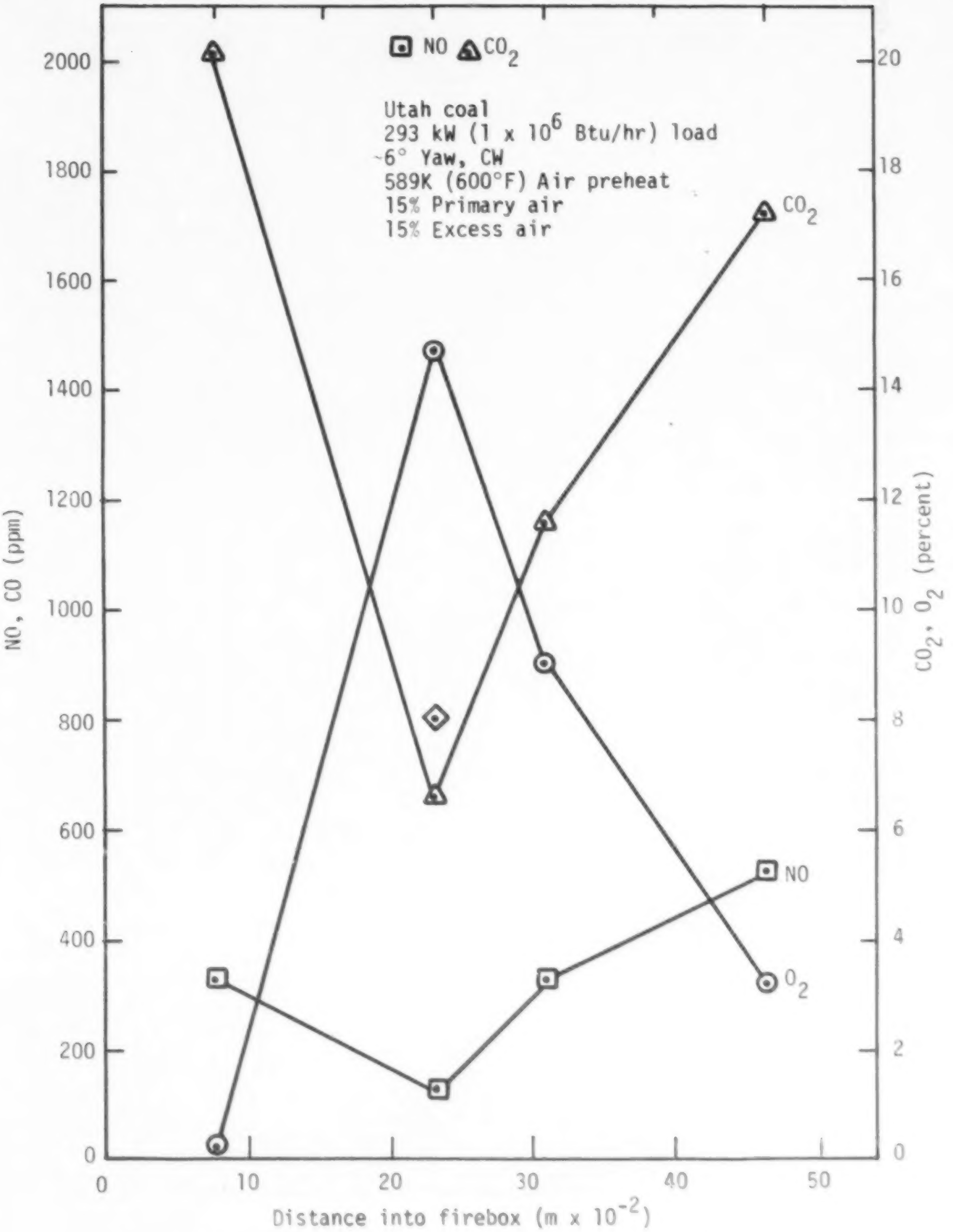

Figure 46. Concentrations across firebox at sampling location 1-2.

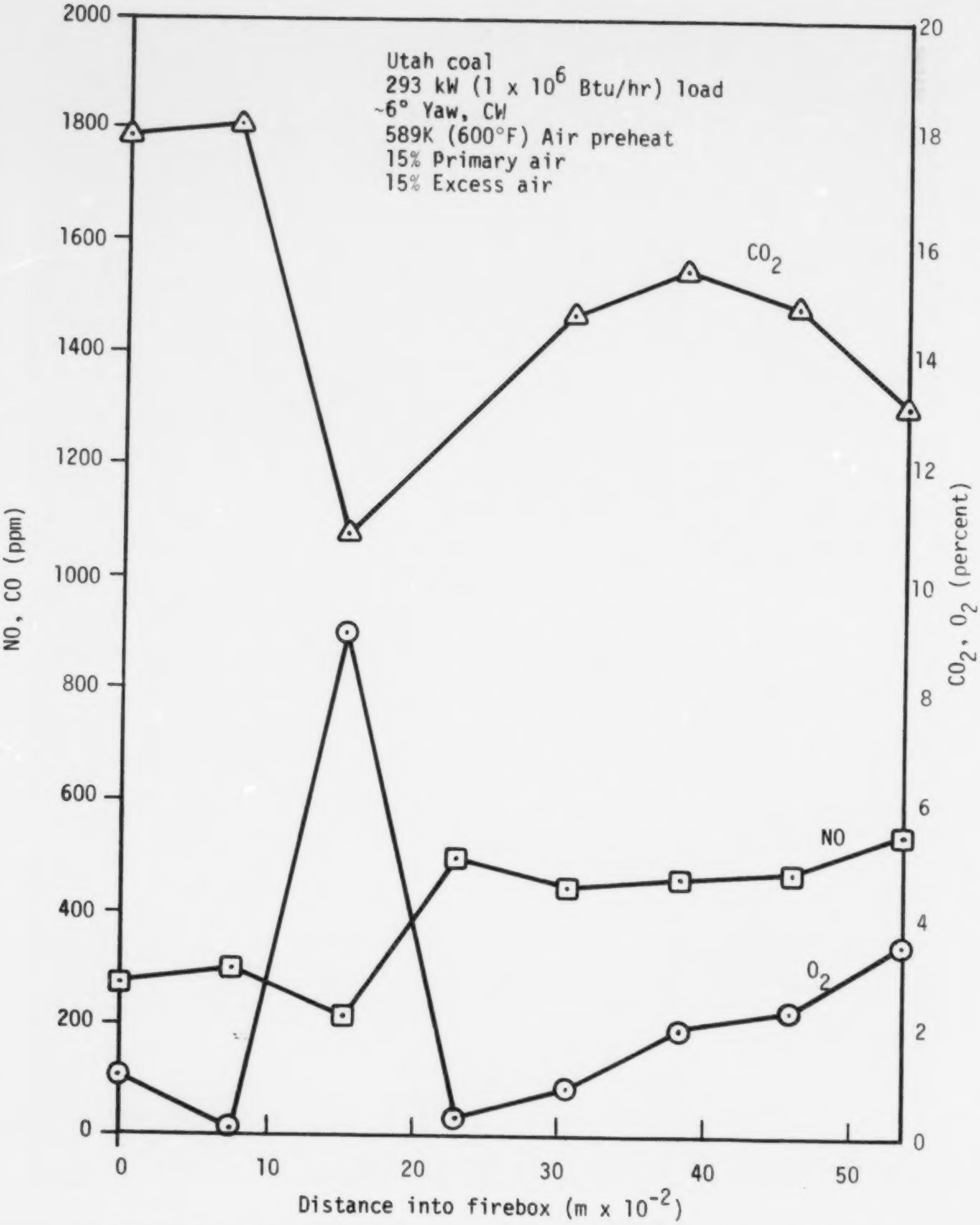

Figure 47. Concentrations across firebox at sampling location 1-1.

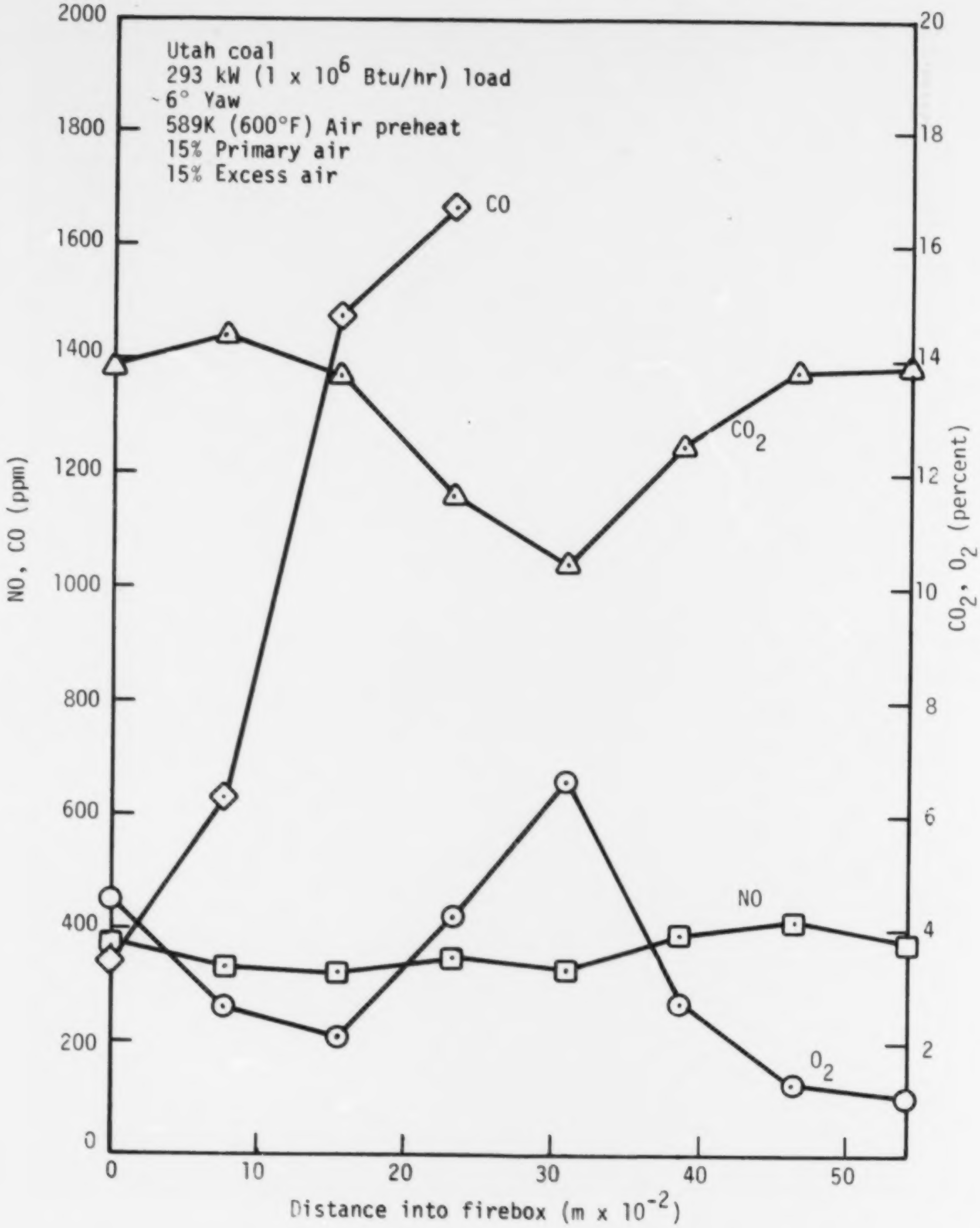

Figure 48. Concentrations across firebox at sampling location 2-1.

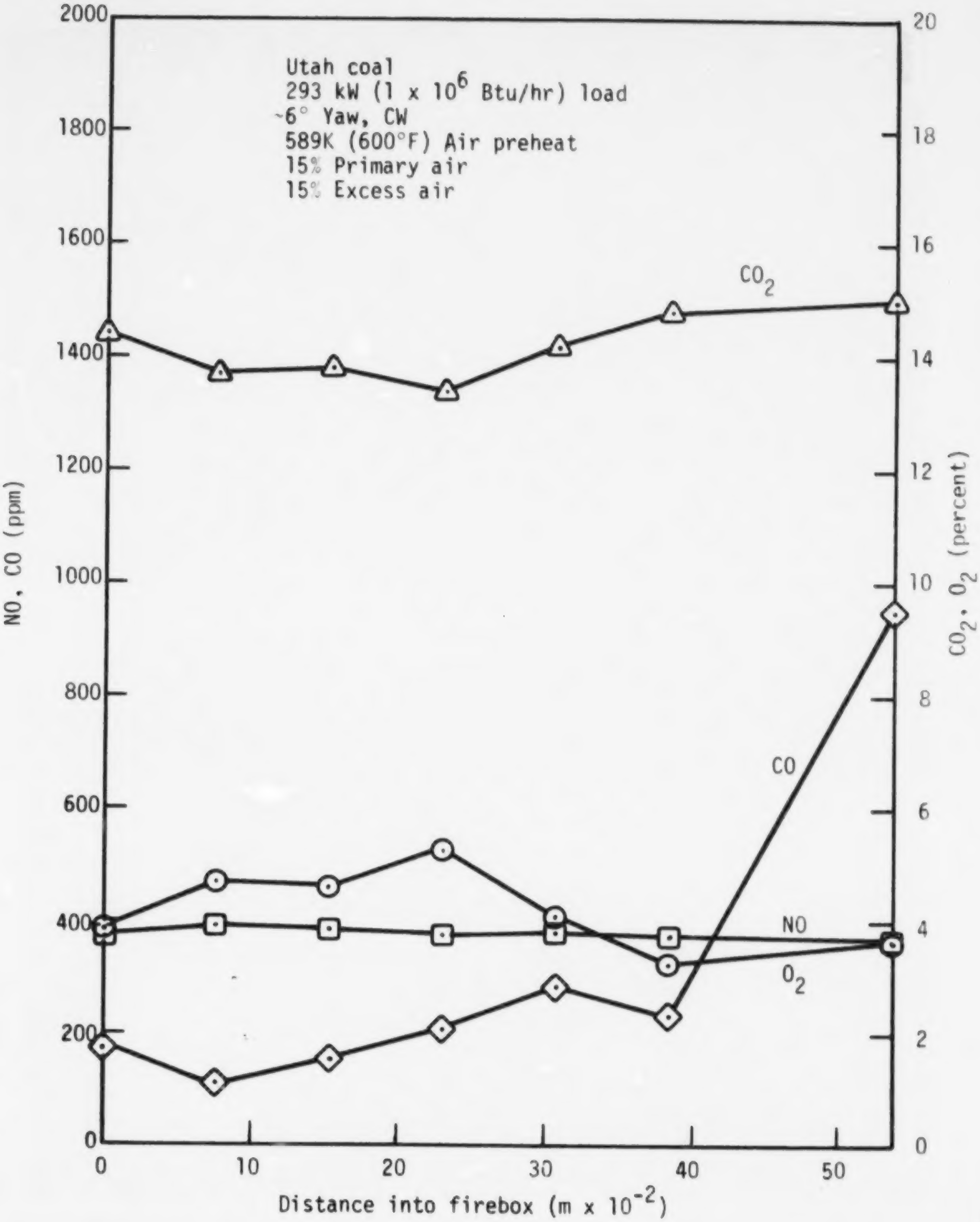

Figure 49. Concentrations across firebox at sampling location 4-2.

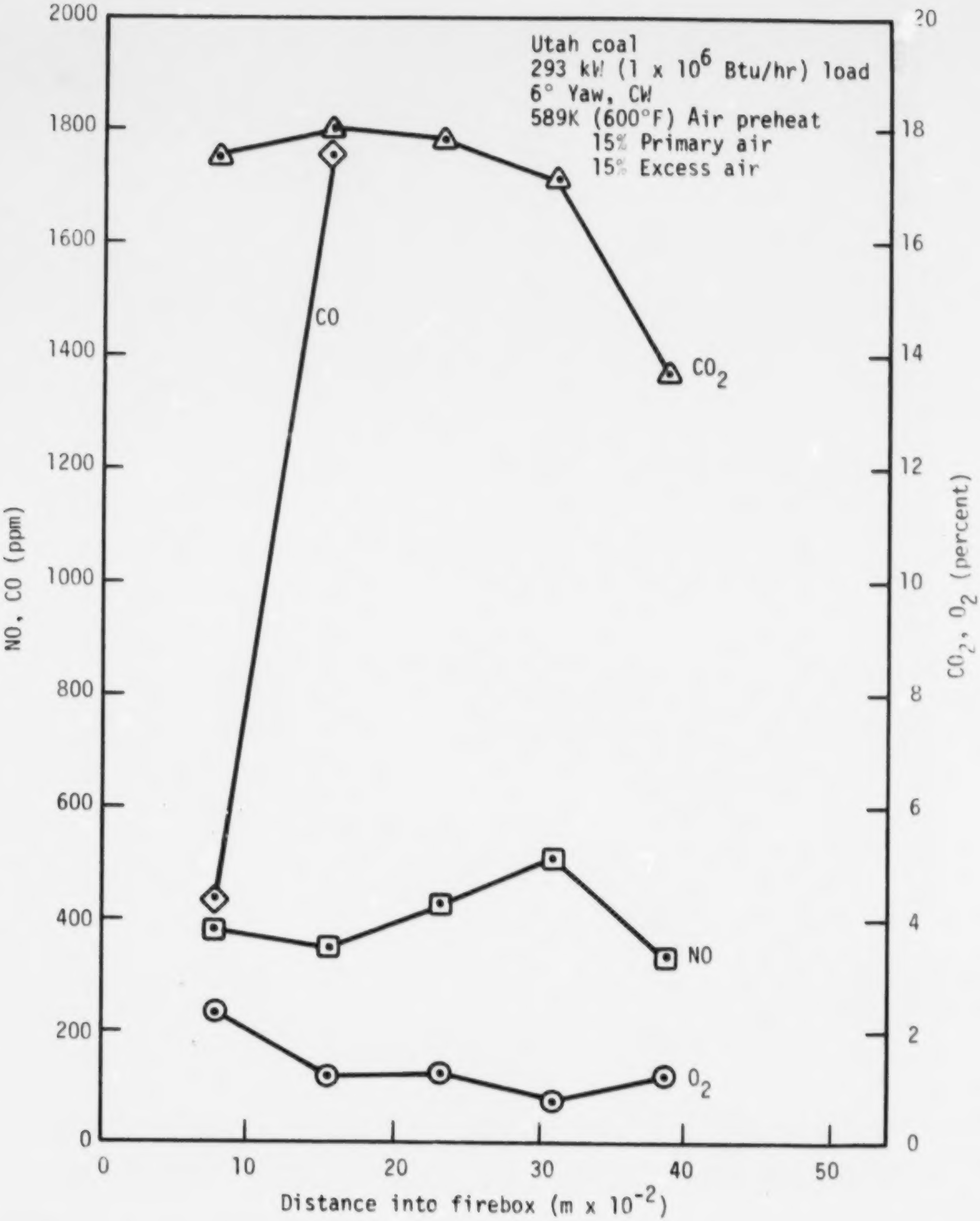

Figure 50. Concentrations across firebox at sampling location 3-1.

jet with hot burnt gases from the adjacent upstream corner burner. Mixing of fuel and air in this zone is enhanced, relative to the wall side of the jet, by the crossflow of hot burnt gases over the burner jets. These hot gases cause a rapid heating and devolatilization of coal particles on the vortex core side of the fuel jet. The fuel is only 60 percent burnt and has been in this zone less than 100 ms; thereby most of the NO production can be associated with volatiles burning. Since the initial volatilized fuel nitrogen sees an abundance of oxygen, the initial NO formation rate in this zone is high. Near the furnace wall NO, CO_2, and O_2 levels are characteristic of firebox burnt gas levels. The bulk of the total net NO production occurs in this near burner region.

Measurements downstream of the burner and above the burner elevation (Figures 44, 45, 48, 49, and 50) show lower peak NO values and much flatter behavior of NO with distance into the firebox. These results show that the dominant NO formation region is on the fuel jet elevation where fuel N, which is evolved from the coal, is locally converted to NO or N_2 fairly rapidly. Above the fuel jet elevation, NO levels do not vary strongly.

Downstream of the burner face and just prior to the next burner interaction (Figures 45 and 50), O_2 and CO_2 concentrations are more uniform and the NO peak is not as pronounced. Oxygen concentrations are low and NO concentrations are high in this zone, and the net NO production is small. This zone is downstream of where the vortex was observed to significantly impact with and cause rapid mixing of the fuel and air jets. Burning in this zone and downstream is mostly char combustion.

Probing results at 26.7 cm above the burner level (Figure 49) show CO_2, O_2, and NO levels relatively flat and consistent with furnace exit conditions. Very little net NO production occurs in this zone and solid samples show that only 10 percent of the fuel is unburnt at this level.

Several brief conclusions can be derived from these data:

- Production of NO on the vortex core side of the jet and at the fuel jet elevation is high

- Conversion of fuel nitrogen in this region is high for partially burnt mixtures

- Regions near walls have conditions characteristic of the burnt gases which exit the firebox

- Above the fuel jet elevation, NO results are smoother with lower peak levels than those observed at the fuel jet elevation

- Downstream of the burner, on the fuel jet elevation, peak NO levels are still evident with minimum NO levels higher than those found near the burner face

Figure 51 also exhibits these effects for a firing configuration in which the yaw angle was set at 12° with the vortex rotating opposite to these cases.

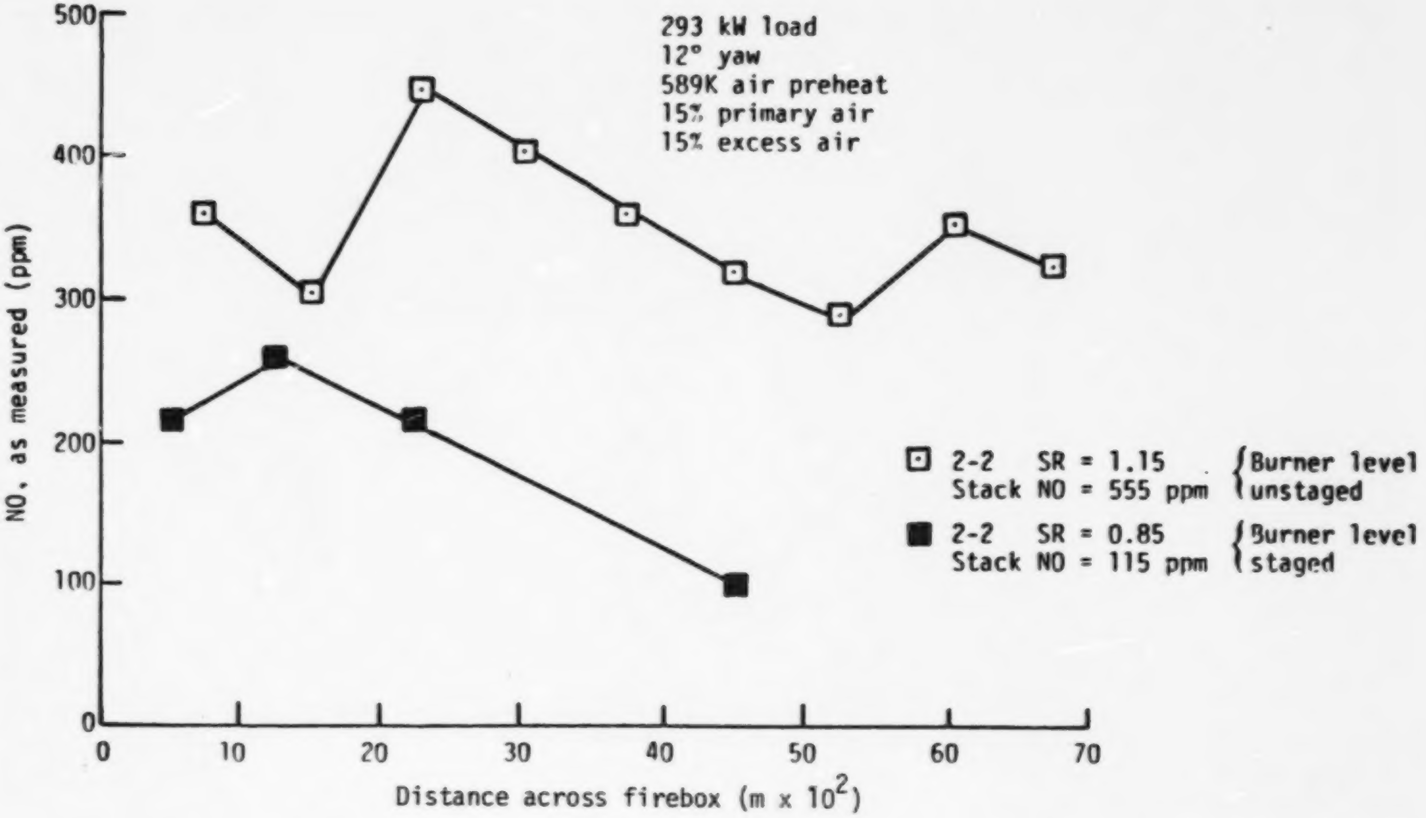

Figure 51. Comparison of unstaged and staged firebox NO probing results.

An interesting effect to note in Figure 51 is the variation of NO at the fuel jet centerline under staged conditions.

These staged combustion probing tests were run at a firebox SR of 0.85 with an overall stack excess air level of 15 percent. As expected, staged combustion significantly lowered stack NO through reduction of prior-formed NO and lower conversion efficiency of fuel N to NO. Of greatest interest were the probing results presented in Figure 51, which showed that, near the burner face, the vortex core side NO formation peak was eliminated by operating the firebox fuel rich. Operating the active zone on the vortex side of the fuel jet under O_2-deficient conditions appeared to eliminate the peak NO formation leading to a low firebox burner elevation NO level which is even further reduced by decay processes occurring above the furnace burner elevation.

In addition to the probing data, observations of flame and vortex flow patterns from the bottom of the furnace were made during the probing tests. Both natural gas and coal flames were observed with both giving qualitatively similar results. At 6° yaw, the vortex was somewhat smaller than observed in full-scale practice with multiple burner levels. By increasing the yaw angle to 12°, the vortex diameter was increased and appeared to give a vortex larger than full-scale systems.

Table 8 gives the stack NO levels for the three different burner yaw angles tested. These results show that overall NO production is not dramatically influenced by yaw angle even though vortex size is observed to change significantly with yaw angle. The relative lack of sensitivity of NO to yaw angle might be due to the role of volatile versus char NO_x formation in tangentially fired systems.

As shown by the probing results, NO processes associated with volatiles combustion occur near the burner face and contribute the bulk of NO. Also, these tests show that the initial diffusion nature of the jet flame does not appear to be strongly impacted by the variations in yaw angles tested. From flame observation and in-flame probing, ignition and initial burning appear to be similar enough for the different yaw angles to not significantly impact

TABLE 8. EFFECT OF YAW ANGLE ON NO

Yaw angle from diagonal	Stack NO ppm (0 Percent O_2)
0° clockwise	565
6° clockwise	506
12° counterclockwise	543

volatile NO processes. Beyond the volatile process zone, or roughly beyond one-half the firebox length, the difference in size and strength of the vortex, caused by yaw angle changes, should significantly impact the aerodynamics and mixing of the jet. However, in this zone, NO production/reduction is dominated by char processes. These processes are slow and therefore unresponsive to local environmental changes on the burner level which have timescales shorter than char burnup and NO decay.

The small variation in stack NO results with yaw angle also shows that NO flame processing by the vortex, if any exists, is unaffected by yaw angle. As noted previously, at the yaw angles tested, vortex blending and mixing of fuel/air/products is significant. Therefore, very chemically active flame zones, where NO processing can occur, are absent in the vortex and NO reduction is small. In addition, vortex mixing destroys any rich zones and the associated potential NO reducing species. Thus, flame processing by this process is also small and very little net flame processing occurs in the vortex.

In summary, the probing results show that near the burner face combustion is asymmetric with ignition, intense burning and peak NO production occurring on the furnace side of the fuel jet. At this location, 60 percent of the fuel is consumed. This amount of fuel consumed and large NO production can probably be associated mostly with coal volatiles. Downstream of this peak NO production, near the burner zone, beyond roughly half the firebox length, mostly char combustion is taking place and NO production is small.

For staged and unstaged combustion, NO levels near the wall are characteristic of firebox exit conditions. Levels of NO near the middle of the jet are similar between the staged and unstaged results. However, the peak NO levels on the vortex core side of the flame, which were observed under lean conditions, are absent under rich conditions. In fact, NO levels on the vortex core side of the flame continually decrease as the center of the firebox is approached. It is hypothesized that the interaction between oxygen-deficient gases from the adjacent flame and the burner flame gives a locally fuel-rich flame zone in which reduction of fuel N to N_2 is favored over oxidation to NO.

4.3.2 Firebox NO Doping

Information on the NO reduction capability of various zones in the firebox was obtained by injecting NO dopant into the firebox. A ceramic injector tube 1.9 cm in diameter, shown in Figure 52, was used to distribute NO over a roughly horizontal line source 15 cm long. The NO flow in the injector was set at a level required to yield 375 ppm in the stack for an inert injectant. Injection locations were chosen above, at, and below the burner centerline to assess the NO reduction potential of the near-burner and vortex zones probed earlier. These locations were based on the flame and vortex observations made earlier. NO dopant was also injected into the primary air/coal supply line to assess the effect of the very-near-burner zone on NO reduction. Figure 53 presents, on a plan view of the furnace, the percent of NO dopant remaining in the stack for the indicated injectant locations. The percent remaining is found by subtracting the exit NO

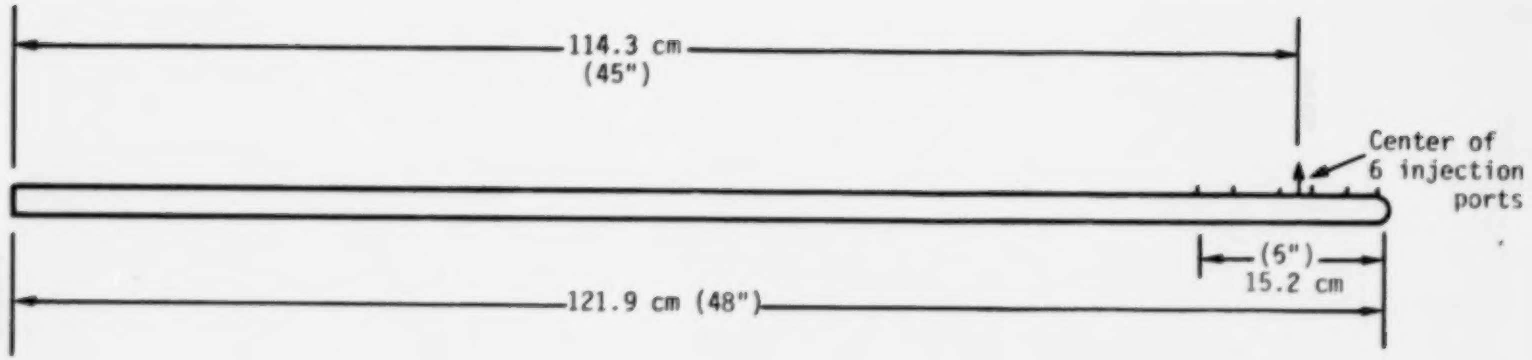
114.3 cm
(45")
Center of
6 injection
ports
(5")
15.2 cm
121.9 cm (48")

Figure 52. Ceramic NO injectors.

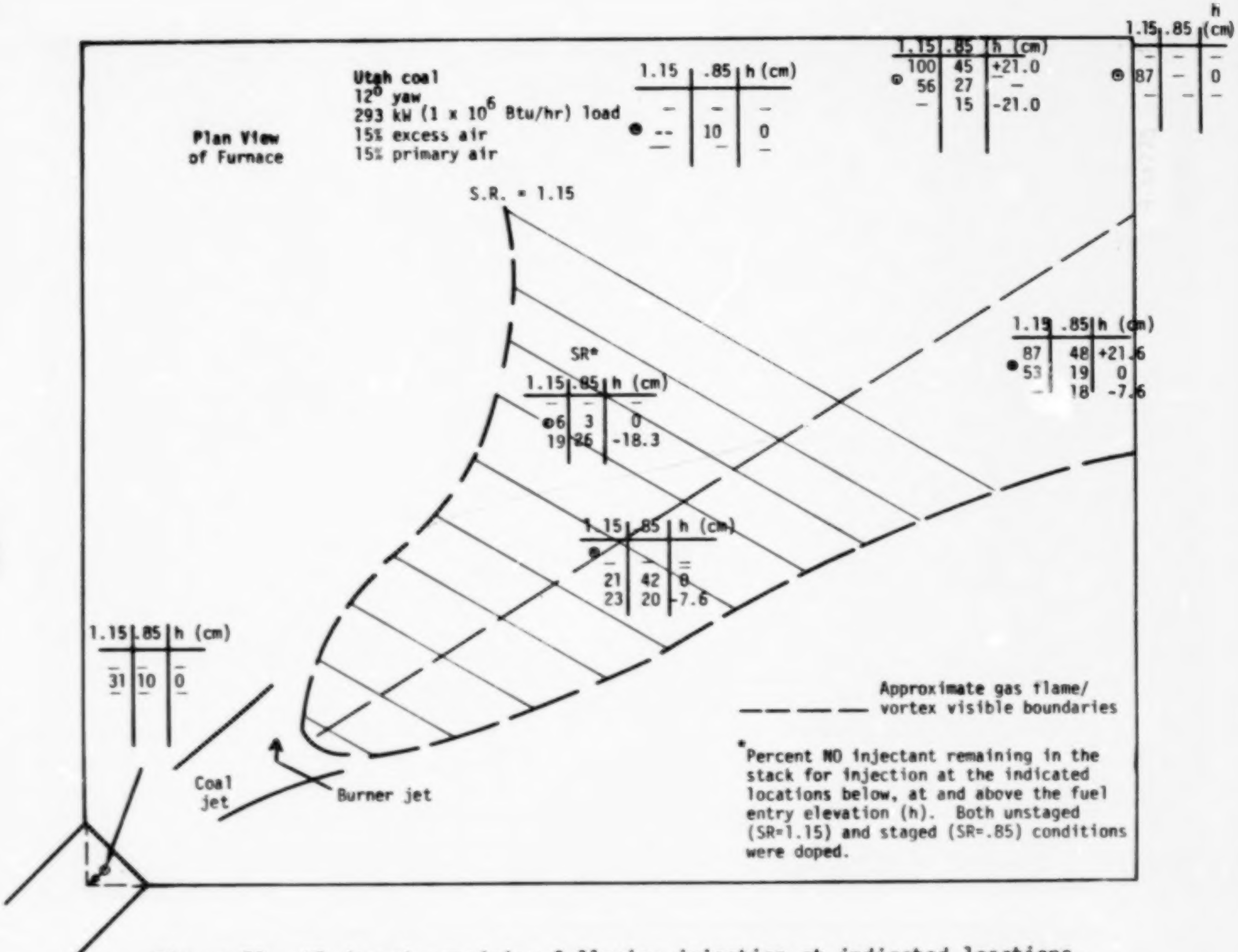
Plan View
of Furnace
Utah coal
12° yaw
293 kW (1 x 10⁶ Btu/hr) load
15% excess air
15% primary air
1.15 | .85 | h (cm)
– | – | –
-- | 10 | 0
1.15 | .85 | h (cm)
100 | 45 | +21.0
56 | 27 | –
– | 15 | -21.0
1.15 | .85 | h (cm)
– | – | –
87 | – | 0
S.R. = 1.15
SR*
1.15 | .85 | h (cm)
– | – | –
6 | 3 | 0
19 | 26 | -18.3
1.15 | .85 | h (cm)
87 | 48 | +21.6
53 | 19 | 0
– | 18 | -7.6
1.15 | .85 | h (cm)
– | – | –
21 | 42 | 0
23 | 20 | -7.6
1.15 | .85 | h (cm)
31 | 10 | 0
Coal
jet
Burner jet
Approximate gas flame/
vortex visible boundaries
*Percent NO injectant remaining in the stack for injection at the indicated locations below, at and above the fuel entry elevation (h). Both unstaged (SR=1.15) and staged (SR=.85) conditions were doped.

Figure 53. NO dopant remaining following injection at indicated locations.

concentration without dopant from the measured doped level and dividing by the theoretical inert injectant concentration of 375 ppm. Conventional, as well as staged, combustion conditions at a first-stage SR of 0.85 were tested.

As shown in Figure 53, for unstaged combustion conditions, injecting NO on the fuel jet centerline near the burner yields NO reduction efficiencies of 70 to 80 percent. Away from the burner and in the vortex, reduction efficiency is about 50 percent. In the active zone on the vortex core side of the fuel jet, explored in the probing tests, reduction is 94 percent. Below the burner level, NO reductions of 80 percent were measured whereas above the burner level reductions were small, being less than 13 percent.

Under staged combustion conditions, at a first-stage SR of 0.85, the results in Figure 53 show that reductions at the burner elevation were better by a factor of two from the unstaged results, except at a single point. Below the burner level, reductions observed were about the same as conventional unstaged reductions. Above the burners, the reductions were significantly better for the staged conditions.

These results show that NO is most effectively reduced if the NO is injected into the active combustion and peak NO production zone formed by the interaction of hot burnt gases and the fuel jet. In this zone, reaction is probably fast and addition of NO can drive the reactions from NO_x production toward a balancing of NO_x production and reduction. Another effective reduction zone is near the burner face at the burner elevation. In this zone, oxygen is not abundant and NO is reduced. Below the burner level, NO reduction is effective for both staged and unstaged conditions. Since reduction is not observed above the burner level for lean conditions, this indicates that NO injected below the burner centerline must get entrained and reduced in burner elevation flame zones.

In summary, the NO injection results show that significant flame processing can occur within the firebox under both staged and unstaged conditions. The degree of processing depends very much on the location of injection, with the maximum reduction occurring when the NO is injected at the initial jet interaction zone. This is a very active flame zone where considerable flame processing can occur. In order of degree of flame processing, the jet/vortex interaction zone is very effective, the fuel jet, fuel-rich zones and below the fuel entry elevation somewhat less effective, and above the burner level ineffective under unstaged combustion conditions.

4.3.3 Burner Biasing

To determine the effect of burner biasing on NO, two opposite corner burners were operated fuel rich with the adjacent corners providing the rest of the combustion air to bring the overall excess air level up to 15 percent. The fuel-rich burners were operated at 0.6 of the overall fuel combustion air requirement. Preheat, yaw, and other combustion conditions were maintained the same as during the baseline testing. Test results given in Table 9 showed only a 10-percent decrease in stack NO from the baseline level for the extreme

TABLE 9. EFFECT OF CORNER BURNER BIASING ON NO

Firing Mode	NO ppm (0 Percent O_2)
Baseline	405
Biased SR = 0.6 for two burners	365

biased condition.* This insensitivity to biasing may be due to having, at an SR of 0.6, sufficient air needed for complete combustion of the volatiles, since the volatiles content of the fuel is only 39 percent by the ASTM method. Thus, early volatile NO processes may not be significantly altered by extreme biasing. In addition, beyond the near-burner zone where NO char processes dominate, the vortex strongly mixes fuel, air, and products, destroying the fuel/air biasing set up by the rich corner burners. Therefore, combustion conditions and NO processes in the vortex are not significantly altered by the extreme biasing.

In summary, probing, NO doping, yaw angle, and biasing tests have shown that NO production in the conventional tangentially fired pilot-scale facility is dominated by near-burner processes where fuel N is volatilized along with the fuel volatiles and these components then react in a diffusion flame environment. NO production can be very significant in these very active flame zones. Downstream of this diffusion flame, beyond roughly one-half of the firebox length from the burner, the vortex interacts with the flame and rapidly breaks up and mixes fuel, air, and products. This environment has fairly uniform concentration levels of CO_2, O_2, and NO, showing very little net NO production or reduction from this zone to the stack. In this zone, very few volatiles are left in the fuel and the processes are dominated by char combustion. With the limited amount of O_2 and the effect of oxygen-deficient boundary layers surrounding the particles, NO production from char nitrogen is probably limited. In addition, the char surface can reduce previously formed NO by either carbon reduction or catalyzing a CO-plus-NO-reduction reaction. These processes, plus homogeneous reduction/production processes, must be sufficiently in balance to yield the observed small net change in NO from this zone to the stack.

4.4 CIRCUMFERENTIAL FLAME-FLAME INTERACTIONS

Having established the general NO emission character of conventional tangential firing, additional tests were carried out to assess in more detail the impact of near-burner diffusion flame and jet/vortex interaction processes on NO and the relationship between design parameters and NO.

---

*During these biasing tests, overall furnace load was reduced thereby giving a lower baseline NO level.

To assess and quantify the impact of adjacent burner flame-flame interactions on NO formation/reduction, two of the tangential burners used in the baseline testing were set up in the firebox as shown in Figure 54 so that the angle between their centerlines, ϕ, and the distance to their centerline intersection point, X_i, could be varied. During these tests, the vortex present in tangential firing was absent. The variation of interaction angle and distance to flame interaction was expected to affect the ignition, mixing, and any NO flame processing occurring between the flames. Further, operating one flame fuel-rich and the other fuel-lean was expected to show if NO flame processing is beneficially impacted by rich zones, as was shown in the tangentially fired NO firebox dopant tests. Firebox firing rate for these tests was 146 kW (0.5 x 10^6 Btu/hr) compared to 293 kW (1 x 10^6 Btu/hr) when firing tangentially. Therefore firebox stirring and temperature were lower for these tests than when firing tangentially.

The NO results for both locally lean and locally rich/lean firing are given in Figures 55 and 56, respectively. The rich flame was the traversing flame. The lean flame was held fixed. These results show that NO, for the most part, is insensitive to distance to intersection, but depends on angle of intersection. This is shown in both the locally lean and locally rich/lean firing cases given in Figures 57 and 58, respectively. The one high point for 90^o angle and 25.4-cm (10-inch) intersection represents an unusual combustion condition where burning was observed to be initiated either at or inside the fuel tube. The locally rich/lean cases are comparable to the locally lean cases.

Two levels, roughly 200 and 400 ppm NO, independent of intersection distance, are evident from the results. If NO flame processing was active, it was expected that NO would change as more of the burnt gas NO was entrained into the earlier portions of the traversing flame. The absence of variation with intersection distance, for all intersection angles, indicates that either NO flame processing is not active or that it is balanced by a NO production effect.

Visual observation of the intersecting flames showed that the 135^o intersection angle flames appeared to be more widely spread out in the firebox than the 90^o and 45^o cases. The firebox backmixing, which is the source of hot gases which ignite the flames, is quite different for the 135^o, 90^o, and 45^o intersection cases. As will be shown in Section 4.4, if backmixing is reduced below a certain level, slow-mixed flames can become widely detached from the burner and NO emissions will rise dramatically. The increase in NO is a result of fuel/air mixing prior to ignition and burning such that the fuel nitrogen from the coal is reacted in a more oxygen-rich environment. Possibly the high NO levels exhibited by the 135^o intersection cases are a result of a lifted flame phenomenon. Unfortunately, limitations on flame visibility did not allow confirmation of this behavior. However, an abrupt increase from the 200- to 400-ppm NO level was observed for a single flame when it became widely detached. This is discussed in Section 4.5.2.

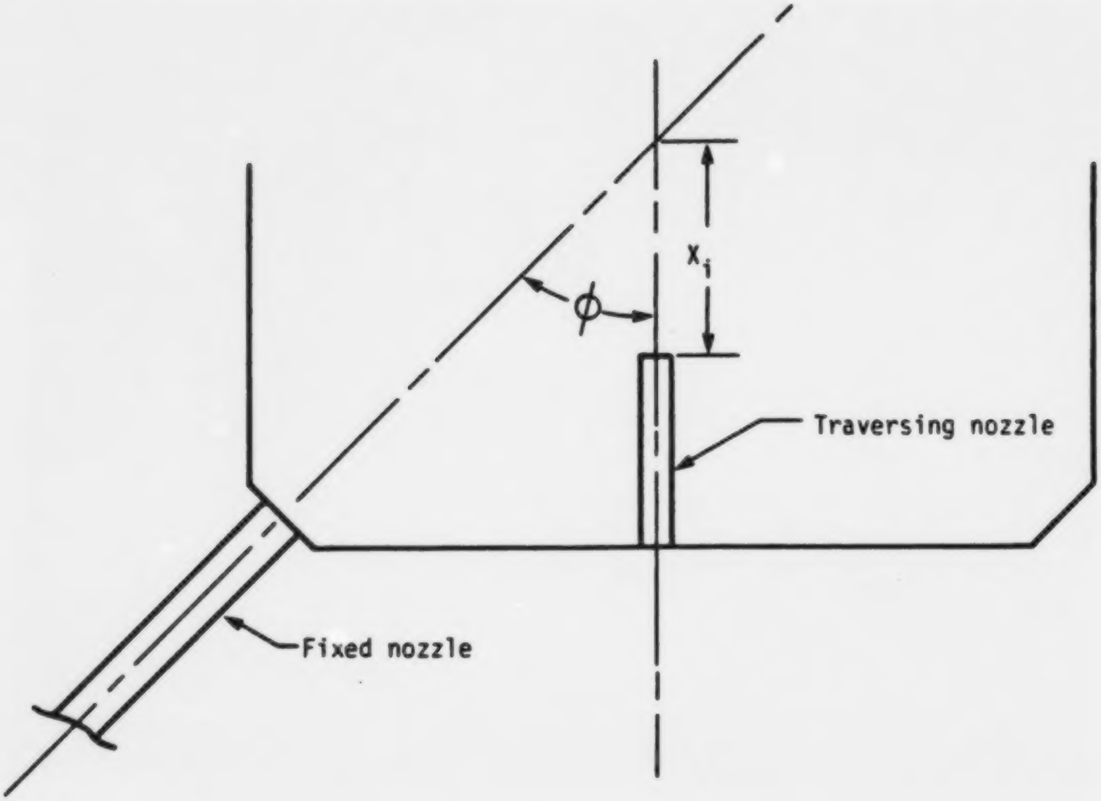
X_i
ϕ
Traversing nozzle
Fixed nozzle

Figure 54. Flame-flame interaction, 45° configuration.

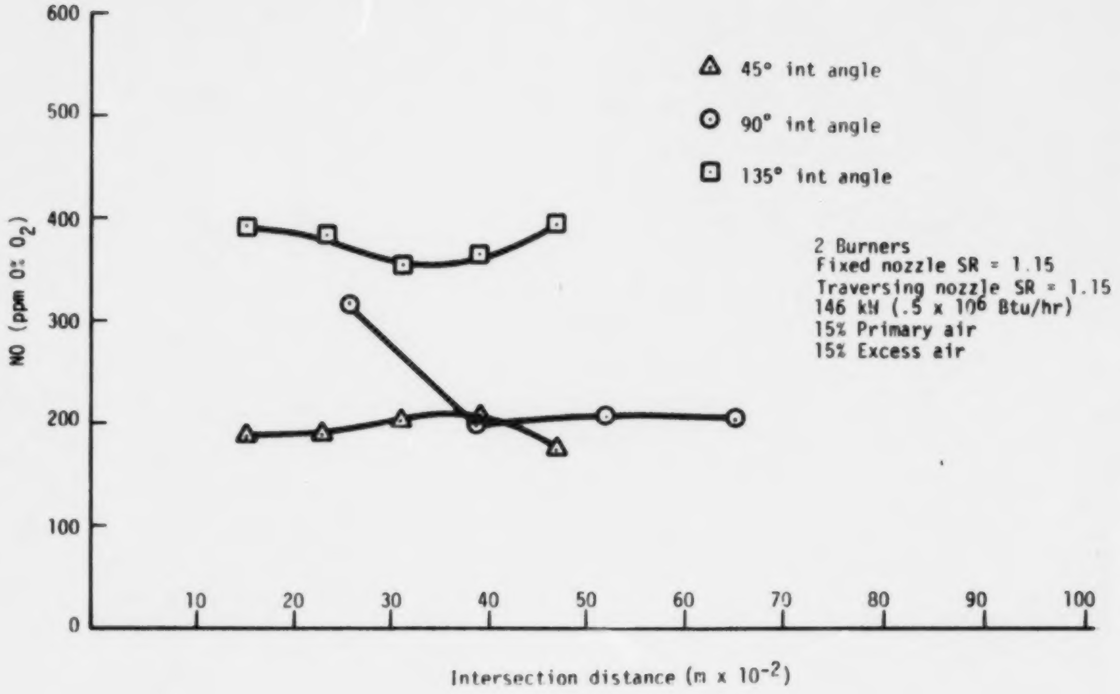

Figure 55. Flame interaction.

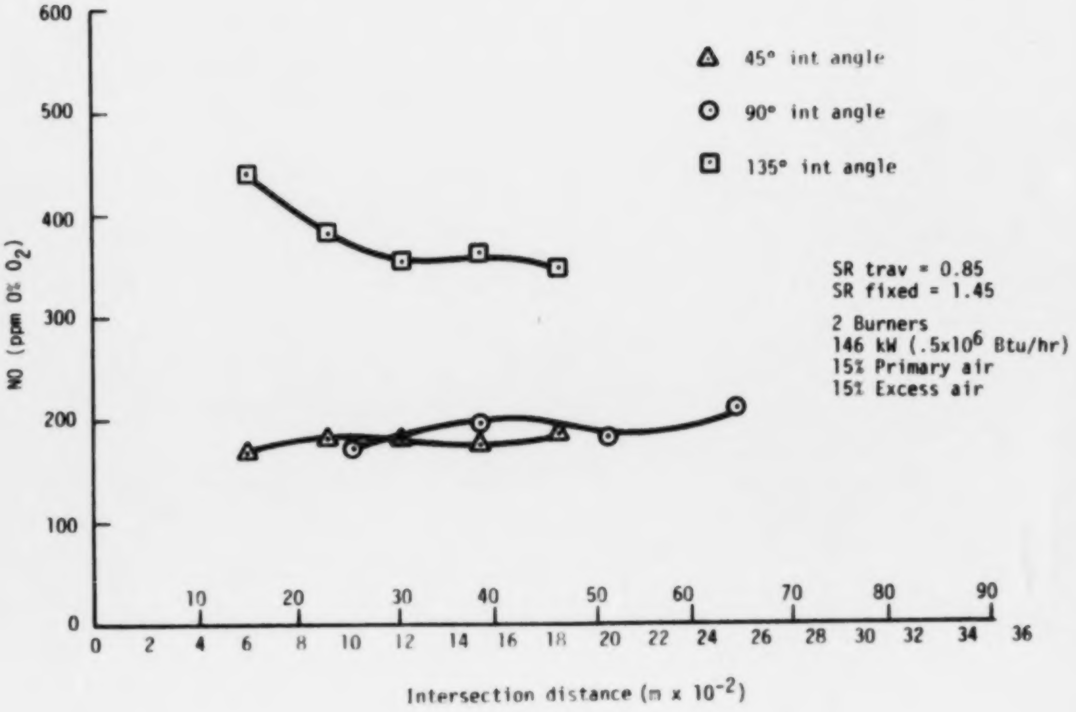

Figure 56. Flame interaction, rich/lean.

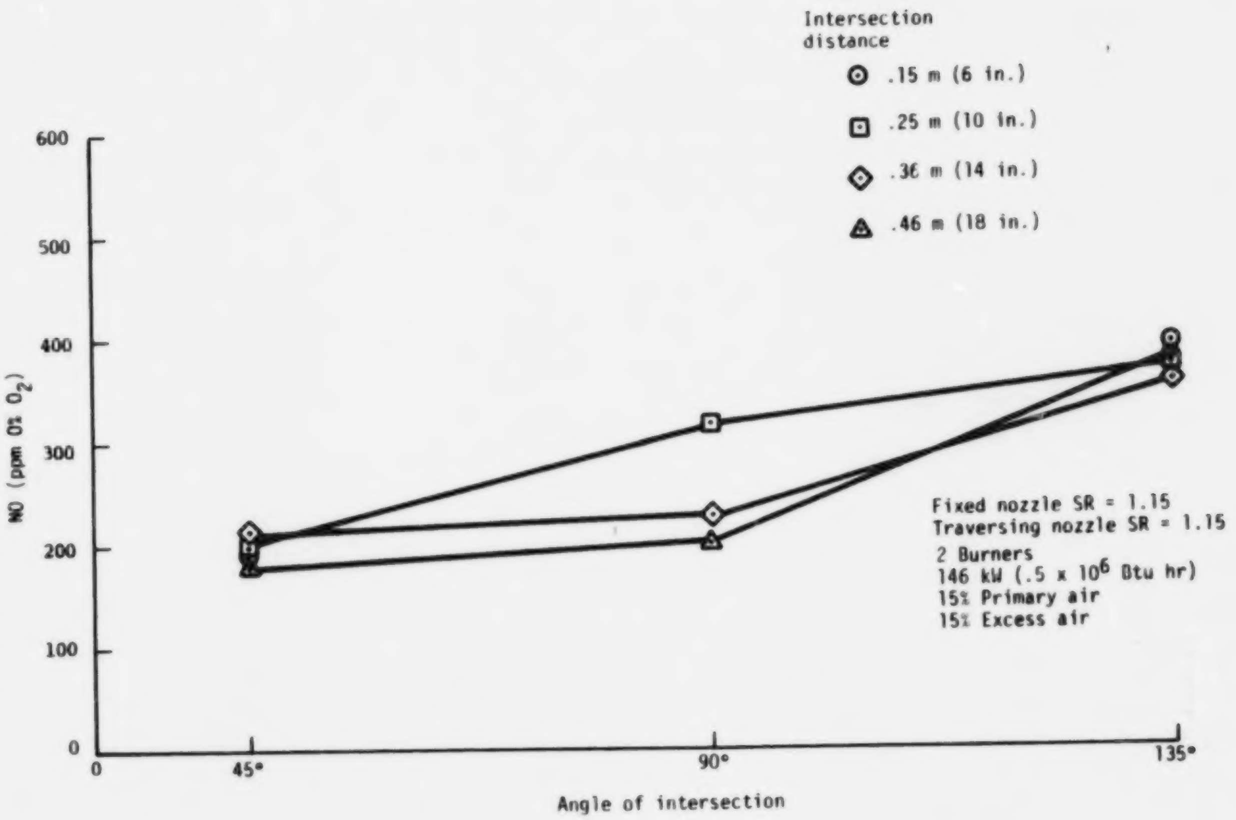

Figure 57. Flame interaction.

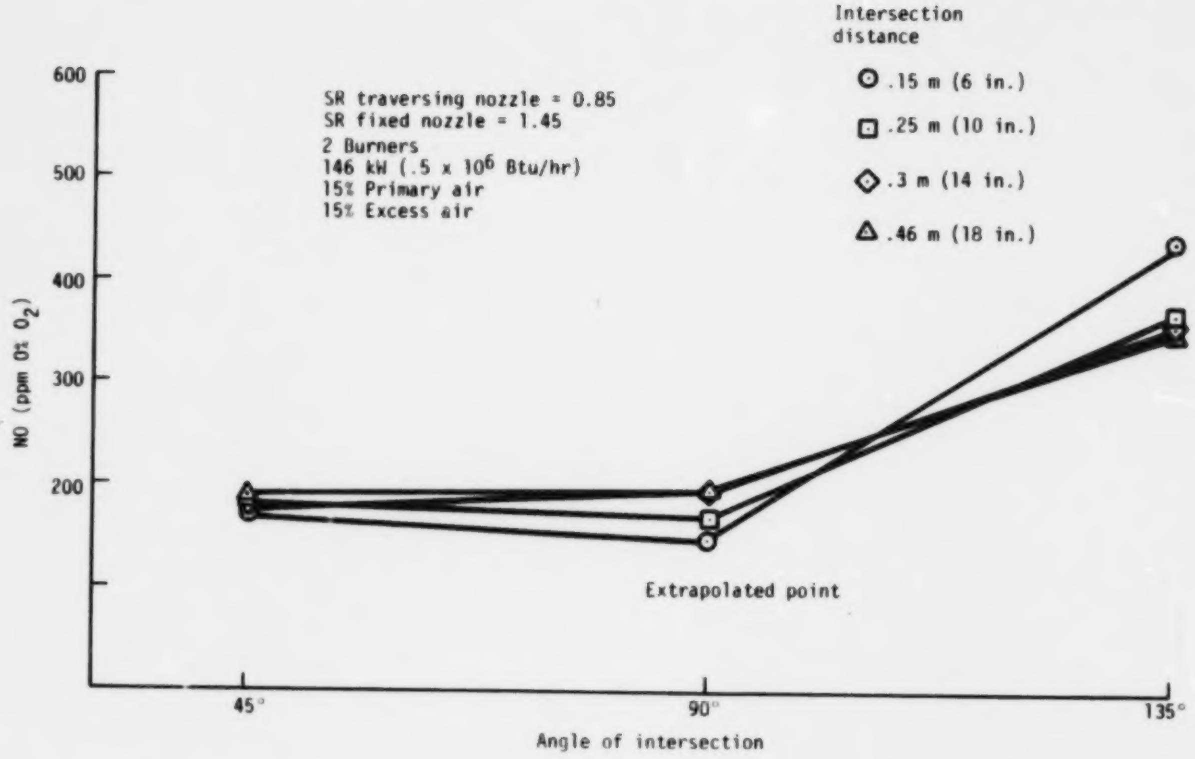

Figure 58. Flame interaction NO results, rich/lean.

The insensitivity of NO to intersection distance for all of the angles tested was surprising. It was observed that bringing the traversing flame into close proximity with the fixed flame caused flame spreading and apparent mixing to change. This change should have affected the diffusion flame behavior and NO production, since the traversing flame was brought to within five burner exit diameters of the fixed flame. At this distance, the diffusion flame effect is still dominant. It is possible that the increase in NO by the enhanced mixing of O_2 into the fuel jet might be balancing the reduction of the previously formed fixed flame NO, giving very little net change in NO.

The insensitivity of NO to operating the traversing flame rich with the fixed flame lean was less surprising. Operating the rich burner at 0.85 SR gives sufficient air for fuel and nitrogen volatiles reaction by the diffusion flame process. Beyond the volatiles reaction region, the char fuel and nitrogen reaction is slow compared to the gas phase mixing. Therefore, the initial rich/lean burner stratification is lost before it has time to significantly impact the char burnout processes.

In summary, depending on how tangential burner type flames interact, possibly lifted flames and high NO levels can be achieved. For attached flames, bringing flames into close proximity alters flame spreading and mixing but not NO levels. Also, operating one flame rich and the other lean does not impact NO levels. Possibly, the adverse impact on NO of mixing O_2 into the fuel jet is balanced by some beneficial NO flame processing. Thus, the mixing of previously formed NO into the flame zone, required for NO flame processing also brings O_2 into the flame zone, the net effect leaving NO levels unchanged. The excellent NO flame processing effect observed when NO dopant was injected in a concentrated form into the firebox cannot be achieved by entraining gases dilute in NO into boundaries of diffusion flames.

The most effective method of flame processing is self-flame processing where NO formed in the fuel jet is reduced by reburning of the fuel jet through staged air addition at a downstream location. In the absence of self-flame processing, regular NO flame processing might be optimized by reducing mixing intensity such that flame stratifications are maintained while mixing in previously formed NO over a period of time. This corresponds to the entrainment of previously formed NO into the upper burner levels of conventional tangentially fired units. The interactions that occur on a single level, like the two burner tests described here, are too severe for NO flame processing benefits to be greater than the negative effect due to the loss of fuel/air stratifications.

4.5 TANGENTIAL BURNER DESIGN CHARACTERIZATION

Recognizing the importance of the near-burner diffusion flame processes on NO emissions, tests of different burner designs were carried out to assess their impact on NO and to determine the relationship between design parameters and NO. Burner designs tested were limited to nonswirling slow-mix designs such as those presently used in tangential systems. Compact intense flames produced by swirl burners are not compatible with corner firing due to potential slagging, deposition, and thermal problems.

The firebox probing tests showed that the furnace side of the fuel jet, where ignition occurs, is a very active combustion zone and is where NO production appears to be a maximum. These tests also showed that NO production in this zone could be reduced by operating the zone fuel rich. Also, previous studies on tangential and other types of firing have shown that the O_2 availability within the fuel jet is important to early peak NO production. Lifted flames, where O_2 availability is high at the ignition point, exhibit very high NO levels compared to attached flames. Based on this information, burner designs were tested with various exposures of the fuel jet to combustion air and recirculated hot gases necessary for ignition. These tests demonstrate the effect of O_2 availability on NO and the benefit of using hot burnt gases to devolatilize the coal prior to combustion air addition. Also, the relative position between the fuel and air was varied to achieve a fuel-rich condition on the vortex side of the fuel jet. Lastly, during some tests, the overall firebox mixing was decreased to demonstrate the effect of firebox mixing and jet breakup on NO.

4.5.1 Burner Configuration

The burner design tests were performed in the firebox at an overall firing rate of 293 kW. Three conventional baseline burners firing on gas and one experimental burner firing on coal were used to generate a conventional tangential system vortex. This test procedure represented a compromise between modifying all four corner burners for each new burner configuration, which would have been expensive, and operating only a single burner without the vortex. It was believed that some vortex would be needed to help maintain positive-ignition and prevent lifted flames which could obscure the results. Most tests were carried out for standard baseline conditions of yaw, preheat, excess air, and velocities. Some staging and reduced overall load tests were also run.

Figure 59 presents the NO results for the various burner configurations. These are given as a function of temperature, since baseline testing showed that NO results increase with temperature. The NO level when all four corner burners are operated on gas is also shown. The results are uncorrected for the dilution effect of the lower NO gas combustion products. Actual differences in NO due to coal burner alterations are then greater by up to a factor of four than the differences appearing in Figure 59. The individual air port configurations are presented schematically at the top of Figure 59. Going from configuration 1 to 5, the ratio of exposure of the fuel jet to hot burnt gases relative to that of the combustion air decreases. Configuration 1 is the fuel jet alone with all of the secondary combustion air distributed to the other three corner burners firing on gas. The NO results in Figure 59 show that configuration 2 has the lowest NO levels for a given temperature and configuration 5 has the highest levels. In configuration 5, the fuel jet is surrounded by combustion air and the entrainment of hot burnt gases into the fuel jet is the lowest of any of the configurations tested. Configuration 2 has the fuel jet located toward the inside of the furnace with the secondary air jets aligned in a vertical row behind the fuel jet. It was observed that configuration 2 had rapid ignition and burning compared to configuration 5. The greater exposure of the fuel jet to the hot burnt gases in the vortex was beneficial to early burning in this case. The later

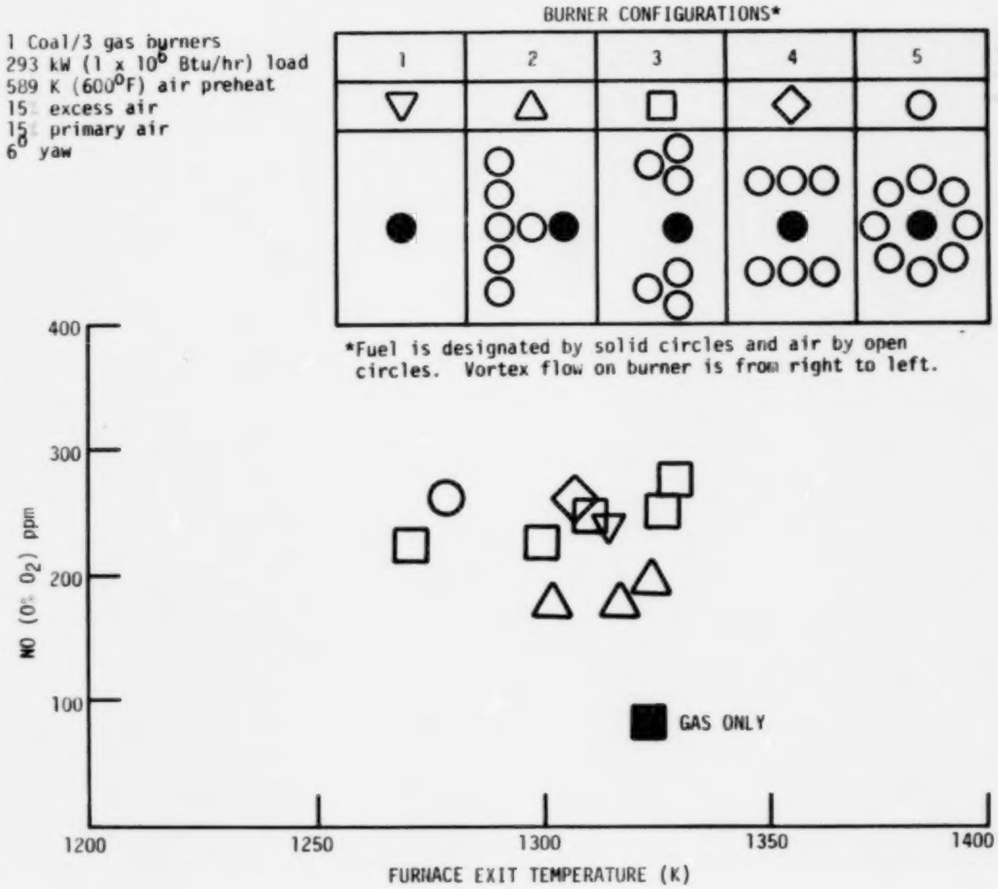

Figure 59. Burner configuration NO levels.

ignition and burning of configuration 5 leads to a more premixed condition and higher O_2 levels at the point where fuel nitrogen is evolved from the coal. This leads to the higher NO values observed for this configuration. Another beneficial effect of configuration 2 is the outward displacement of air with respect to the fuel. This configuration maintains the ignition and intense burning zone in a fuel-rich mode leading to lower NO.

Configuration 1, the fuel jet by itself, had the greatest exposure to hot burnt gases of all the configurations tested, and had NO results similar to conventional tangential burner type arrangements such as configurations 3 and 4. It was observed that the fuel jet by itself was heavily impacted by the vortex flow, and fuel jet spreading, mixing, and stripping of the fuel was extreme compared to other configurations. The intermediate NO results achieved by configuration 1 may be a result of the beneficial effect of hot gas mixing being balanced by the undesirable effect of spreading the fuel throughout the firebox rather than maintaining the fuel in a concentrated column. Utilizing the secondary air jets to create a pressure field, as in configuration 2, helps to shield the fuel jet from stripping by the vortex flow and is beneficial to NO emissions.

Tests were also run with a firebox stoichiometry of 0.95 to evaluate combined new burner concepts and overfire air. The remainder of the combustion air was introduced just beyond the firebox exit to give an overall excess air level of 15 percent. As shown in Figure 60, NO decreased significantly with staging to levels of around 130 ppm for configurations 2, 3, and 4. The NO results varied very little between the configurations tested at a SR of 0.95. Previous staging tests also showed little influence of the early firebox mixing processes on NO (Reference 9).

In summary, the burner design tests showed that increased exposure of the fuel jet to hot burnt gases was beneficial to early ignition and burning and resulted in the lowest NO. Placing the fuel jet towards the inside of the furnace causes the hot ignition zone to operate more fuel rich, which from earlier probing test results leads to lower NO. However, if the fuel jet is not backed up by secondary combustion air jets or some other means, the fuel jet could be dispersed by vortex impact which would then counterbalance the beneficial NO effect of hot burnt gas exposure. Operating the firebox at less than the theoretical air requirements lowers NO for all the burner configurations tested. Under staged combustion conditions at a firebox SR of 0.95, the final NO level is independent of configuration.

4.5.2 Firebox Mixing

Load variation in previous conventional tangentially fired tests was found to affect NO levels primarily through changes in mixing intensity in the firebox. Burner configurations 2, 3, and 4 were tested for the effect of firebox mixing intensity by varying the three burner gas firing rates while maintaining the new burner design configuration at a constant 73 kW. Varying the gas firing rate was expected to change the vortex strength and the turbulence intensity in the firebox.

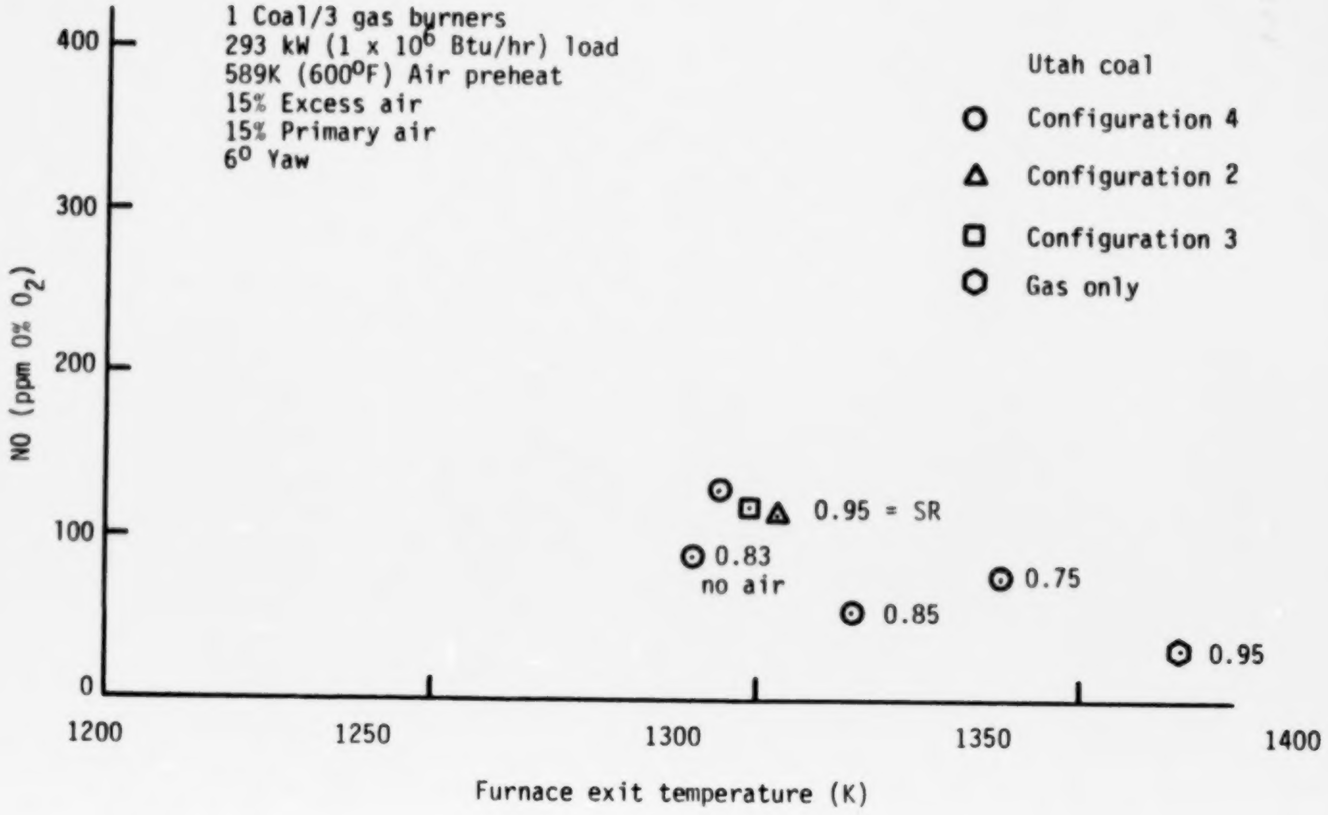

Figure 60. Burner configuration effect on NO during staging.

Figure 61 shows the NO results for configurations 2, 3, and 4 for gas firing rates from 0 to 293 kW (1 x 10^6 Btu/hr). At 0 kW gas firing, the vortex is absent and the burner flames are long and narrow. As the gas firing rate increases, the firebox vortex develops and the coal flame begins to broaden near the burner face and bend slightly, with ignition and burning increasing on the vortex side of the fuel jet. With further increases in gas firing rate, the fuel jet is dispersed about 20 fuel tube exit diameters from the burner face as shown in Figure 62. At this location, vortex interaction with the jet is significant enough to destroy the original collimated character of the burner jet. Dispersing the fuel in an overall oxygen-rich environment is detrimental to NO_x emissions. It should be noted that at 220 kW, the individual gas burner firing rates are the same as the coal burner firing rate. The results presented in Figure 61 show that the as-measured NO results do not increase significantly in going from 0 to 293 kW (1 x 10^6 Btu/hr). However, these results are uncorrected for dilution by the considerably lower NO content gas combustion products. Assuming a gas-only NO level of 75 ppm, a simple correction for dilution would show a consistent and large (an estimated 900 ppm at maximum firing rate) increase of NO for the coal burner as the gas firing rate is increased. This is a significant increase and demonstrates the importance of firebox mixing on NO. It should be noted that the 210 ppm level at 0 kW gas firing rate is consistent with long pulverized coal diffusion flames.

It should be note that during these vortex mixing intensity tests, some variation in temperature was experienced. This is the primary reason why the NO ranking of the configurations is different from the cases shown in Figure 59.

The results in Figure 61 also show the importance of the vortex to maintaining ignition and preventing high NO lifted flames. From Figure 61, it can be seen that at 147 kW (0.5 x 10^6 Btu/hr) gas firing rate, or higher, the difference in NO results between the configurations is small. At this firing rate, ignition of the coal flame by the vortex is very positive. However, at 0 kW gas firing rate, the vortex is absent and ignition is somewhat tenuous. Whereas configuration 3 experienced positive ignition at the burner face, configuration 4 did not and the flame was observed to detach from the burner face. This resulted in the large increase in NO as has been observed elsewhere for detached flames.

During all of these tests, CO and UHC emissions were small and combustion efficiency was good.

In summary, mixing tests showed that vortex mixing is very important to NO emissions. Increased vortex mixing leads to increasing NO. This is primarily a result of the dispersion of the latter part of the fuel jet beyond 20 burner exit diameters. However, the absence of vortex mixing can lead to a loss in burner ignition and high NO emission lifted flames can occur. Therefore, an optimal configuration might be to reduce mixing to the lowest level possible consistent with good positive ignition and CO, UHC, and carbon loss emissions.

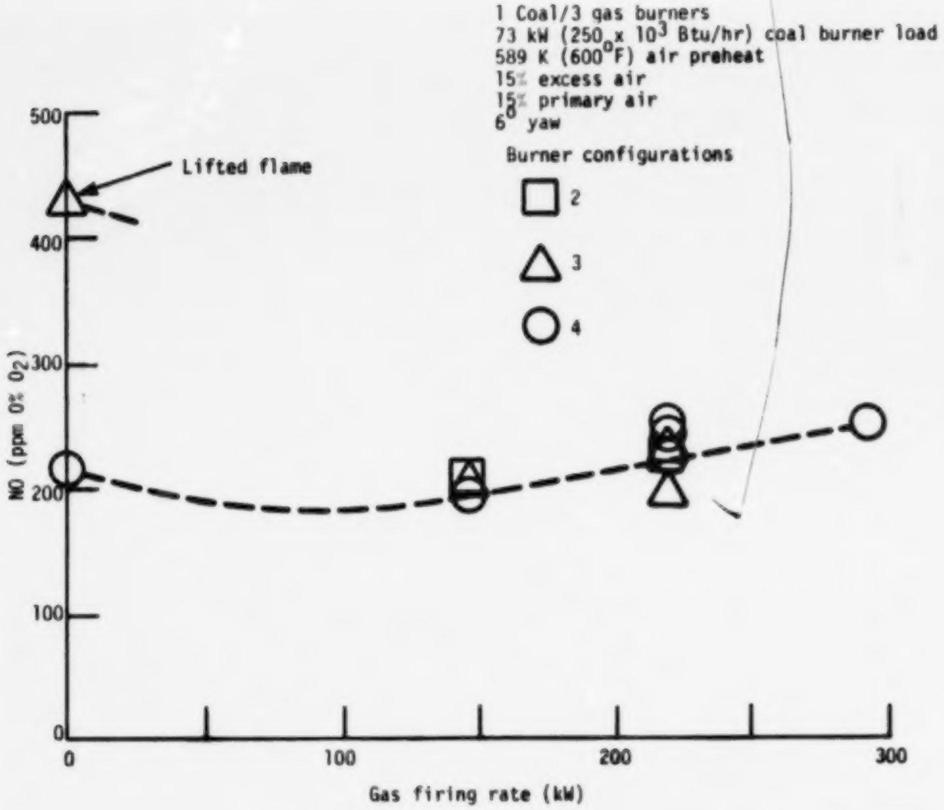

Figure 61. Burner configuration NO level variations with firing rate.

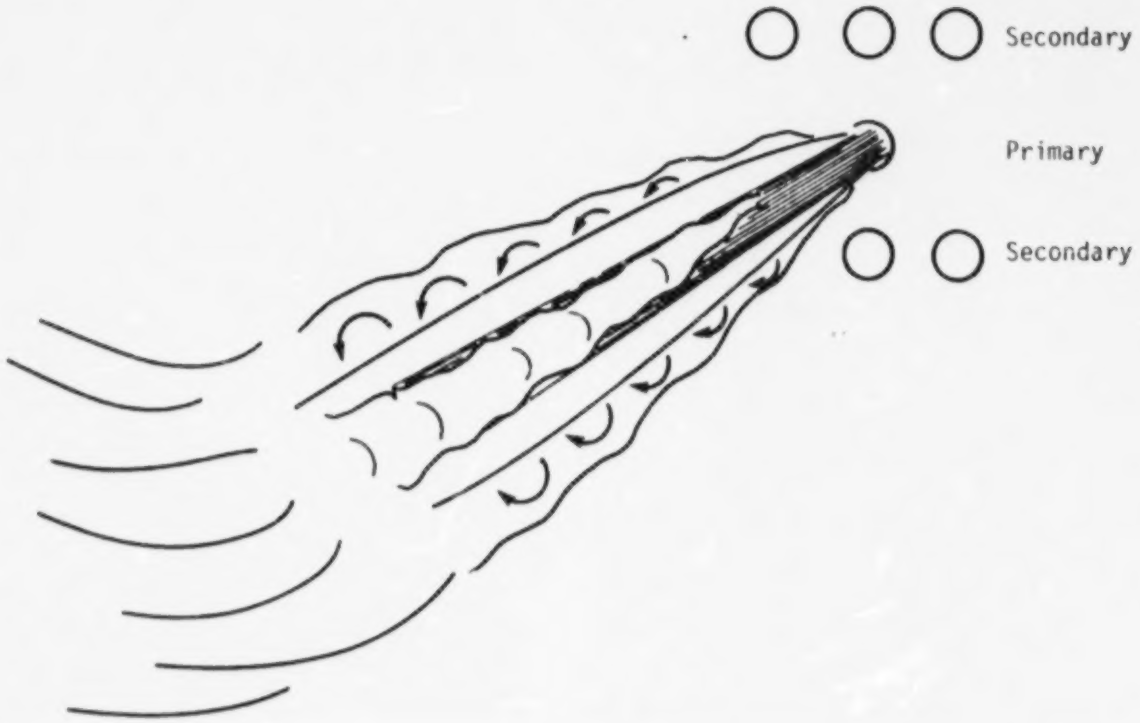
Secondary
Primary
Secondary

Figure 62. Flame visualization for configuration 4.

SECTION 5

LOW-NO_x SYSTEM DEFINITION

The purpose of the second phase of the study was to develop a low-NO_x combustion modification technique for retrofitting into existing, or incorporating into new, tangentially fired boiler designs. The understanding gained from the testing in the first phase of the study was fully applied in this development effort.

5.1 LOW-NO_x SYSTEM CONCEPT

Based on the observations detailed in Section 4, the following requirements for a low-NO_x tangential system were identified: (1) initiate burning sooner to minimize O_2 availability at the ignition point, (2) operate the jet interaction zone fuel-rich, (3) protect fuel jet from dispersion by vortex flow, (4) lower firebox mixing with the constraint of positive ignition, and (5) operate a portion of the char burnout zone oxygen-deficient to promote NO decay. In addition to these low-NO_x requirements, constraints must be applied regarding boiler size and efficiency, wall corrosion and slagging, and heat transfer. To minimize corrosion and slagging problems, oxygen-deficient combustion gases should not contact the walls. Also, sufficient time and oxygen must be available to fully burn the fuel and minimize carbon loss, and CO and UHC emissions. Finally, furnace volume and exit gas temperatures must be limited to those typical of presently operating units.

Figure 63 presents a top and side view schematic of the low-NO_x system with rich and lean zones identified. The major system features are: (1) fuel directed at a conventional tangential yaw angle into the center of the furnace, (2) some secondary air directed parallel to the fuel jet, either displaced toward the outside of the firebox relative to the fuel or surrounding the fuel jet, and (3) the bulk of the secondary air directed along the wall at and above the fuel jet elevation.

These major system features create oxygen-deficient conditions in the active near-burner and char burnout zones, and fuel-lean conditions on the furnace walls at and above the fuel jet elevation. These system characteristics address both the low-NO_x requirements and the operational constraints noted above.

The initial low-NO_x system tests used a configuration that had variable wall air injection angles with respect to both the furnace wall and the horizontal plane. This configuration, denoted System 1, is shown

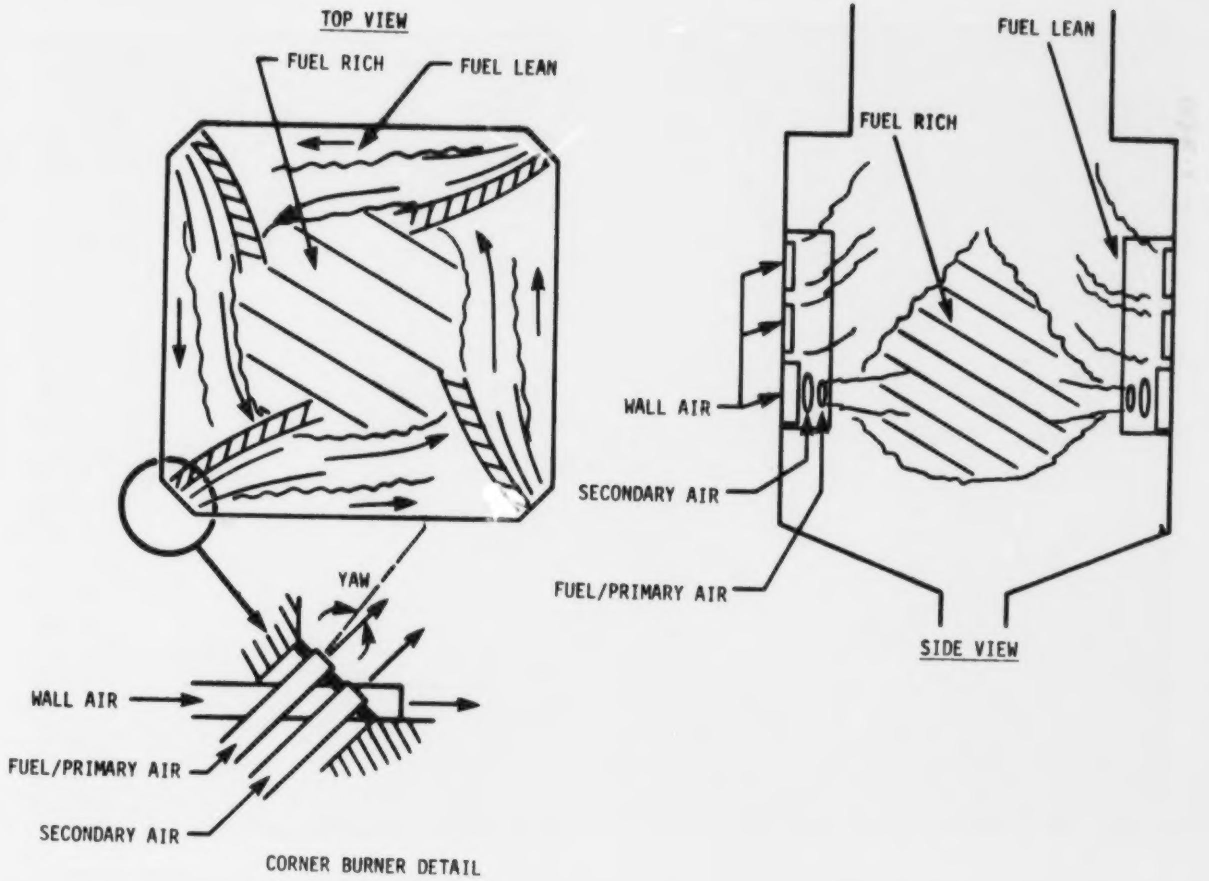
TOP VIEW
FUEL RICH
FUEL LEAN
YAW
WALL AIR
FUEL/PRIMARY AIR
SECONDARY AIR
CORNER BURNER DETAIL
FUEL LEAN
FUEL RICH
WALL AIR
SECONDARY AIR
FUEL/PRIMARY AIR
SIDE VIEW

Figure 63. Low-NO_x air-on-wall system schematic.

schematically in Figure 64. Subsequent testing used a configuration where all the wall air jets were confined to the burner blocks set in the corners of the firebox. This configuration, denoted System 2, is also shown schematically in Figure 64. Though less flexible than the initial configuration, System 2 is a closer representation of how the system might be retrofitted into a full-scale boiler. The primary emphasis of System 2 testing was to define the benefits of distributing the secondary combustion air over a wider elevation of the firebox. It should be noted that the true optimal low-NO_x configuration would probably require secondary combustion air to be more uniformly distributed over the furnace wall than is possible using the few discrete jets tested. However, the primary emphasis of this program is on retrofittable concepts that can achieve significant NO_x reductions without requiring major changes to tangentially fired boiler hardware. This confines the wall air jets to the corners of the firebox.

Both Systems 1 and 2 used refractory burner blocks, which for ease of modification, were cast onsite. The final testing used the System 3 burner schematicized in Figure 64. This burner had metallic burner ports to closely simulate a minimum modification retrofit of the concept into a modern tangentially fired boiler. Test results showed that all three burner systems were capable of significantly reducing NO_x under good combustion conditions.

5.2 LOW-NO_x SYSTEM 1 BURNER TEST RESULTS

For System 1 testing, the corner burners in the pilot-scale facility were modified as shown in Figure 64 to simulate the low-NO_x system illustrated in Figure 63. Tests were then initiated to optimize the primary, center, and wall jet configuration, placement, direction, and velocity. The purpose of these tests was to define the primary, center* and wall jet configurations and angles for optimal NO reduction under acceptable combustion conditions.

5.2.1 Low-NO_x System 1 Burner Design

For ease and economy of fabrication, the low-NO_x System 1 burners were cast of high-temperature refractory material. As shown in Figure 64, the center air port was cast into the blocks with the primary air and fuel being supplied through a metallic pipe or cast into the burner blocks. This method of fabrication demonstrated great durability during the test program. Of course, utilizing refractory blocks constrained the possible burner port geometries to those having significant section thicknesses for needed strength. This did not present a problem since System 1 burner testing focused only on the concept's general emissions and combustion performance. Systems 2 and 3 burner designs, particularly System 3, focused more on packaging the low-NO_x concept into designs which could be retrofitted into modern full-scale tangential utility boilers.

---

*Defined as the fraction of secondary combustion air which is directed into the center of the furnace at conventional burner yaw angles.

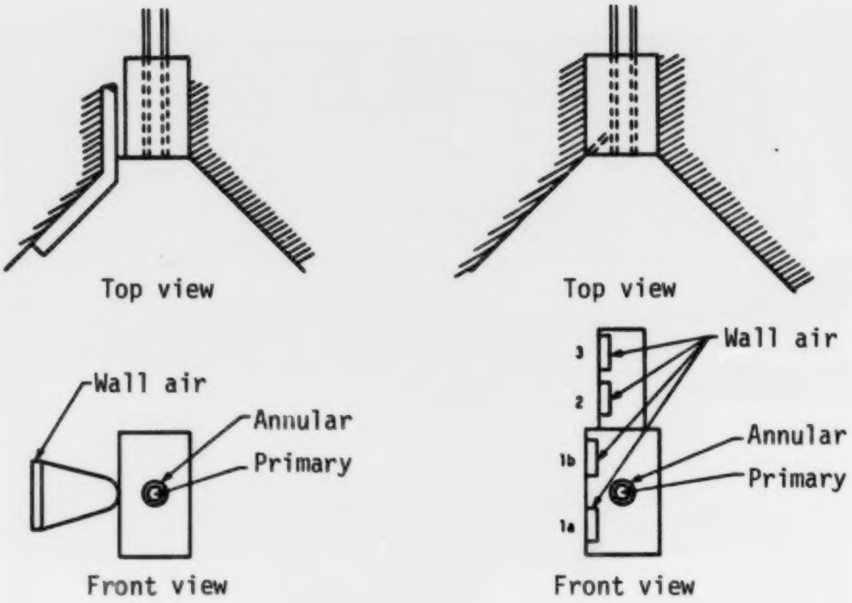
Top view
Wall air
Annular
Primary
Front view
Top view
3
2
1b
1a
Wall air
Annular
Primary
Front view

System 1

System 2

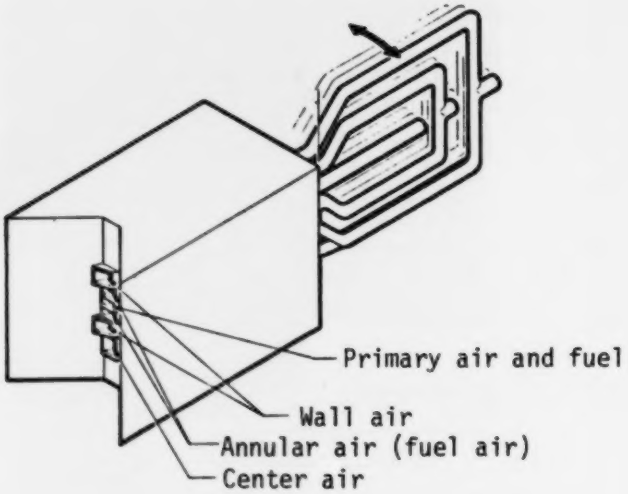
Primary air and fuel
Wall air
Annular air (fuel air)
Center air

System 3

Figure 64. Schematic of Systems 1, 2, and 3 low-NO_x burners.

The wall jets for the System 1 burners consisted of independent supply pipes which terminated in either circular or flat diffuser exit nozzles (see Figure 64). The tips of these nozzles were located roughly one-third of the distance down the furnace wall. These independent wall jets could be either rotated in the vertical plane or directed angularly away from the wall in the horizontal plane to assess the impact of wall jet orientation on NO and combustion performance.

The primary, center, and wall airflows were independently controlled. The center and wall air was preheated to 589 K (600°F) while the primary air was unheated. The staged performance of these burners was tested by utilizing the existing staged air ports described in Section 1. The staged air was also heated to 589 K (600°F) for all tests.

For most cases, the primary airflow nozzle was designed to yield the same exit velocity as the baseline burner tests described in Section 4. Since the center and wall air port geometries changed between configurations, the exit velocity of these jets varied both with these changes and as a percent of the secondary airflow split between the center and wall air ports. Velocities lower and higher than the primary jet velocity were tested.

5.2.2 Primary, Center, and Wall Jet Configuration Testing

Figures 65 through 67 provide schematics of the System 1 burner primary, center, and wall air port configurations tested. As shown in Figure 65, while configuration G was similar to configuration 2 tested in the near-burner mixing study, it departed from configuration 2 by integrating a 5.8-cm (2-inch) diameter wall air jet. Configuration H was identical to configuration G except the circular tube wall jet was replaced by a 15.2 x 0.95 cm (6 x 3/8 inch) slot jet.

Configurations I, J, and K, also given in Figure 65, had similar center air ports and slot wall jets directed along the wall, but different primary configurations. These variable primary configurations were used to define the effect on NO of exposing a greater surface area of the fuel jet flow to the hot vortex gases for a given amount of flow area. The circular primary configuration represented the case of minimum surface area per flow area. The long slot primary configuration had the greatest surface area per flow area of all configurations tested.

Figure 68 presents the NO results for configurations G, H, I, and J as a function of the percent of secondary combustion air flowing in the wall jet. With configuration G as well as all subsequent configurations, the presence of a strong vortex, similar to that in conventional tangential firing, was observed at both low and high percent air on the wall; the rotational velocity of the vortex increased with percent wall air. Configuration G results show that NO decreased as percent wall air increased until a minimum level of about 320 ppm was reached at 50 to 70 percent wall air. For configuration H, NO decreased monotonically with increasing percent wall air. At lower and higher percent wall air, configuration H results were, respectively, higher and lower than configuration G results. Configuration H reached minimum NO levels of about 250 ppm at 100 percent air on the wall. As

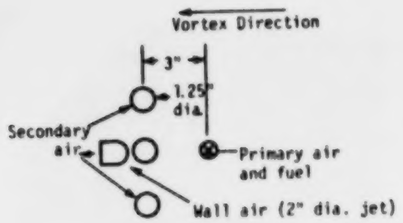
Vortex Direction
3"
1.25" dia.
Secondary air
Primary air and fuel
Wall air (2" dia. jet)

Configuration G

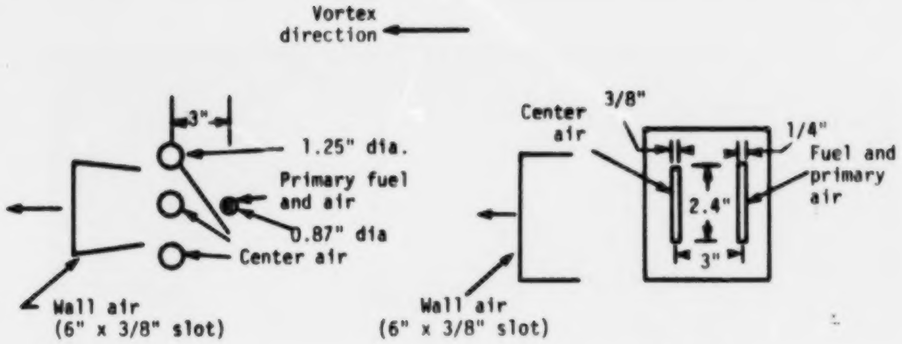
Vortex direction
3"
1.25" dia.
Primary fuel and air
0.87" dia
Center air
Wall air (6" x 3/8" slot)
Center air
3/8"
1/4"
Fuel and primary air
2.4"
3"
Wall air (6" x 3/8" slot)

Configuration H

Configuration I

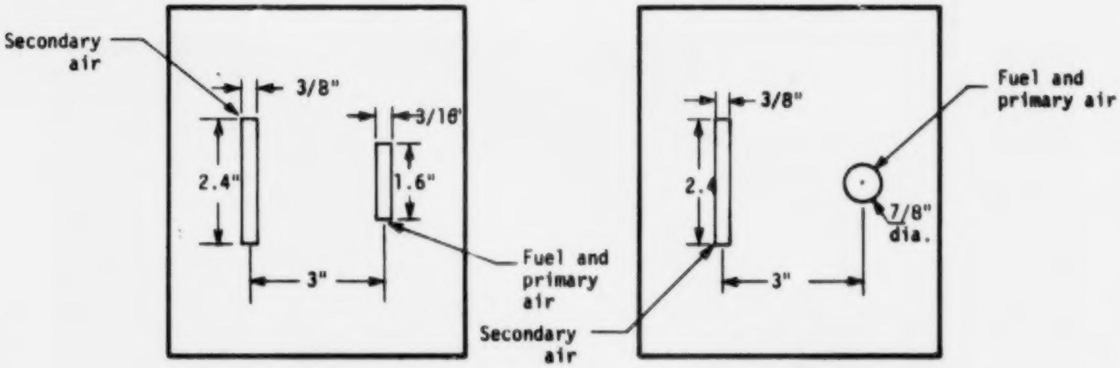
Secondary air
3/8"
3/16"
2.4"
1.6"
3"
Fuel and primary air
Secondary air
3/8"
2.4
Fuel and primary air
7/8" dia.
3"

Configuration J

Configuration K

Figure 65. Corner burner configurations G, H, I, J, and K.

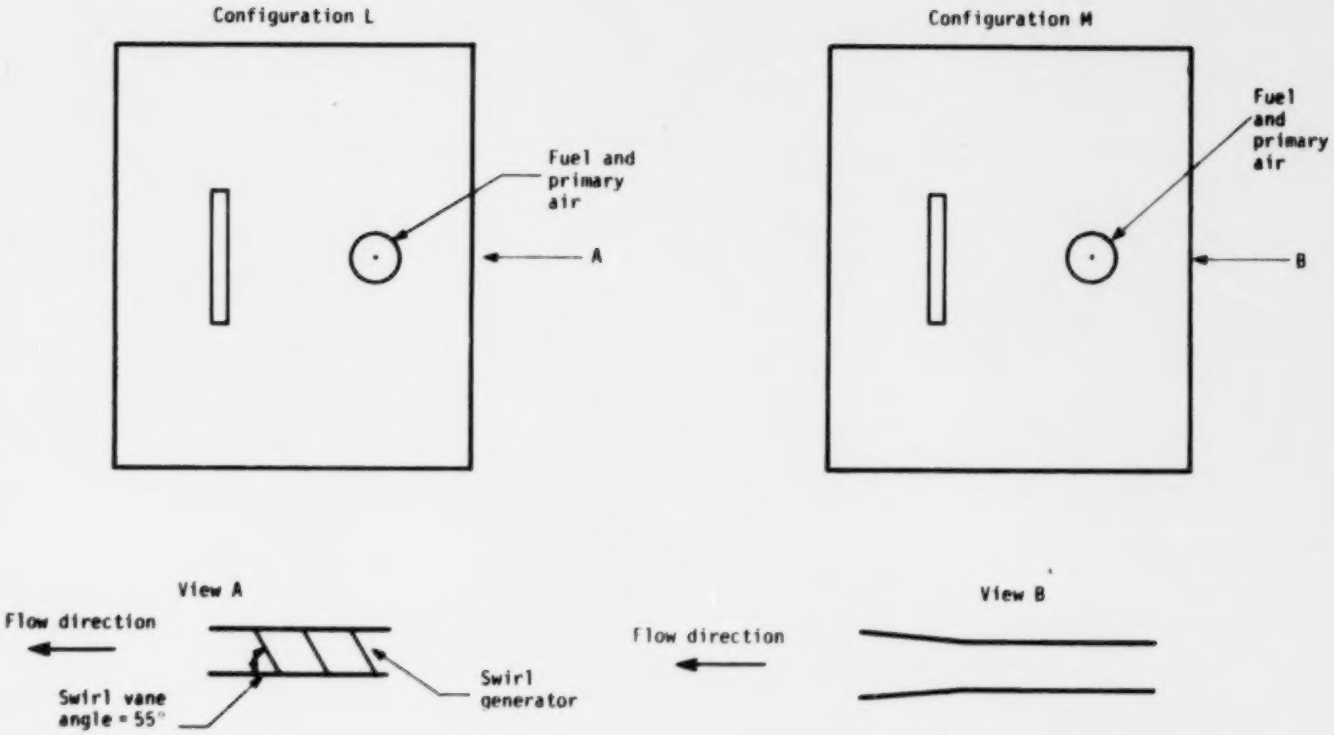
Configuration L
Configuration M
Fuel and primary air
Fuel and primary air
A
B
View A
View B
Flow direction
Flow direction
Swirl vane angle = 55°
Swirl generator

Figure 66. Corner burner configurations L and M.

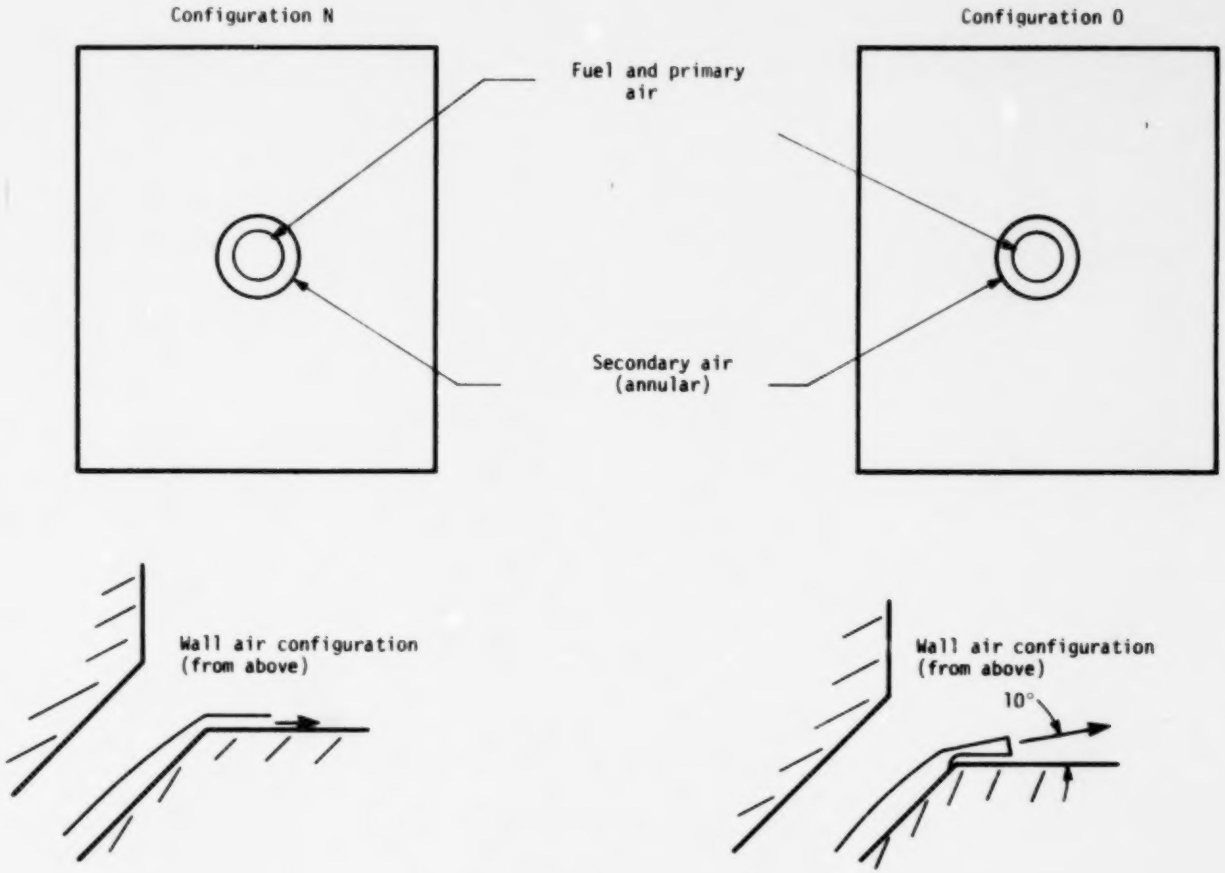
Configuration N
Configuration O
Fuel and primary air
Secondary air (annular)
Wall air configuration (from above)
Wall air configuration (from above)
10°

Figure 67. Corner burner configurations N and O.

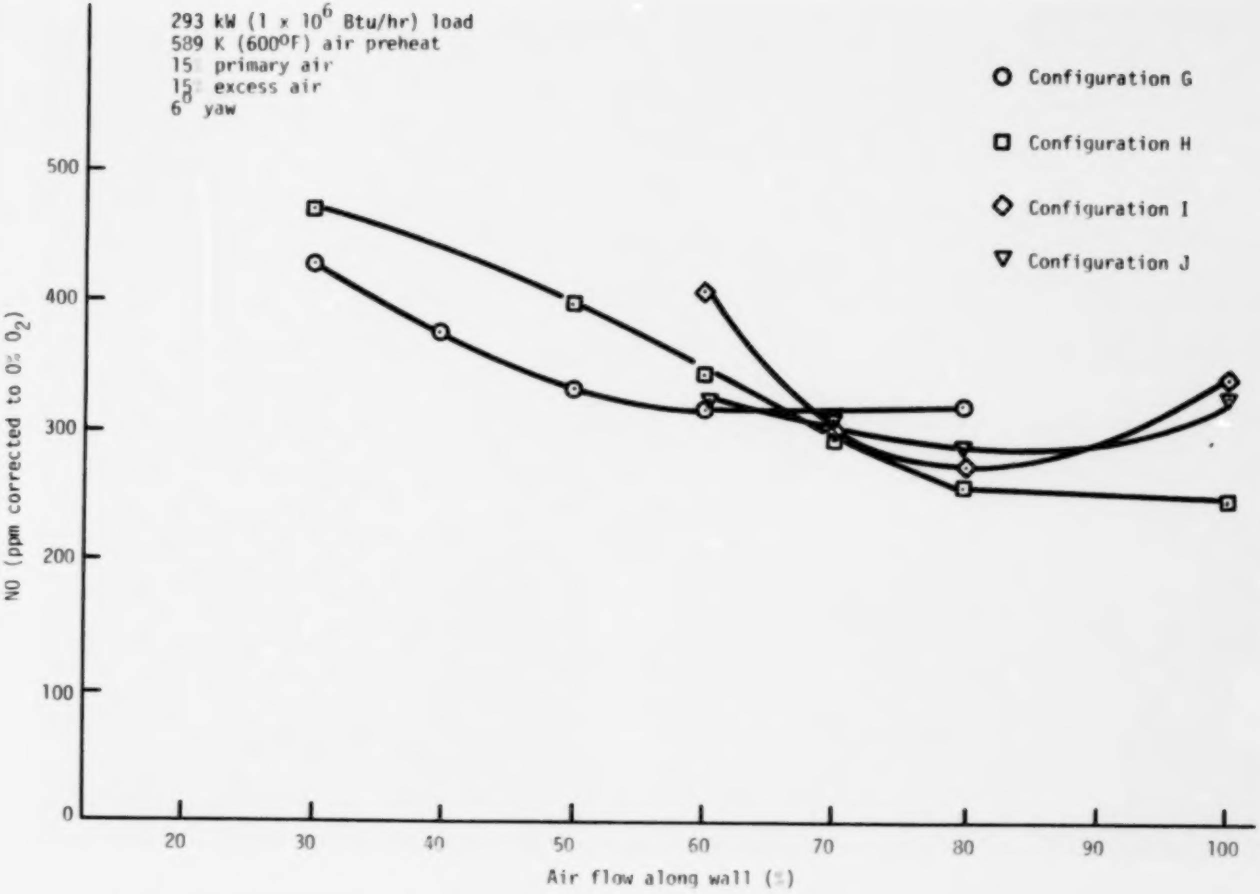

Figure 68. Configurations G, H, I, and J NO versus percent wall air.

indicated above, the only difference between configurations G and H was the change from a circular to a slot wall air jet. The slot wall jet for configuration H was expected to reduce fuel/air mixing by spreading the air in the relatively aerodynamically quiescent region along the wall. Comparison of configuration G and H results confirms that slot wall jets are beneficial to NO at high percent wall air.

For 100 percent air on the wall, only 15 percent of the total combustion air is directed into the center of the furnace in the primary stream with the fuel. However, due to the entrainment of wall air into the center of the furnace by the primary jets, the fuel/air separation remains fairly modest even at 100 percent air on the wall. This is demonstrated by in-flame probing test results (see Figure 69) which show that, as percent wall air was increased from 30 to 80 percent, the oxygen concentration in the central core region of the furnace (measured at 0.20m or 8 inches above the fuel entry elevation) decreased to nearly zero. Since solids sampled in the center of the furnace showed that the fuel was consumed to the extent of oxygen available, the high average oxygen concentrations in the center of the furnace with 30 percent wall air indicated that the center of the furnace, on the average, was not very fuel-rich. At 80 percent air on the wall, the center of the furnace was fuel-rich, and solid samples showed that roughly 80 percent of the fuel was consumed in the center of the furnace. This indicated a local SR of approximately 0.8 in the center of the furnace, which has been found in staging tests to be effective for NO reduction (Reference 9).

It is of interest to note that 80 percent of the secondary combustion air is needed to achieve, roughly, a SR of 0.8 in the center of the furnace. Obviously, in this case air which is directed along the wall immediately begins to mix into the center of the furnace and continues mixing with vertical height until fuel, air, and combustion products are fully mixed. Figure 70 gives the firebox concentrations of NO and O_2 at 0.45m (18 inches) above the fuel entry elevation. By comparing these results to those for 0.20m (8 inches) above the fuel entry elevation (Figure 69), it can be seen that the fuel-rich region, where O_2 concentrations are near zero, has become smaller, and NO concentrations are more uniform.

These probing results clearly show that the wall air approach develops a fuel-rich region in the center of the firebox, similar to that which develops in the lower furnace of a staged combustion system. As the stack NO_x emission results show, fuel burned in this region will have a lower potential for producing NO_x.

Configurations I and J introduced center and primary air into the furnace as rectangular jets. The greater surface area to flow area of these jets caused more rapid ignition of the fuel and a greater amount of burning prior to mixing with the vortex. These configurations explored the benefits of increasing diffusion burning while decreasing the amount of burning in the center of the furnace. To limit initial mixing between the primary and center air streams, the secondary air ports of configurations I and J were sized to yield equal velocities for the primary and center air jets at 80 percent air on the wall.

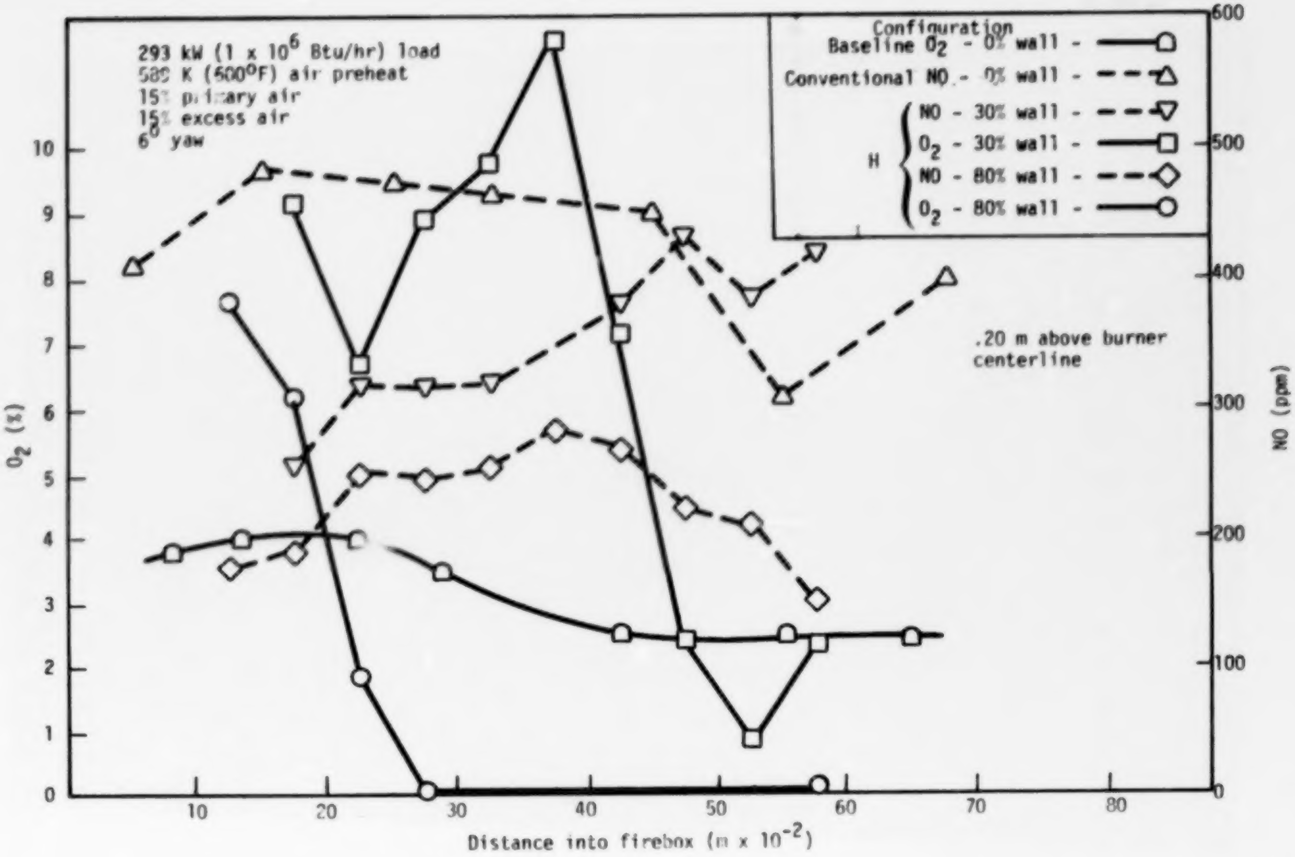

Figure 69. Configuration H NO and O_2 firebox concentrations 0.20m above the fuel entry elevation.

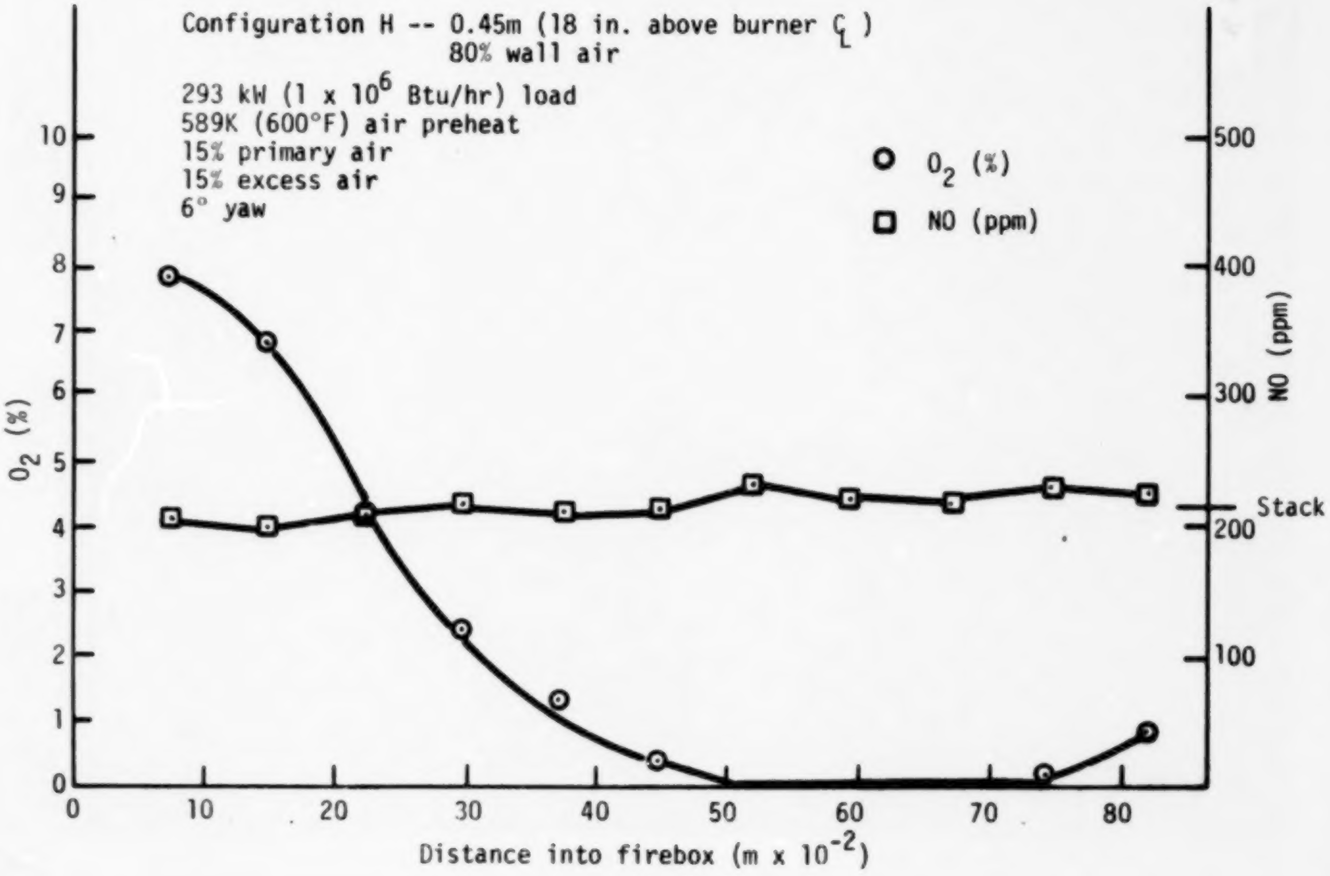

Figure 70. Configuration H NO and O_2 concentrations across firebox at 0.45m above the fuel entry elevation.

NO results for configurations I and J, given in Figure 68, show that the slot jets had higher NO minimums than the circular jets (configuration H), the long slot primary jet (configuration I) giving the highest NO minimum. Also, with configurations I and J the NO minimums occured at a percent wall air of around 80 percent.

Greater exposure of the fuel to hot gases using these slot primary configurations was not beneficial to NO. The more rapid initiation of fuel burning, which was proven beneficial in the burner definition tests in Section 4, probably was offset by the reduced penetration of fuel into the center of the furnace. For these configurations, diffusion burning of the fuel jet was traded for less burning in the fuel-rich core at the center of the furnace. Also, the larger surface area of the slot jets entrained more wall air into the center of the furnace. Flame observation also showed that significant fuel jet stripping took place due to wall air and vortex flow impact on this larger surface area jet. This impact dispersed some of the fuel into the wall air, further reducing the fuel-rich nature of the center of the furnace.

This is supported by comparing in Figures 71 and 70 the probing results 0.45m (18 inches) above the fuel entry elevation for configurations I and H, respectively. The configuration I slot primary results, given in Figure 71, show no evidence of a fuel-rich region, whereas the configuration H circular primary results in Figure 70 show a significant fuel-rich region in the center of the furnace.

Since the center air jets of configurations H, I, and J were different, configuration K, a circular primary jet with a center air port identical to configurations I and J, was also tested. Figure 72 compares the slot primary cases (configurations I and J) to the circular primary case (configuration K) for equivalent center and wall air configurations. These results show that the circular primary jet gave better NO results for percent wall airflows above 60 percent. Flame observation also showed that the circular primary jet had better penetration to the center of the furnace than the slot primary cases. This better penetration causes the center of the furnace to operate more fuel-rich, as can be seen in Figures 73, 74, and 75 which present the probing results at 0.20m (8 inches) above the fuel entry elevation for configurations I, J, and K, respectively. Configuration K had the most extensive fuel-rich core, followed by configuration J and then I. This order corresponds to the primary jet's decreasing amount of surface area versus flow area and confirms the benefit of fuel penetration to NO.

Primary configurations L and M were schematized previously in Figure 66. These configurations were similar to configuration K except that configuration L had a helical swirl generator inserted in the primary jet and configuration M had a diverging primary flow.

Configuration L was an attempt to increase the fuel residence time prior to the fuel-jet/vortex interaction without lowering the primary jet exit velocity; this would maintain the fuel in a more highly stratified form for a longer period of time. Unfortunately, along with providing a longer residence time, the swirl increased fuel-jet/wall-air mixing; observations of the fuel

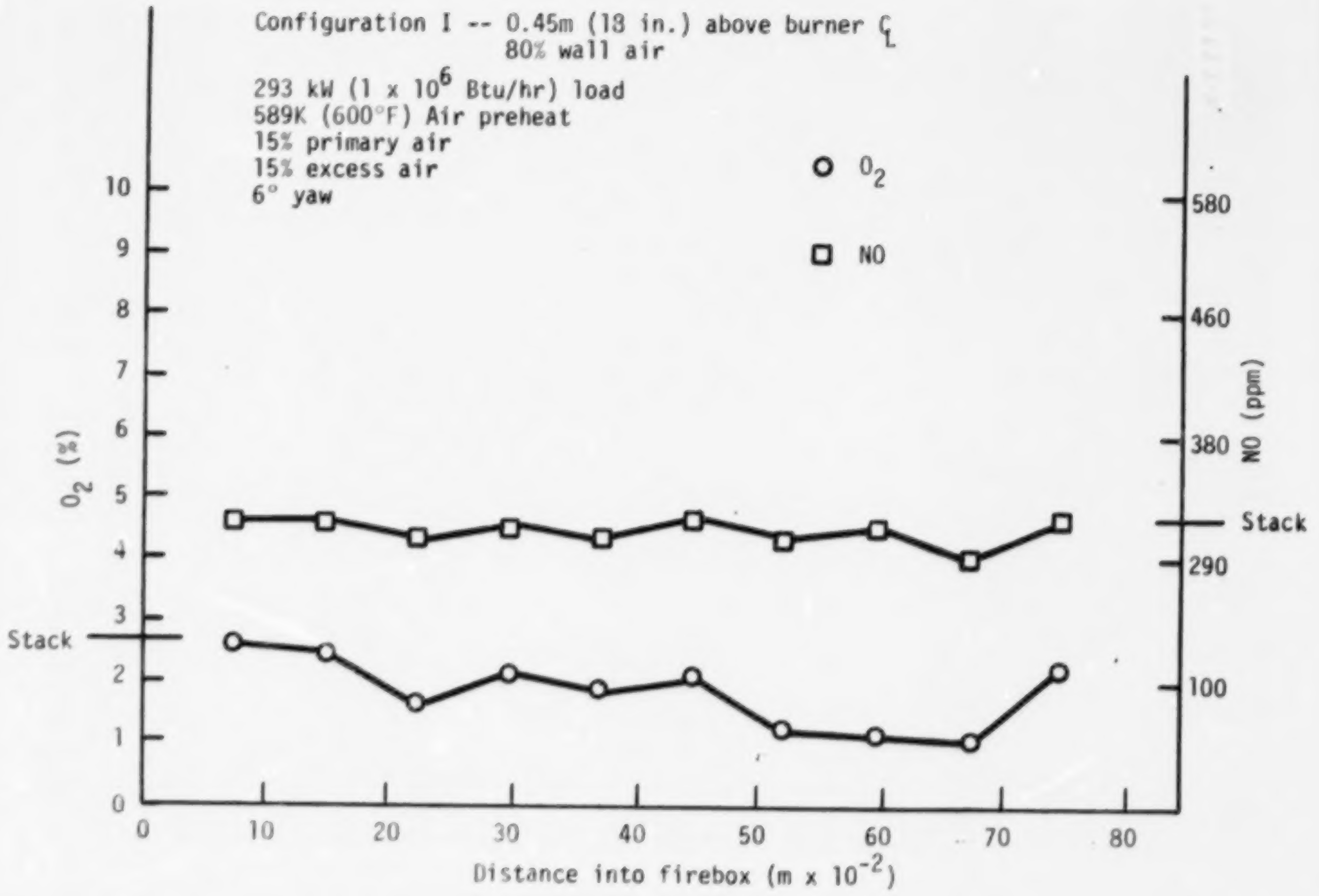

Figure 71. Configuration I NO and O$_2$ concentrations across firebox at 0.45m above the fuel entry elevation.

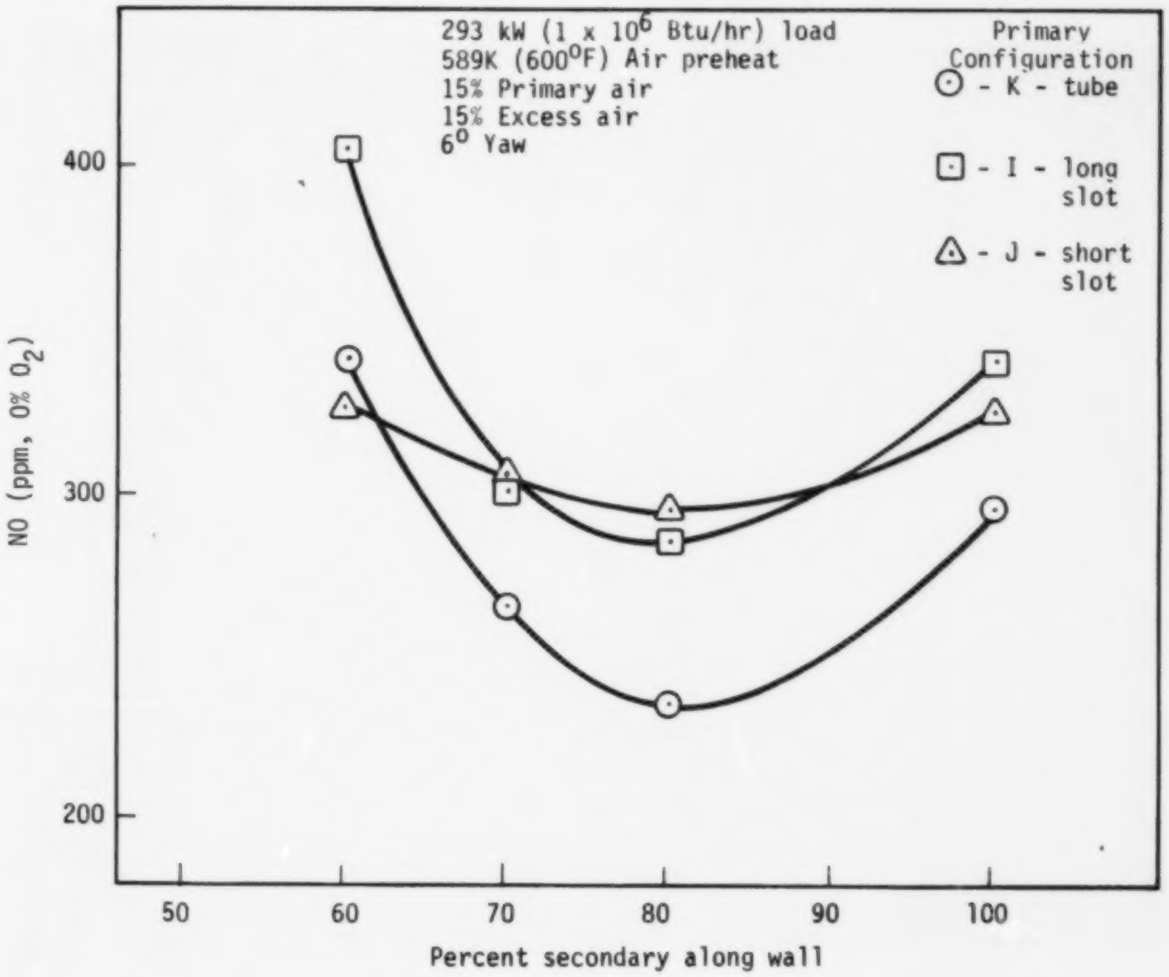

Figure 72. Configurations I, J, and K NO results versus percent wall air.

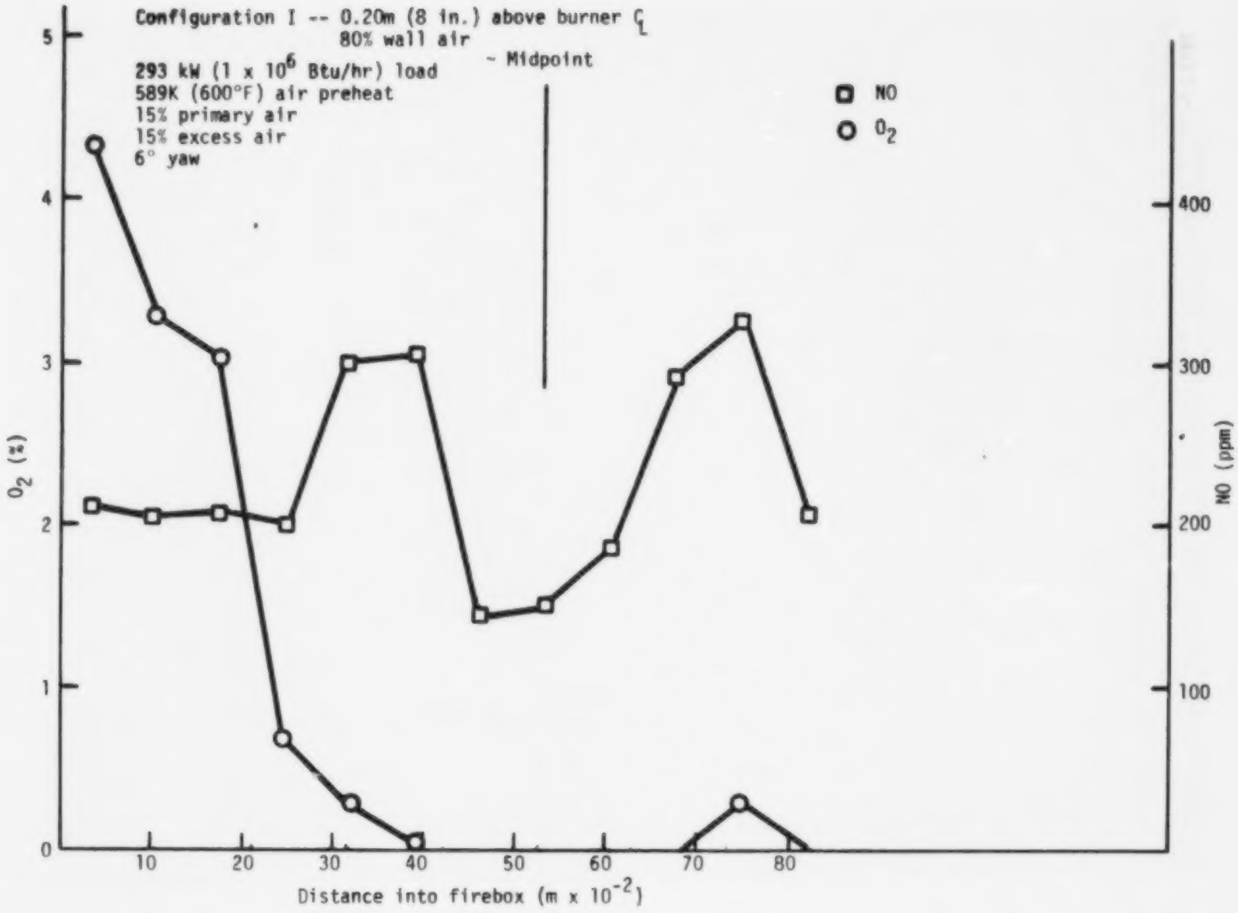

Figure 73. Configuration I NO and O_2 firebox probing results 0.20m above the fuel entry elevation.

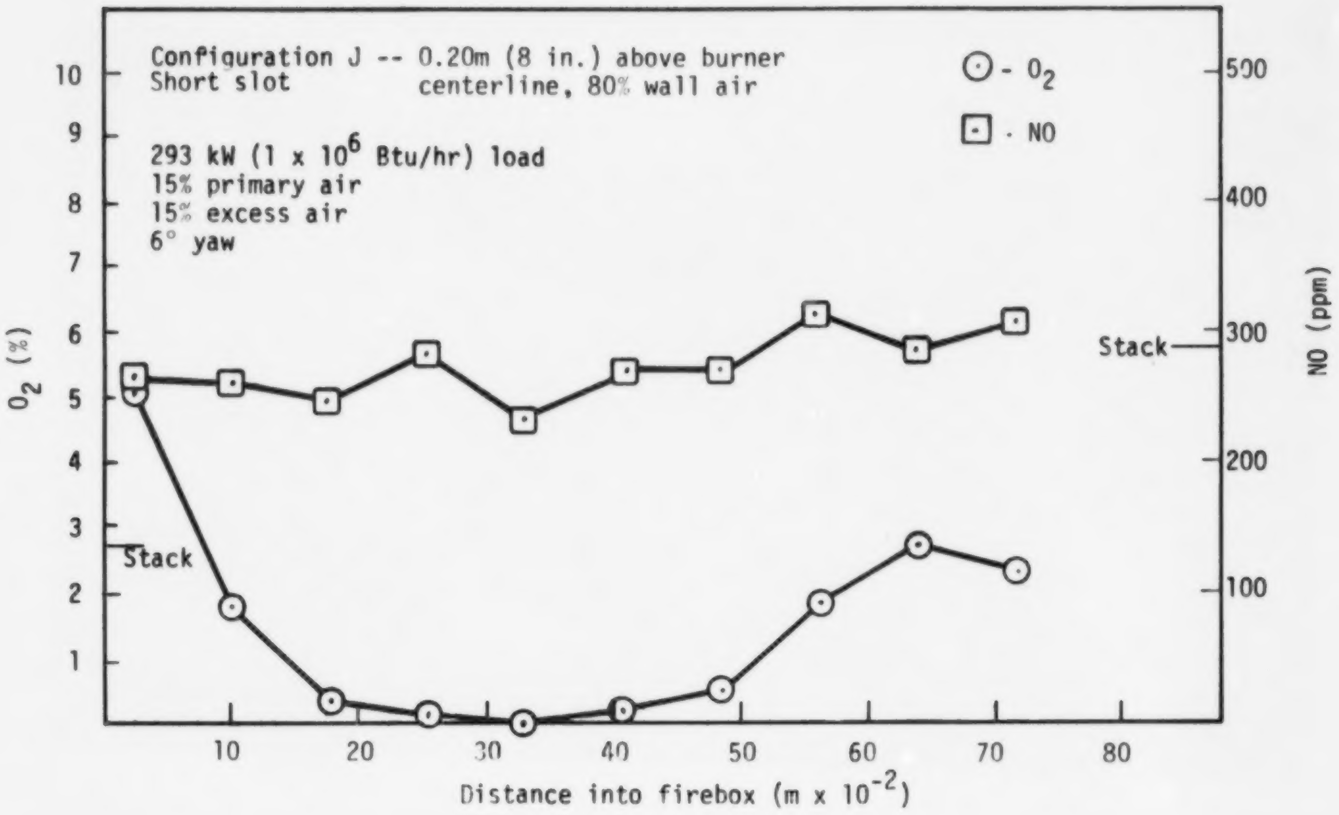

Figure 74. Configuration J NO and O_2 firebox probing results 0.20m above the fuel entry elevation.

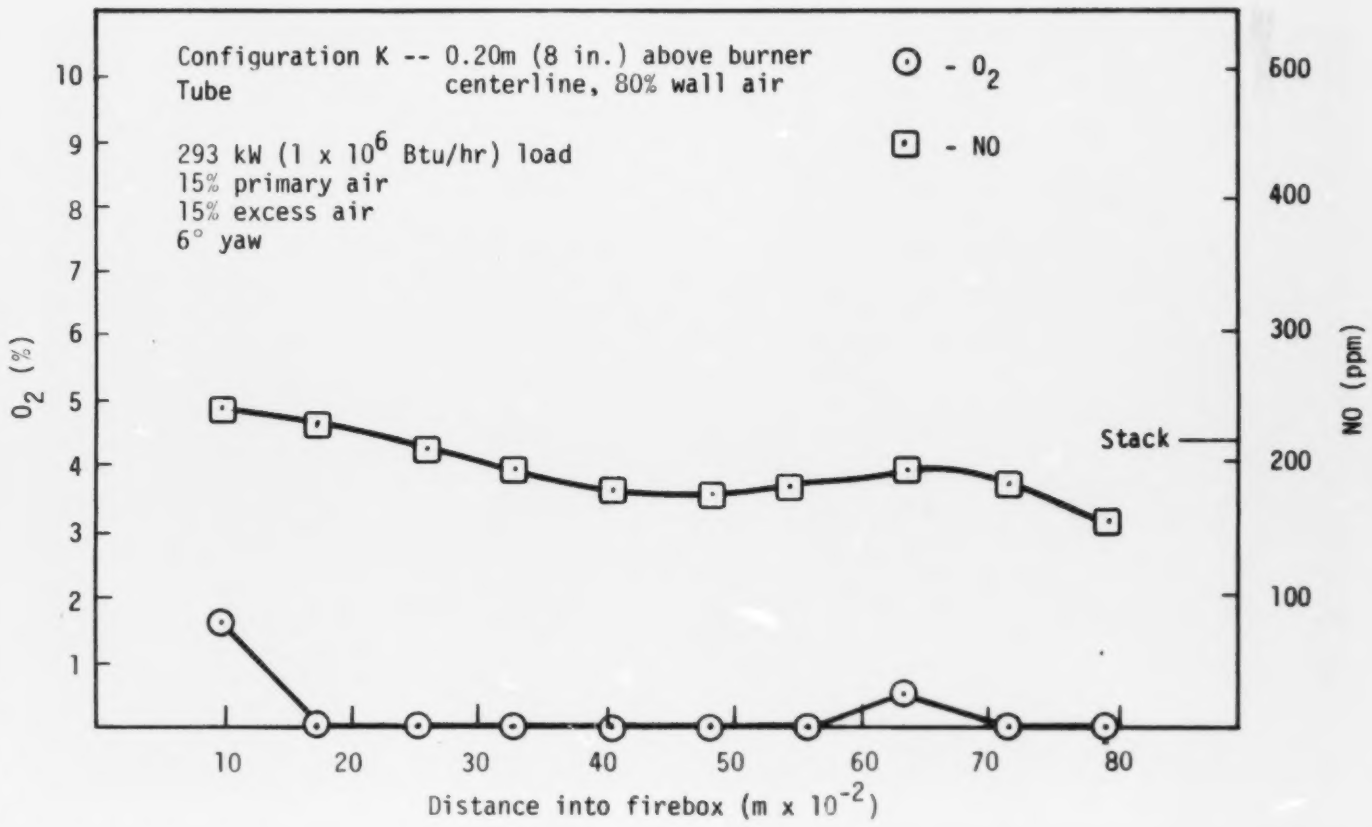

Figure 75. Configuration K NO and O_2 firebox probing results 0.20m above the fuel entry elevation.

jet showed that fuel was stripped from the jet and dispersed into the wall air region. This resulted in the disappearance of the fuel-rich zone from the center of the furnace and in higher NO levels, as can be seen in Figures 76 and 77, respectively. For this configuration, the detrimental effect of dispersing the fuel in the firebox offset any benefit of increased residence time prior to vortex interaction.

Configuration M was an attempt to collimate the fuel into a dense core in the center of the primary jet prior to exiting the burner. With this diverging primary flow, it was hoped that any primary jet stripping by the vortex or wall airflow would not disperse the fuel as much as in configuration K. However, observation showed that the diverging nature of the primary airflow resulted in more mixing of fuel and air than did configuration K. This was detrimental to the creation of the fuel-rich core and therefore stack NO, as can be seen from the probing results in Figure 78 and the stack NO results in Figure 77.

Based on results from configurations G through M, it was concluded that fuel jet penetration to the center of the furnace without significant fuel jet stripping by the wall jets or vortex was very important to NO. Configuration N, shown previously in Figure 67, surrounded the primary fuel jet with the air jet. The purpose of the coannular center air jet was to protect the primary fuel jet from stripping by the wall jet or vortex flow. With the coannular configuration, only the center air jet would be impacted by the wall jet and vortex flow, and more fuel would penetrate to the center of the furnace. Figure 79 shows that configuration N produced a significant fuel-rich region in the center of the furnace, and Figure 77 shows that the stack NO results were significantly better than those for configurations L and M at 80 percent air on the wall. However, at 60 and 100 percent air on the wall, configuration N results were not significantly better than those for configuration M. As indicated previously, the center air port area for configuration N was designed to match primary and center air velocities at 80 percent air on the wall. At 60 and 100 percent air on the wall, the velocity differences between the primary and center jets caused shear which mixed the fuel and center air rapidly, reducing fuel penetration to the center of the furnace.

As found for configuration K, configuration N probing results 0.45m (18 inches) above the fuel entry elevation (Figure 80) show a significant fuel-rich core.

5.2.3 Wall Jet Orientation

The purpose of these tests was to determine the impact of wall jet orientation on NO_x and combustion performance. Configuration N primary, center, and wall air port arrangements were used in configuration O to test the effect on NO_x of moving the wall jet away from the wall in the horizontal plane. Configuration G primary, center, and wall air port arrangements were used to test the effect on NO_x of inclining the wall jet in the vertical plane.

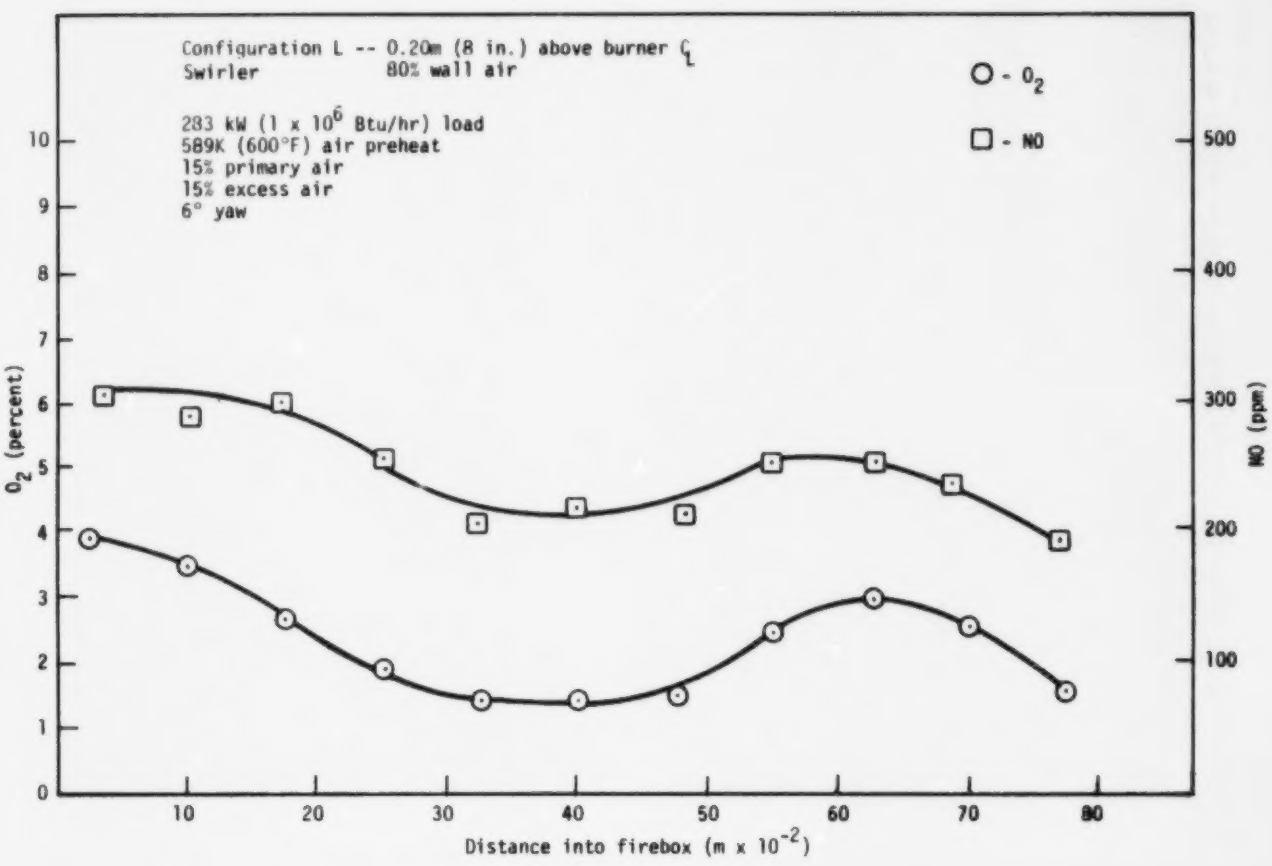

Figure 76. Configuration L NO and O_2 firebox concentrations 0.20m above the fuel entry elevation.

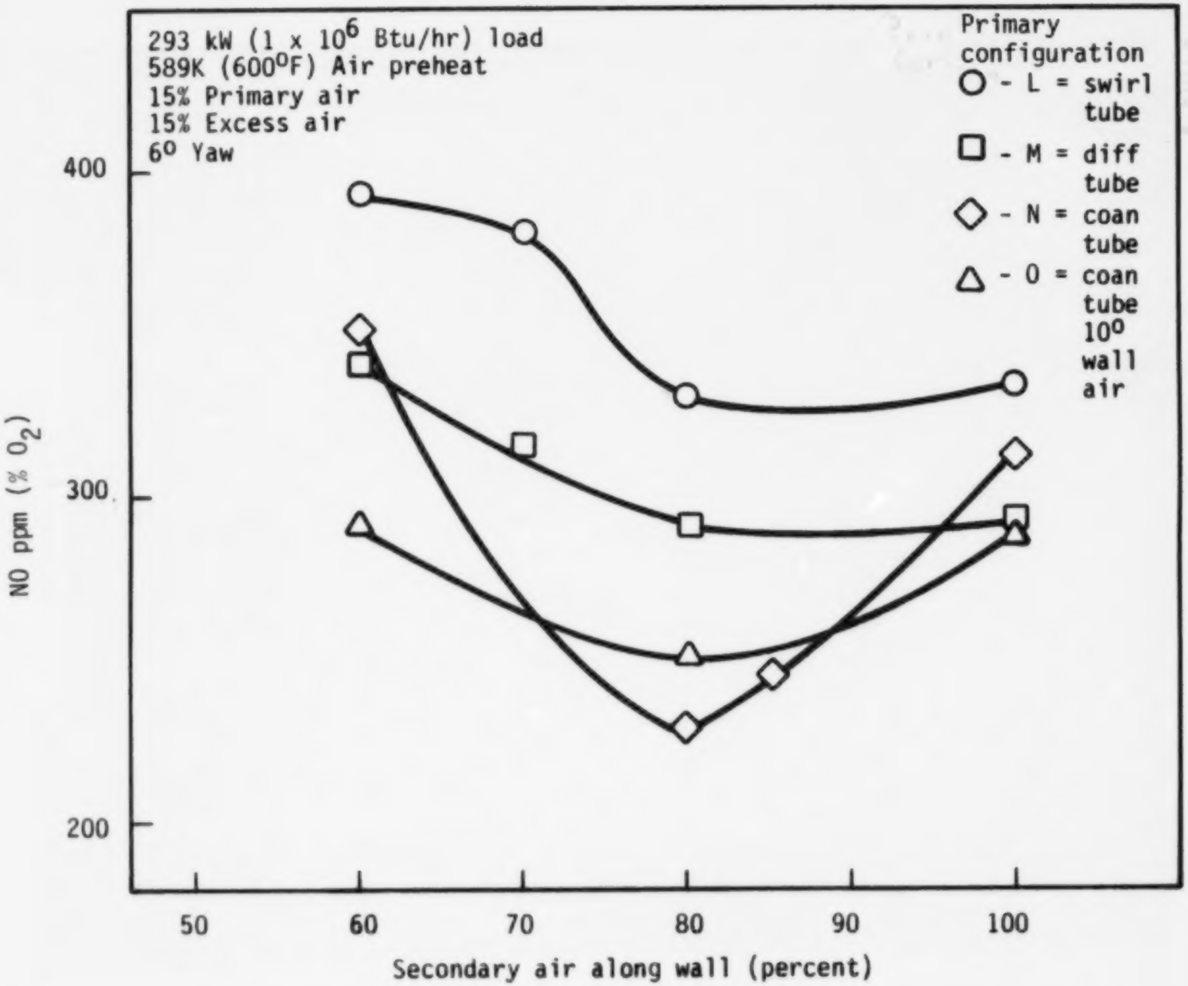

Figure 77. Configurations L, M, N, and O NO concentrations versus percent wall air.

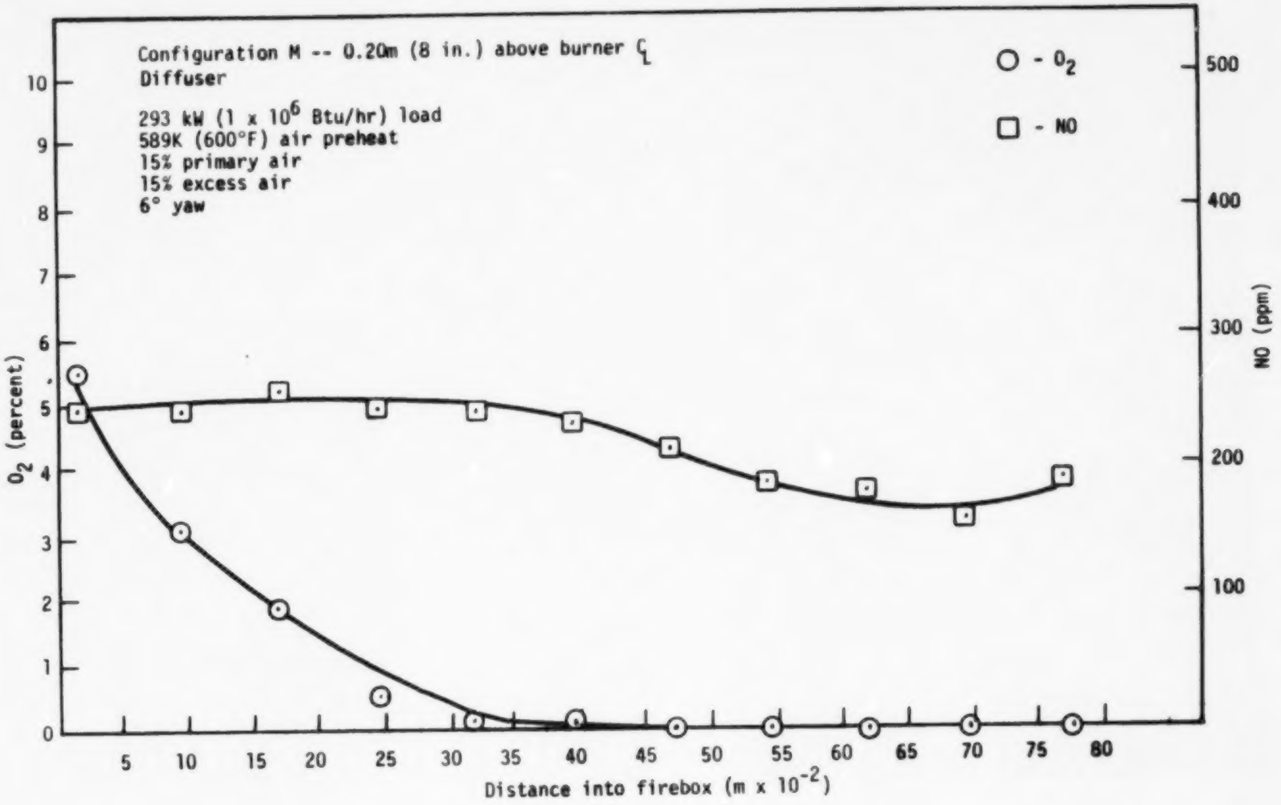

Figure 78. Configuration M NO and O_2 firebox concentrations 0.20m above the fuel entry elevation.

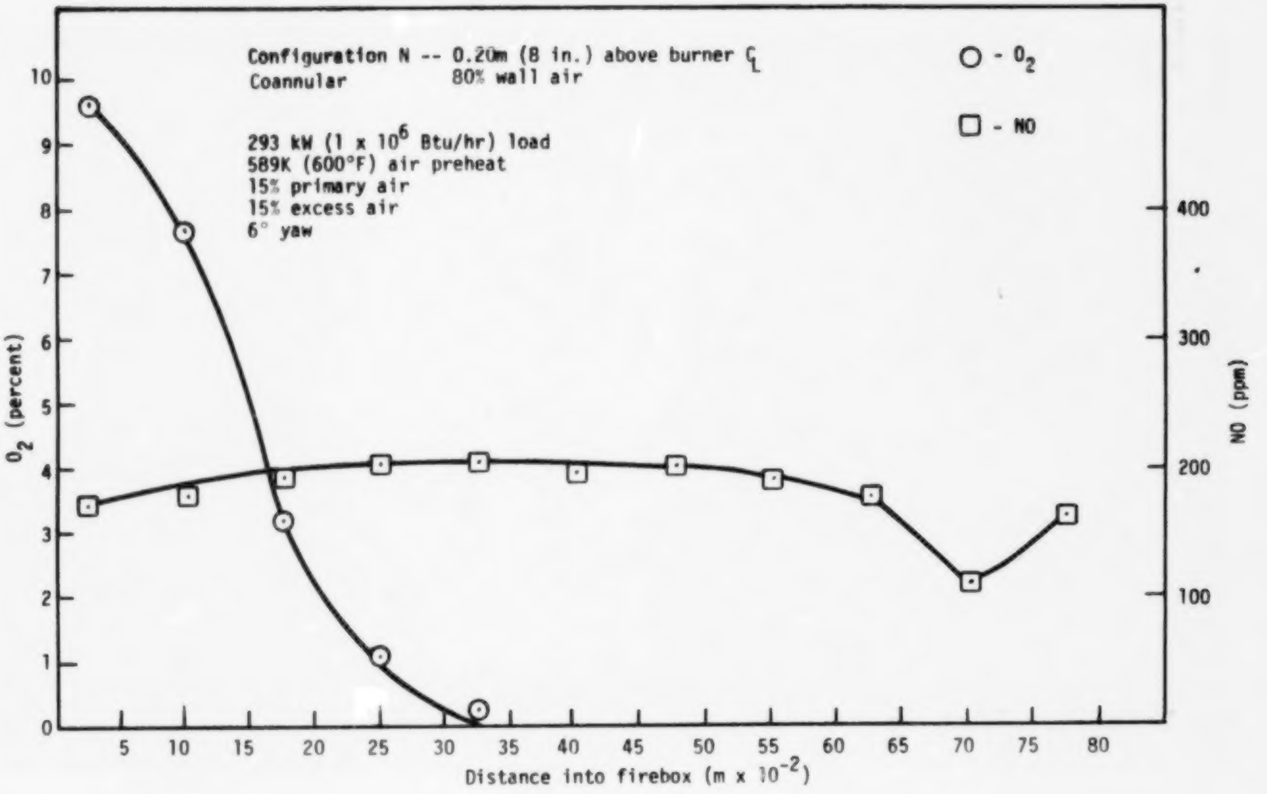

Figure 79. Configuration N NO and O_2 firebox concentrations 0.20m above the fuel entry elevation.

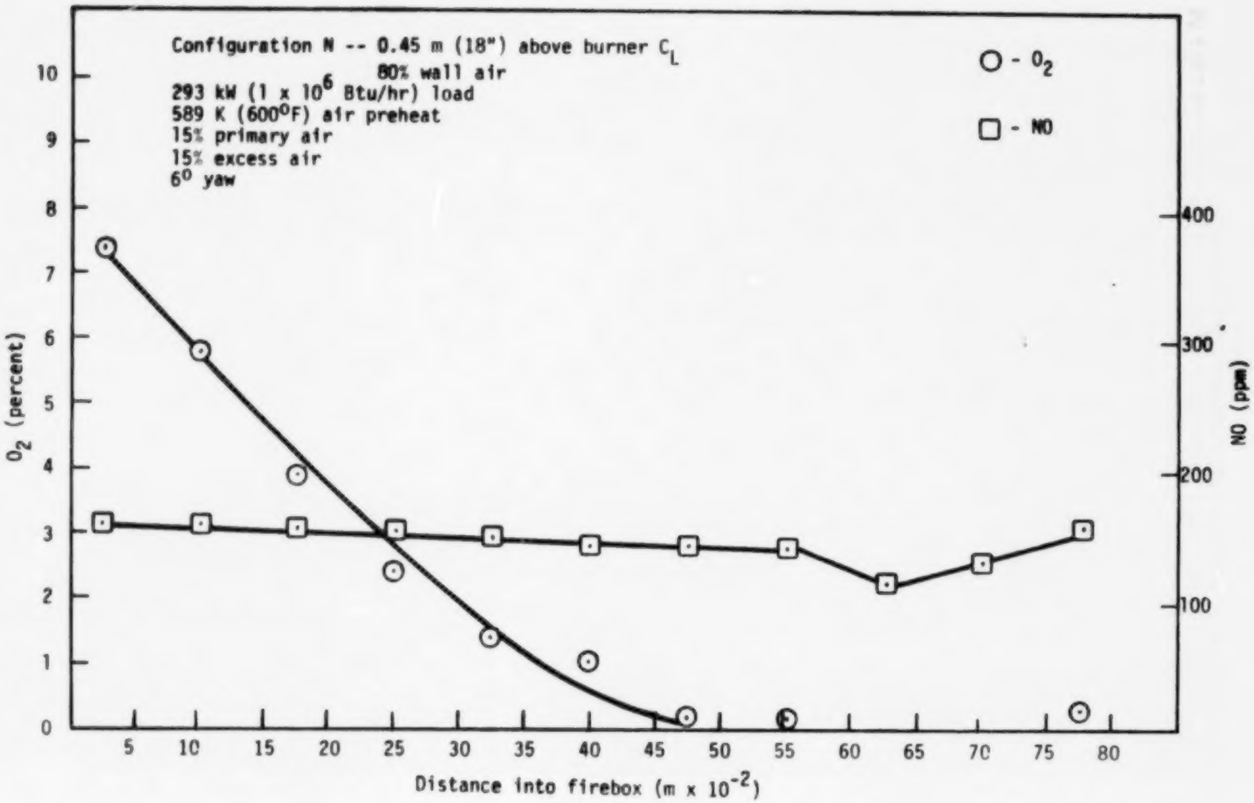

Figure 80. Configuration N NO and O_2 concentrations 0.45m above the fuel entry elevation.

As shown previously in Figure 67, configuration O used the same coannular primary/center air configuration as did configuration N. However, in configuration O the wall air jet was directed at a 10° angle off the furnace wall to determine the effect on NO of directing the wall air at an angle to the wall. The NO results in Figure 77 show that configuration O had marginally better results than configuration N at 60 and 100 percent air on the wall and marginally poorer results at 80 percent air on the wall. More importantly, the probing results for configuration O in Figure 81 show that the oxygen-deficient gases from the center of the firebox had penetrated behind the wall jets, reducing the vicinity of wall O_2 concentration to 3 percent, one-third the level found for configuration N (Figure 79). At the 3 percent O_2 levels characteristic of configuration O, any penetration of the wall air layer would lead to unfavorably low O_2 concentrations. The high wall O_2 concentrations for configuration N are attractive in that, even in areas where the fuel-rich vortex gases penetrate the wall air layer, wall O_2 concentrations will still be reasonable. Because of this difference in wall air O_2 concentrations, configuration N is favored over configuration O.

Figure 82 shows the effect on NO of varying the wall air jet inclination angle for configuration G. The primary and secondary air jets for this case, similar to the configuration 2 jet locations, were shown schematically in Figure 65. At a 0° angle, the wall air jet is behind the fuel jet and is shielded from the direct impact of the vortex flow. As the wall jet inclination angle is varied from the horizontal, the wall jet is directed out from behind the fuel jet and, due to the lack of fuel jet shielding, becomes more easily entrained into the fuel-rich core. The decrease in fuel/air separation caused by this mixing might explain the observed NO increase for positive and negative wall air jet angles with respect to the horizontal.

Besides yielding minimum NO, directing the wall air jet horizontally is desirable for multiburner-level firing. For a system with several burner levels, directing the wall air upwards or downwards with respect to the fuel jet might result in undesirable burner-to-burner air jet interactions.

5.2.4 Effect of Temperature and Load Variation on System 1 Burner Performance

An additional feature of the low-NO_x System 1 configuration is the improvement in NO emissions as temperature rises. Figure 83 shows that, as gas temperature was increased for two different air-on-wall system configurations, NO decreased. As discussed earlier, under the fuel-rich conditions existing in the center of the furnace, increases in temperature will lead to more volatilization of the fuel nitrogen in the rich zone, and more conversion of this nitrogen to molecular nitrogen rather than to NO. This attractive emission behavior with temperature might be used to reduce boiler size and capital costs for a given heat release.

Also shown in Figure 83 is the NO reduction caused by decreasing the load at a fixed gas temperature. As discussed previously, reducing the load decreases firebox mixing, thereby maintaining rich zones in which NO is minimized.

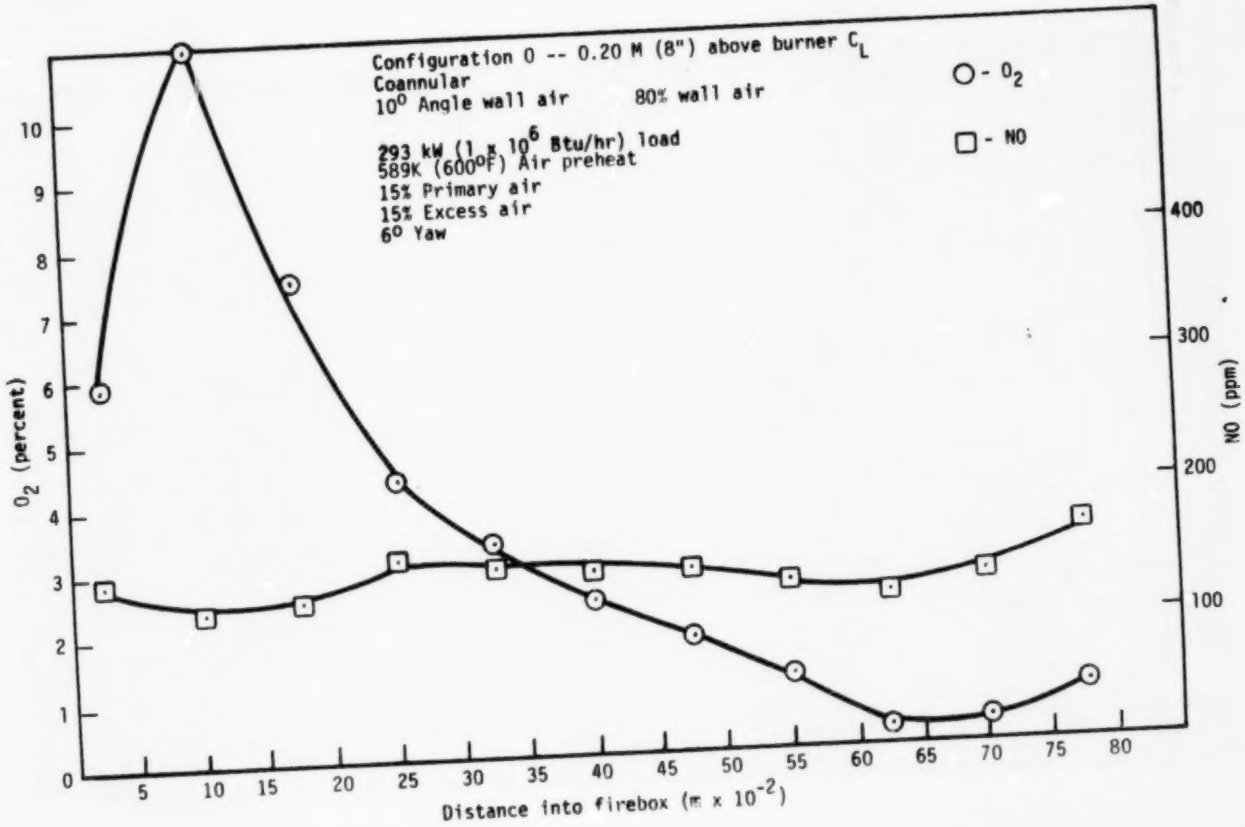

Figure 81. Configuration 0 NO and $0_2$0 firebox concentrations 0.20m above the fuel entry elevation.

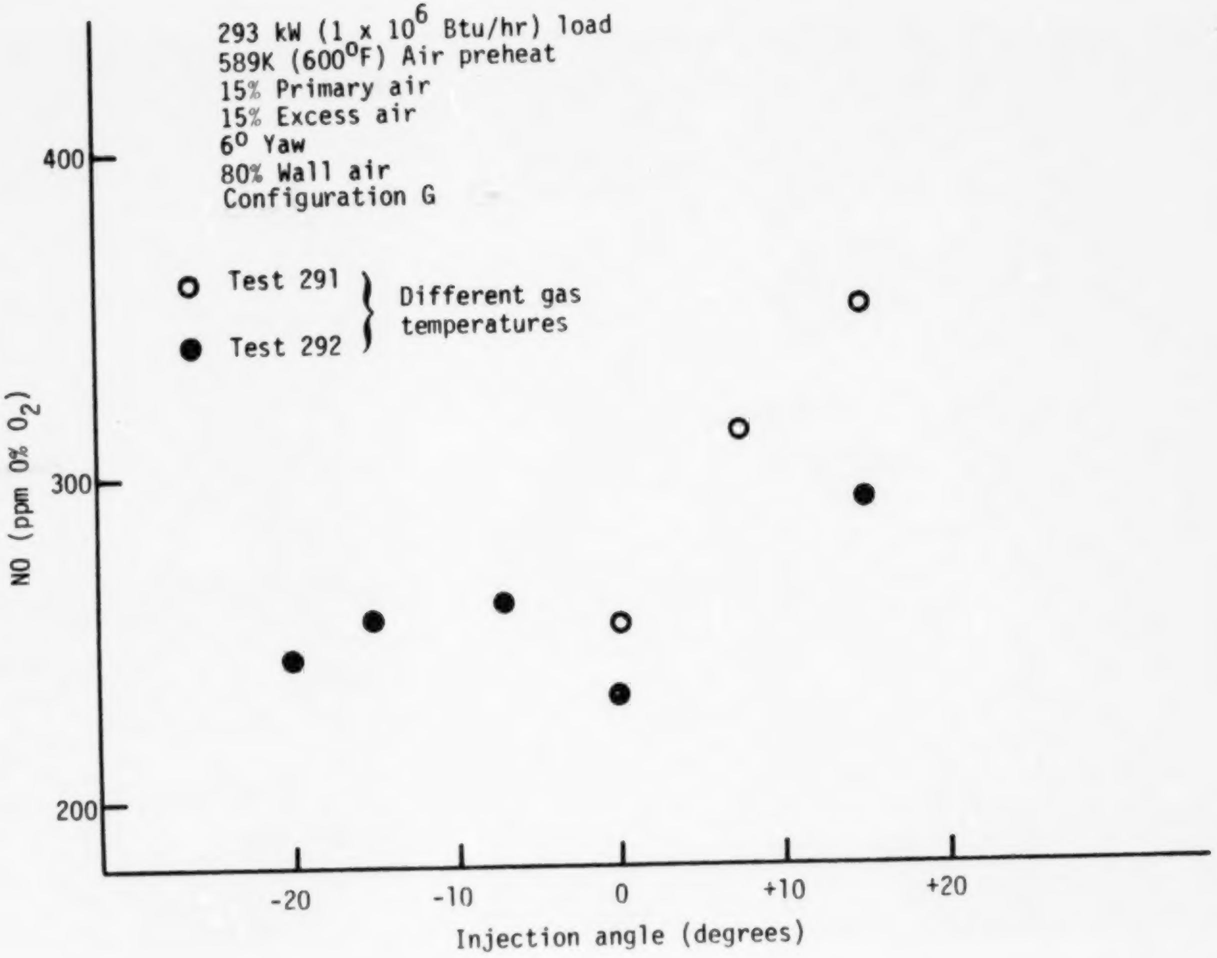

Figure 82. Effect of wall jet inclination angle.

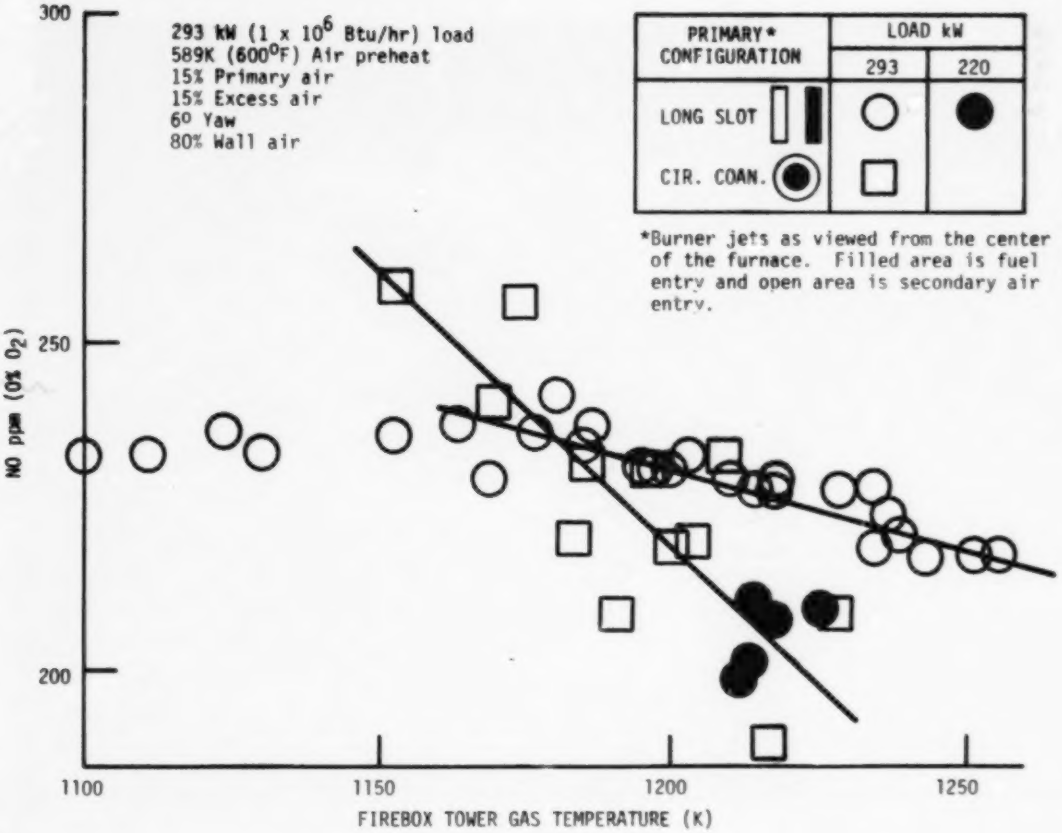

Figure 83. NO versus gas stream temperature for air-on-wall low-NO_x system.

5.2.5 Results Summary and Comparison with Conventional Tangential Firing

In summary, as shown in Figure 84, tests where the primary fuel and seconday jet configurations were varied showed that directing approximately 20 percent of the secondary combustion air into the center of the furnace and 80 percent along the walls at the fuel jet elevation yielded the lowest NO for most of the System 1 primary configurations tested.

Configuration N produced the lowest NO of all the configurations. Moving the wall jet away from the walls (configuration O) resulted in marginally higher NO but much lower wall O_2 levels which is less beneficial to wall corrosion and slagging. Also, inclining the wall air jet from the horizontal increased NO emissions.

For the cases tested with fixed air jet areas, increasing the percent air on the wall increased the velocity of the wall jet, as well as distributed more of the air on the wall. The minimum NO levels achieved may represent a balance between the benefits of the outward displacement of the combustion air for a wider separation of fuel and air, and the negative effects of increased fuel/air mixing caused by the wall jets' higher velocity. Higher percentages of wall air than optimal will give high wall air velocities and excessive mixing; lower percentages of airflow will place too much air in the center of the furnace.

At 80 percent air on the wall, probing results show that the center of the furnace was oxygen-deficient in a zone typically occupying 40 percent of the firebox 20 cm above the burner level for most configurations tested. As the wall air mixed into this oxygen-deficient zone, the zone typically shrank to 20 percent at 46 cm above the burner centerline. At this location, NO formation/reduction processes are essentially complete, and NO levels are comparable to stack values. With most configurations, there appeared to be a correlation between the extent of the fuel-rich core in the center of the furnace and stack NO levels: a more extensive fuel-rich core resulted in lower stack NO.

Table 10 presents the approximate vicinity of wall O_2 and NO concentrations for configurations H through O at 0.20m (8 inches) above the fuel entry elevation. These wall O_2 concentrations are much higher than the approximately 4 percent for conventional tangential firing. For configuration N, the coannular primary/center air yielded a wall O_2 concentration over twice the conventional levels. Even under staged combustion conditions at an SR of 0.66, configuration N had wall O_2 concentrations equivalent to conventional levels for tangential firing in the pilot-scale facility, as shown in Figure 85 and Table 10.

Figure 86 shows the effect of excess air at the optimal 80 percent air-on-wall conditions for several primary configurations. As shown in Figure 86, the best configuration was a coannular primary/secondary air arrangement in which the circular primary jet was surrounded by an annular passage that contained 20 percent of the secondary combustion air. Flame observation showed that this configuration produced the smallest amount of fuel dispersion prior to entering the fuel-rich core zone. Slot primary jets

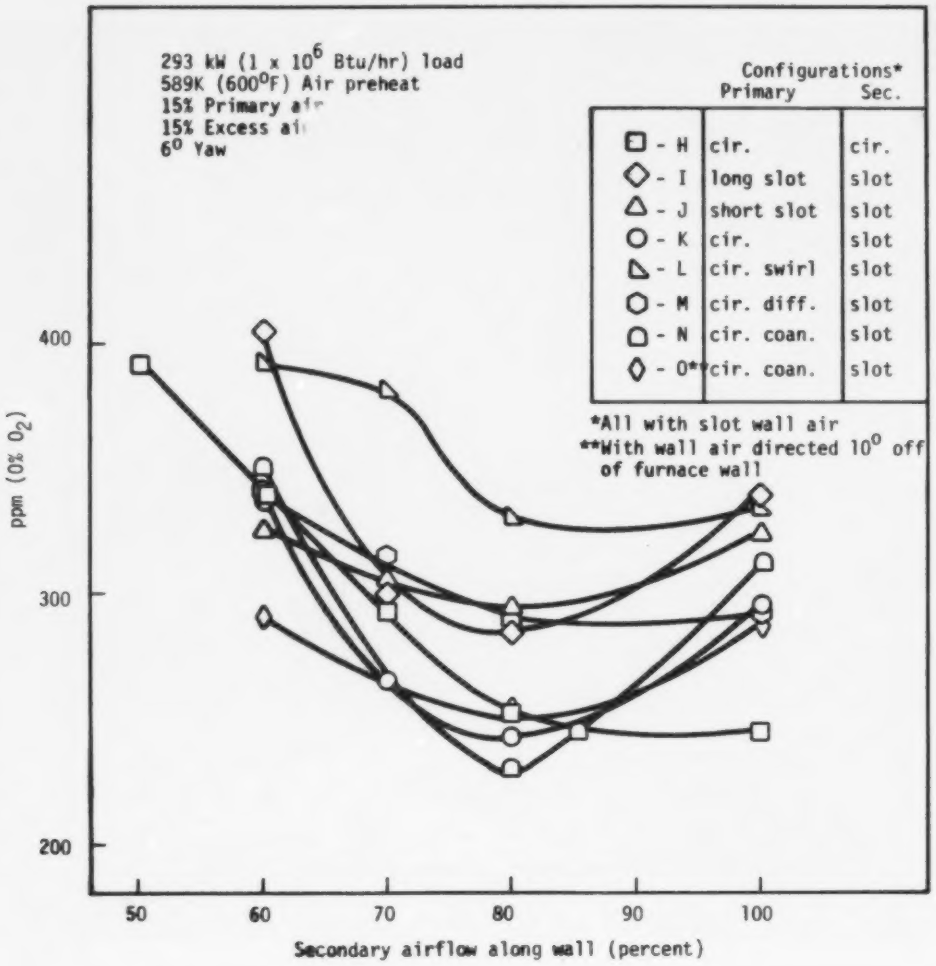

Figure 84. Configurations H through O NO results with percent wall air.

TABLE 10. AIR-ON-WALL PRIMARY CONFIGURATION WALL GAS CONDITIONS

	Configuration			0.20m (8") Above Burner C_L Probing Wall	
	Primary	Center	Wall	O_2 (%)	NO (ppm)
H	Cir	3 cir	Slot	7.5	180
I	Long shot	Slot	Slot	4.5	200
J	Short slot	Slot	Slot	7.0	210
K	Cir	Slot	Slot	1.5	238
L	Cir. swirl	Slot	Slot	4.0	312
M	Air. diff.	Slot	Slot	5.5	250
N	Conc. circular		Slot	9.6 4.0[a]	172 140
O	Conc. circular		Slot	11.0	160
Conventional Baseline	Cir	Cir	--	4.0 0.8[b]	400 200

[a] Staged SR = 0.66
[b] Staged SR = 0.85

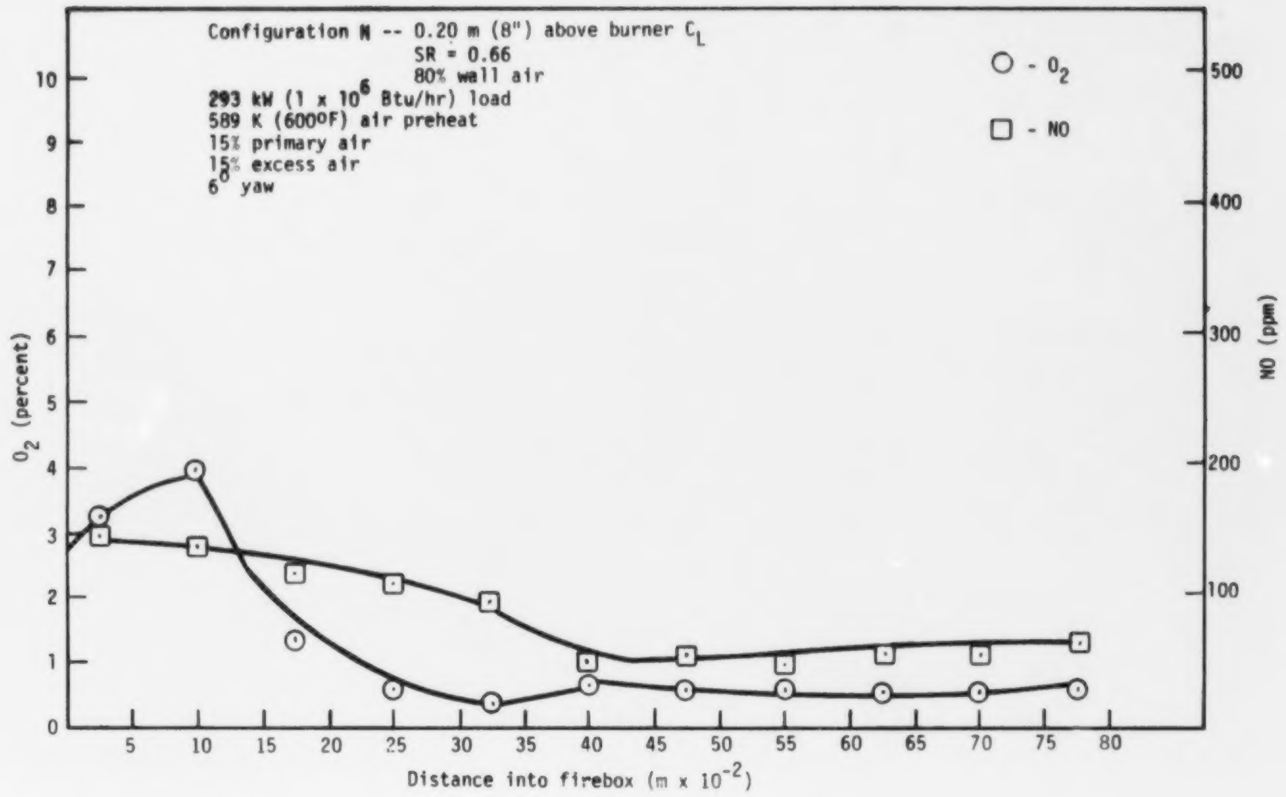

Figure 85. Configuration N staged NO and O_2 firebox concentrations 0.20m above fuel entry elevation.

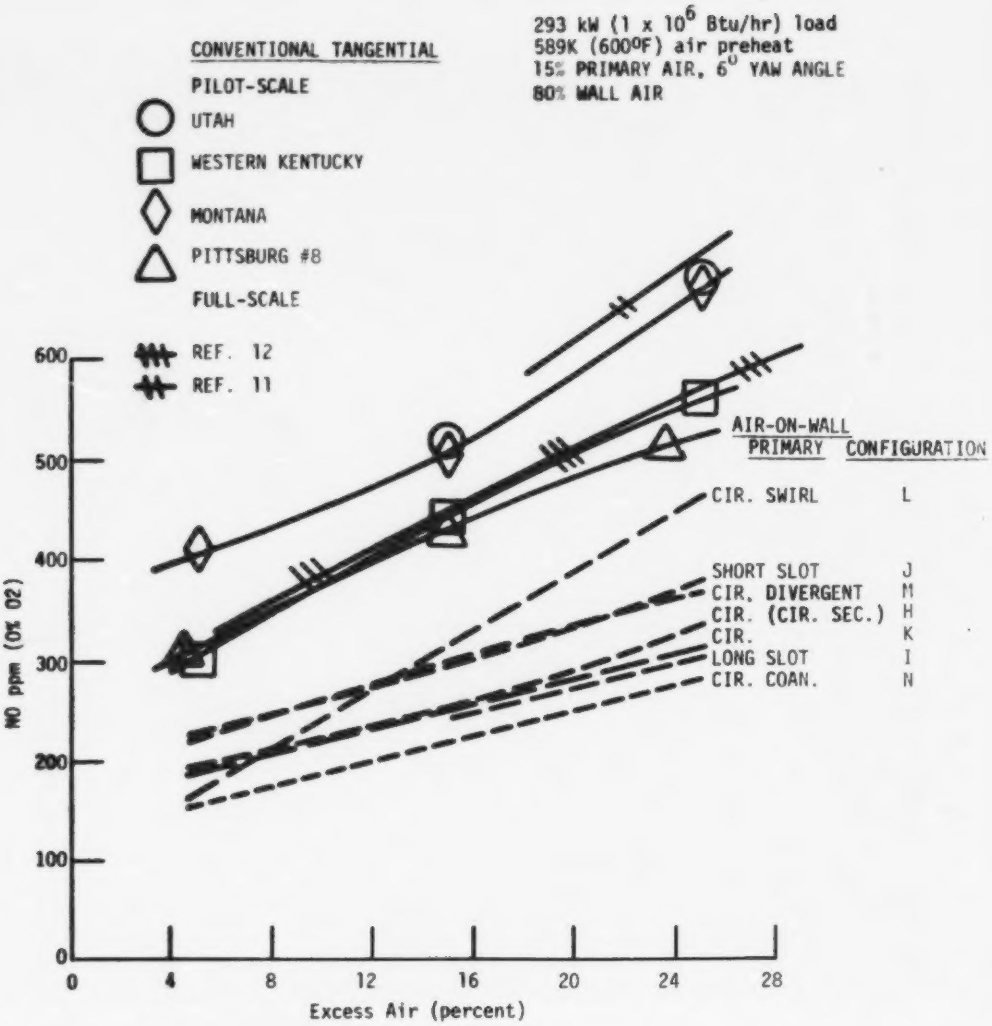

Figure 86. Effect of excess air on conventional pilot-scale, full-scale, and pilot-scale air-on-wall system NO emissions.

of various lengths though initially burning fuel much sooner than the other configurations, created fuel dispersion problems: the dispersed fuel would burn in fuel-lean zones, yielding high NO. Circular primary jets having swirling or diverging flows also yielded higher NO at 15 percent excess air.

Figure 87 shows the effect on NO of combining the wall air at the 80 percent air-on-wall condition with staging. These results, an indication of the system performance to be expected when combining the air-on-wall system with overfire air in a full-scale system, show that staged combustion augments the NO reduction potential of the air-on-wall system for all configurations tested. With relatively modest staging, at an SR of 1.0 in the lower firebox, all configurations yielded NO levels of 200 ppm or lower. As indicated above for configuration N, these reductions were achieved at vicinity of wall O_2 concentrations near those for unstaged conventional tangential firing. Therefore, wall corrosion and slagging should not be a problem when staging is combined with the air-on-wall system.

Comparison of the best low-NO_x concept results to conventional pilot- and full-scale tangential firing results in Figure 86 shows that the System 1 concept reduced NO emissions by roughly 60 percent and lowered the sensitivity of NO to excess air. This reduced sensitivity may be a result of the more diffuse burning in the fuel-rich core. Comparison of the best low-NO_x staged results to conventional pilot-scale tangential firing results in Figure 87 shows that the System 1 concept had much lower NO than the conventional system at moderate staging and equivalent results under heavy staging; the latter is due to the insensitivity of the NO results to the early mixing processes required for extreme staging (Reference 9). However, existing boilers can only be moderately staged, and the low-NO_x system has a clear advantage under these conditions. In addition, even with staging, the low-NO_x system wall O_2 concentrations were near 4 percent. This is about the same as wall O_2 concentrations for unstaged conventional tangential systems and much higher than the 0.8 percent O_2 concentration for staged conventional tangential firing shown in Table 10.

5.3 LOW NO_x SYSTEM 2

A major emphasis of the System 2 burner development was on retrofittable system concepts that can achieve significant NO_x reductions without requiring major changes to full-scale tangentially fired boiler hardware. While the System 1 burner demonstrated the effectiveness of the air-on-wall concept in reducing NO_x, it was not an easily retrofittable design but a design which might be useful as a future new design. Specifically, in the System 1 burner, secondary wall air was injected approximately one-third of the distance along the furnace wall (see Figure 64). Applying the System 1 burner design to full-scale units would require a significant redesign of the furnace waterwalls. The objective of the System 2 burner development was to apply the air-on-wall low-NO_x concept to a burner design more representative of full-scale practice. Another objective of this burner design was to define the benefits of distributing the combustion air over a wider elevation in the firebox.

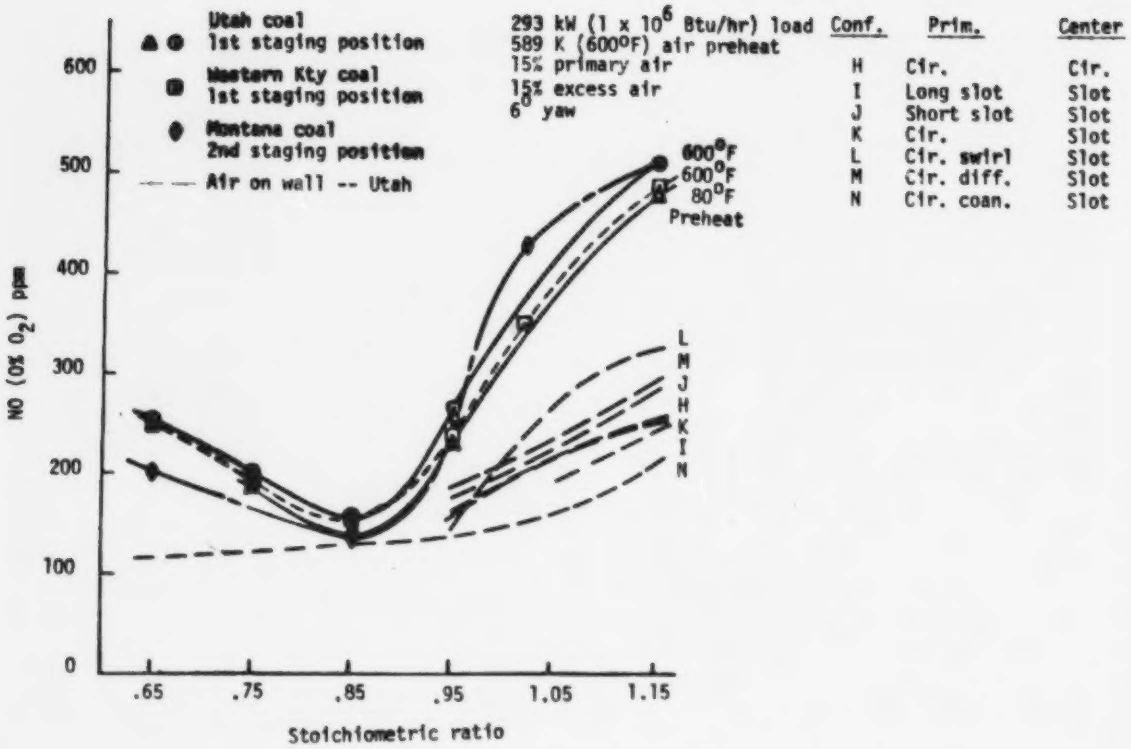

Figure 87. Configuration H through N staged NO results.

5.3.1 Low-NO_x System 2 Burner Design

The System 2 burner, which more closely resembles full-scale practice, was shown previously in Figure 64. The wall air jet, at a 45° angle to the firebox diagonal, was situated in the corner burner block, split into two ports above and below the fuel entry elevation. These wall air jets, labeled 1A and 1B in the figure, maintained the separation of the fuel and the bulk of the secondary air, and kept a blanket of air on the furnace walls.

These jets were connected to one airflow controller and a valving system, so that either or both jets could be selected. This allowed three different configurations of airflow injection at the fuel entry level (jet 1A, jet 1B, or jets 1A and 1B (1AB) together) with two different jet velocities (1A, and 1B were high velocity, while 1AB, with twice the flow area, was low velocity).

The annular jet of air surrounding the fuel was retained from System 1 for two reasons: (1) System 1 results show that for coannular primary/center port arrangements, some annular air (about 20 percent of the secondary air) was required for lowest NO_x levels, and (2) CE's full-scale units have a similar air jet surrounding the primary jet, making it likely that this feature would be retained in any retrofit of existing units.

A further addition to the System 2 design was its ability to distribute the wall air over a larger vertical distance by diverting a fraction of the air to wall ports 2 and 3 shown in Figure 64. Similar to and of the same dimensions as jets 1A and 1B, ports 2 and 3 were directed at a 45° angle to the firebox diagonal. Use of wall air ports 2 and 3 further separated the fuel and air, thereby maintaining an oxidizing atmosphere over a larger wall area. This design might be retrofitted into a full-scale unit through a combination of windbox modifications and/or burners out of service.

The System 2 burners utilized the same castable refractory construction developed for System 1. This allowed burner parameters to be varied with a minimum of downtime. In all, four different System 2 burner configurations were tested. Configuration S, shown in Figure 88, was used for the baseline characterization tests. Configuration T, also shown in Figure 88, studied the effect of primary jet placement on NO_x and combustion performance. Configurations U and V, similar to configuration S, were used to test the effect of reduced center and wall jet velocities. Table 11 summarizes the velocity and yaw angle parameters of these four burner configurations.

5.3.2 Configuration S Baseline Testing

Initial testing in this phase characterized System 2 NO emissions as compared with System 1 results. Operating parameters investigated were excess air, percent secondary air on wall, first stage stoichiometry for staged combustion, firebox gas temperature, and 1A, 1B and 1AB wall air jets flow splits.

As shown in Figure 89, configuration S had higher baseline NO emissions over a range of excess air than did the System 1 optimum, configuration N.

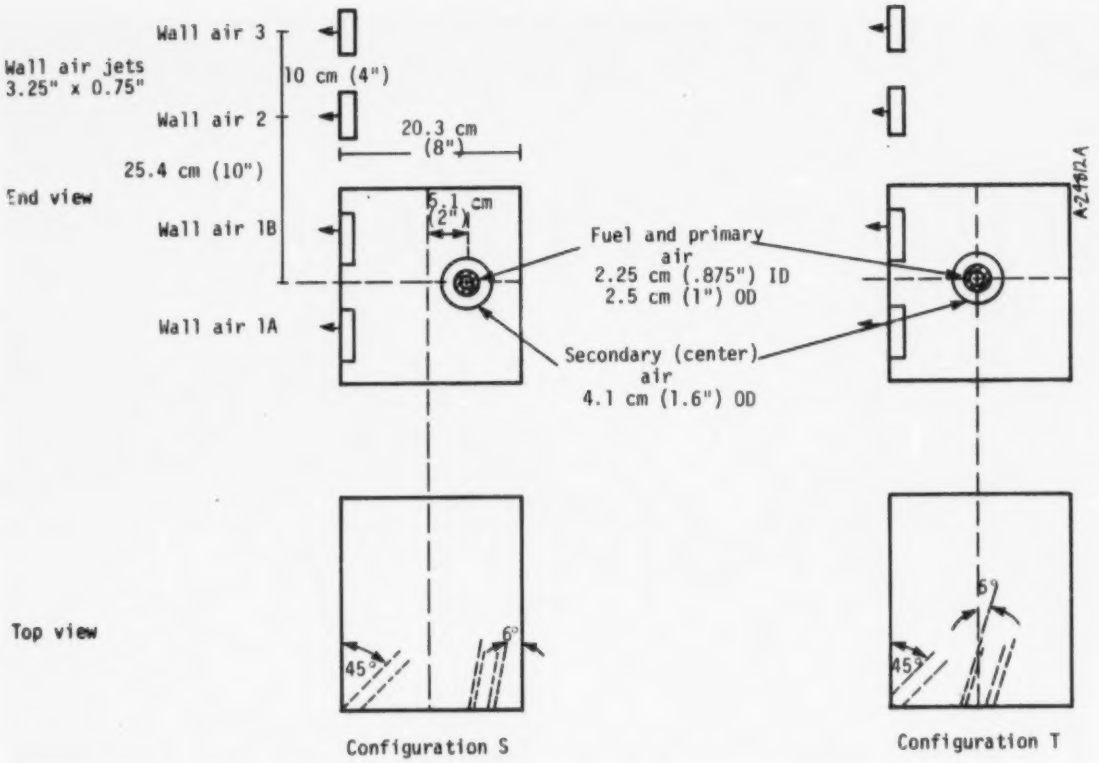
Wall air 3
Wall air jets
3.25" x 0.75"
10 cm (4")
Wall air 2
20.3 cm
(8")
25.4 cm (10")
End view
5.1 cm
(2")
Wall air 1B
Fuel and primary
air
2.25 cm (.875") ID
2.5 cm (1") OD
Wall air 1A
Secondary (center)
air
4.1 cm (1.6") OD
A-24812A
Top view
45°
6°
45°
6°
Configuration S
Configuration T

Figure 88. Comparison of System 2 burner configurations.

TABLE 11. SYSTEM 2 BURNERS

Configuration	V_{ann} m/s (ft/sec)	V_{1A}, V_{1B} m/s (ft/sec)	V_{1AB} m/s (ft/sec)	$V_{primary}$ m/s (ft/sec)	Yaw (degrees)
S	8.23 (27)	16.5 (54)	8.23 (27)	9.14 (30)	6-offset
T	8.23 (27)	16.5 (54)	8.23 (27)	9.14 (30)	6
U	8.23 (27)	12.8 (42)	6.40 (21)	9.14 (30)	6-offset
V	5.49 (18)	12.8 (42)	6.40 (21)	9.14 (30)	6-offset

Velocities based on jet area and baseline mass flows

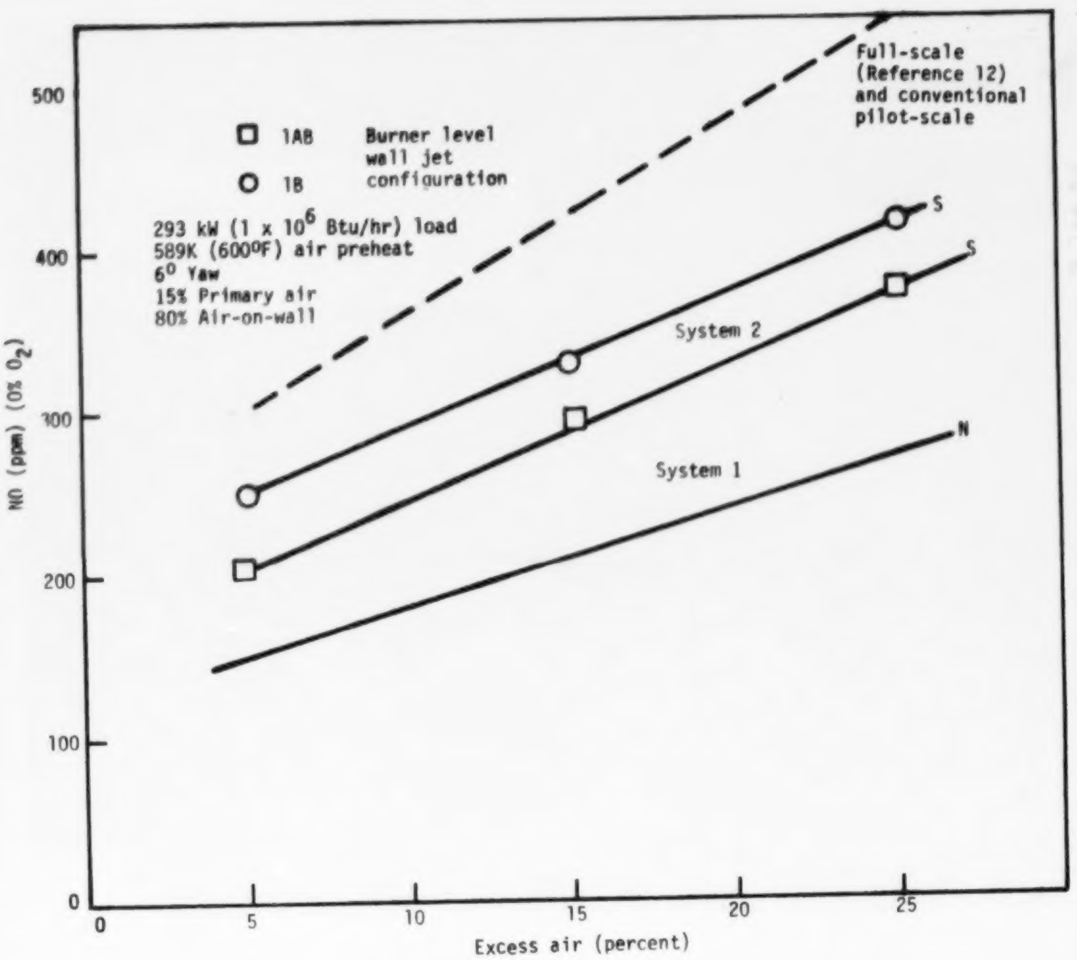

Figure 89. NO versus excess air for configuration S.

NO levels for System 2 ranged from 50 to 100 ppm higher than those for System 1, depending on temperature, and wall jet configuration. Also, the higher slope of System 2 NO as compared to that for System 1 suggested more premixing of fuel and air in System 2 which was not surprising since the fuel and air were less separated in System 2 than in System 1. However, System 2 NO levels and the trend with excess air were still below those of full-scale units.

As shown in Figure 90, NO versus percent secondary air on the wall also followed a trend similar to the System 1 results, with the optimum NO levels at 80 to 85 percent wall air. As in System 1, a balance can be seen between the benefits of wider fuel/air separation at higher percent air on the wall and the negative effects of increased fuel/air mixing yielding an NO minimum.

With overall excess air remaining constant, the variation of NO with first-stage stoichiometry under staged combustion can be seen in Figure 91. At very fuel-rich conditions, Systems 1 and 2 NO levels approached each other, indicating that burner differences (first-stage fuel/air mixing) between the two systems were no longer the dominant factors in overall NO formation. This independence from local mixing effects at low first-stage stoichiometries was seen in earlier work (Reference 9).

The dependence of System 2 burner NO on gas temperature can be seen in Figure 92. The temperature was measured in the heat exchange tower near the furnace exit at location T_{26} as defined in Section 4.3. Although there is radiation error in this measurement, it is useful as a relative correlation parameter. As shown in Figure 92, System 1 NO levels were lower than System 2 levels but both followed a similar trend with temperature. The significant scatter in data is due to the large time intervals between taking data over which firebox and burner ash deposition was significant.

Figure 92 also illustrates the effect on NO of the wall air jet configuration. Injecting the air below the fuel tube level in port 1A yielded NO levels at least 70 ppm higher than either the 1B or 1AB configurations. Using the 1A jet also yielded a high air injection velocity which might have excessively impacted the downstream adjacent fuel jet, thereby increasing fuel/air mixing and leading to higher NO levels. The 1B jet, while also yielding high velocities, injected air slightly above the fuel tube, which might have reduced its impact on the downstream jet because of its upward movement. The 1AB jet injected air at half the velocity of the 1A or 1B jets, which reduced its impact on adjacent fuel jets. As can be seen in Figures 89, 90 and 92, the 1AB wall jet configuration yielded slightly lower NO levels than the 1B and 1A configurations, suggesting that lowering velocity and thereby lowering mixing is beneficial to NO.

The velocity effect on the vortex was determined by observing natural gas flame patterns from the bottom of the firebox. The 1A or 1B jets produced a large diameter vortex (two-thirds the firebox length), while the 1AB configuration produced a smaller vortex (one-half the firebox length). Furthermore, the high-velocity 1A or 1B jets produced significant bending of

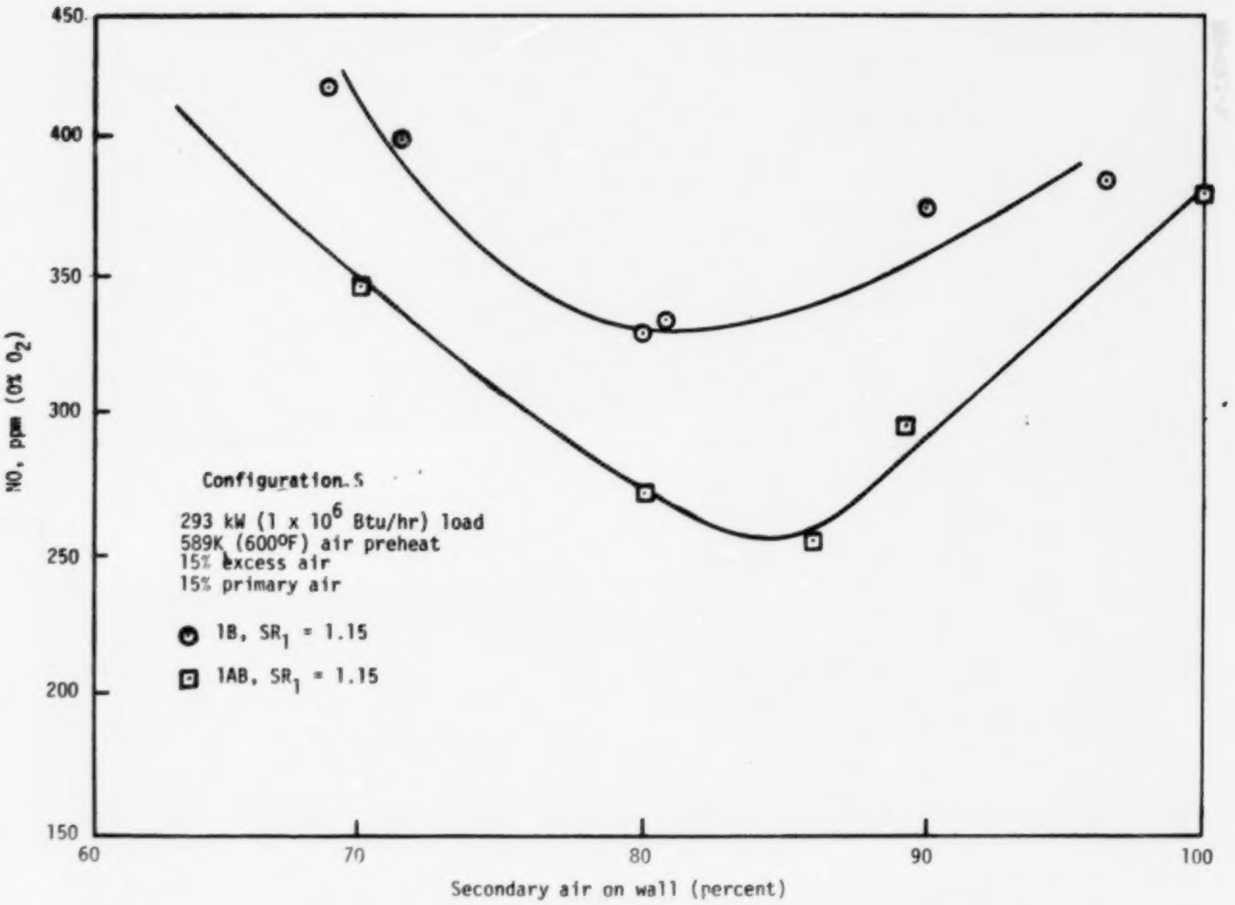

Figure 90. Configuration S NO versus percent secondary combustion air-on-wall.

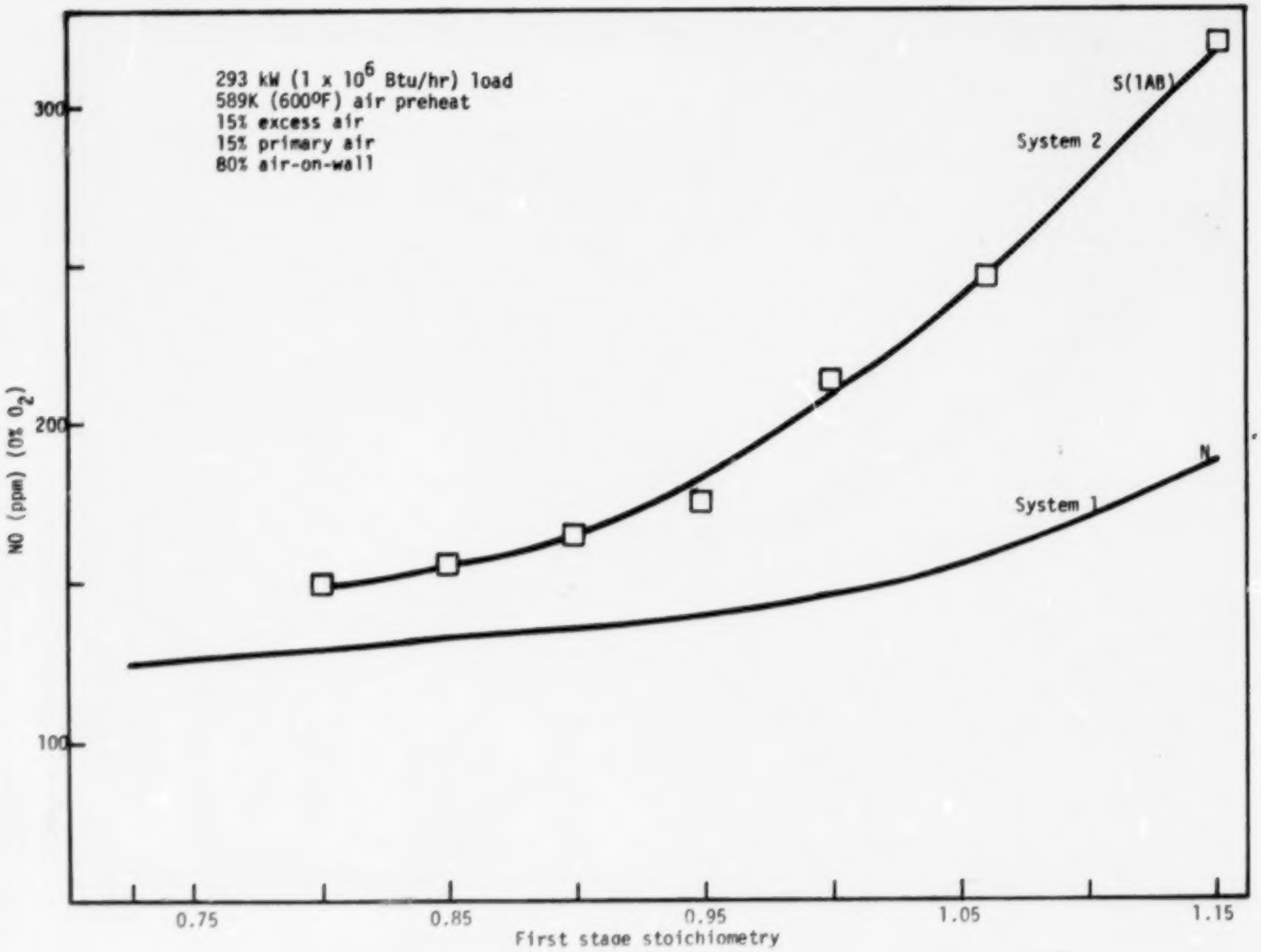

Figure 91. Staged NO levels for configurations N and S.

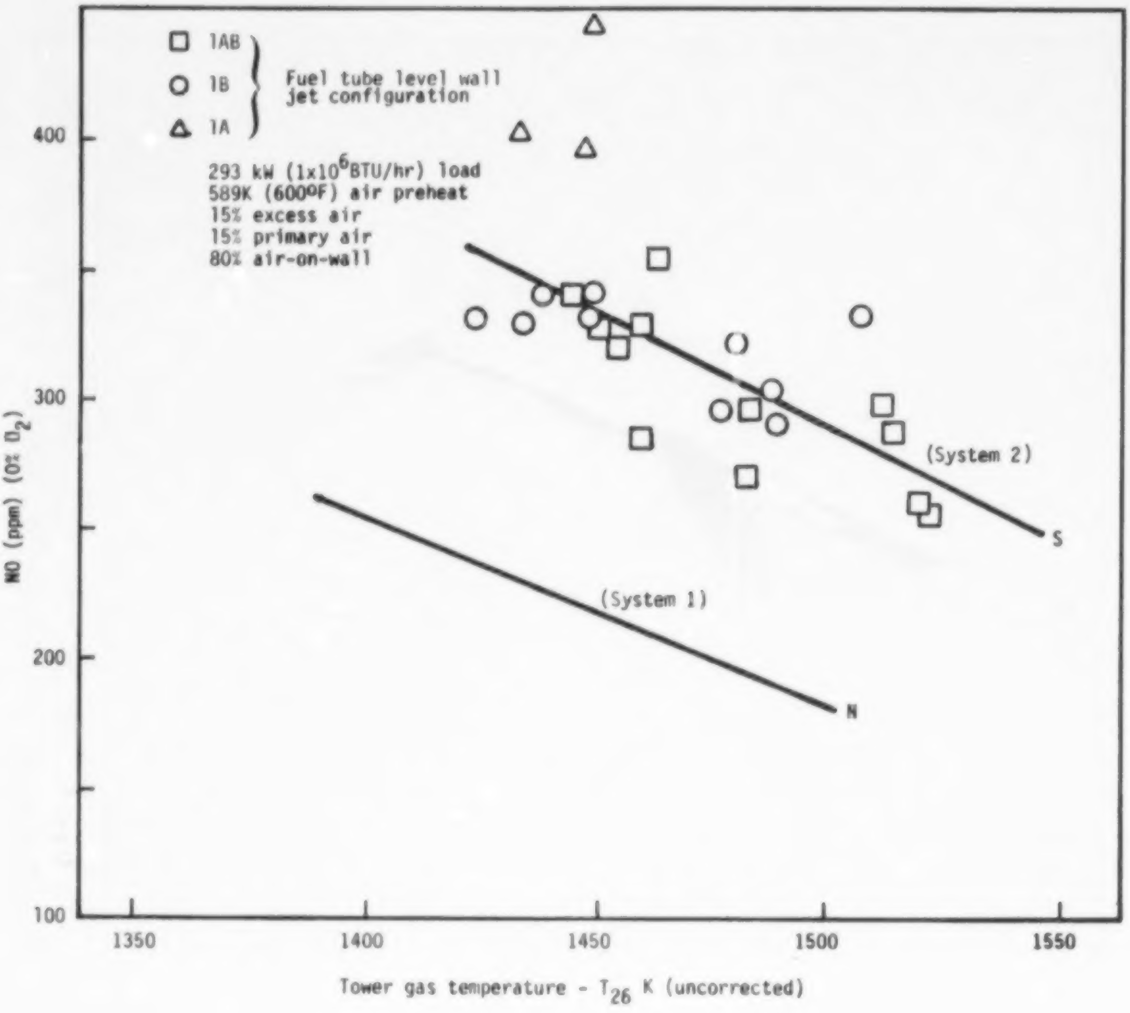

Figure 92. NO versus temperature for configurations N and S.

the downstream adjacent fuel jet, while such bending was not as significant with the low-velocity 1AB jet.

To help understand why System 2 levels were higher than System 1 levels, flame zone probing data were obtained. As discussed earlier, the lowest NO emissions in System 1 were found with an oxygen-deficient core in the middle of the firebox; NO levels were higher when oxygen was present in the center of the firebox. System 2 probing results given in Figure 93 show significant O_2 concentrations in the center of the firebox, at the fuel tube centerline and 0.20m (8 inches) above. This is in contrast to System 1 configuration N results where no O_2 was found in the center of the firebox. The presence of O_2 in the center of the firebox probably caused the higher baseline NO levels for System 2. If the oxygen could be eliminated, NO levels might decrease.

An interesting comparison can also be made between the System 2 1B and 1AB probing data. Although the configurations were probed on different days and had a 100°F difference in average gas temperature (T_{26}), the structure of their vortices in terms of O_2 and NO results as presented in Figures 93 and 94 shows an excellent correspondence. This indicates that, even though the velocities and locations of the wall air jets were different, the fuel/air mixing in the firebox was similar. Apparently, the global (i.e., corner wall jets) rather than the detailed (i.e., 1B versus 1AB) burner configuration parameters are causing O_2 to be present in the center of the furnace.

5.3.3 Vertically Distributed Wall Air Testing

In these tests, configuration S was used with the fuel and air further separated by distributing a portion of the wall air above the fuel tube elevation in wall jets 2 and 3.

In the following discussion, SR_1 will refer to the stoichiometry in the firebox due to air injected at the fuel tube level. Therefore, an SR_1 of 1.15 means no air was injected in wall jets 2 or 3, while an SR_1 less than 1.15 indicates some air was distributed into wall jets 2 or 3. The upper wall air is divided equally between wall ports 2 and 3, unless otherwise noted. 1AB23 means air injected in wall jets 1A, 1B, 2, and 3, while 1B23 means air injected in 1B, 2, and 3 only. During testing, both percent air on the wall and SR_1 were varied in alternate runs in order to quickly zero in on minimum NO conditions. For clarity, only the final optimum conditions are presented.

In Figure 95, it can be seen that NO levels decreased from baseline levels as wall air was distributed to wall ports 2 and 3, with the minimum NO shifting to higher amounts of air on the wall. Since each wall jet had less airflow, injection velocities were lower than those for previous System 2 baseline tests. Thus, when wall jets 2 and 3 are used, the effects of lower velocity and vertical separation of fuel and air combine to lower NO_x.

Figure 96 shows the variation of NO at a fixed percent air on the wall (i.e., constant center air for a range of vertical distributions of wall air). These results were taken at different temperatures than the results in

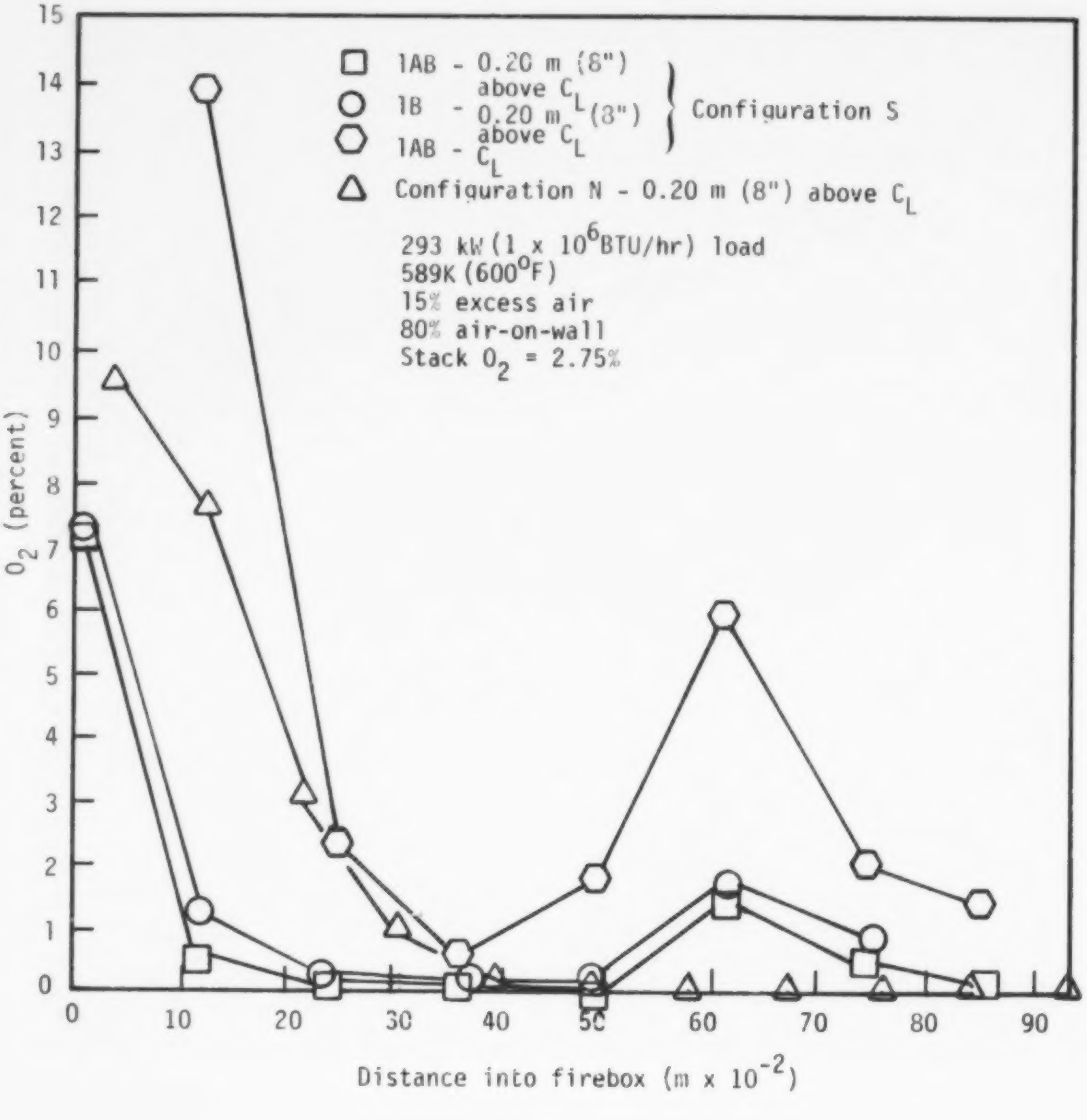

Figure 93. Firebox probing O_2 results for configurations N and S.

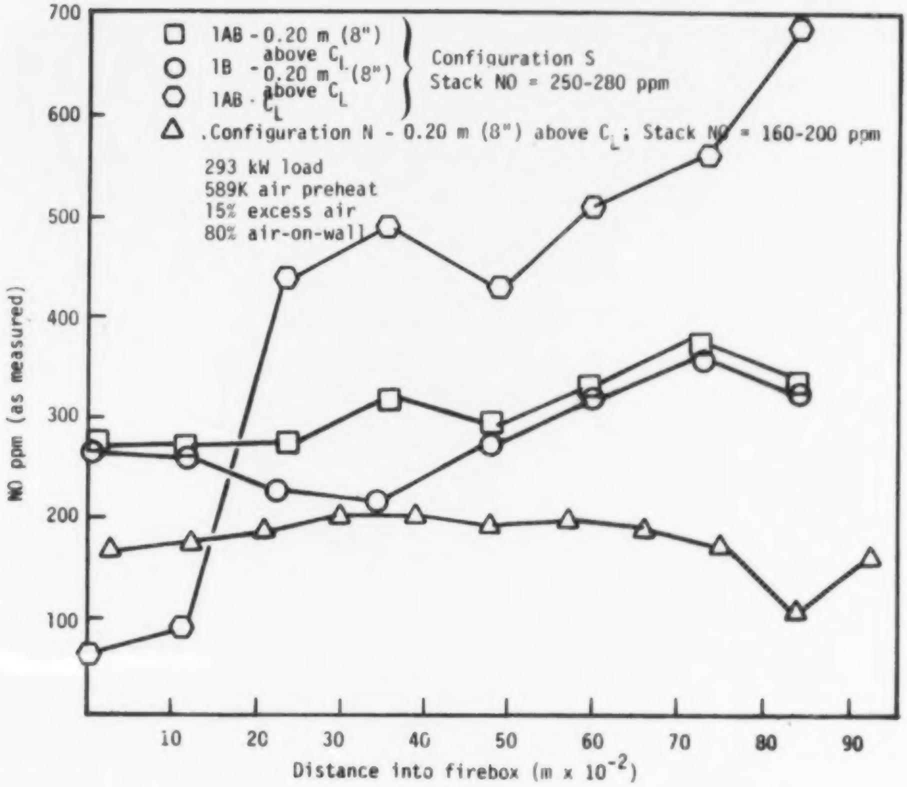

Figure 94. Firebox probing NO results for configurations N and S.

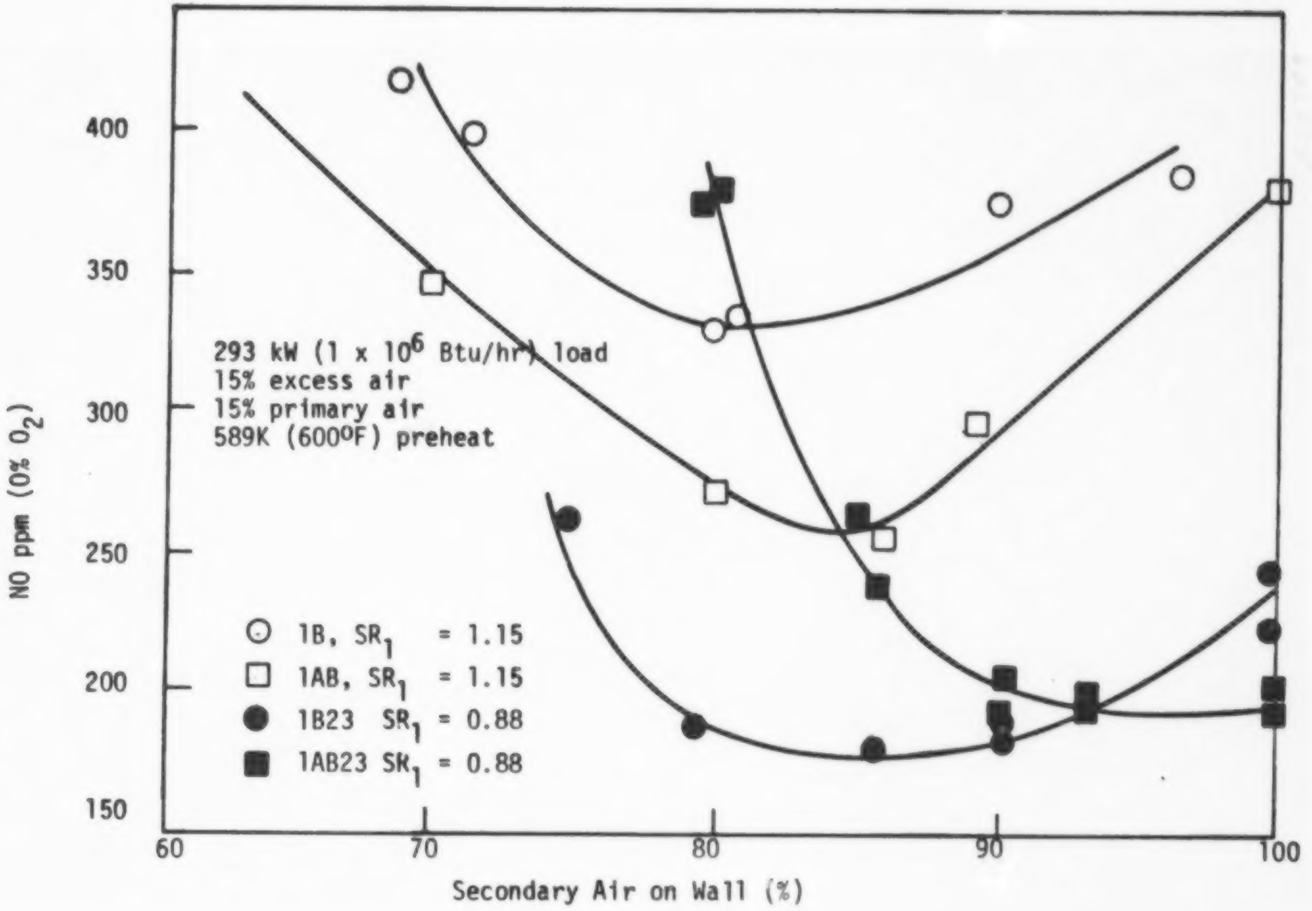

Figure 95. NO versus percent secondary combustion air on wall -- configuration S.

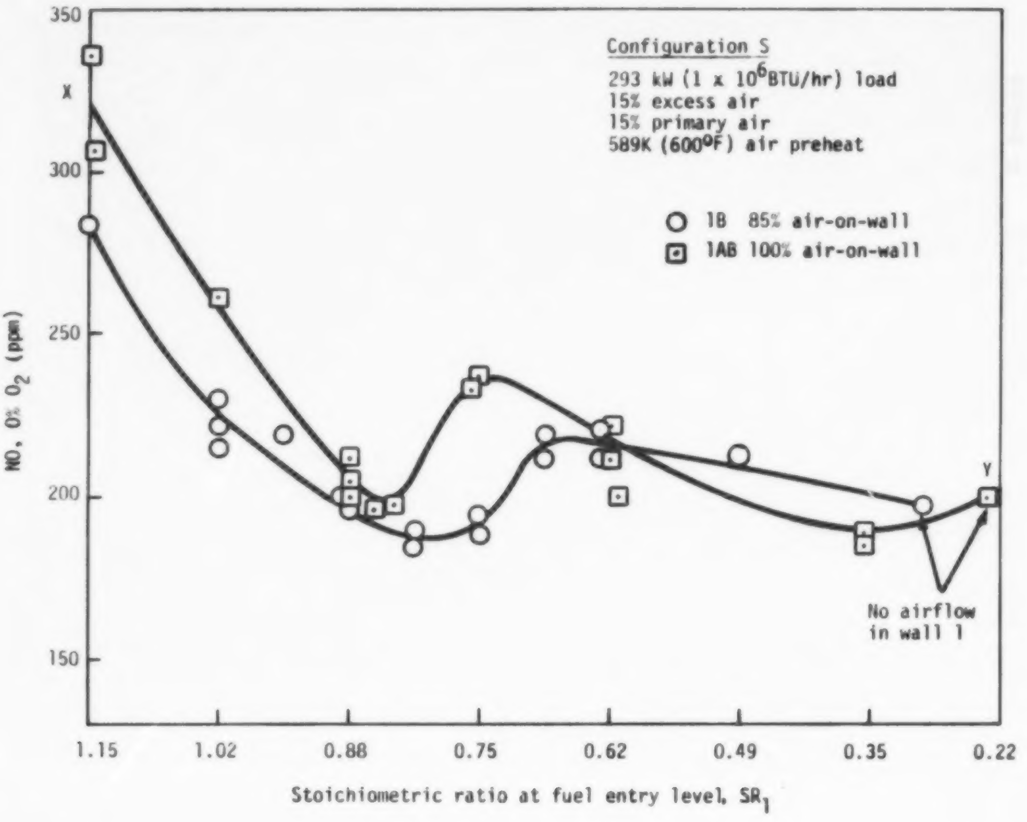

Figure 96. NO variation with fuel tube elevation stoichiometry for configuration S.

Figure 95; thus, at an SR_1 of 1.15 NO levels do not match. As can be seen in Figure 96, NO decreased as SR_1 decreased, reaching a local minimum near an SR_1 of 0.88, then increasing before finally reaching a second low level when all the wall air was evenly distributed between ports 2 and 3. As before, both velocity and fuel/air separation change as SR_1 varied. At the two extreme conditions for 1AB ($SR_1 = 1.15$ and $SR_1 = 0.22$, labeled x and y in Figure 96), wall airflow was entirely in either 1AB or 2 and 3. Since the jets had an equal area and therefore equal velocity, the observed NO reduction was entirely due to the vertical displacement of air. At intermediate air splits, the jet velocities were lower and the NO results show the combined effect of velocity and air displacement.

Figure 97 gives NO versus temperature for System 1, System 2 baseline, and vertically distributed wall air. In contrast to the System 2 baseline (configuration S) and System 1 (configuration N) results, a negative temperature correlation was not evident for the vertically distributed wall air case. However, data were taken only at high temperatures, so the negative temperature correlation might have reached an asymptotic condition beyond which further NO reductions due to temperature effects were not possible.

The effect of wall jet 2 and 3 velocities on NO was determined by distributing the upper wall air between the two jets. Wall jet 2 and 3 velocities ranged from 11m/s to 22m/s (36 to 72 f/s), depending on whether the flow was split between the two jets or only one jet was used. Figure 98 shows that wall jet 2 and 3 velocities influenced NO only slightly. Apparently, the local staging effect of delaying mixing by injecting air above the fuel tube elevation was the dominant factor; upper wall jet velocity and placement played only minor roles.

To determine whether oxygen in the vortex core had decreased for the vertically distributed wall air case, in-flame probing was used at the fuel tube elevation, as well as at 0.20m (8 inches) and 0.45m (18 inches) above this level. The 1AB and 1B configurations used the optimal 100 percent and 85 percent air on wall, respectively, for these tests. The relationships between probing ports and wall air jet elevations are illustrated in Figure 99, as well as the corresponding bulk residence times up to these locations. The probing results in Figures 100 and 101 show that at 0.20m (8 inches) above the fuel entry elevation the oxygen had not been eliminated for the 1AB configuration, although the 1B configuration was definitely oxygen-deficient. For the 1AB wall jet case, the oxygen levels increased from the fuel tube to the 0.20m (8 inches) elevation, while the total NO was reduced* to stack levels by the 0.20m (8 inches) elevation. Clearly, the oxygen in the core was mixing with the combustion gases after most of the significant NO formation had taken place (note the small reduction in NO levels from 0.20m (8 inches) to 0.45m (18 inches). The confinement of NO formation to near the fuel entry level is desirable for multilevel burner, full-scale applications of the air-on-wall concept.

---

*The reduction from peak values might be due to dilution by the wall air rather than significant chemical reaction.

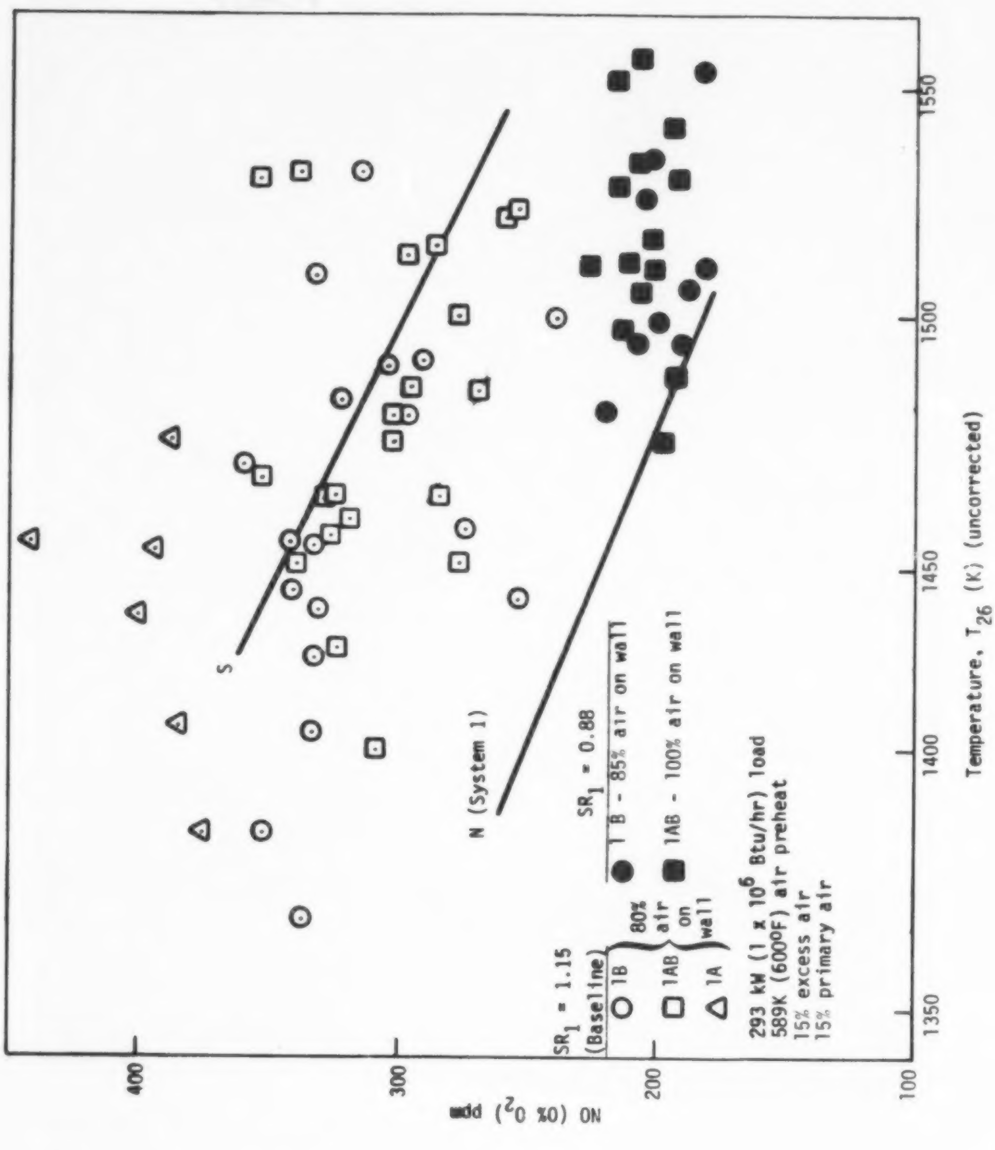

Figure 97. NO versus tower gas temperature for configuration S.

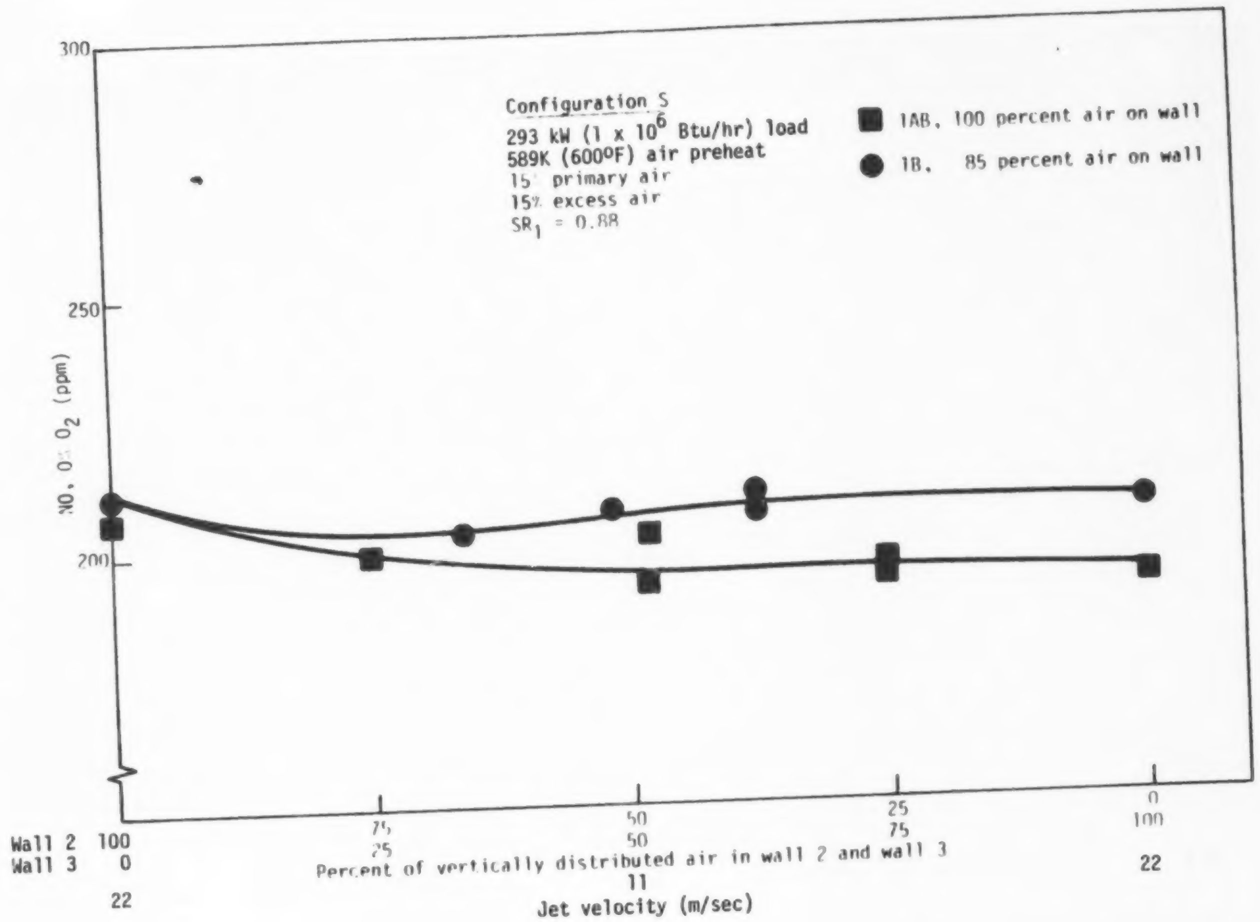

Figure 98. Effect of wall jet 2 and 3 velocities on NO levels.

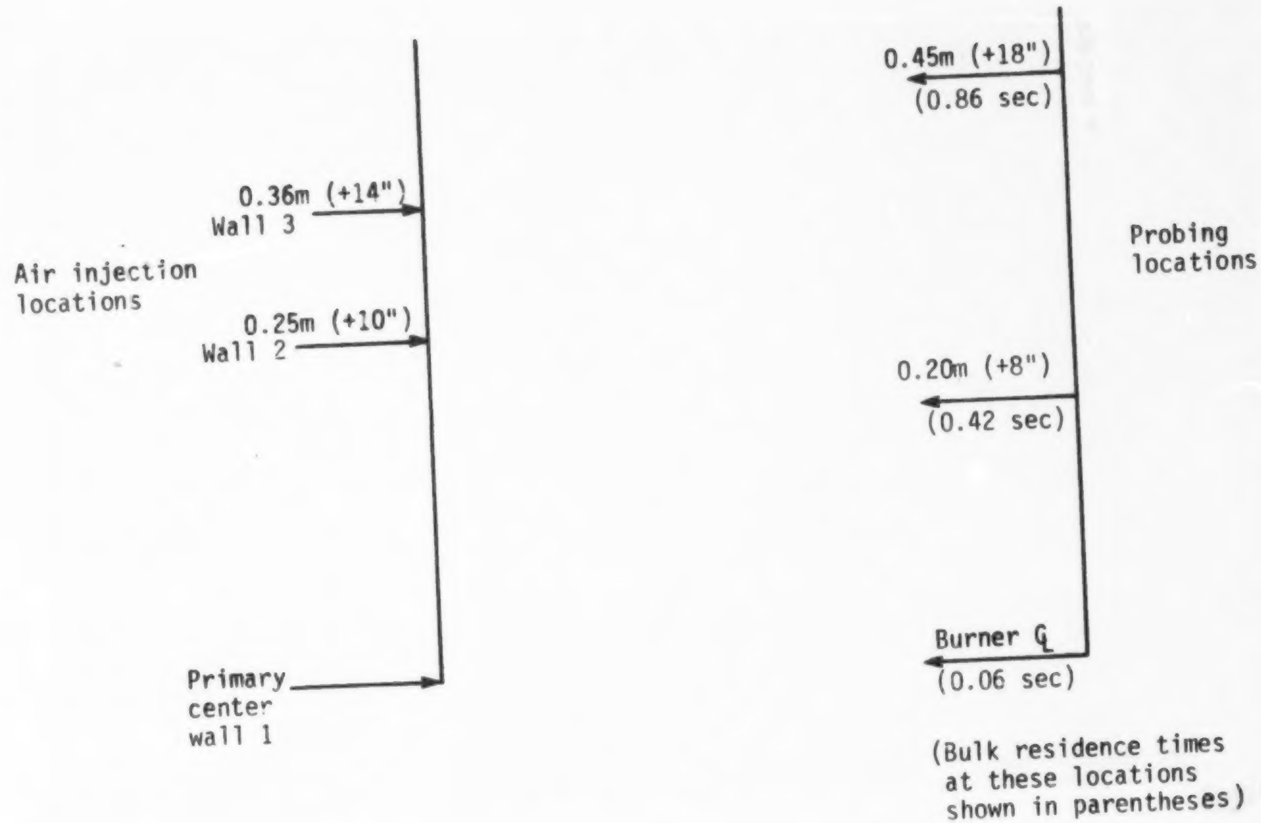
Air injection locations
0.36m (+14")
Wall 3
0.25m (+10")
Wall 2
Primary center wall 1
0.45m (+18")
(0.86 sec)
Probing locations
0.20m (+8")
(0.42 sec)
Burner ℄
(0.06 sec)
(Bulk residence times at these locations shown in parentheses)

Figure 99. Probing ports versus air port locations for configuration S.

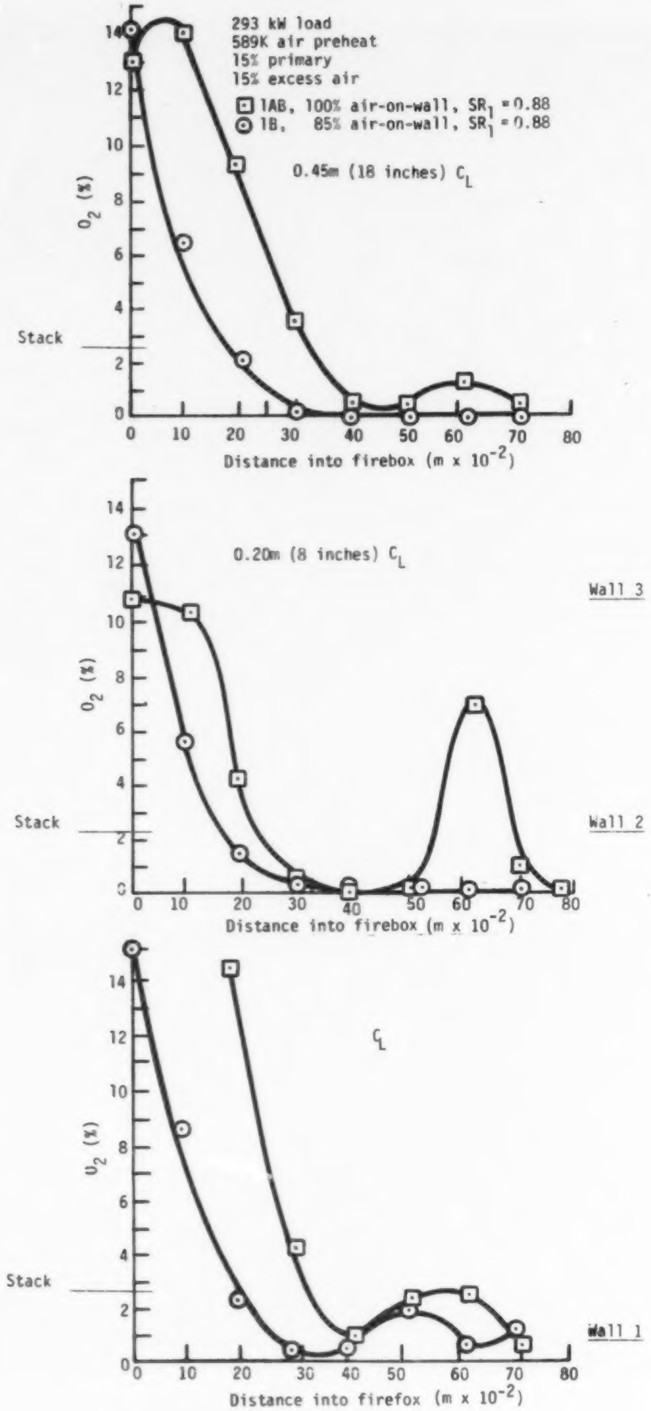

Figure 100. O_2 concentrations across firebox at 0.20m (8 inches) Above and 0.45m (18 inches) above the fuel tube elevation.

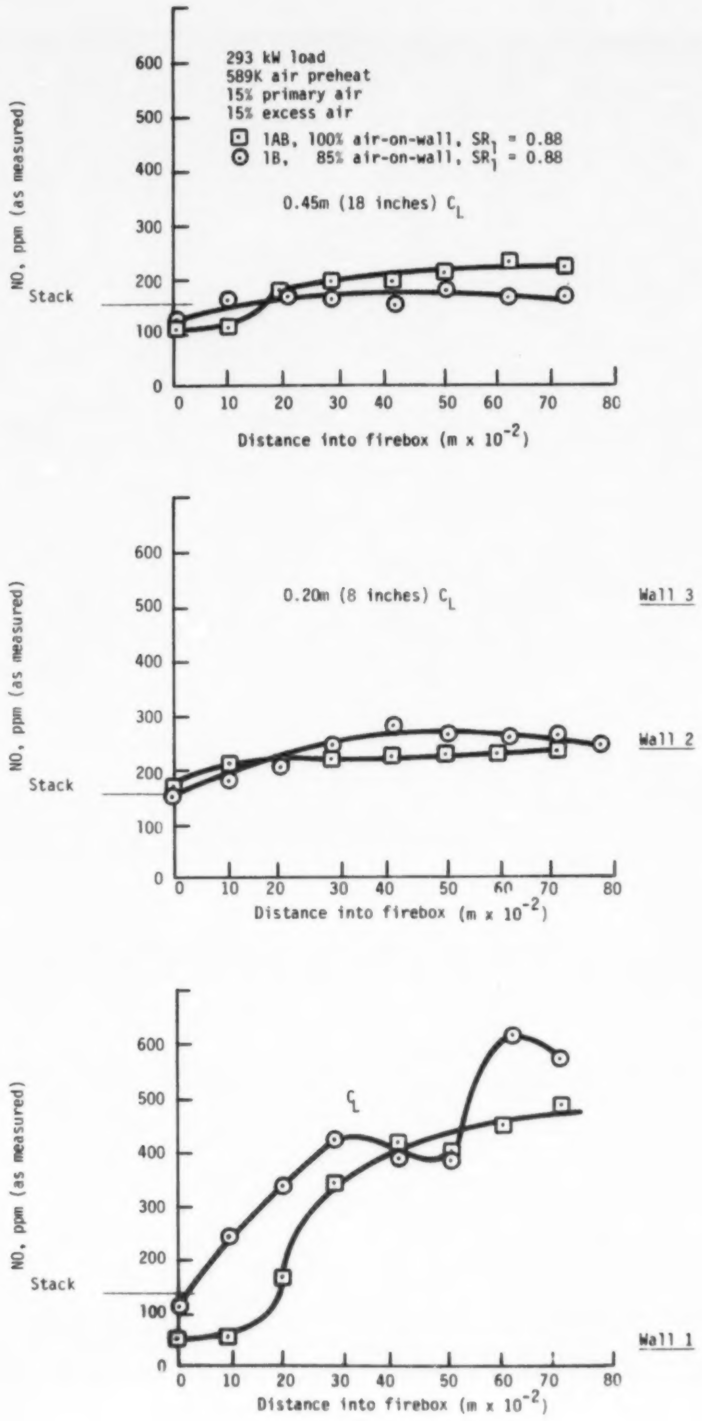

Figure 101. Firebox probing results for configuration S with vertically distributed wall air.

In addition to in-flame gaseous samples, char samples from the probing tests were analyzed. Figure 102 shows the percent of combustibles and nitrogen remaining in the char at the various heights/residence times in the firebox. As can be seen in the figure, most of the combustibles (up to 86 percent) has been consumed by 0.45m (18 inches) above the fuel entry elevation (residence time of 0.86 sec). Assuming that the fuel is consumed to the extent of oxygen available, this indicates a local SR at that point on the order of 0.86. However, from the figure the fuel-nitrogen can be seen to evolve from the coal more quickly than the total combustibles. Early evolution of nitrogen in the gas phase promotes NO reduction in the fuel-rich fireball, allowing the formation and reduction of NO to be completed sooner. This agrees with previous conclusions that most NO is formed before reaching the 0.20m (8 inches) level.

Vertically distributing the wall air had no discernible impact on combustion efficiency. Analysis of particulate samples obtained just upstream of the heat exchangers (residence time of 2.54 sec) yielded values of carbon in flyash of 1.6 to 2.4 percent. CO emissions during the testing were under 50 ppm, while UHC levels were under 15 ppm. A summary of System 1, System 2, and pilot-scale conventional tangential efficiencies and wall oxygen levels appears in Table 12.

5.3.4 Primary Jet Position

With low-NO_x System 2 burners (configuration S) well characterized and operating conditions optimized, attention was focused on the effect of burner parameters. The effect of primary jet placement was tested using configuration T burners, shown in Figure 88. The only change from configuration S was the movement of the primary jet to the firebox diagonal. All angles, velocities, and test conditions were unchanged from previous configuration S testing. This change increased vortex swirl, as well as moved the fuel entry tube to a position in line with full-scale units.

Initial observations of natural gas flame patterns showed fuel jet bending by the upstream wall jet. Vortex size was qualitatively larger than the configuration S vortex, with flames scraping the walls. After firing on coal, the walls showed a large increase in deposits, indicating flame impingement. This was not surprising, given the increased swirl of the vortex with configuration T.

Several standard parametric tests were run on configuration T. The trend of NO versus excess air, shown in Figure 103, established configuration T in line with previous low-NO_x configurations N, R, and S (Note that the data for configuration T in this figure were taken at an SR_1 of 0.88; all other curves in this figure were at an SR_1 of 1.15).

Figure 104 shows a comparison of NO versus percent secondary air on the wall for configurations T and S, both with vertical wall air. That the 1AB curves were taken in different thermal environments partly accounts for the difference in absolute NO levels. However, the trends were similar, with 1B NO levels essentially the same. This similarity in trends shows that the

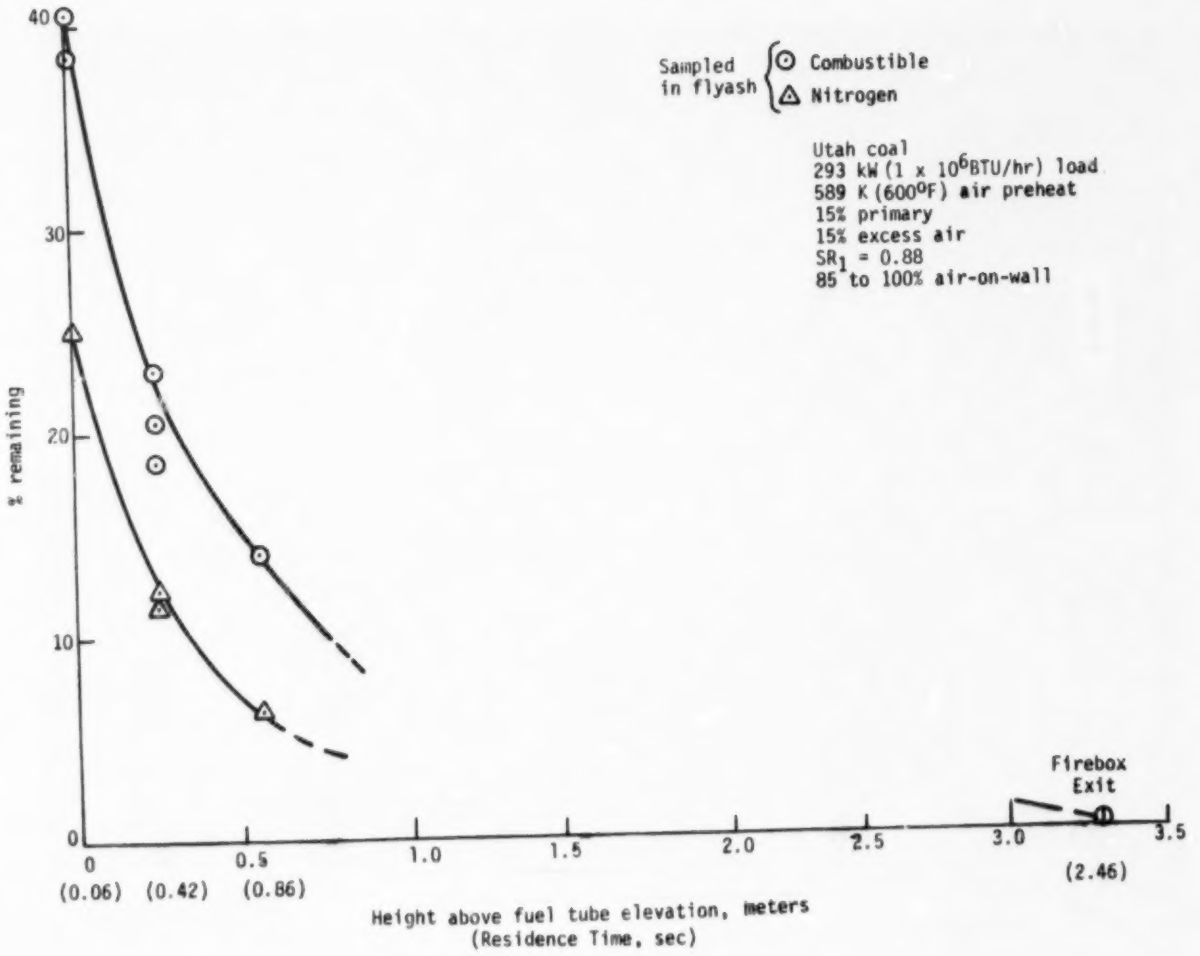

Figure 102. Combustion losses for configuration S.

TABLE 12. PILOT-SCALE COMBUSTION RESULTS COMPARISON

	Conventional T-fired	System 1 air on wall	System 2 vertical wall air
CO	16 ppm	36 ppm	50 ppm
Carbon in flyash	7%	3%	1.6 - 2.4%
Efficiency	99.3%	99.7%	99.7 - 99.9%
O_2 @ .025 m (1") from wall			
.20 m (8") elevation	4.0%	9.6%	11-13%
.45 m (18") elevation		7.3%	13-14%

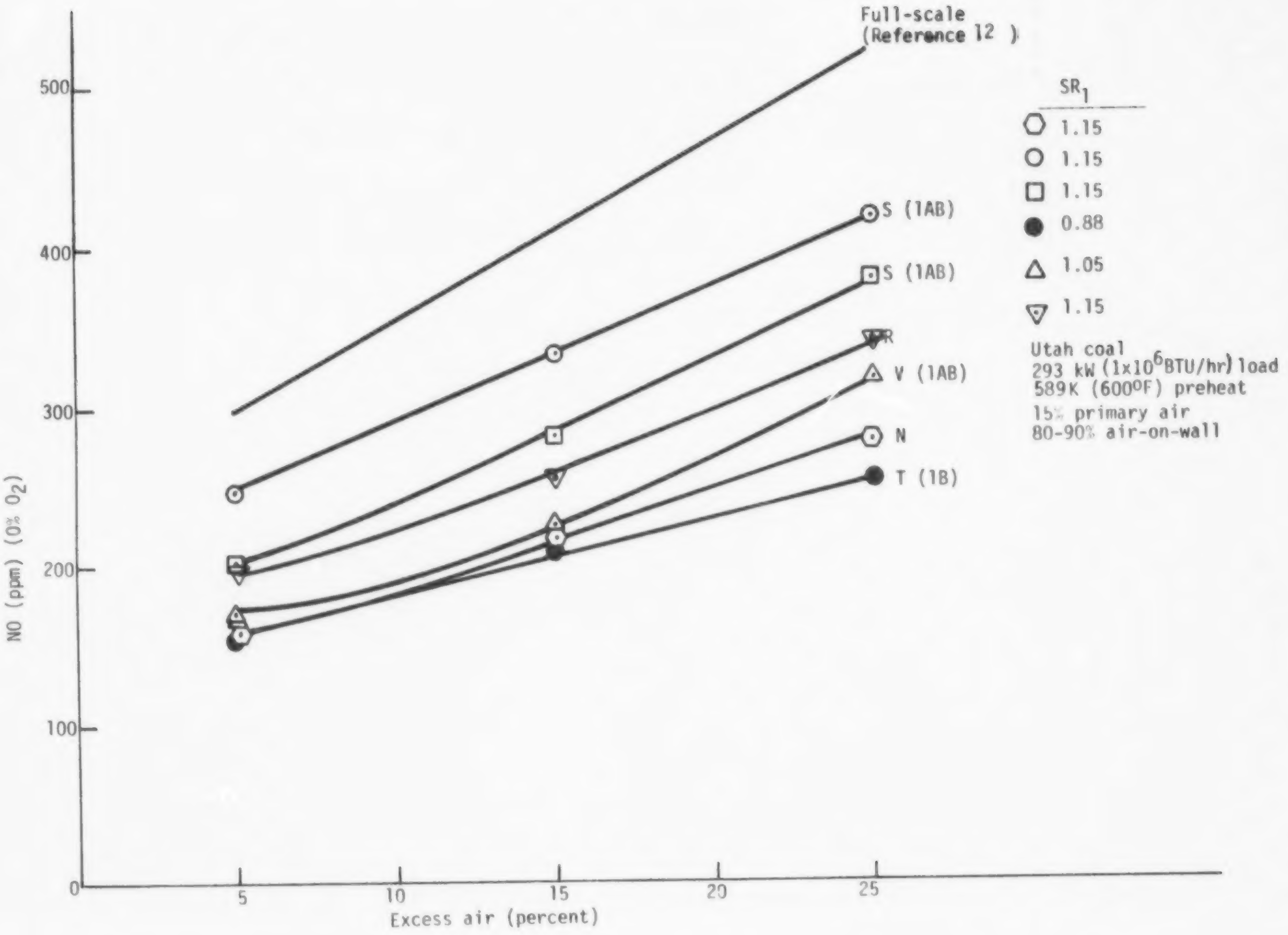

Figure 103. NO versus excess air.

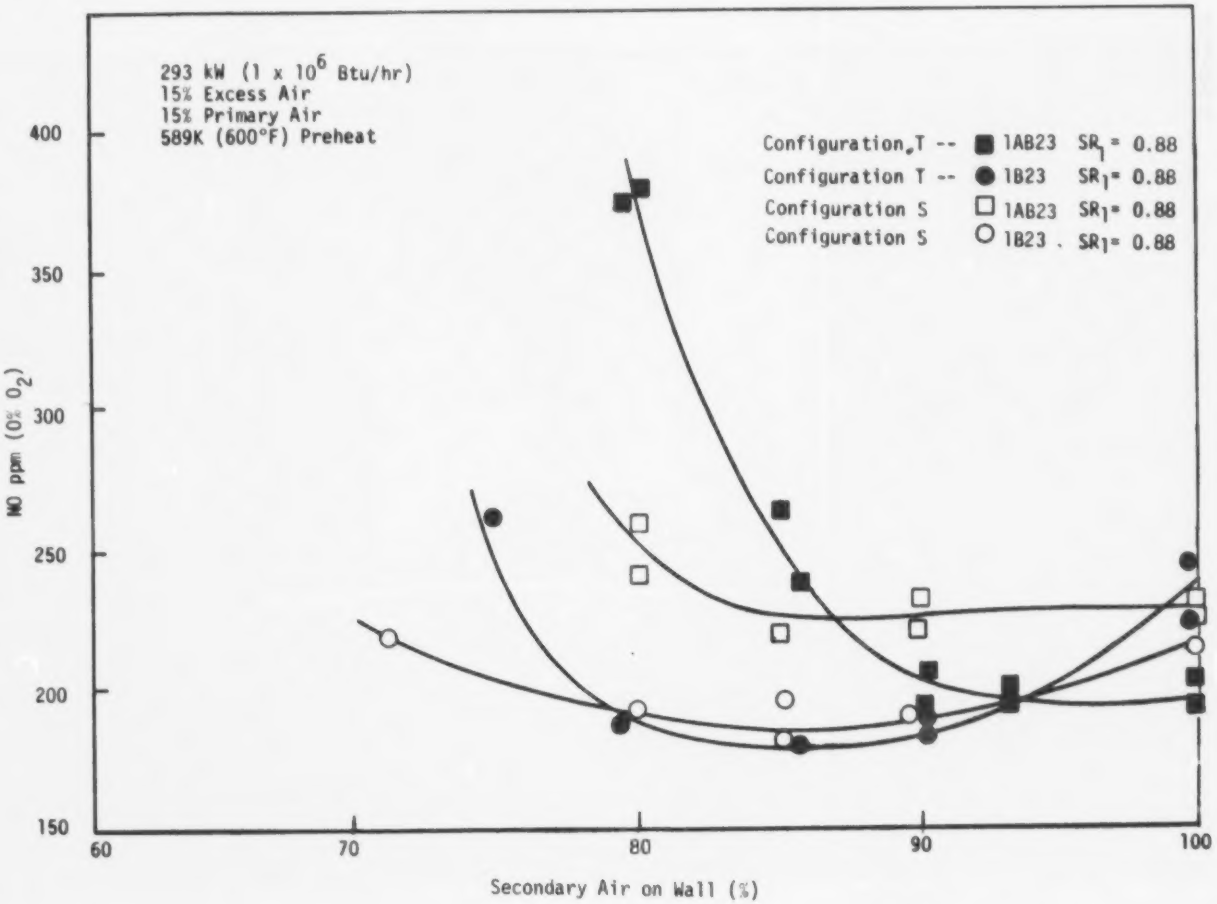

Figure 104. NO versus percent secondary combustion air on wall for configuration S and T with vertical wall air.

velocity/mixing effects of the wall/center air splits were not affected by changing the primary jet location.

The NO versus fuel tube elevation stoichiometry (SR_1), results for configuration T are shown in Figure 105. The local NO minima seen with configuration S at an SR_1 between 0.75 and 0.88 were not clearly seen with configuration T. Instead, NO decreased monotonically with SR_1, with almost no difference between the 1B and 1AB configuration results. The thermal conditions shown in this curve are cooler than those in Figure 104.

In summary, moving the primary jet location (from configuration S to configuration T) did not bring substantial reductions in NO levels, although levels in the 180 to 220 ppm range were reached at some conditions. However, a large increase in the amount of wall deposits was seen, and vortex observation showed a potential wall flame impingement problem.

5.3.5 Center and Wall Air Velocity Effects

Two burner blocks, designated as configurations U and V, were fabricated to study the effects of wall air velocity and center air velocity, respectively. The new burner blocks were similar to configuration S in design with minor modifications to the secondary air passage areas. The 1AB wall air passage areas of both configurations U and V were increased by approximately 30 percent in comparison to configuration S. The center air passage area of configuration V was increased by 50 percent in comparison to configurations S and U. Accordingly, in comparison to configuration S the velocity of the 1AB wall air was reduced by 30 percent for configurations U and V, and the center air velocity was reduced by 50 percent for configuration V. Table 11 gives the velocities for the different configurations.

Several parametric tests were run on both configurations U and V. The results from these tests are given in Figures 106 through 109. Figure 106 compares the results without vertical wall air as a function of air on the wall. By reducing the secondary wall air velocities in configurations U and V, NO emissions were reduced. This agrees with conclusions about wall air velocities from configuration S. Reducing center as well as wall air velocity in configuration V resulted in lower NO levels for a wall air of about 80 percent. Qualitatively, no strong NO minimum with percent wall air was observed for configurations U and V, as was observed for configuration S. The rapid increase in NO emissions at a percent wall air greater than 86 percent for configuration S can probably be attributed to its higher wall air velocity compared to the other two configurations. As indicated previously, increasing the wall air velocity will not only increase mixing but will also bend the primary fuel jet towards the wall, thereby enhancing the fuel/air mixing process and raising NO levels.

Figure 107 compares the NO results for configurations U, V, and S at an SR_1 of 0.88 as a function of percent wall air. When the percent wall air was less than 80 percent, NO emissions decreased as secondary air velocities decreased. This was similar to the NO behavior for an SR_1 of 1.15. But, as the percent wall air exceeded 85 percent, the opposite behavior was true. Apparently the lower wall air velocity at an SR_1 of 1.15 already dominated

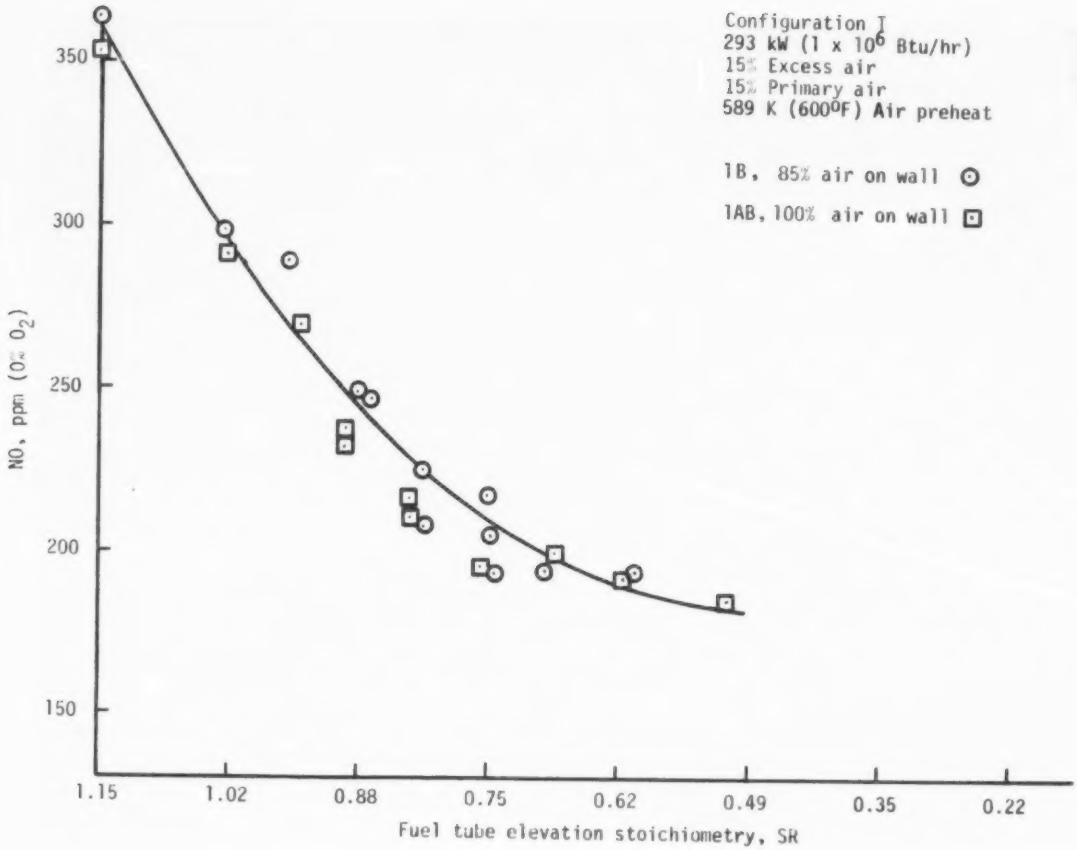

Figure 105. NO variation with fuel tube elevation stoichiometry for configuration T.

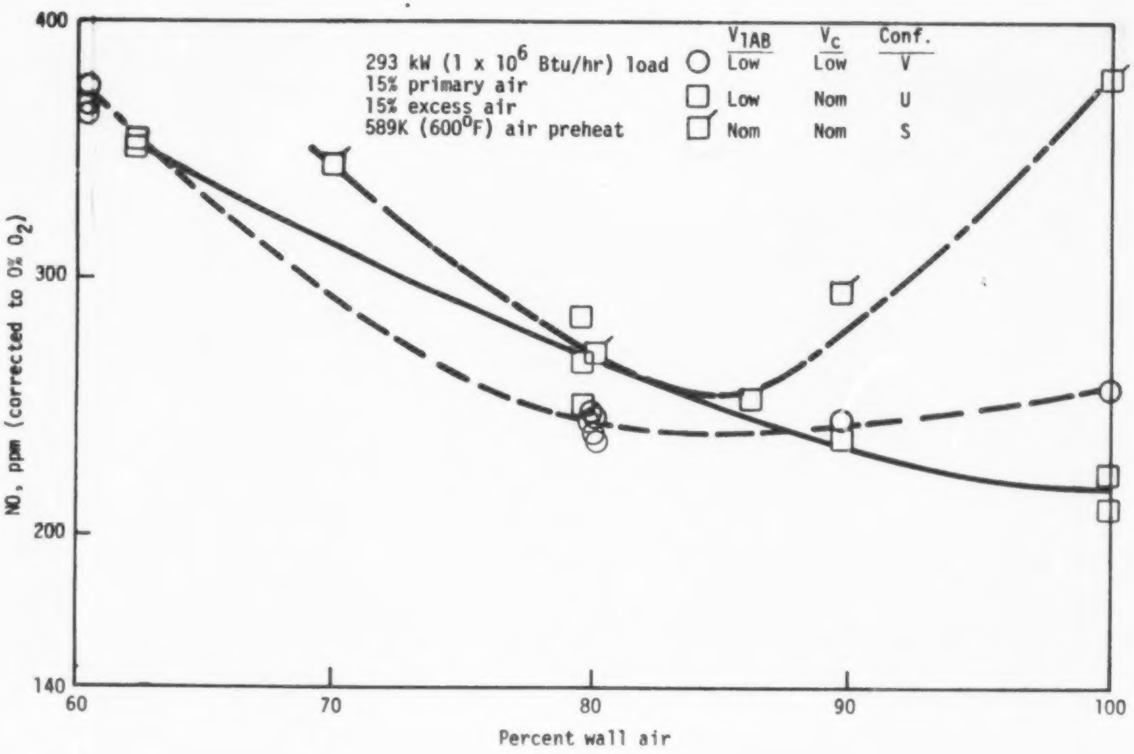

Figure 106. Configuration U, V, and S NO versus percent wall air results (SR_1 = 1.15).

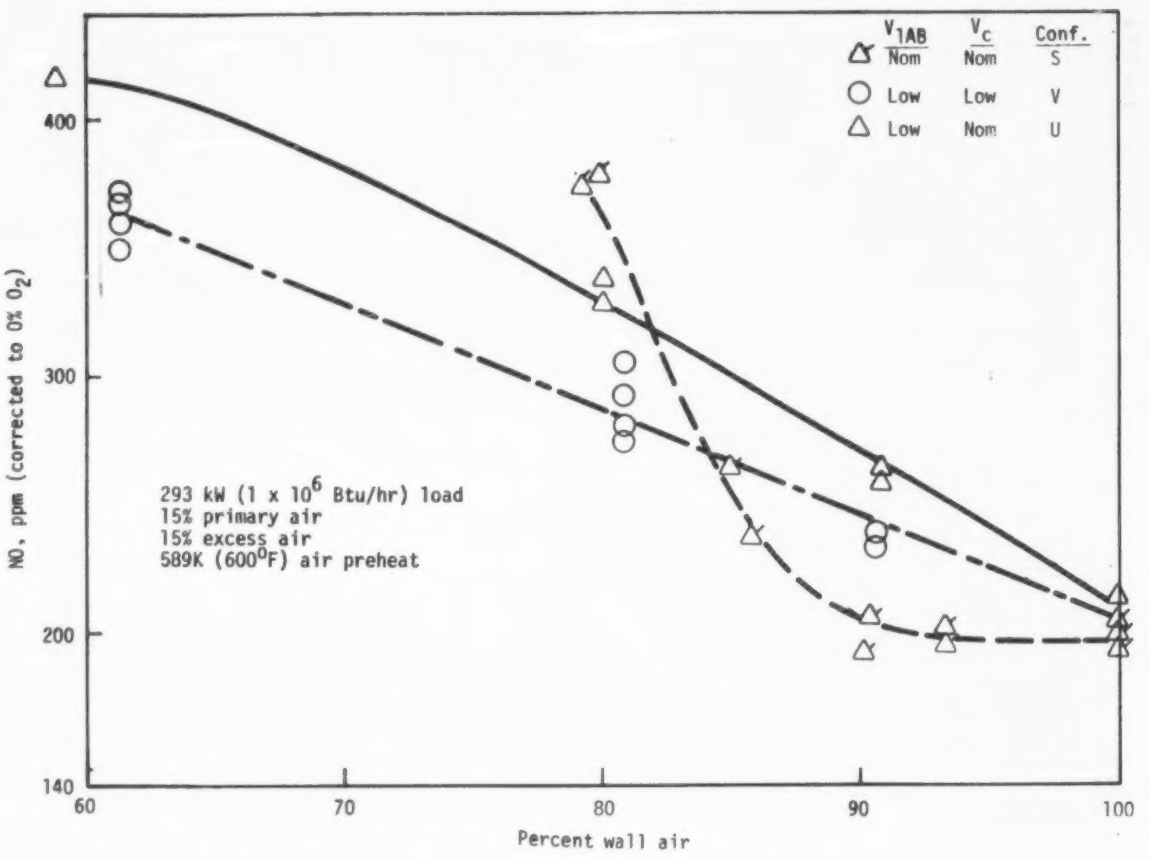

Figure 107. Configurations U, V, and S NO versus percent wall air results (SR_1 = 0.88).

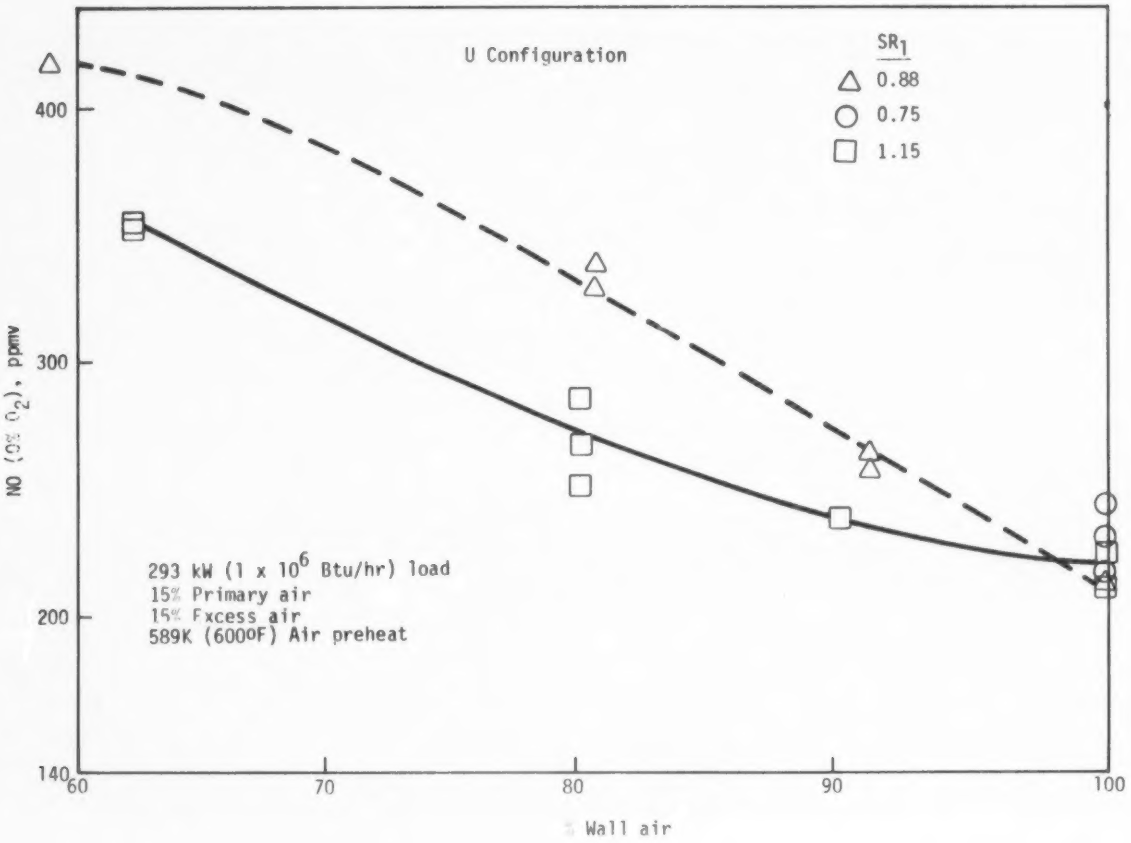

Figure 108. Effects of SR_1 on NO emissions for configuration U.

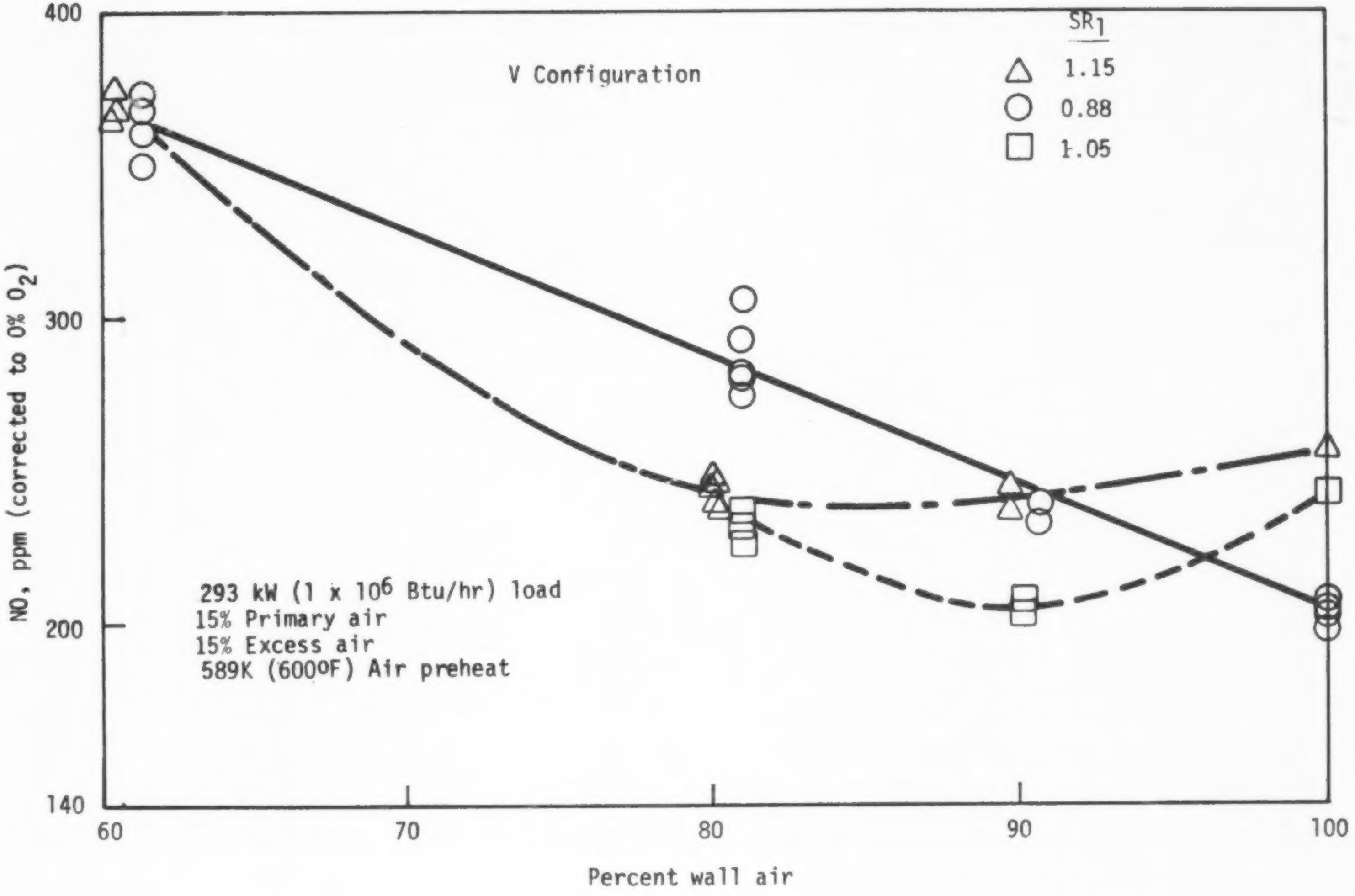

Figure 109. Effects of SR_1 on NO emissions for configuration V.

the NO reduction process in configurations U and V. Further, reductions in the lower wall air velocity, by injecting some of the air in wall air ports 2 and 3, did not benefit NO.

Observation of the flames from the side of the furnace for these low-velocity cases at an SR_1 of 0.88 showed that the swirling motion was much reduced and the flames had a considerable upward velocity compared to the high-velocity cases. With much reduced vortex strength, the impingement of hot gases on the fuel jets possibly is not sufficient to maintain stable positive ignition. This could cause the higher NO levels for the low-velocity wall jet cases at an SR_1 of 0.88.

Figures 108 and 109 show the effects of SR_1 on NO emissions for configurations U and V, respectively. Figure 108 shows that NO emissions increased as SR_1 decreased for configuration U, which was contrary to configuration S results. As mentioned previously, this behavior was probably due to the poor vortex motion of the lower SR_1 case. Similar behavior below 80 percent wall air was also found for the configuration V results in Figure 109. Near 100 percent wall air, as SR_1 decreased NO decreased.

In summary, without vertical wall air (i.e., $SR_1 = 1.15$), lower wall 1AB velocities, such as in configurations U and V appear to reduce NO emissions. However, with vertical wall air (i.e., $SR_1 = 0.88$), NO increases or decreases depending on the percent air on wall. Apparently, some minimal vortex swirling motion is required to stabilize the flames and the fuel rich and lean zones for minimal NO production. Below this level of swirl, NO increases as wall air velocity is decreased.

5.3.7 Coal Particle Size

Due to coal transport velocity limitations, pilot-scale system jet velocities were too high by a factor of roughly five to properly match local residence time with full-scale systems. For example, the residence time for a scaled mixing condition in the pilot-scale facility, given by the adjacent and fuel jet interaction, was one-fifth the time experienced by coal particles in a full-scale facility. Since particle processes are slow compared to gaseous combustion reactions, the mismatch in residence time can be compensated, to some extent, by using smaller particles in the pilot-scale facility. Since a smaller particle will heat up, volatilize, and oxidize more quickly than a larger particle, a smaller particle size fuel supply would give a better simulation of full-scale combustion conditions in the pilot-scale facility.

A fine coal particle fuel supply was briefly tested to more closely simulate full-scale combustion conditions and to demonstrate if local residence time mismatches are important to NO emissions. A sieve analysis of both normal and fine coals is shown in Figure 110. Fine coal is mostly below 44 μm, while normal coal ranges evenly from 0 to 140 μm.

Unfortunately, only a limited amount of fine coal was available. As the coal system did not feed well with the fine coal, very limited data were obtained before the supply of coal ran out. The NO results are within 5 percent of the normal coal results under optimal conditions with

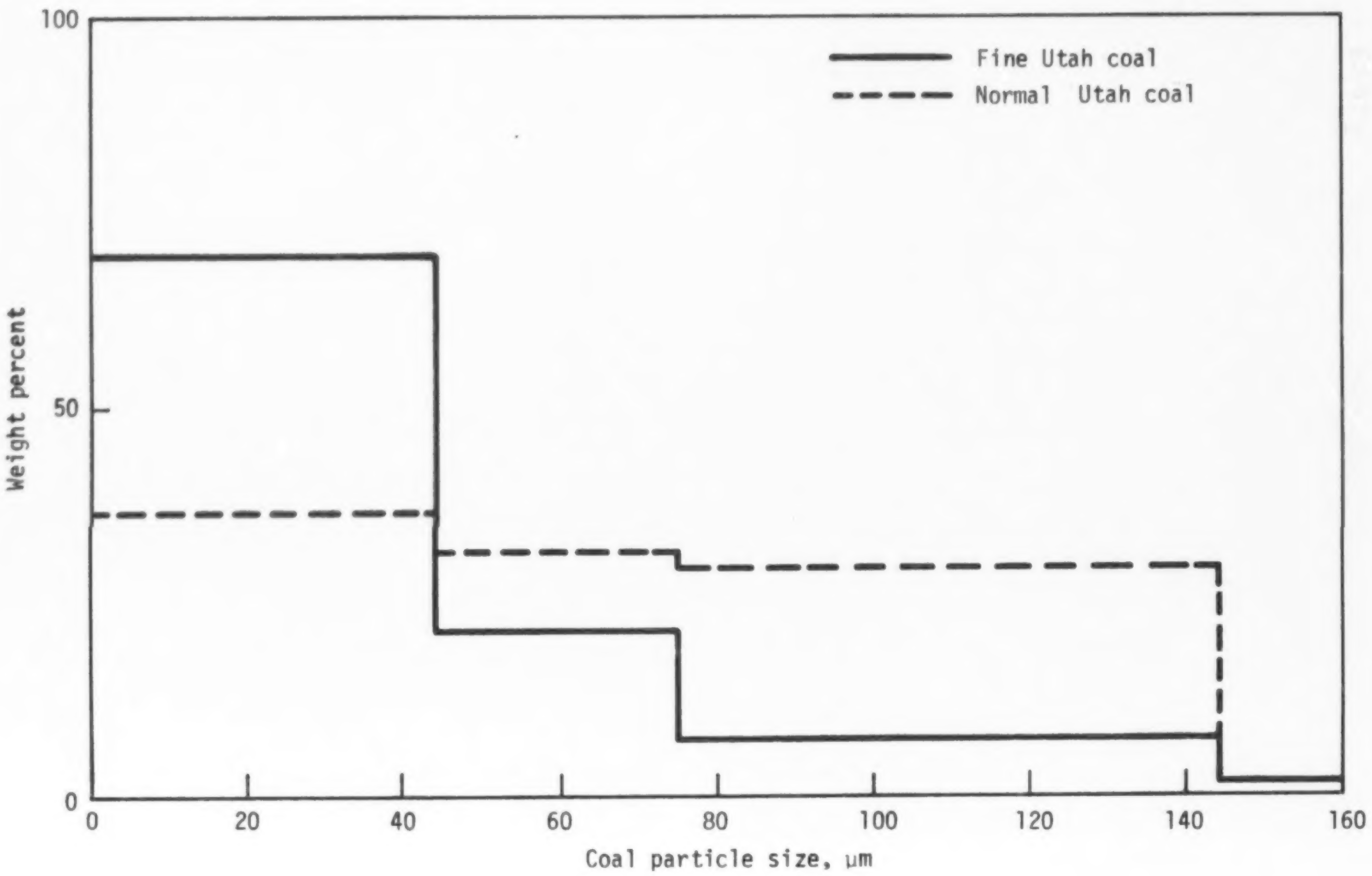

Figure 110. Coal particle size distribution.

configuration V. The close agreement of fine and normal coal data indicates that coal particle size, and hence local particle residence time, did not influence NO results. This would tend to support arguments put forth earlier that fuel/air mixing dominates NO emissions, with local residence times playing a secondary role.

5.3.8 Flue Gas Recirculation Simulation

As a NO_x control technique, flue gas recirculation (FGR) has been used principally as a diluent to control flame temperatures. Although this is an effective method for thermal NO_x control, over one half of the NO_x from coal combustion is believed to be derived from the nitrogen bound in the fuel. At normal combustion temperatures, fuel-derived NO_x is not strongly influenced by temperature (Reference 9). However, under staged combustion, low second-stage temperatures strongly influence coal NO_x emissions (Reference 24).

Testing in this task explored two possible uses of FGR in the low-NO_x system. In the first application, FGR was injected into the center air port surrounding the fuel jet to act as an oxygen-free shield between the fuel and secondary combustion air from the wall jets. This FGR shield would reduce fuel/oxygen contacting and possibly lower NO.

In the second application, FGR was injected into wall jets 2 or 3 only. As shown in staged combustion tests, lowering second-stage temperatures inhibits NO_x formation during the fuel-lean second-stage burnout (Reference 24). The present air-on-the-wall configuration may be considered a locally staged configuration. Since probing results for configuration S suggest that most fuel-rich NO production occurs below the wall 2 level, it was speculated that lowering gas temperatures at the wall 2 and 3 levels, through FGR injection, would function like lowered second-stage temperatures in inhibiting NO_x formation during burnout.

For the FGR tests, configuration S burners were used with N_2 as the FGR simulator. The results are shown in Figures 111, 112, and 113 as NO versus FGR percent of total airflow, and NO versus SR_1 at the fuel entry elevation. As shown in Figure 111, after correcting for the diluent effect of the FGR, NO levels actually increased as FGR flow increased for all SR_1's and injection locations tested. Combustion efficiencies were high for these tests, with combustible losses of 0.16 to 0.56 percent.

For a given FGR flow, the effect of injection location can be seen in Figure 112 (10 percent FGR) and in Figure 113 (20 percent FGR). From these results it appears that increasing FGR was definitely detrimental to NO. The lack of significant NO reduction with FGR injection in the center/annular air jet of a low NO_x tangential burner for coal combustion has also been shown recently in pilot-scale tests reported by Kawanura and Frey (Reference 30).

As expected, gas temperatures were reduced by up to 83K (150°F), as measured by a bare thermocouple, with the addition of FGR. As explained previously, injecting FGR in the wall air ports was expected to lower second-stage temperatures which would lower NO. However, the benefits of

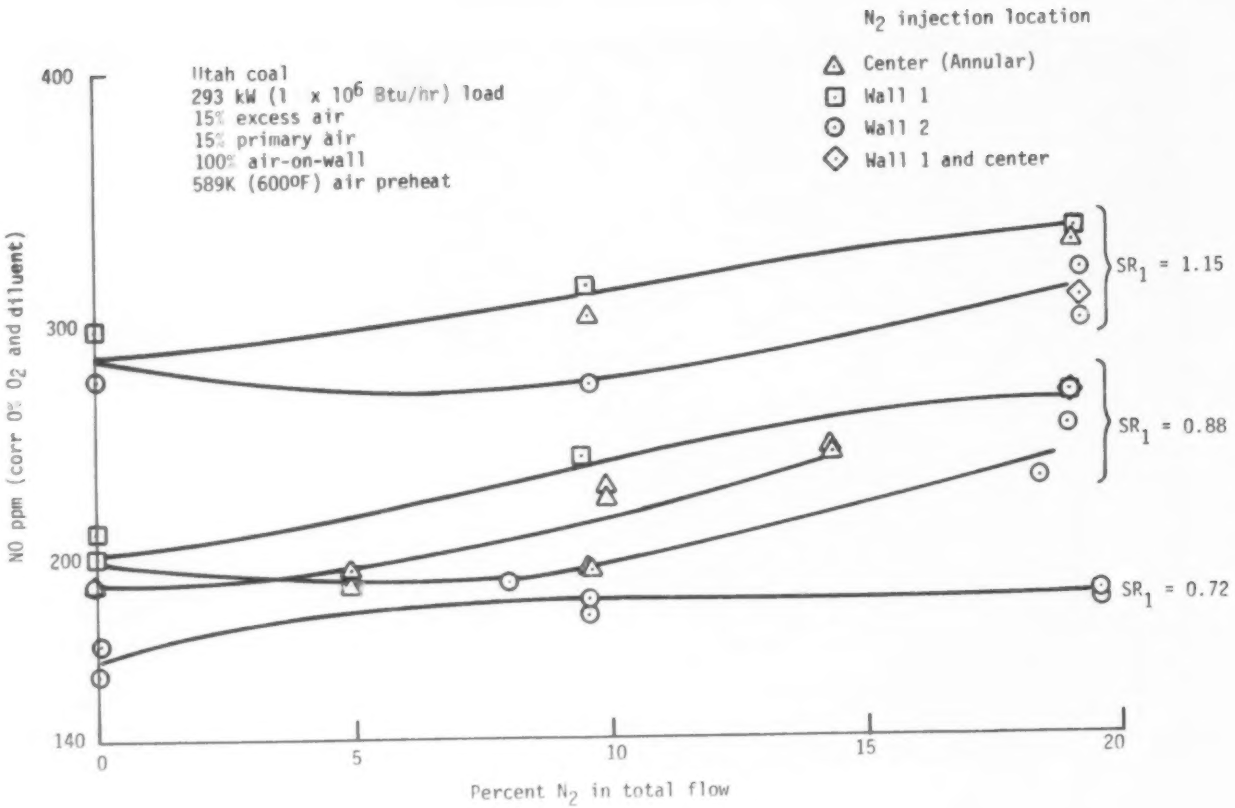

Figure 111. FGR simulation -- NO versus percent N_2.

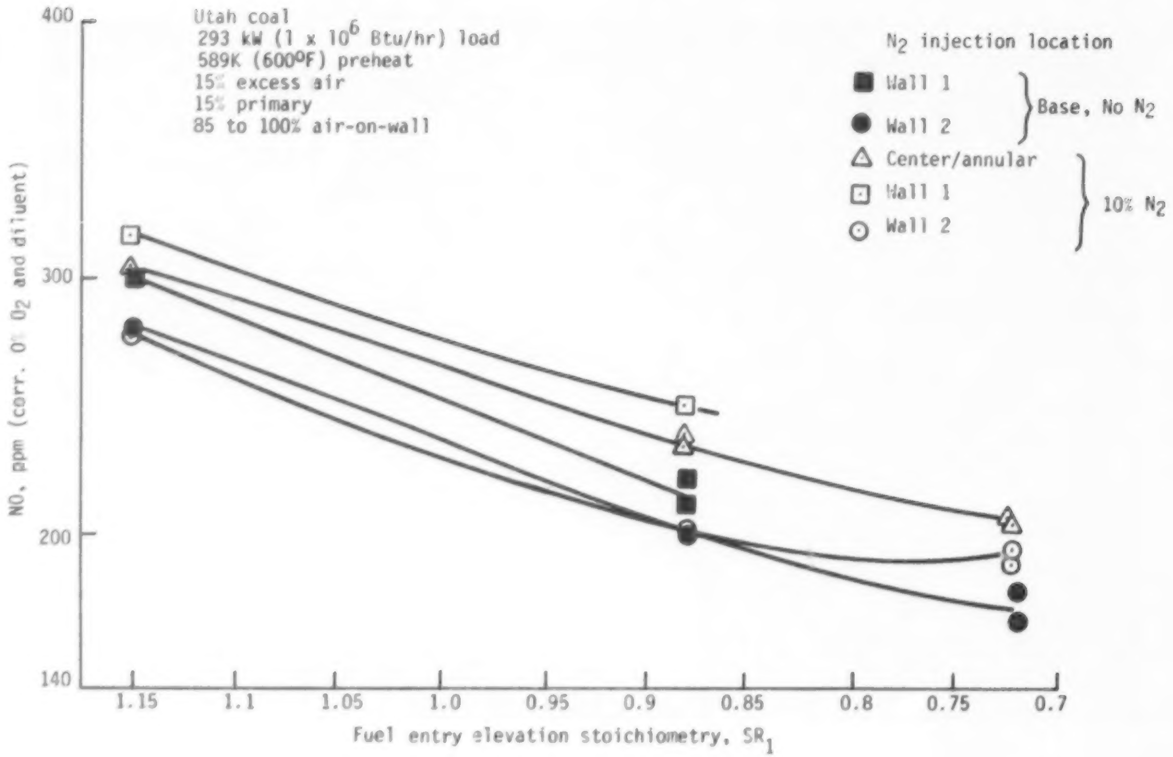

Figure 112. FGR simulation -- NO versus SR_1 (10 percent N_2).

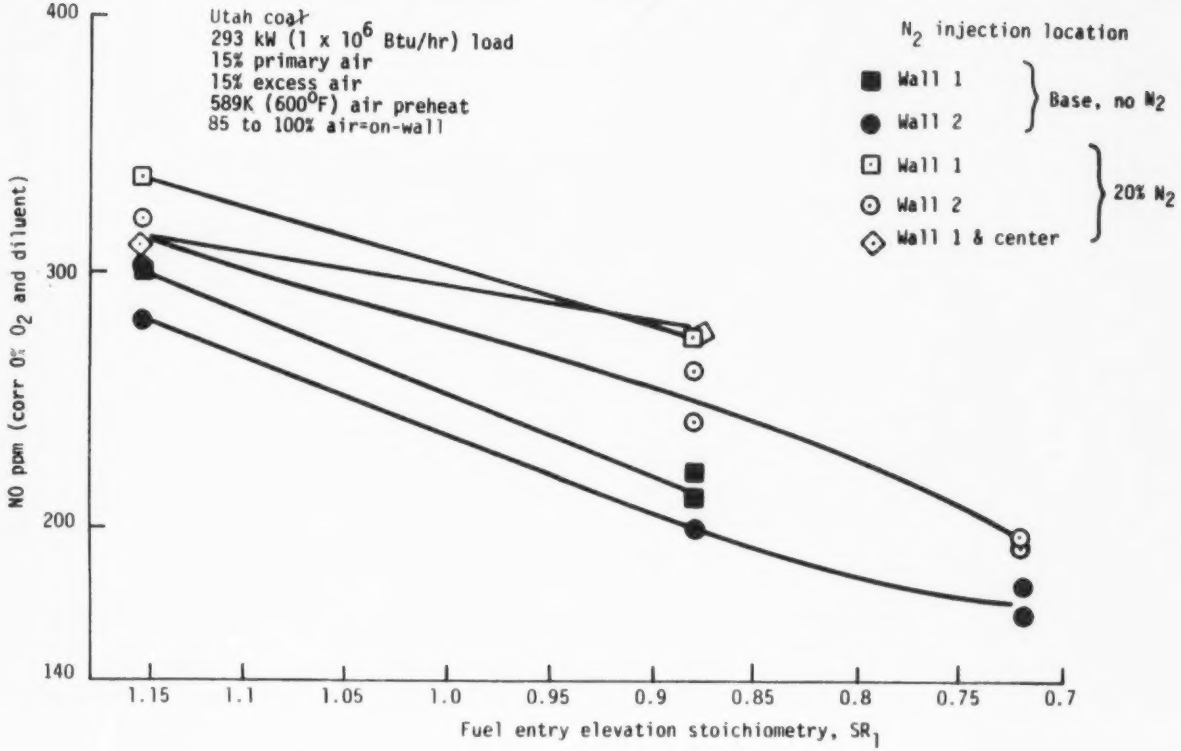

Figure 113. FGR simulation -- NO versus SR_1 (20 percent N_2).

lower second-stage temperatures could have been negated by increased fuel/air mixing and lower temperatures in the early combustion zone. Since first and second stages in the air-on-the-wall system are not well defined, putting FGR in wall ports 2 and 3 may have lowered the first stage as well as the second stage temperature. This may not be beneficial to NO. Similarly, the beneficial fuel shielding effect of the FGR in the center air passage may have been negated by increased center jet velocity and subsequently increased fuel/air mixing in the early combustion zone. The use of FGR without a corresponding reduction in airflow (which would require a reduction in load without hardware changes) increased mixing and decreased bulk residence time due to increased mass flowrates. Since a long residence time allows NO reduction reactions to occur in the fuel-rich zones, decreased residence time could lead to higher NO.

In summary, a quick test of FGR with the low-NO_x system indicated corrected NO emissions are not reduced by FGR. The ineffectiveness of FGR is thought to be related to increased overall firebox mixing, and lower gas temperatures in the lower part of the furnace as well as in the upper furnace zone. A more careful application of FGR (i.e., redesign of injection ports and possibly separate FGR-only injection ports) might benefit the low-NO_x system NO emissions. However, the cursory tests performed here did not demonstrate that a significant potential exists for this NO_x control approach.

5.3.9 System 2 Summary and Conclusions

Based on the System 2 testing, a number of summary statements can be made. System 2 baseline NO levels at an SR_1 of 1.15 were higher than System 1 levels. As in System 1 tests, optimal System 2 NO levels were found with 80 to 100 percent of the secondary air directed along the wall. Distributing wall air to the upper wall air ports at an SR_1 of 0.88 reduced NO levels to the minimum NO range for System 1. This represents a 64 percent reduction in NO from conventional tangentially fired levels.

Most NO is produced quickly at the fuel entry level, and in some cases decays at higher elevations. Thus, a fuel-rich vortex core at the fuel entry level is important for minimizing NO. Velocity, air distribution, and mixing effects are crucial to NO formation at the fuel entry level and less crucial at the upper wall air levels. The negative correlation between NO and bulk gas temperature seen in System 1 may reach an asymptotic condition at a tower gas temperature of 1,506 K (2,250°F).

Combustion efficiency, as measured by stack carbon loss, and CO and UHC emissions, was high (>99.7 percent). As in the System 1 testing, the high O_2 levels measured at the walls should minimize wall corrosion and slagging in a full-scale system.

With the primary jet placed to increase vortex swirl, NO levels were not significantly affected. However, flame impingement on the wall becomes a problem for high swirl levels.

Wall 1 and center air jet velocities strongly influence mixing and NO levels. Moderately reducing the wall jet 1 velocity reduced premixing of fuel and air and lowered NO. However, further velocity reductions can weaken the vortex until stability and positive ignition may be compromised; under these conditions, NO increases.

Particle residence time to jet interaction is much shorter in pilot-scale, as compared to full-scale facilities. Fine coal particle sizes were used to compensate for this residence time mismatch. NO results were essentially equivalent for the normal and fine particle cases. Therefore, local residence time mismatch did not appear to be a primary factor in NO formation/reduction. Thus, the use of normal size coal particles in pilot-scale simulations appears to adequately model local combustion environments and thereby NO formation.

Injecting FGR in the center or upper wall air jets to control combustion temperatures failed to reduce NO levels. In fact, NO levels increased. The disadvantages of decreased residence time, increased mixing, and lower first-stage gas temperatures apparently outweigh the benefits of fuel jet shielding and reduced second-stage gas temperatures.

5.4 SYSTEM 3 BURNER TESTING

The purpose of these tests was to simulate, in pilot-scale, low-NO_x burner conditions for a potential full-scale demonstration burner design. Results of these tests would help guide demonstration burner design and the selection of parameters to be tested.

Pilot-scale System 1 and 2 burner tests showed that low NO_x can be achieved in coal-fired tangential systems by diverting a portion of the secondary combustion air at an angle to the conventional burner yaw. The angle and the amount of this wall air was found to have strong effects on controlling NO_x emissions: the lowest NO_x was achieved when a large portion of secondary air was diverted nearly parallel to the wall.

In conjunction with this pilot-scale testing effort, CE tested a similar burner concept at Richmond Power and Light's Whitewater No. 2 unit in Richmond, Indiana. The Whitewater unit is a nontilting, pulverized coal, tangentially fired boiler having a generating capacity of 65 MW_e with a heat input of 191 MW through three elevations of coal nozzles. Similar to the pilot-scale testing results, the wall air angle was found to have a strong effect on NO_x reduction. In addition, increased carbon loss was observed as the secondary air was diverted toward the walls, resulting in flame impingement. During these tests, flame impingement was controlled at a moderate wall air angle by varying the fuel/air momentum using damper settings. However, under the optimal low-NO_x wall air angle, fuel/air momentum control was only marginally effective in reducing wall flame impingement.

As in the Richmond tests, flame impingement was experienced during some tests conducted in the pilot-scale facility. This condition was found in configuration T System 2 burner tests when the primary and annular yaw angle was significant and wall air velocity was high, i.e., where the stokes (St)* and swirl (Sw)** numbers of the vortex flow were high. However, for most pilot-scale tests with System 1 and 2 burners, wall flame impingement and high carbon loss were not problems, even when the wall air was directed parallel to the walls. With these systems, primary and annular yaw angles, and wall air velocities were controlled to achieve St and Sw numbers which allowed good fuel/air separation for low NO_x while simultaneously limiting wall flame impingement. In addition to the control of these parameters, the pilot-scale System 1 and 2 burners separated the primary/annular and wall air jets by several fuel tube diameters. This reduced the interaction between the primary/annular and wall jets and thereby reduced the potential for flame impingement.

Pilot-scale burners with geometries similar to the baseline demonstration burner design (System 3) were tested to define the NO_x and combustion performance of burners simulating demonstration burner design features. In particular, the effect on NO_x and combustion performance of primary/annular and auxiliary wall air jet angle, velocity, and separation was examined. The performance of wall air combined with overfire air (OFA) was also examined.

5.4.1 Description of Burner Design

The System 3 burner design in this test program made maximum use of the refractory burner block technology developed during the System 1 and 2 burner studies. Figure 114 is a drawing of the System 3 burners. These burners were based on a demonstration burner design for potential retrofit to a full-scale facility. A schematic of this demonstration burner design along with configurational information is presented in Figure 115. The proposed demonstration burner represents a modest modification of a modern, 5-level coal-fired, CE tangential burner incorporating OFA ports immediately above the uppermost auxiliary air port.

To allow air to be diverted toward the walls as in the pilot-scale tests, turning vanes will be incorporated into the auxiliary air compartments in the top three burner levels of a full-scale system. The lower two burners, however, will have secondary air projected towards the center, as in conventional tangential firing. The overall secondary air distribution is given in Figure 115. As can be seen from the figure, the percent wall air for this full-scale design will be less than the levels typically run in the pilot-scale tests.

---

*$St = \frac{p V_t d_p^2}{g R_b}$ where p and d_p are particle density and diameter, respectively, V_t is vortex velocity, g is gas viscosity, and R_b is vortex scale.

**$Sw = \frac{G_a}{G_x R_b}$ where G_a and G_x are angular and axial momentum, respectively, and R_b is firebox scale.

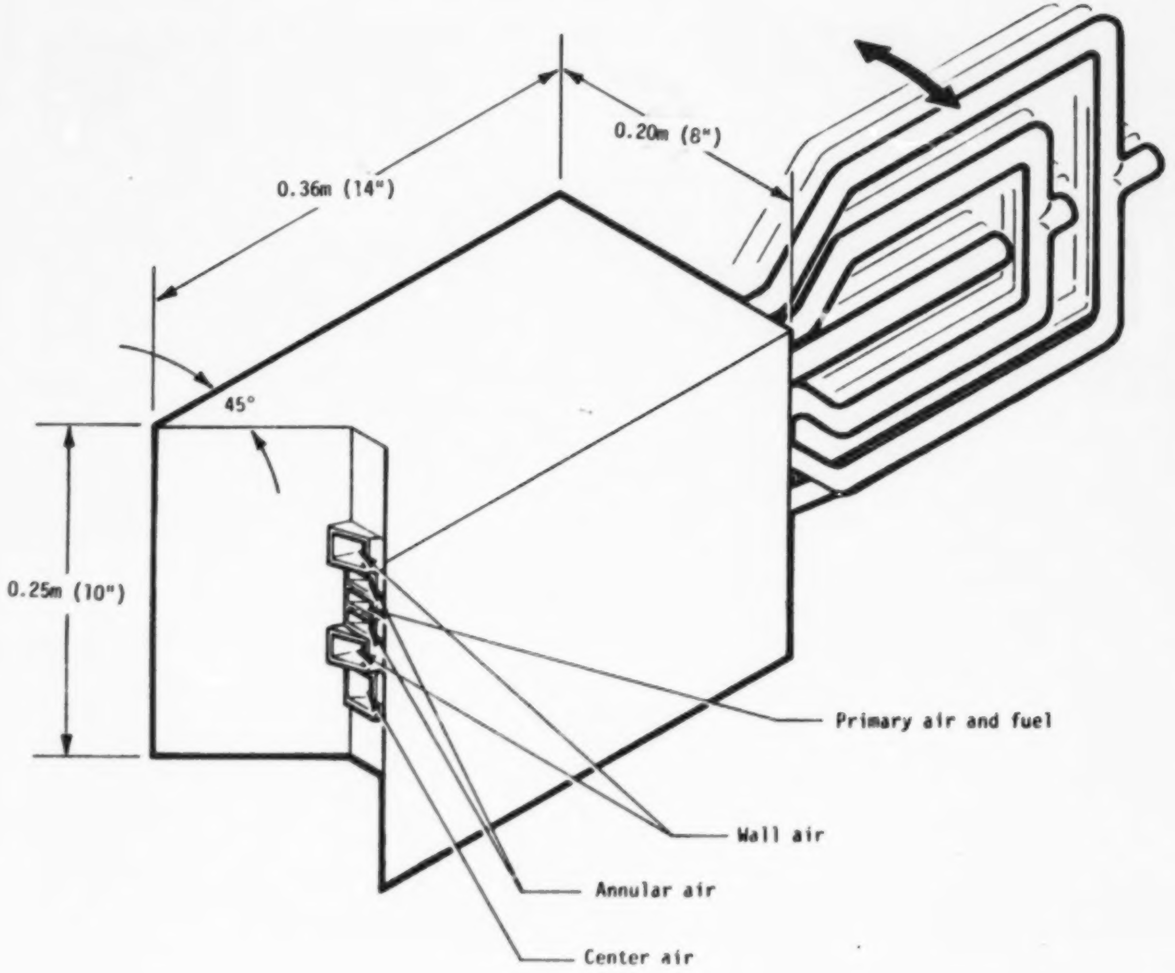
0.36m (14")
0.20m (8")
45°
0.25m (10")
Primary air and fuel
Wall air
Annular air
Center air

Figure 114. System 3 burner schematic.

Air flow splits
(% secondary air flow)

Annular	27
Center	29
Wall	29
OFA	15

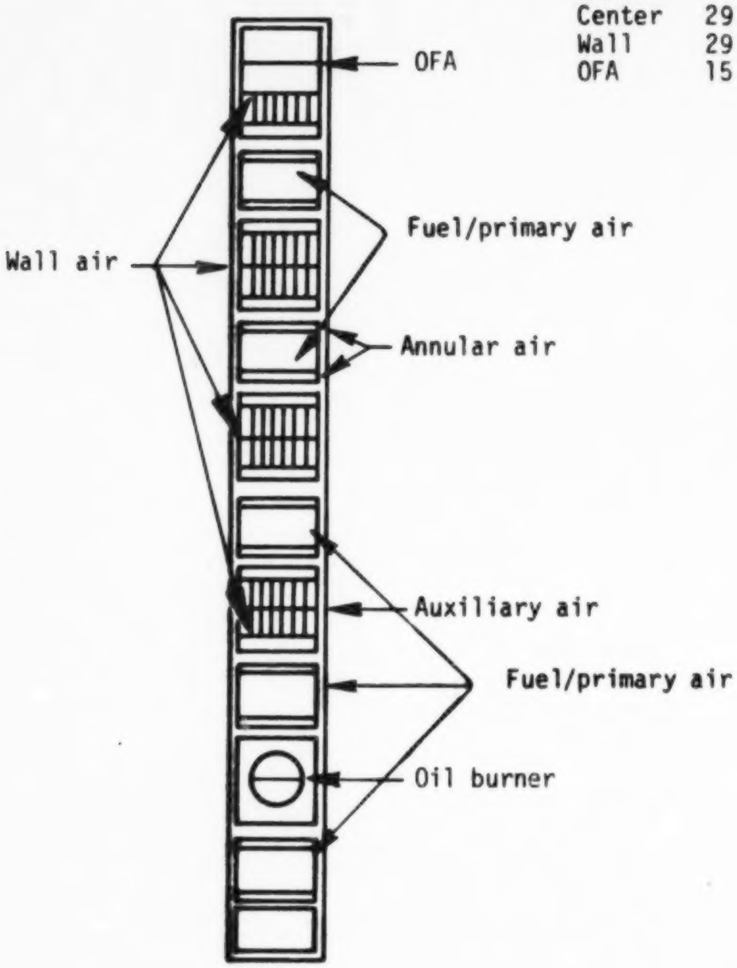
OFA
Fuel/primary air
Wall air
Annular air
Auxiliary air
Fuel/primary air
Oil burner

Head-on view of five-level burner

Figure 115. Demonstration burner design.

As can be seen in Figure 114, the System 3 burners utilized refractory blocks to provide fulcrums upon which stainless steel primary, annular, and wall air jets pivot. The center air jet, which simulates the bottom row of the demonstration burner, was fixed at a 12° yaw angle in the lower part of the refractory block. The OFA ports were located in an upper refractory block to provide either 8° or 45° yaw angle airflows. Primary and annular air jet angles can be adjusted from 0° to 8° yaw, and wall air angle can be adjusted from 31° to 45° yaw.

In addition to air jet angle variation, air port inserts can be used to establish the effect of primary/annular or annular/wall air jet separation and velocity increases on NO and combustion performance. Inserts were sized to give 80 and 116 percent increases in annular and primary air jet velocities, respectively.

To simulate multiburner level full-scale system performance, the System 3 burners modeled the relative velocity ratios, port geometries, and jet directions of the potential demonstration burner design. The matching of these parameters was expected to simulate the flow and mixing patterns between the pilot- and full-scale facilities. To simplify the air supply in the pilot-scale facility, the full-scale system annular port and the portion of auxiliary air at a conventional yaw angle were simulated by a single annular air port in the pilot-scale burner as can be seen by comparing Figures 114 and 115. This departure from the demonstration design was not expected to impact the simulation.

As shown in Figure 115, the lower level of the demonstration burner does not have turning vanes. Therefore, all the airflow in the lower burner level will be projected into the center of the furnace. To simulate in pilot scale the effect of this lower burner level, a center air port was incorporated into the single-level System 3 burners. The center air port simulates the air introduced into the middle of the furnace by the lower burner level of the full-scale system. The angle and exit area of the System 3 burner's center air ports were chosen to simulate the average effect of the full-scale lower burner level secondary airflow on system performance. The detailed processes near the full-scale system's lower level burner face are probably not modeled by the center air port. However, the global effect of more combustion air in the center of the furnace at the lower burner level in the full-scale system was probably adequately modeled by the center air port in the pilot-scale facility.

Modeling the full-scale OFA ports in the single-level pilot-scale facility was not straightforward. In a full-scale system, the residence time of the fuel combustion products to the point of OFA addition varies, depending upon the entry elevation of the fuel. Combustion products from the lower burner level have the longest residence time, and those from the upper level have the shortest residence time before OFA addition. To model this nonuniform residence time distribution in pilot scale, an average residence time to OFA addition was used.

The average residence time to OFA addition in the full-scale system was obtained by assuming the flow at each burner level to be a well-stirred reactor fed by the gas flow from lower burner levels and by the gas flow from the burners at that particular level. Proceeding up the burner levels in this manner, the individual burner level flow and average residence time to the bottom of the full-scale OFA ports were calculated. The average residence time was then used to determine the spacing between the pilot-scale system's fuel entry elevation and OFA ports, assuming well-stirred conditions between these two locations. Based on this analysis, the OFA ports were placed 0.30m (12 inches) above the fuel entry elevation.

It should be noted that separating the fuel entry and OFA ports places these ports closer to the exit of the firebox. At the exit of the firebox, the gases must contract to enter the heat exchange tower. This contraction probably influences the OFA flow which is 0.38m (15 inches) away from this contraction. The impact of the contraction on OFA NO performance is not known. For this study, the proximity of the OFA ports to the contraction had to be accepted to adequately model the residence time from fuel entry to OFA addition.

To simulate full-scale multiple-burner level firing, airflows were distributed between the burner ports as indicated in Table 13. With these airflows, both full-scale percent airflows and relative velocities were simulated by the pilot-scale System 3 burners. This matching should give the correct flow patterns and shear between burner jet flows within the firebox. To simulate full-scale single-level firing, airflows were distributed between the burner ports, as indicated in Table 13. Without burner inserts, these airflows should give a wall-to-primary/annular relative velocity ratio about 40 percent higher than full scale. With burner port inserts, the relative velocity ratio would be 44 percent lower than full scale. Although fixed geometry ports and inserts did not permit the testing of a full-scale relative velocity ratio for single-level simulation, the full-scale airflow splits were achieved in pilot-scale testing.

Because of fuel/air mixture transport limitations, primary air velocity was fixed at 30 ft/sec. At this velocity, the relative velocity scaling, described above, should give annular, wall, and center air exit velocities of 50 ft/sec for the non-OFA, multiburner level simulation case. While properly simulating relative velocities, the pilot-scale System 3 burner velocities yielded St and Sw numbers, respectively, 4.1 and 5.3 times as large as full-scale system values for a similar burner geometry. In addition, due to a fixed burner exit area, the St and Sw number ratios between pilot- and full-scale systems increased to 5.7 and 6.8 for airflow splits simulating the single burner level case.*

Since St and Sw numbers are a measure of particle centrifuging, and vortex and recirculation behavior in the firebox, respectively, the significant mismatch of the pilot- to full-scale numbers might result in differences in system behavior. For example, the relatively high St number

---

*As a point of reference, the ratios of St and Sw for full-scale wall air to conventional tangential burners are 3.5 and 3.7, respectively.

TABLE 13. SYSTEM 3 BURNER AIRFLOW SPLITS

Secondary air variable	Airflows (percent of secondary air)			
	Multiple level simulation		Single level simulation	
	non-OFA	OFA	non-OFA	OFA
Annular	32	27	32	26
Center	34	29	10	10
Wall	34	29	58	49
OFA		15		15

for the pilot-scale facility could cause the fuel to move outward towards the wall more easily than would be experienced by a full-scale burner. Therefore, flame impingement might be expected to be more of a problem for the pilot-scale system than for the full-scale system.

When the System 3 burners were designed, relative velocity simulation was judged to be more important than St and Sw number modeling. Tests results showed that flame impingement with System 3 burners was a problem. Since flame impingement is influenced by St and Sw, a compromise between relative velocity simulation and St and Sw number simulation probably would have been the best approach to modeling full-scale burner performance in pilot scale.

5.4.2 Results and Discussion

The results of the System 3 burner tests are summarized in Table 14. Each data point represents an average of at least two points taken at the same conditions over a period of approximately 1/2 hr. The standard test procedure was to heat up the system on natural gas for a period of approximately 2 days. Upon reaching a nearly steady state thermal condition, the system would then be switched to coal firing. Data taking would commence after reaching nearly steady state thermal coal combustion conditions. This typically occurred after approximately 3 hrs of coal firing. Most test points consisted of at least 1 hr of operation under the required test conditions with data being taken during the later half of the period.

Calibration of the gaseous emission monitoring equipment occurred several times a day. No less than three calibrations/day of the instruments were performed during the System 3 burner testing. In general, the

TABLE 14. SYSTEM 3 BURNER RESULTS

Data number	1	2	3	4	5	6	7	8	9	10	11	12	13	14	15
Test point	376D	376E	376F	376G	376H	376I	376J	376L	376M	376N	377C	377E	378B	378C	378D
Load (10^6 Btu/hr)	1.01	1.02	1.01	1.02	0.99	0.99	1.01	0.99	0.99	0.99	1.00	1.01	1.00	1.02	0.99
Excess Air (%)	15	15	15	15	15	15	15	15	15	15	15	15	15	15	15
NO (ppm @ 0% O_2)	410	342	441	399	431	432	426	490	553	368	362	414	348	295	350
O_2 (%)	2.79	2.76	2.73	2.70	2.76	2.77	2.76	2.76	2.76	2.76	2.61	2.75	2.78	2.74	2.79
Carbon Burnout (%)											99.9	99.9	100	100	99.9
Total Air (lbm/hr)	875	880	877	883	860	856	873	857	858	858	868	874	862	882	858
Primary (lbm/hr)	132	130	129	128	126	129	129	130	130	127	130	131	130	131	131
Airflows (% of secondary)															
Annular	34	21	21	26	31	31	26	35	42	42	26	26	31	26	26
Wall	37	44	44	30	35	35	30	14	16	43	49	49	58	48	49
Center	15	21	35	28	34	34	29	35	43	15	10	10	11	11	11
OFA	15	14	0	16	0	0	15	16	0	0	15	15	0	15	14
Stage															
Air Jet Angles (degrees)															
Primary	8	8	8	8	8	8	8	8	8	8	0	8	0	0	8
Wall	45	45	45	31	31	45	45	45	45	45	31	31	45	45	45
OFA	45	45	--	8	--	--	8	8	--	--	8	8	--	45	45
Air Jet Velocities (ft/sec)															
Primary*	31	31	30	30	30	30	30	31	31	30	31	31	31	31	31
Annular**	54	34	34	42	49	48	41	54	65	66	41	41	49	42	40
Wall**	54	65	65	45	51	50	44	20	23	62	72	72	84	71	70
Center**	22	32	52	42	50	49	43	51	63	22	15	15	16	16	16
Inserts															

*Assume t_{air} = 100°F
**Assume t_{air} = 500°F

TABLE 14. CONTINUED

Data number	16	17	18	19	20	21	22	23	24	25	26	27	28	29
Test point	378E	378G	378H	378I	378J	381A	381B	381C	381E	381F	381G	381H	381J	381K
Load (10^6 Btu/hr)	1.01	1.02	1.02	1.02	1.02	1.02	1.02	1.01	1.02	1.00	1.01	1.01	1.02	1.01
Excess Air (%)	15	15	15	15	15	15	15	15	15	15	15	15	15	15
NO (ppm @ 0% O_2)	392	332	371	320	313	287	342	341	318	335	345	389	375	256
O_2 (%)	2.76	2.79	2.76	2.77	2.79	2.75	2.77	2.73	2.73	2.72	2.75	2.74	2.77	2.77
Carbon Burnout (%)	100	100	100	100	99.9	99.9		99.9						
Total Air (lbm/hr)	874	881	880	880*	881	882	879	876	881	866	872	876	883	874
Primary (lbm/hr)	131	131	132	132*	132	132	131	130	132	129	128	131	133	133
Airflows (% of secondary)														
Annular	32	26	27	27*	27	26	26	26	26	25	32	32	32	27
Wall	59	49	50	50*	49	49	49	49	49	49	59	58	59	48
Center	9	10	10	10*	10	10	10	10	10	11	10	10	10	10
OFA	0	15	14	14*	15	16	16	16	16	15	0	0	0	0
Stage														15
Air Jet Angles (degrees)														
Primary	8	8	8	0	0	0	8	8	0	0	0	0	0	0
Wall	45	37	31	31	37	31	31	45	45	37	37	45	31	31
OFA	--	45	45	45	45	45	45	45	45	45	--	--	--	--
Air Jet Velocities (ft/sec)														
Primary	31	31	31	31	31	68	67	67	68	66	66	67	68	68
Annular	51	42	43	43	43	75	75	75	75	71	92	92	93	77
Wall	87	73	74	74	73	73	73	72	73	72	87	86	88	70
Center	13	15	15	15	15	15	15	15	15	16	15	15	15	15
Inserts						X	X	X	X	X	X	X	X	X

*From 378H

TABLE 14. CONCLUDED

Data number	30	31	32	33	34	35	36	37	38	39	40	41	42	43	44
Test point	381L	381M	381N	381O	382B	382C	382D	382E	382F	382G	382H	382I	382J	382K	382L
Load (10^6 Btu/hr)	1.00	1.05	1.03	1.03	1.02	0.99	0.98	1.02	1.02	1.01	1.14	1.13	1.01	1.04	0.71
Excess Air (%)	15	15	15	15	15	15	15	15	15	15	15	15	25	5	15
NO (ppm @ 0% O_2)	280	542	302	315	446	298	289	310	258	251	279	249	306	186	201
O_2 (%)	2.71	2.72	2.74	2.76	2.76	2.72	2.76	2.72	2.72	2.77	2.77	2.76	4.27	1.01	2.77
Carbon Burnout (%)															
Total Air (lbm/hr)	861	909	895	891	882	856	853	882	880	874	983	977	947	783	613
Primary (lbm/hr)	133	133	133	134	131	131	131	132	132	130	130	145	129	131	97
Airflows (% of secondary)															
Annular	27	42	30	11	37	27	22	27	19	10	25	27	27	28	28
Wall	49	48	60	79	52	48	39	48	47	47	49	47	48	48	48
Center	10	10	10	10	11	10	10	10	19	27	10	10	10	9	9
OFA	0	0	0	0	--	15	28	15	15	15	15	16	15	15	14
Stage	14														
Air Jet Angles (degrees)															
Primary	0	0	0	0	0	0	0	0	0	0	0	0	0	0	0
Wall	45	31	31	31	31	31	31	31	31	31	31	31	31	31	31
OFA	--	--	--	--	--	45	45	45	45	45	45	45	45	45	45
Air Jet Velocities (ft/sec)															
Primary	68	68	68	69	67	67	67	68	68	67	67	74	66	67	50
Annular	76	126	88	32	107	76	61	78	55	29	82	87	85	71	56
Wall	71	74	90	118	77	69	56	71	70	69	83	77	78	62	49
Center	15	16	15	15	17	15	14	15	28	40	17	17	16	12	9
Inserts	X	X	X	X	X	X	X	X	X	X	X	X	X	X	X

instruments were found to drift no more than 5 percent between calibrations. Data have been corrected for calibration drift.

After 20 hrs of testing on coal, the system was shut down and allowed to cool. The inside walls of the firebox and burner faces were then cleaned of deposits to maintain a consistent internal firebox geometry for all test conditions.

The initial System 3 burner tests were scoping tests to quickly establish the performance of the burner with respect to design variables. Also, these tests provided data for comparison to previous System 1 and 2 test results and Richmond Power and Light full-scale system results.

Figure 116 schematicizes some System 1 and 2, and Richmond Power and Light burner designs. Comparison of these designs with the System 3 and full-scale demonstration designs in Figures 114 and 115 respectively, shows that System 1 and 2 designs were significantly different from the Richmond Power and Light, full-scale demonstration, and System 3 designs. The Richmond Power and Light design had similarities to the demonstration and System 3 designs in fuel/air placement, but it differed significantly in the design of the annular air compartment. The Richmond design provided a circumferential shielding of the primary fuel jet by the annular air, while the demonstration design had annular air mostly above and below the fuel jet.

Based on previous System 1 and 2 burner results, percent of secondary air diverted along the walls was expected to be a strong variable in controlling NO_x for the System 3 burners. Therefore, the initial System 3 burner testing examined the performance of the burner with respect to the percent wall air. Figure 117 gives the NO results for these burners as a function of percent of secondary air* along the wall. As shown on the figure, the wall and primary/annular air angles were set at 45° and 8°, respectively. Non-OFA and 8° and 45° angle OFA cases were included.

Other details of the test conditions are given in Table 14 and Figure 117. Also included in Figure 117 are some System 1 and 2 burner results obtained previously, and a single data point from the Richmond Power and Light full-scale boiler tests** (Reference 31). As shown in Figure 117, System 1, 2, and 3, burner NO decreased significantly as the percent of secondary air on the wall increased. This was the case for non-OFA as well as OFA cases. Further, the System 3 results were roughly comparable to System 1 (configurations G and H) results and the single estimated Richmond Power and Light result.

No 8° wall air angle baseline tests were performed with the System 3 burners. However, extrapolating the non-OFA percent wall air results presented in Figure 117 from 15 percent back to 0 percent wall air would

---

*All percent air values, except primary air, will be given in subsequent discussions as a percent of secondary air.

**Scaled from reported percent reduction and estimated baseline levels.

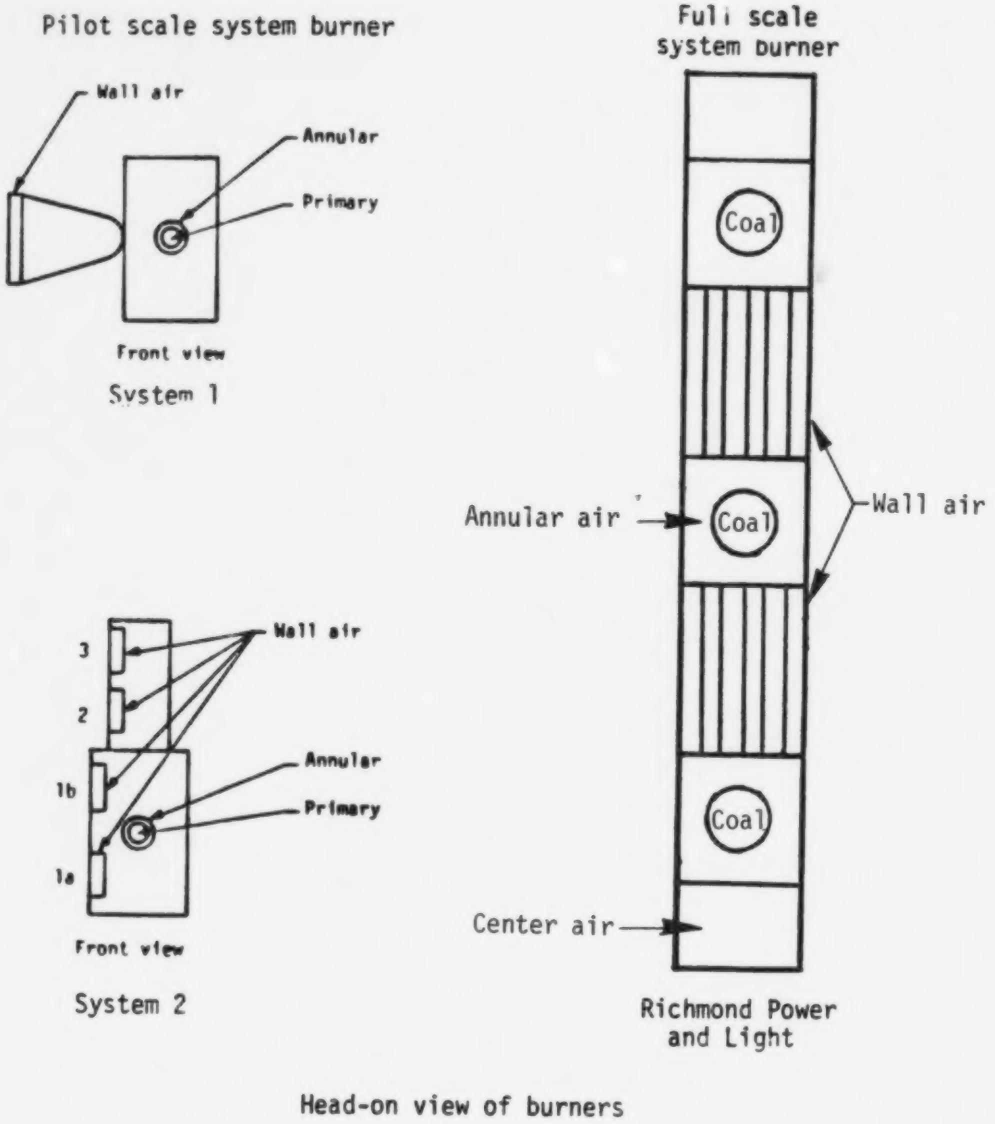
Pilot scale system burner
Wall air
Annular
Primary
Front view
System 1
3
2
1b
1a
Wall air
Annular
Primary
Front view
System 2
Full scale system burner
Coal
Coal
Coal
Annular air
Wall air
Center air
Richmond Power and Light
Head-on view of burners

Figure 116. Systems 1 and 2 and Richmond Power and Light burner designs.

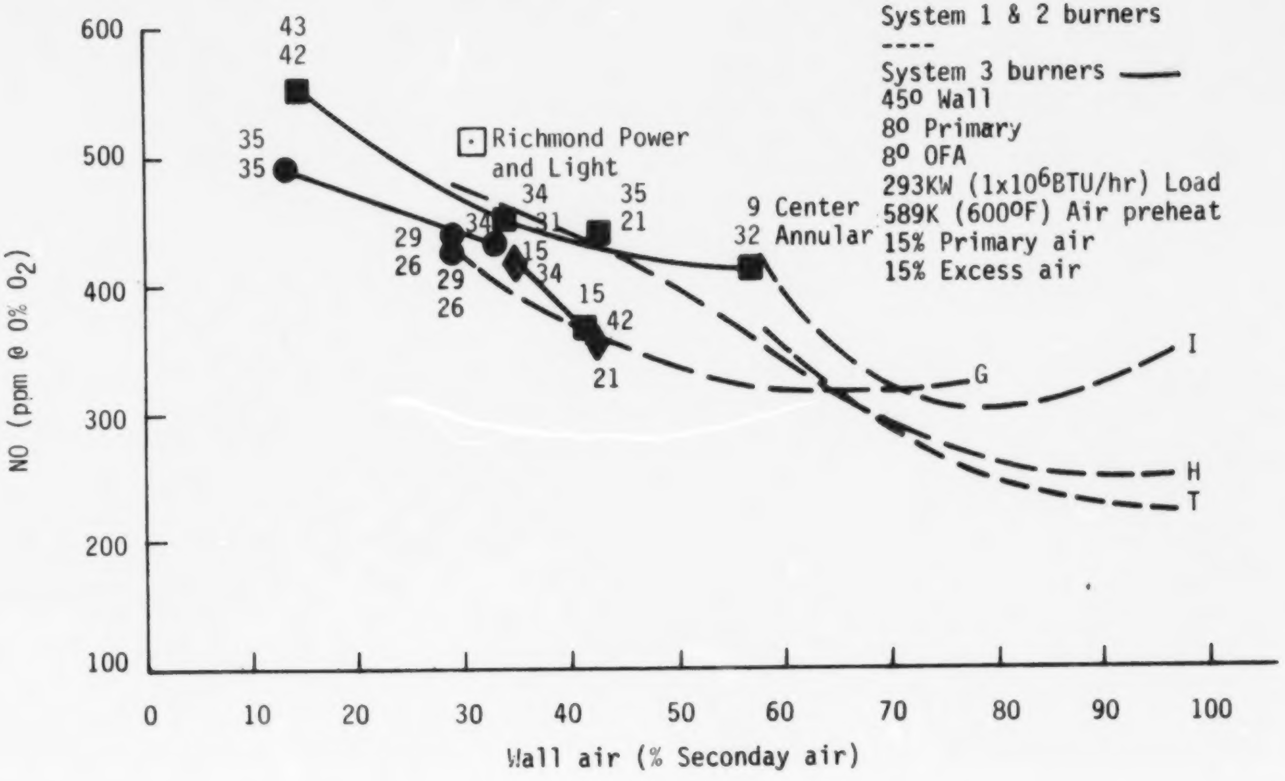

Figure 117. Comparison of Systems 1, 2, and 3, and full-scale NO results.

conservatively yield 600 ppm NO at baseline conditions. This level seems reasonable based on conventional tangential firing results and gives NO reductions of approximately 25 and 33 percent from baseline for 35 and 48 percent wall air, respectively. As discussed previously, the 48 percent wall air condition utilized the same percent wall-to-primary/annular airflow splits as projected for a single burner level of the demonstration burner. The 35 percent wall air case, with 34 percent of the secondary air in the center air port, was an attempt to simulate the wall-to-primary/annular airflow split projected for the average of five burner levels of the demonstration burner. As can be seen from the System 1, 2, and 3 results in Figure 117, greater reductions in NO can be achieved simply by increasing the percent wall air.

After performing these scoping tests, it was decided that the System 3 burner performance was acceptable relative to previous System 1 and 2 burner results and Richmond Power and Light data. In addition, it was decided that the most appropriate modeling condition was with 48 percent wall air, 10 percent center air, and 26 percent annular air. This airflow split, an approximate modeling of a single level of the demonstration burner, was chosen as our baseline condition.

Operating the Systems 3 burners under this percent airflow split yielded a high wall air velocity (approximately 72 ft/sec). As discussed previously, this condition caused a significant mismatch between pilot- and full-scale St and Sw numbers. The ratio of pilot-scale and similarly configured full-scale St and Sw numbers are estimated to be 5.7 and 6.8, respectively.

These significant differences can lead to flame impingement problems in the pilot-scale facility which might not be experienced in the full-scale facility at similar percent airflow splits. Therefore, the pilot-scale results represent a conservative test for flame impingement.

Center air was maintained at 10 percent for these single burner level simulation tests, more to cool the metallic part of the burner jets than to simulate any aspect of the demonstration burner design.

System 3 burner testing will be discussed in detail below. Specifically, the influence of the following list of parameters on NO_x and combustion performance will be addressed:

- Wall air angle
- Primary/annular air angle
- Primary/annular air velocity
- OFA
- Percent wall and annular air
- Excess air
- Load
- Fuel effects

5.4.2.1 Wall Air Angle

Having selected a percent wall/annular airflow split, tests were then run to establish the effect of wall air angle on NO. Figure 118 presents the wall air angle results for 8° and 0° primary/annular air angles with and without OFA. Most of the data was taken with 45° OFA, which seemed to be the most effective orientation. Detailed test conditions can be found on the figure and in Table 14.

As shown in Figure 118, the major result from wall angle testing is that NO was insensitive to wall air angle in the range of angles tested. For 8° and 0° primary/annular angle and 45° OFA, NO did not change significantly as wall air angle increased. The 8° primary/annular case exhibited a NO minimum at 37° wall air angle, while NO for the 0° primary/annular case seemed to decrease monotonically as wall air angle increased.

From previous System 1 burner and Richmond Power and Light results, it was expected that the System 3 burner NO results would be strongly influenced by wall air angle. As the wall air angle was increased, the separation of fuel and air was expected to increase and NO formation in the center of the furnace to decrease. However, as wall air angle was increased, the vortex swirl also increases. Increasing swirl tends to bend the fuel jet towards the wall which reduces the amount of fuel reaching the center of the furnace and the fuel richness of the core. This has a detrimental effect on NO formation. Thus, the beneficial effect of separating fuel and air, as wall air angle is increased, can be offset by the increased vortex swirl's bending of the fuel jets towards the wall. It is speculated that these compensating effects could lead to the observed System 3 burner NO insensitivity to wall air angle.

In support of this hypothesis, gas flame and flow pattern observations from the bottom of the furnace for the System 3 burner 45° wall air angle case showed that, upon exiting the burner, the fuel jets turned abruptly towards the furnace wall, the flames impinging on the walls. In these tests, flame impingement was defined as where the fuel jet flow and resulting flames were observed to be in close proximity (less than a few burner exit diameters in distance) to the wall. As wall and primary/annular angles were reduced, the fuel jet bending and flame impingement were reduced. However, in all cases, some degree of flame impingement was evident. In addition, inspection of furnace ash deposition patterns after shutdown showed that most of the ash was deposited in a fairly narrow band at the burner fuel entry level around the periphery of the firebox. In particular, deposition was heaviest near the burner faces. This deposition pattern suggests that a portion of the fuel or ash is moving outward into the wall air layer and being selectively deposited at the fuel entry level.

This type of flame impingement and ash deposition pattern was not evident in System 1 and 2 burner tests. Flame observation for these burner systems showed a fairly small vortex with fuel jets penetrating into the center of the furnace. Also, deposition was not as selective or extensive for these burners as was found for the System 3 burner. Deposits for System 1 and

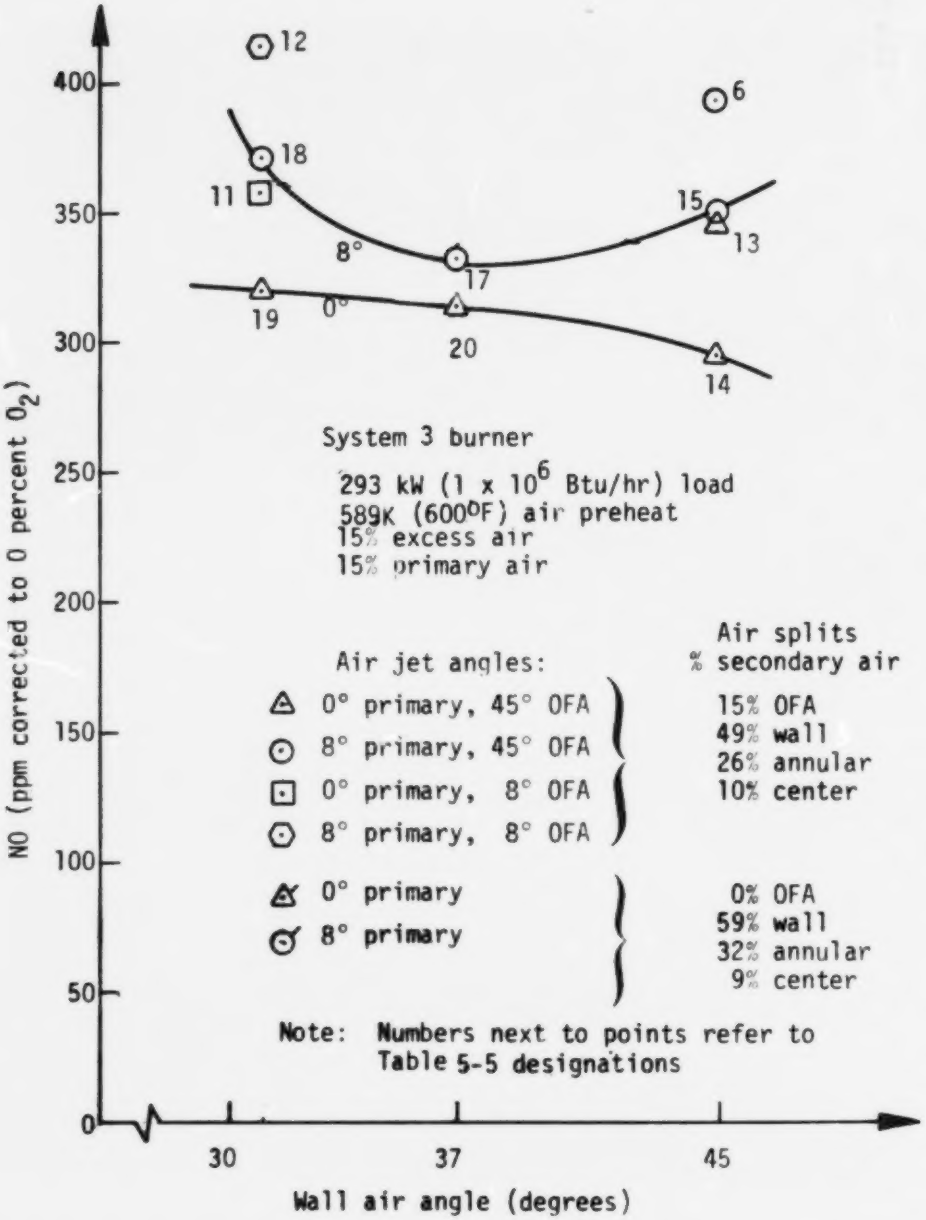

Figure 118. NO versus wall angle using variable angle burner blocks without inserts.

2 burner tests were more evenly distributed over the entire firebox, indicating that fuel and ash were moving outward towards the walls in a less selective manner.

The difference in flame impingement behavior between the System 1 and 2 and the System 3 burners is probably due to the relative velocity differences between these burners. For the System 1 and 2 burners, particularly the System 2 burners, the wall air was distributed to fairly large exit area jets giving a lower wall jet velocity compared to the System 3 burners. Figure 119 presents the burner port geometries and relative areas for some System 1, 2, and 3 burners. For similar percent airflow splits in the different burners, the System 3 burners clearly will have the highest wall air exit velocities. The differences in velocity lead to significant St and Sw number differences between the three burner systems as indicated in Table 15. High St and Sw numbers associated with System 3 burners compared to System 1 and 2 burners causes the movement of fuel out towards the wall which yields poor fuel/air separation and consequent insensitivity of NO with respect to wall air angle.

In the full-scale demonstration burner, scale and velocity differences will give lower St and Sw numbers. As discussed previously, the ratio of pilot-scale System 3 burner St and Sw numbers to full-scale values are 5.7 and 6.8, respectively. Therefore, flame impingement should be less of a problem with the full-scale system. Additional support for less flame impingement in the full-scale system can be found in the System 2 burner results. As shown in Table 15, System 2 burners have St and Sw numbers comparable to full-scale values. Since impingement was not a problem with System 2 burners, it might be speculated that impingement with full-scale burners should not be as severe as with System 3 burners.

TABLE 15. VORTEX PARAMETERS FOR PILOT-SCALE SYSTEMS 1, 2, AND 3, AND FULL-SCALE DEMONSTRATION AND CONVENTIONAL TANGENTIAL SYSTEMS

	System				
Parameter	Pilot scale			Full scale	
	1	2	3	Demonstration	Conventional
Stokes	0.46	0.18	0.80	0.14	0.04
Swirl	3.29	1.37	5.83	0.86	0.23

*Calculated for 55 percent wall air (including 45° OFA) at 45°, 15 percent primary air, and the balance annular air at 8° yaw angle.

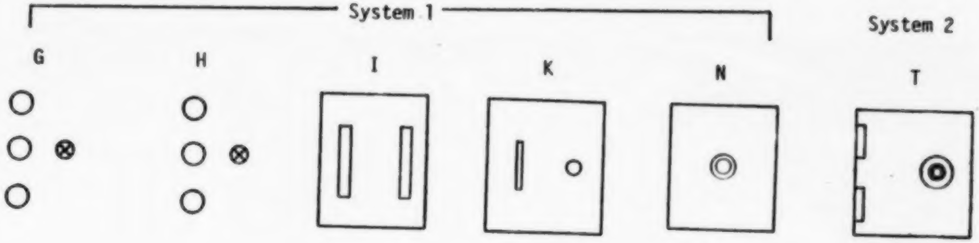
System 1
System 2
G
H
I
K
N
T

Exit Area/* Relative Area	G	H	I	K	N	T
Primary	0.59/1.0	0.59/1.0	0.60/1.0	0.60/1.0	0.60/1.0	0.60/1.0
Annular	3.68/6.24	3.68/6.24	0.90/1.50	0.90/1.5	0.94/1.57	1.23/2.05
Wall	3.14/5.32	2.25/3.81	2.25/3.75	2.25/3.75	2.25/3.75	4.88/8.13

*Exit area in in^2

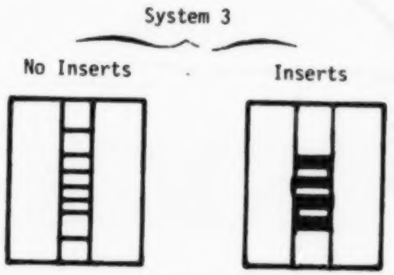
System 3
No Inserts
Inserts

Exit Area/ Relative Area	No Inserts	Inserts
Primary	0.54/1.0	0.22/1.0
Annular	1.20/2.22	0.70/3.18
Wall	1.19/2.20	1.19/5.41

Figure 119. Systems 1, 2, and 3 configurations and jet exit areas.

It should be noted that it is not clear what the impoact of flame impigement of the type observed in pilot-scale testing would be in a full-scale facility. In conventional full-scale systems, some intermittent brushing of the flames along the furnace walls is possible. As observed in Richmond Power and Light tests, this brushing can be increased by diverting some of the secondary air towards the wall. Flame impingement in full-scale units is typically associated with increased boiler tube wastage and carbon loss. Tube wastage was not monitored in the Richmond Power and Light full-scale tests. Carbon loss was measured, and at 44 MW load, carbon loss doubled as wall air angle was increased from roughly 8^{0} to 45^{0}.

Unlike the full-scale test results, excellent carbon burnup was observed in the System 3 burner results, even for the cases with flame impingement. As can be seen from the carbon burnout data presented in Table 14, carbon burnout approached 100 percent for all conditions tested. This degree of carbon burnout was greater than that experienced in System 1 and 2 burner tests (approximately 99.7 percent) and conventional tangential firing tests in the pilot-scale facility (approximately 99.3 percent). Since carbon burnup was nearly complete for all conditions tested, in only a few subsequent extreme cases (45^{0} wall air and OFA, and 8^{0} primary/annular air angle conditions) were carbon loss measurements taken during the pilot-scale tests to ensure carbon burning was complete.

The extremely good carbon burnout achieved with the System 3 burners can probably be attributed to the hot refractory walls in the pilot-scale facility. The St and Sw numbers of the System 3 burners are sufficiently high to cause migration of some of the coal, particularly the bigger particles, to the furnace walls. Coal particles that impact the hot refractory wall probably stick and oxidize until only ash is left. Therefore, carbon burning is hypothesized to be a combination of suspension burning and some large coal particle fixed-bed burning on the hot walls. Through the fixed-bed burning process, carbon burning is more complete than if the big coal particles did not impact the walls and were burned in a suspension manner.

Recognizing the flame impingement problem for System 3 burners, metallic inserts for the primary and annular air jets were installed to increase exit velocity and reduce the relative velocity ratio between the wall and the primary/annular jets. This reduced the primary jet bending and thereby helped prevent flame impingement. Using this approach, St and Sw numbers were still too high relative to full scale. Geometry changes (i.e., bigger wall jets) needed to reduce these parameters to values more characteristic of full-scale values were not made in this test program. Only relative velocity changes were available to alleviate flame impingement.

Gas flame and flow pattern observations from the bottom of the furnace with inserts in the burners showed that the fuel jets penetrated further into the center of the firebox. The degree of penetration increased as wall and primary/annular air angles were reduced. With the bottom of the furnace off, flames appeared not to impinge on the walls for any of the angles tested. This was in contrast to the noninsert case, where some degree of flame impingement was observed for all angles tested.

Figure 120 presents the NO results as a function of wall air angle for the case with burner inserts at 8° and 0° primary/annular angles, with and without OFA. For the most part, these results show that NO increased slightly with wall air angle for the cases tested. As in the noninsert case, the change in NO with wall air angle was not very significant. Comparing the results in Figure 118 to Figure 120, it appears that utilizing inserts did not change NO significantly. However, as shown by flame observation, flame impingement was reduced to some extent by inserts, making operation with inserts the more desirable condition. When the system was fired with a 45° wall air angle for a considerable period of time, ash was deposited similar to that deposited under noninsert test conditions for System 3 burners. Apparently, gas flame pattern observations with the bottom of the furnace off may only provide a relative indicator of flame position. With the bottom of the furnace in place, recirculation patterns inside the furnace may displace flames to positions different from those observed with the furnace bottom off.

As in the noninsert cases, wall air angle was not a strong parameter influencing NO. Flame observations from the bottom of the furnace showed that wall flame impingement was reduced in the insert case. However, ash deposition patterns indicated that flame impingement was still present. This was certainly possible since St and Sw numbers were not significantly changed by using inserts. The outward movement of fuel into the wall air for large St and Sw numbers might offset the advantage to NO formation of fuel/air separation as wall air angle increased. This could lead to the insensitivity of NO levels with respect to wall air angles for both the insert and the noninsert cases.

5.4.2.2 Primary/Annular Air Angle

As shown in Figures 118 and 120, reducing the primary/annular air angle from 8° to 0° decreased NO by up to 50 ppm. This was the case for a variety of wall air angles and OFA angles, and cases with and without inserts. The benefit to NO of reducing primary/annular angles was significant in all test cases. In addition, flame observation from the bottom of the furnace showed that fuel jet bending and consequent flame impingement was reduced by decreasing primary/annular air angle.

Based on the above discussion of the influence of St and Sw numbers on NO and flame impingement, the benefit of reducing primary/annular air angle is clear. As primary/annular air angle is reduced, the angular momentum of the vortex and the St and Sw numbers are reduced. For 48 percent wall air, the St and Sw numbers are reduced approximately 10 percent by reducing the primary/annular angle to 0°. Fuel bending and flame impingement is thereby reduced improving fuel/air separation and NO. Since the primary/annular jet has a small angle relative to the wall angle, reductions of St and Sw numbers by reducing primary/annular angle are small.

As indicated in Table 15, the ratios of full-scale wall air to conventional tangential firing St and Sw numbers are 3.5 and 3.7, respectively. Reducing the full-scale primary/annular jet angle to 0°, as performed in the System 3 burner tests, would reduce the wall air St and Sw numbers by about 10 percent. This reduction still leaves the full-scale wall

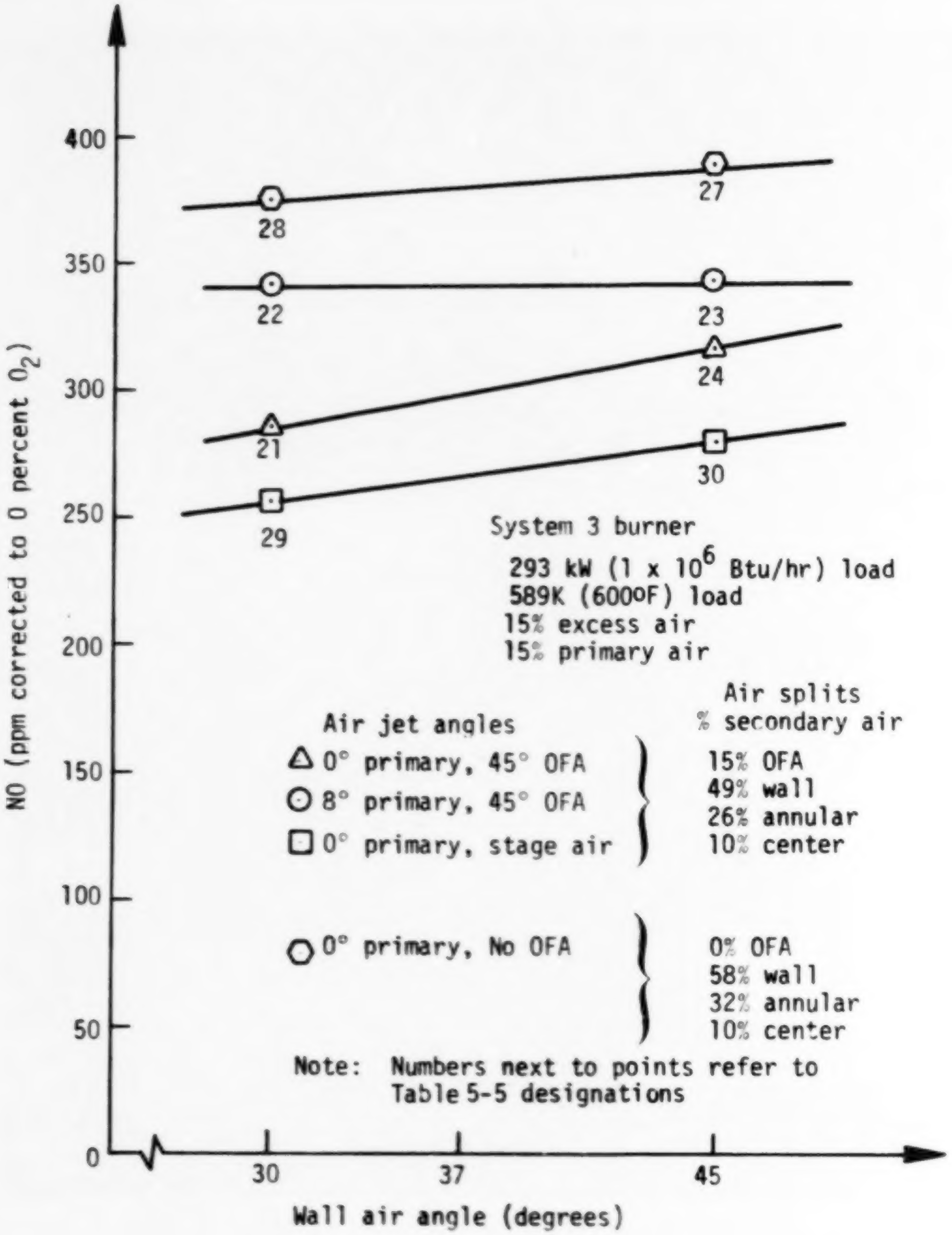

Figure 120. NO versus wall angle using variable angle burner blocks with inserts.

air system St and Sw numbers far above conventional values. Therefore, vortex swirl for the wall air case at 0° primary/annular angle should be very strong, resulting in good mixing and combustion efficiency.

5.4.2.3 Primary/Annular Air Velocity

Using the inserts in the primary and annular air jets increased their velocities by factors of 2.2 and 1.7, respectively, as can be seen by comparing noninsert and insert test conditions given in Table 14. This represented a large increase in velocity which was expected to improve the resistance of the fuel jet to bending, thereby reducing the flame impingement problem. However, some flame impingement might have still been present, even though the gas flame pattern tests seemed to show some improvement.

As can be seen by comparing the results in Figures 118 and 120, NO did not seem to be significantly impacted by the use of inserts. Apparently the benefits to NO of reduced fuel jet bending were offset by the negative aspect of increased firebox mixing for the higher jet velocities.

Simple jet theory shows that turbulence intensity increases with jet velocity squared. Therefore, increasing velocity by a factor of roughly two significantly increases firebox mixing. This would destroy fuel/air stratifications and thereby fuel-rich zones where NO_x formation is minimized. That NO was maintained constant, or slightly reduced, as primary/annular velocity was significantly increased might indicate that reduced fuel jet bending is beneficial to NO and, in the absence of increased firebox mixing, might reduce NO.

These results indicate that increasing the primary/annular air velocity is not an effective approach to preventing the fuel jets from bending towards the walls due to high St and Sw numbers. Flame impingement problems persisted and NO emissions remained high. A better approach would be to reduce wall air velocity while maintaining constant primary/annular velocity. Under these conditions it is hypothesized that fuel jet bending and firebox mixing would be reduced thereby reducing NO and alleviating flame impingement.

5.4.2.4 Overfire Air

To test the combined effect of wall air and air staging, OFA ports were built into the burners. A conventional OFA injection angle of 8° and a nonconventional angle of 45°, simulating the limiting case of putting OFA on the wall, were tested. These ports were located approximately 0.30m (12 inches) above the burner level. This separation was an attempt to simulate the bulk residence time achieved before OFA addition in the demonstration burner.

In addition to OFA tests, a few brief tests were run with staged air added in the heat exchange tower above the firebox. These tests were run to illustrate the effect of staged air separation and residence time on NO reduction. The tower staged results represent the maximum benefit of air staging.

For the most part, OFA was held to 15 percent of the secondary combustion air, giving a firebox stoichiometry prior to staging of approximately 1.0. This degree of staging corresponds with the maximum design flowrate specified for the demonstration system. A single test condition was run at a higher percent OFA to determine the benefit of increased OFA.

Figures 117, 118, and 120 present some of the OFA test results. Figure 117 shows that, at approximately 15 percent air on the wall, 15 percent OFA at an 8° angle reduced NO approximately 11 percent. This reduction was low compared to conventional tangential firing results where reductions of 20 to 30 percent were observed for 15 percent OFA (Reference 5). For wall air greater than 30 percent, the percent reduction for 15 percent OFA at an 8° angle was even less than at 15 percent wall air.

Figure 120 shows that at 49 percent wall air, adding the staged air in the tower instead of the OFA ports reduced NO by about 29 percent from the non-OFA case at 59 percent wall air. Primary angle in these staged cases was 0°, and percent wall air at the comparison point was higher than the 8° OFA cases presented in Figure 117. However, the results clearly show that staging in the tower is superior to staging in the OFA air ports at 8° injection angle.

The reductions achieved by staging in the tower are more typical of reductions observed in full-scale systems and indicate the maximum benefit to be derived from combining low-NO_x OFA with wall air approaches.

The rather limited reduction achieved by the 8° angle OFA case at a near baseline condition (i.e., small percent wall air) suggests that OFA has not been properly modeled in the pilot-scale facility. As discussed in section 5.4.1, the separation of the OFA port from the burner fuel entry level was based on matching the full-scale and pilot-scale facility bulk gas residence times to the OFA ports. The actual residence times were, of course, different from these because velocities are not uniform within the firebox; there are locally low and high velocity zones with respect to the average velocity. In addition to these differences, which are not easily accounted for, the full-scale facility had five burner levels followed by the OFA ports, whereas the pilot-scale facility only had a single burner level. Therefore, in the full-scale facility, some fuel had a very long residence time prior to mixing with OFA, whereas some fuel had a very short residence time prior to OFA addition. The effect on NO of nonuniform fuel residence time distribution prior to staged air addition in the full-scale facility is not known at this time. This nonuniform fuel residence time distribution could only be approximated in the single burner level pilot-scale facility by using an average residence time.

The differences noted above might be the reason the case with OFA at the near baseline condition did not exhibit as significant a NO reduction as is typically observed in a full-scale system. A greater separation of the OFA and fuel entry elevation, characteristic of the staged air condition, might be required for a better simulation of full-scale OFA effects in the pilot-scale facility. However, the presence of the firebox exit contraction between the present OFA and staged air ports makes it difficult to move the OFA ports higher and still achieve a reasonable modeling of full-scale OFA. It might be speculated that, with a properly modeled OFA, non-baseline as well as near-baseline OFA NO reductions would be improved. Therefore, OFA NO reductions for all pilot-scale facility test conditions are probably the lower bounds of what is achievable in the demonstration burner.

Figures 117, 118, and 120 show the benefit to NO reduction of injecting the OFA at a 45° angle. For the cases both with and without inserts at 0° or 8° primary angles and 31° and 45° wall air angles, the 45° OFA injection angle appeared to reduce NO more than the 8° injection OFA. The case of 31° wall angle and 0° primary angle appeared to have the best reduction, showing a maximum reduction of 21 percent over the non-OFA case. When 45° OFA was increased to 28 percent, the maximum NO reduction increased to 23 percent over the non-OFA case. This reduction was smaller than that expected based on conventional tangential system field data (Reference 5).

Figures 121 and 122, particularly Figure 122, show that 45° OFA NO results, for an equivalent percent wall air at the fuel entry elevation, were below the non-OFA and 8° OFA cases. When 45° OFA flow was added to the percent wall air and NO was plotted versus this total wall airflow, the NO results correlated more closely than when just wall air was used as the correlating parameter. This better correlation of NO with total wall air suggests that the OFA at 45° functions more like wall air than classical OFA, maintaining a rich core for a longer residence time than the 8° OFA case. Assuming this is the case, the effect of OFA on NO can be explained as follows.

For non-wall-air cases, the use of OFA reduces the oxygen concentration in the lower furnace, creating a fuel-rich region where NO production is minimized. This fuel-rich region becomes fuel-lean at the point of OFA addition. When wall air is employed without OFA, a fuel-rich core is developed. However, the rich core occurs in the center of the furnace and may extend vertically further than the rich region with OFA. The rich core becomes fuel-lean as the wall air gradually mixes into it.

When OFA is combined with wall air, the effectiveness of OFA in reducing NO is dependent on the angle of OFA injection, the percent wall air, and the percent OFA. When the percent wall air is high, the rich core is extensive and probably elongated, extending beyond the OFA injection location. Under these conditions, injecting OFA at 8° angle into the center of the furnace probably shortens the length of the fuel-rich core, somewhat offsetting the benefit to NO of reduced overall stoichiometry in the lower furnace. Thus, NO reductions may not be very significant for 8° OFA under these conditions.

On the other hand, if under these conditions OFA is injected at 45°, the central core of the furnace operates fuel-rich at the OFA location, and the 45° injection angle prevents the air from being entrained immediately into the center of the furnace. Thus, a much more positive NO reduction effect is achieved. In addition, the wall air in the lower and upper furnace blankets the walls with oxygen, achieving wall oxidizing conditions even for firebox stoichiometries less than one.

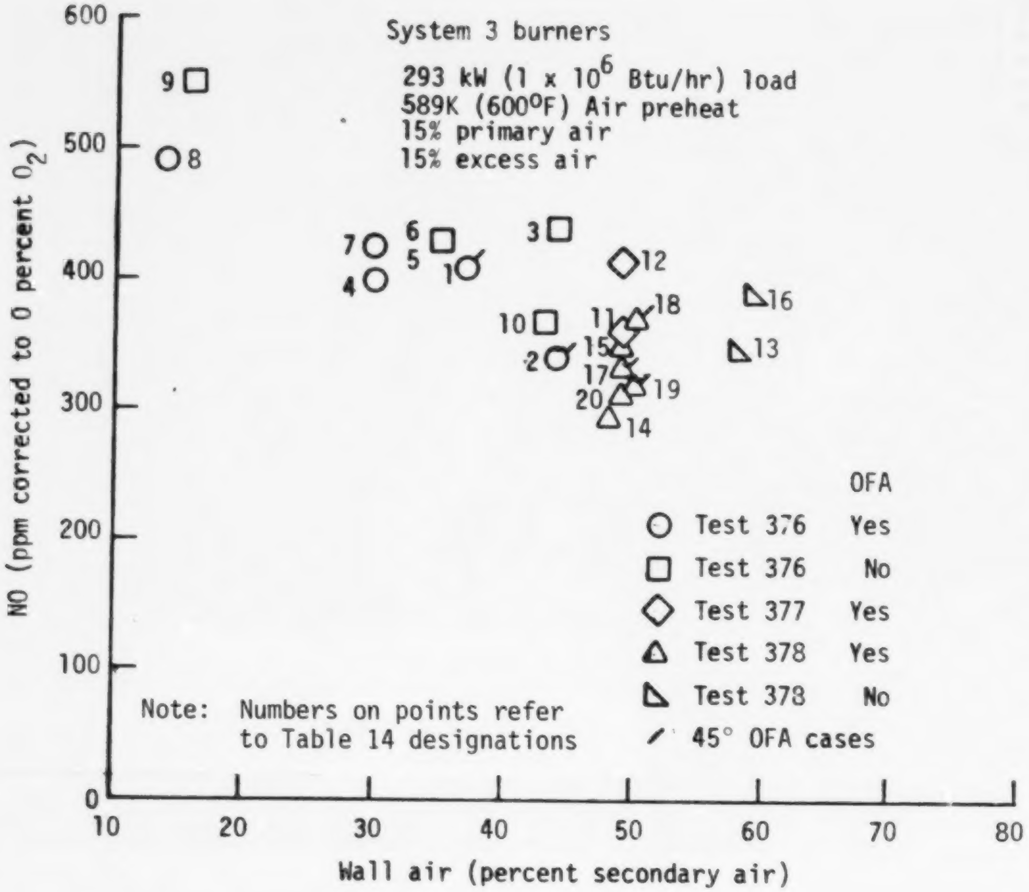

Figure 121. NO versus wall air for mixed conditions using variable angle burner blocks without inserts.

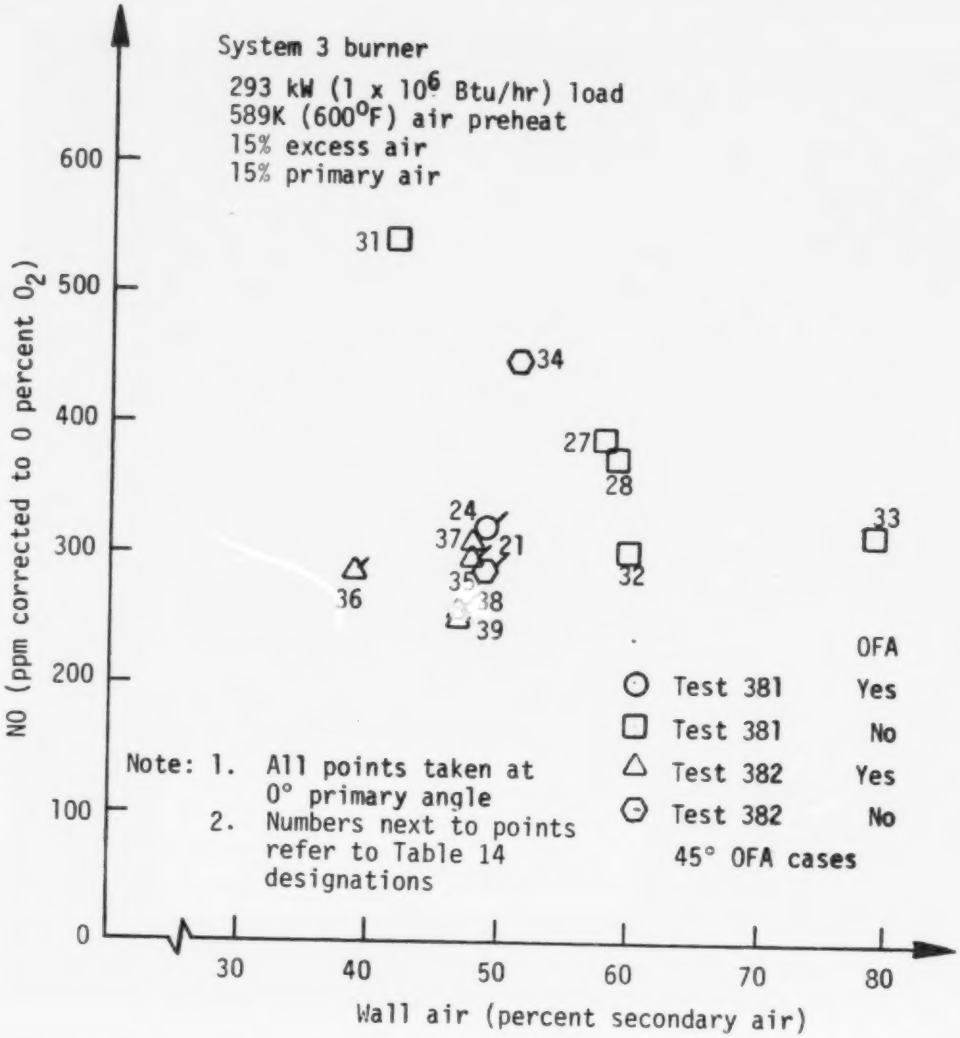

Figure 122. NO versus wall air for mixed conditions using variable angle burner blocks with inserts.

For the case of low percent air on the wall, using the 8° OFA injection angle would not be that detrimental since the impact of wall air on the extent and degree of core fuel richness would be small. For this case, the major NO reduction would be due to OFA. However, even in the low percent wall air case, it is believed that the 45° OFA angle injection case would yield lower NO than the 8° angle case since the mixing of fuel rich gases and OFA would be delayed.

Besides the benefit of reduced NO, 45° OFA might also reduce slag formation in full-scale systems. Slagging typically occurs immediately above the top burner elevation where wall oxygen concentrations reach near exit levels and gas temperatures are still high. Under the reduced oxygen conditions in this zone, the iron in the ash is in the ferrous form which yields a lower ash fusion temperature so running slag forms easily. By directing the OFA at 45°, the OFA blankets the walls above the burner level with oxygen; this tends to maintain the iron in the ferric form which has a higher fusion temperature. Under these conditions, the slagging potential of the ash is reduced. Thus, by applying 45° OFA, both NO and furnace slagging might be reduced.

5.4.2.5 Percent Wall and Annular Air

Figures 123, 124, 125, and 126 present the NO results as a function of both percent total wall air and percent annular air for the cases with and without inserts. As discussed previously, total wall air, which includes the 45° air angles OFA flow, is a better correlating parameter for NO than just percent wall air at the fuel entry elevation. These test conditions include all wall air and primary/annular angles, and OFA conditions tested.

Similar to what was found in the scoping tests discussed previously, NO decreased significantly as percent wall air increased for cases both with and without inserts as shown in Figures 123 and 124. The case with inserts seemed to have a stronger decrease of NO with percent wall air. Comparison of Figures 123 and 124 show that the cases with and without inserts achieved the same NO levels in the range of 60 percent wall air.

Figures 125 and 126 show the effect of percent annular air on NO for the cases without and with inserts, respectively. As percent annular air was varied, the percent wall air changed accordingly in most cases. Therefore, the independent effect of percent annular air was not clear from most of these results. However, a few tests were performed with inserts where percent wall air was held fixed, and percent annular and center air were varied. Figure 127 shows the results of these tests along with the test conditions. These brief results show that percent annular air influenced NO independently of percent wall air. Increasing the percent annular air from 19 to 28 percent increased NO by 20 percent. Below 19 percent annular air, changes in annular air did not affect NO.

These results indicate it is beneficial to reduce percent annular air even with fixed percent wall air. In the pilot-scale test, this was easily accomplished by diverting some of the air to the center air port. In a

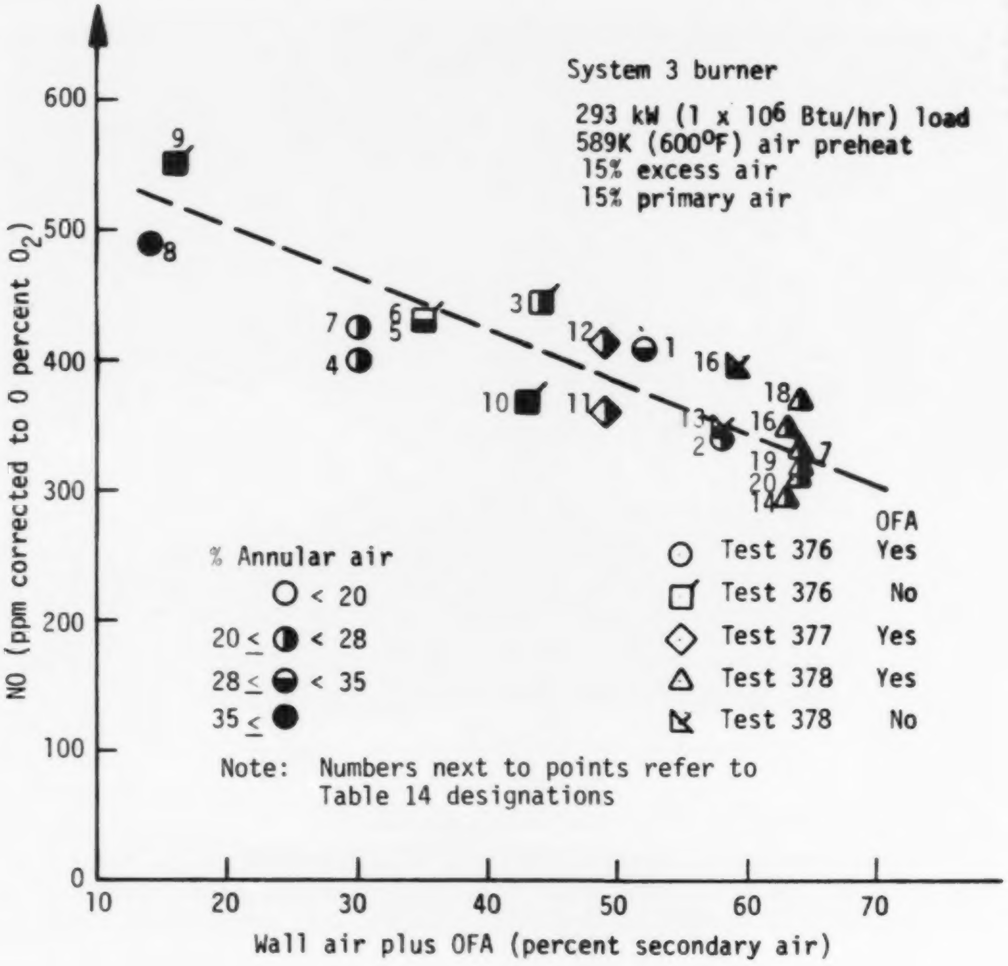

Figure 123. NO versus wall air and OFA for mixed conditions using variable angle burner blocks without inserts.

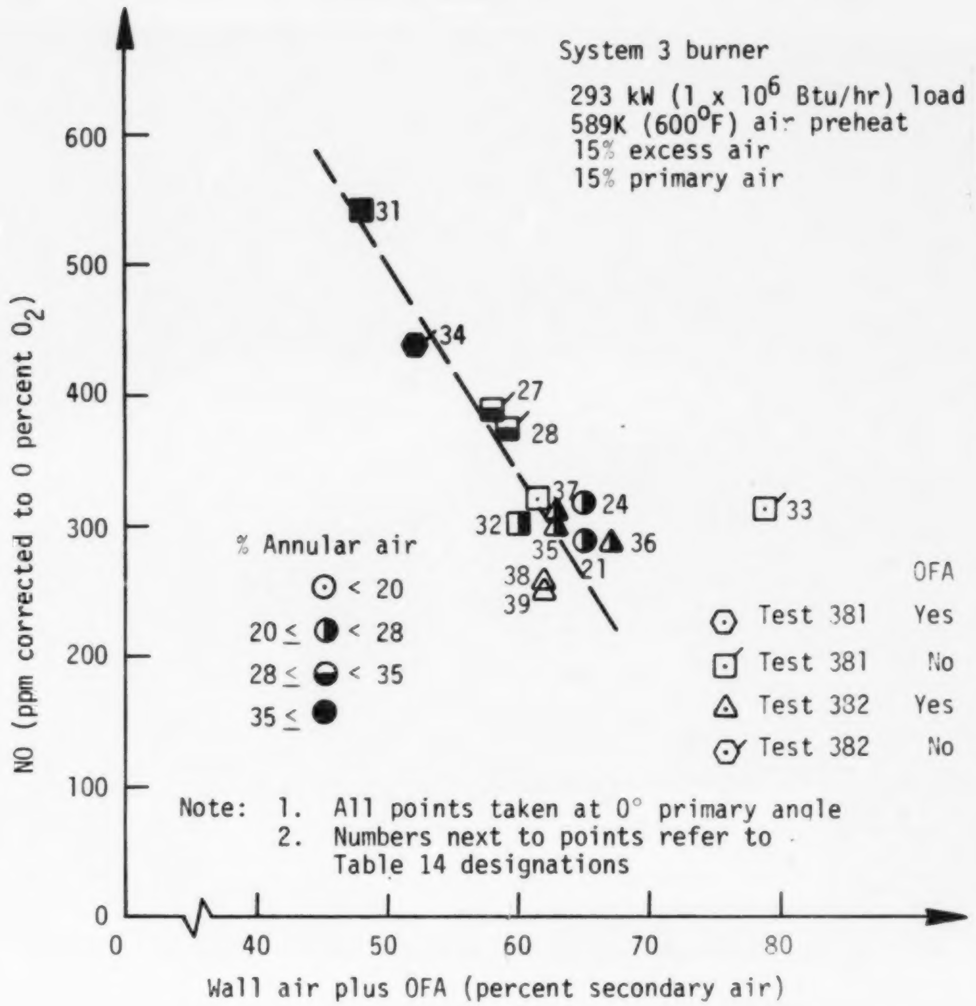

Figure 124. NO versus wall air and OFA for mixed conditions using variable angle burner blocks with inserts.

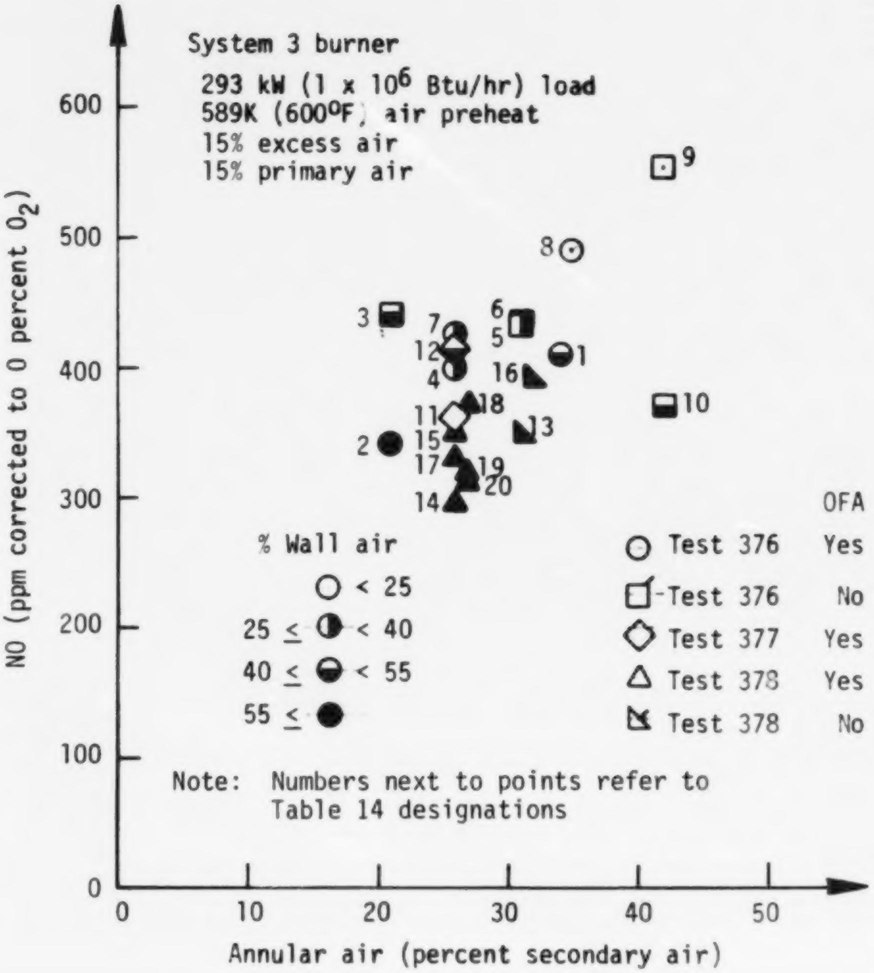

Figure 125. NO versus annular air for mixed conditions using variable angle burner blocks without inserts

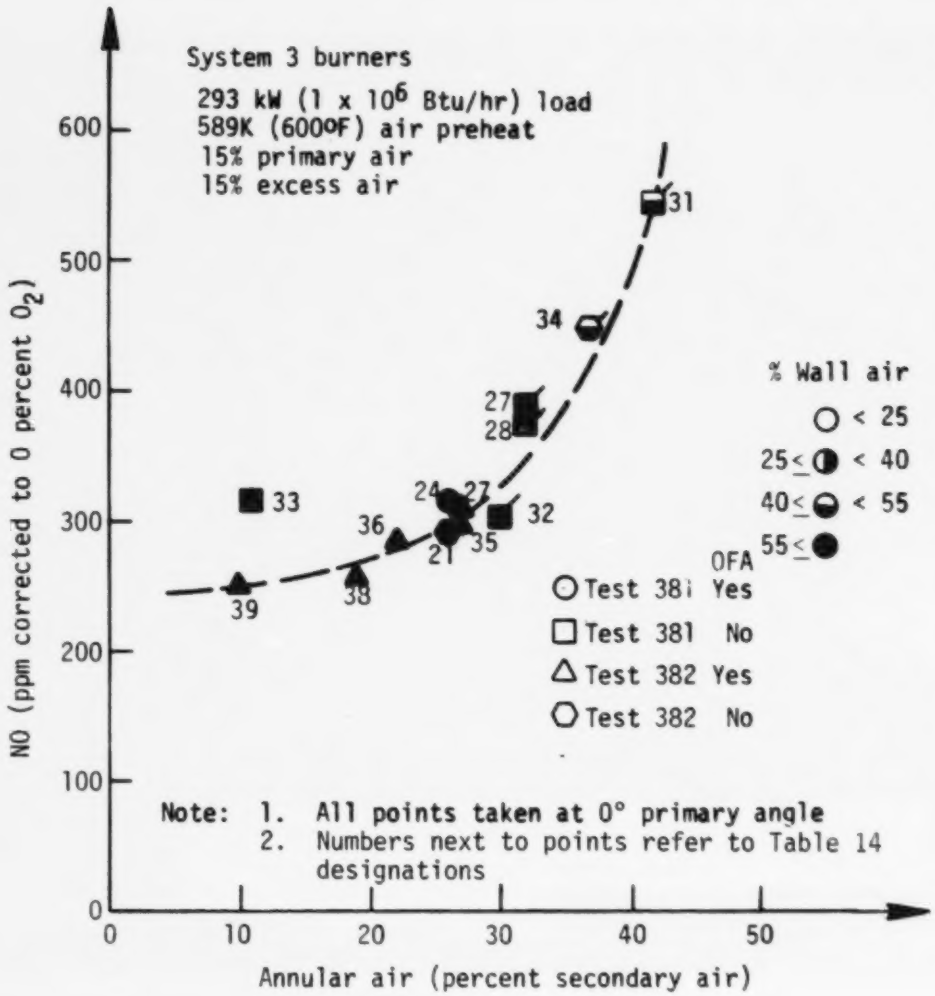

Figure 126. NO versus annular air for mixed conditions using variable angle burner blocks with inserts.

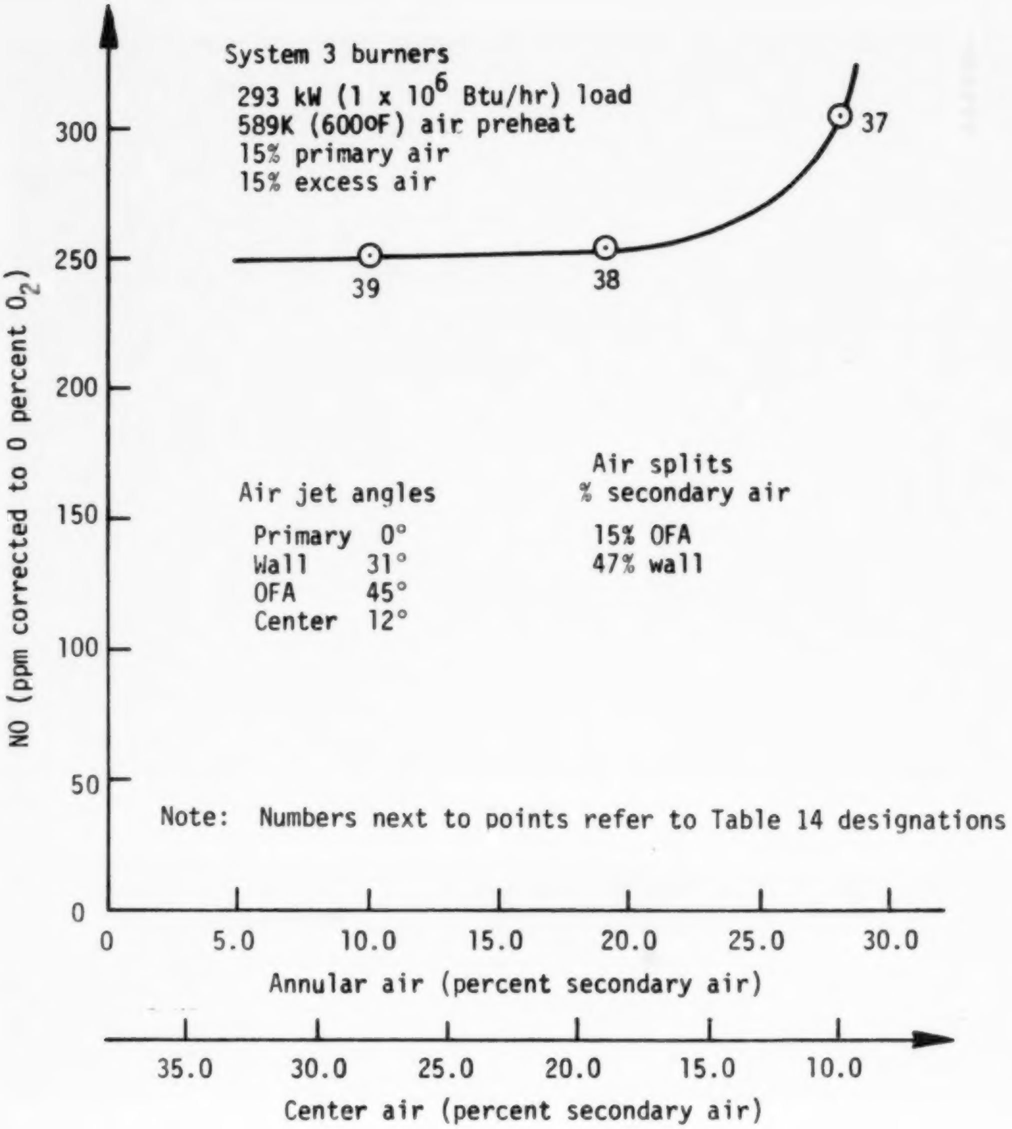

Figure 127. NO versus center/annular air ratio using variable angle burner blocks with inserts.

full-scale system, a similar effect might be accomplished by diverting some of the air to the lower burner level or the OFA ports.

The influence of reduced percent annular air and increased percent wall air is complementary. Reducing the percent annular air limits the amount of oxygen the fuel contacts in the early combustion zone. In the reduced oxygen environment of this zone, early NO formation is retarded. Increasing the percent wall air decreases the amount of oxygen in the center of the furnace, creating a fuel-rich environment. In this zone, the previously formed early NO is reduced. In addition, the remaining fuel nitrogen reacted in this zone has a very low percent conversion to NO. The combined effect of these processes is to yield low NO levels.

Figure 128 compares the System 3 burner results with and without inserts to the System 1 and 2 results as a function of percent wall air. As shown by the scoping tests, System 3 burner NO levels were not drastically different from previous System 1 and 2 burner results. The System 3 results with inserts matched most closely the System 2 configuration T results and the System 1 configurations I, N, and K results. The System 3 results without inserts matched most closely the System 1 configurations H and G results. These different configurations were presented in Figure 119 along with corresponding port areas and port areas relative to the primary port area. These areas and relative areas are a measure of the exit velocities of the jets. Comparing System 1, 2, and 3 port areas show that the configurations which yield NO levels comparable to those for System 3 burners with inserts have annular exit areas smaller than their corresponding wall jet exit areas. Configurations which yield NO levels comparable to those for System 3 burners without inserts have annular exit areas larger than their corresponding wall jet exit areas. At a given percent air on the wall, the System 3 burners with inserts will have a higher annular-to-wall-jet exit velocity ratio than the case without inserts. As in Systems 1 and 2 burner results, the higher velocity ratio for the insert case yields more NO at a lower percent air on wall. At a percent wall air approaching 60 percent, the differences in NO between the configurations is small.

Apparently, at low percent air on the wall, the small annular exit area configuration yields excessive jet velocities which tend to destroy fuel-rich zones in the firebox thereby increasing NO. This negative impact of mixing overcomes the positive aspect of less fuel jet bending at higher primary/annular exit velocities.

5.4.2.6 Excess Air

The variation of System 3 burner NO with excess air is presented in Figure 129 along with the conditions chosen for these tests. These conditions were believed to represent good performance conditions for this burner configuration under baseline, 15 percent excess air conditions. As can be seen in Figure 129, NO increased significantly from 5 to 15 percent excess air and remained flat from 15 to 25 percent.

Also plotted in Figure 129 are some System 2 burner results, both with and without vertical air distribution. In contrast to the System 3 burner

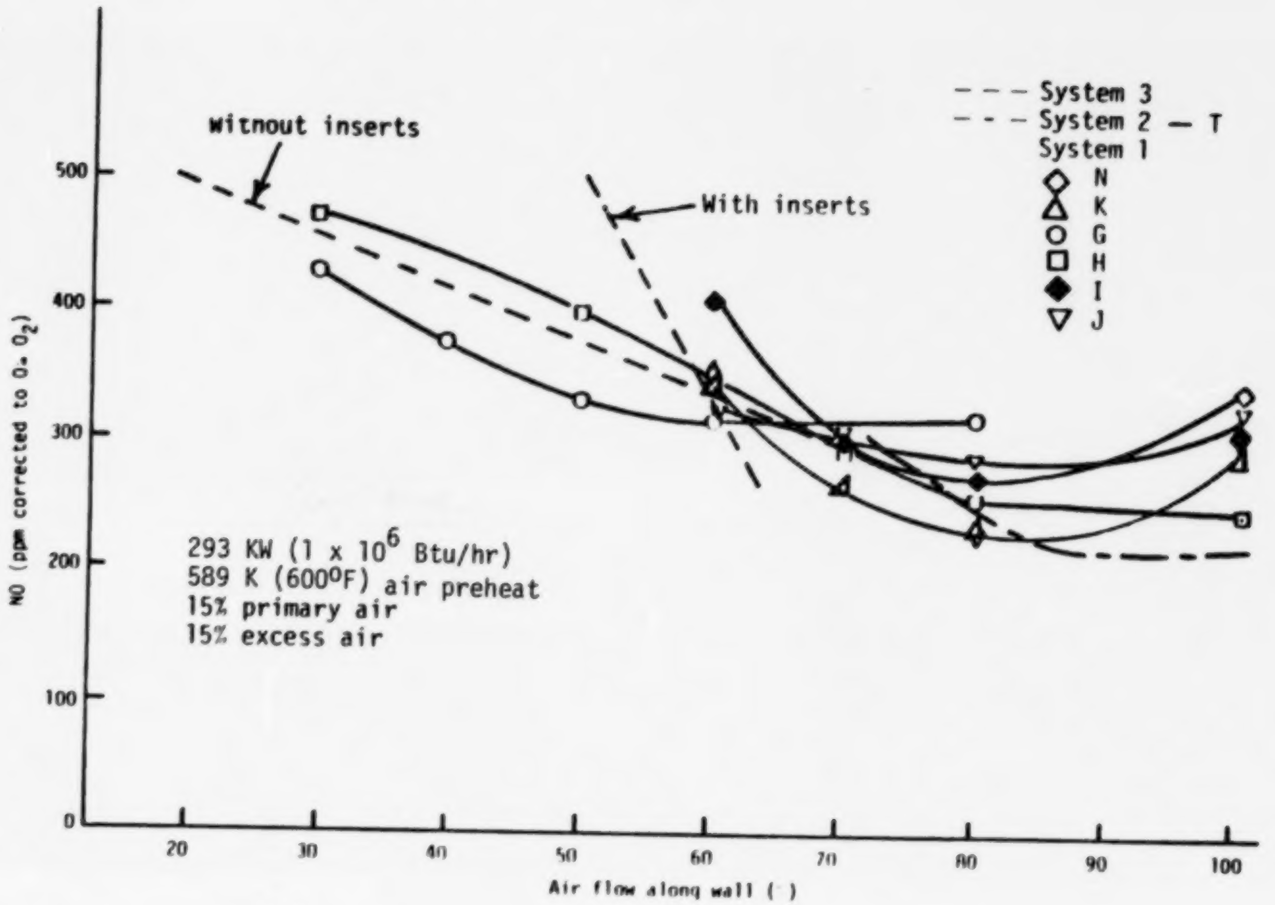

Figure 128. Comparison of System 1, 2, and 3 burner NO variation with percent total wall air.

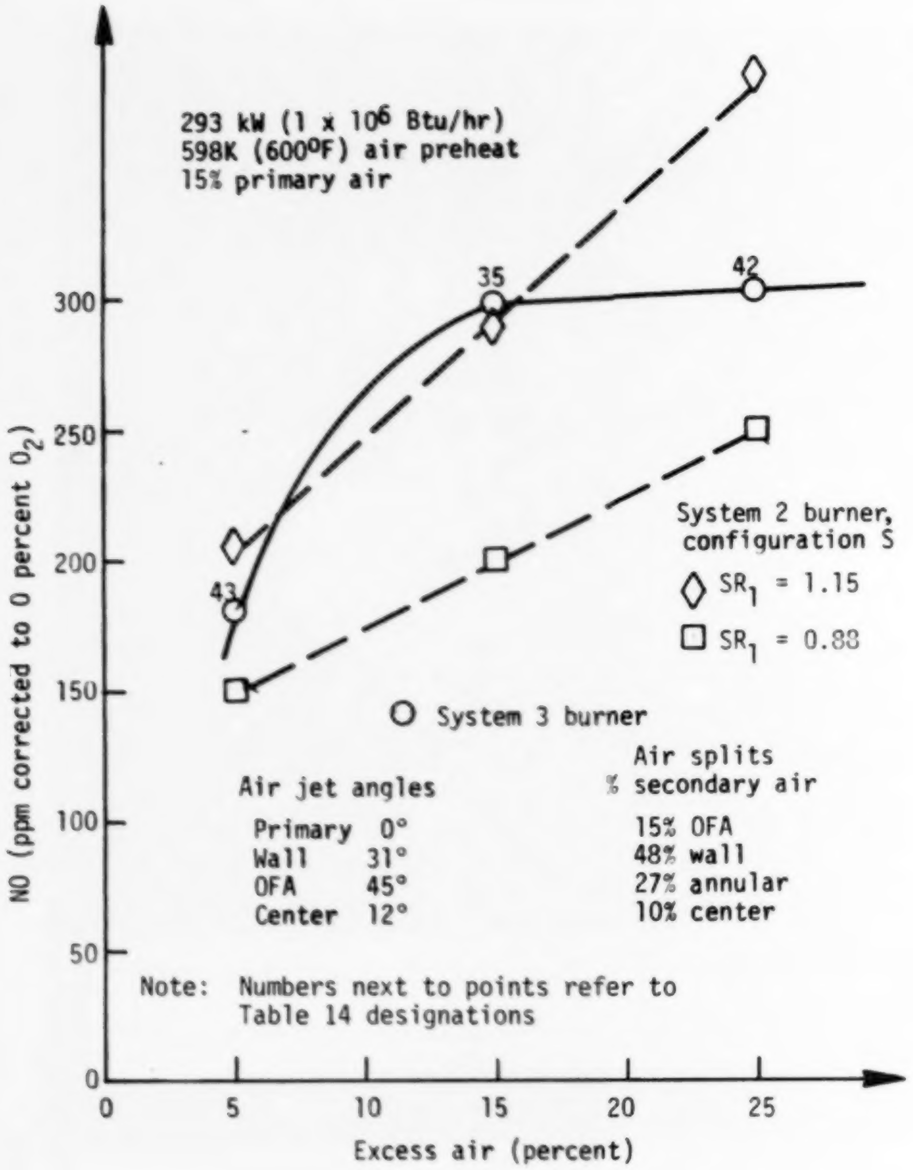

Figure 129. NO versus excess air using variable angle burner blocks with inserts.

results, NO linearly increased with percent excess air for the System 2 burners. However, the System 3 results are bracketed by the System 2 results.

5.4.2.7 Load

Figure 130 presents the variation of System 3 burner NO as a function of firing rate. The nominal test conditions, as given on Figure 130, were the same as those used during the excess air tests. As can be seen in this figure, NO rose as the load increased from 220 to 293 kW (0.75 to 1.0 x 10^6 Btu/hr) and then fell off above 293 kW (1.0 x 10^6 Btu/hr). This fall-off occurred for both a constant primary flow of 59.1 kg/hr (130 lbm/hr) and for an increased primary flow of 65.9 kg/hr (145 lbm/hr). The 65.9 kg/hr (145 lbm/hr) primary airflow is equivalent to 15 percent of the total airflow.

The rise in NO observed in Figure 130 as load increased from 211 to 293 kW (0.72 to 1.0 x 10^6 Btu/hr) can be attributed to increased mixing in the firebox which reduced fuel-rich stratification zones where NO is reduced. Gas temperatures did not change significantly during load variations because of the large thermal mass of the system. Therefore, the NO behavior in Figure 130 cannot be attributed to temperature changes.

The fall-off in NO as load increased beyond 293 kW (1 x 10^6 Btu/hr) cannot be explained on the basis of overall firebox mixing or thermal effects. However, the effect on NO of changing percent primary air at high load offers a reason why NO falls with increasing load. At 334 kW (1.14 x 10^6 Btu/hr), the results in Figure 130 show that NO increased as percent primary flow decreased. This was contrary to conventional tangential firing, where NO was typically reduced as percent primary air was lowered. For the wall air System 3 burners, NO might have increased as percent primary was reduced because of the inability of the lower momentum primary jet to penetrate into the center of the furnace, where NO formation is minimized. Therefore, at reduced percent primary air or reduced load, fuel jet momentum might not be sufficient to penetrate into the center of the furnace, resulting in increased NO. The lower NO at the higher load and fixed percent primary might be the result of better fuel penetration into the center of the furnace for the higher momentum fuel jet case.

It is interesting to note that most of the data for the System 3 burners was obtained at a load condition where, as shown in Figure 130, peak NO is found; lower or higher load reduces the NO formation. The 293 kW (1 x 10^6 Btu/hr) load condition approximates the firing intensity of a full-scale system at maximum continuous rating.

5.4.2.8 Fuel Effects

Testing was performed on a Western Kentucky and a Pittsburgh No. 8 coal to assess the impact of fuel effects. The ultimate and proximate analyses of these coals are given in Table 2. The testing considered load and excess air variation. These tests were conducted using System 3 burner blocks with inserts. The percentage airflow splits and nozzle angles were consistent with previous tests and were kept constant during these tests.

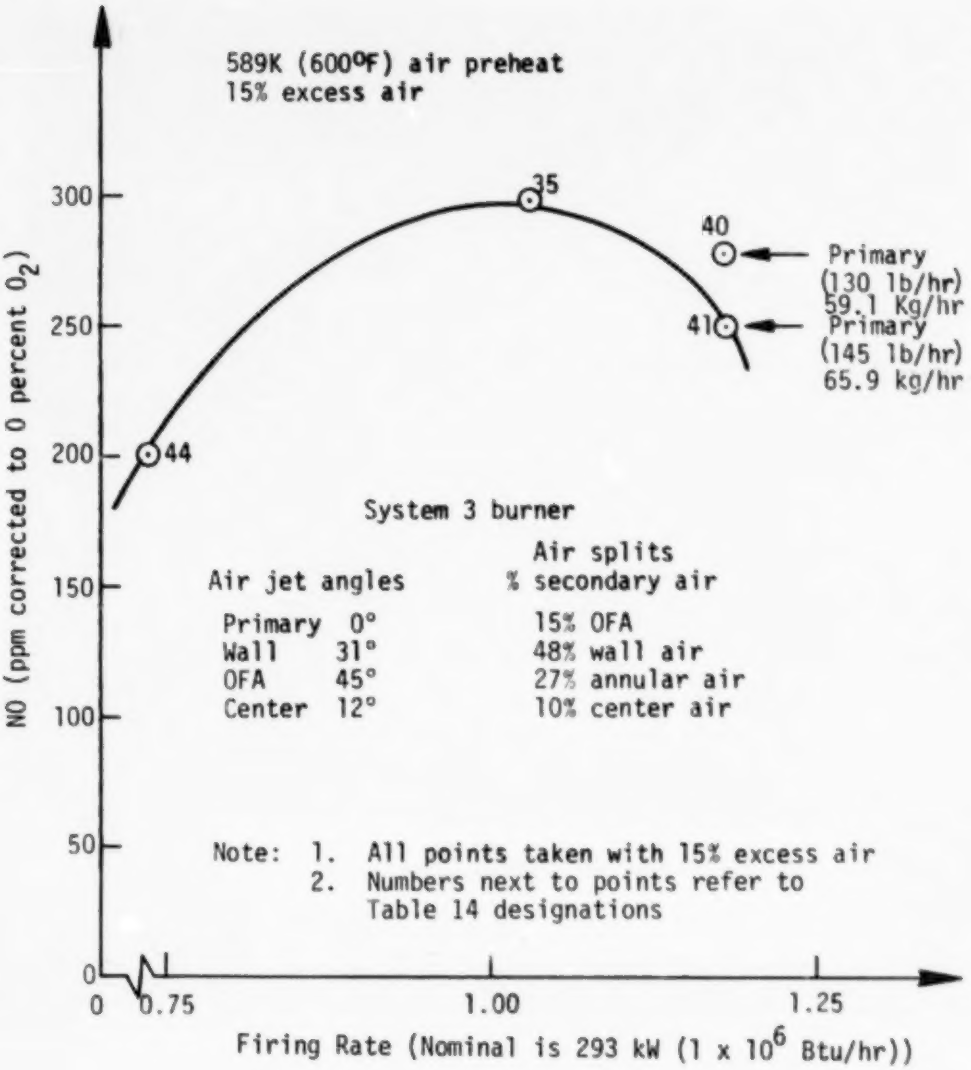

Figure 130. NO versus load using variable angle burner blocks with inserts.

Figure 131 shows the NO versus load for Utah, Western Kentucky, and Pittsburgh No. 8 coal. The baseline Utah coal delivered the lowest level of NO at all firing rates. This may be in part due to the rapid volatilization of the fuel nitrogen in this coal. In general, NO increased with increasing load for the coals tested, except for the low load point on the Pittsburgh No. 8 coal. The high NO level at this point is believed to be caused by a nonuniform coal feed rate at this low flowrate condition. Also, since it is the last point in the testing sequence, the wall and burner deposits could have had a significant impact on firebox aerodynamics, thereby affecting NO.

The increasing NO for conventional burners is generally believed to be associated with increasing turbulence intensity and gas temperatures in the firebox. However, for low-NO_x burners, other factors could also become important. The higher flame temperature resulting from increasing the firing rate could enhance the fuel nitrogen reduction process in the fuel-rich core, thereby offsetting the adverse effect of increasing turbulence intensity. This compensation may make the low-NO_x burner less sensitive to load variation than conventional burners.

The effect of excess air on NO concentration is shown in Figure 132 for the three coals tested. As shown in Figure 132, the Western Kentucky and Pittsburgh No. 8 coal NO exhibited the roughly linear increase typical of NO with excess air. The Utah coal NO exhibited a flattening of the NO curve with high excess air, as was discussed previously.

It should be noted that, in these fuel tests, furnace temperature did not vary significantly as either load or excess air was changed. This is due to the large thermal mass of the system which requires many hours to adjust to a new temperature after a major load change. In a full-scale system, dropping load would result in a more significant drop in gas temperatures. This departure in temperature between the full-scale and pilot-scale systems must be considered in extrapolating the pilot-scale data to real systems.

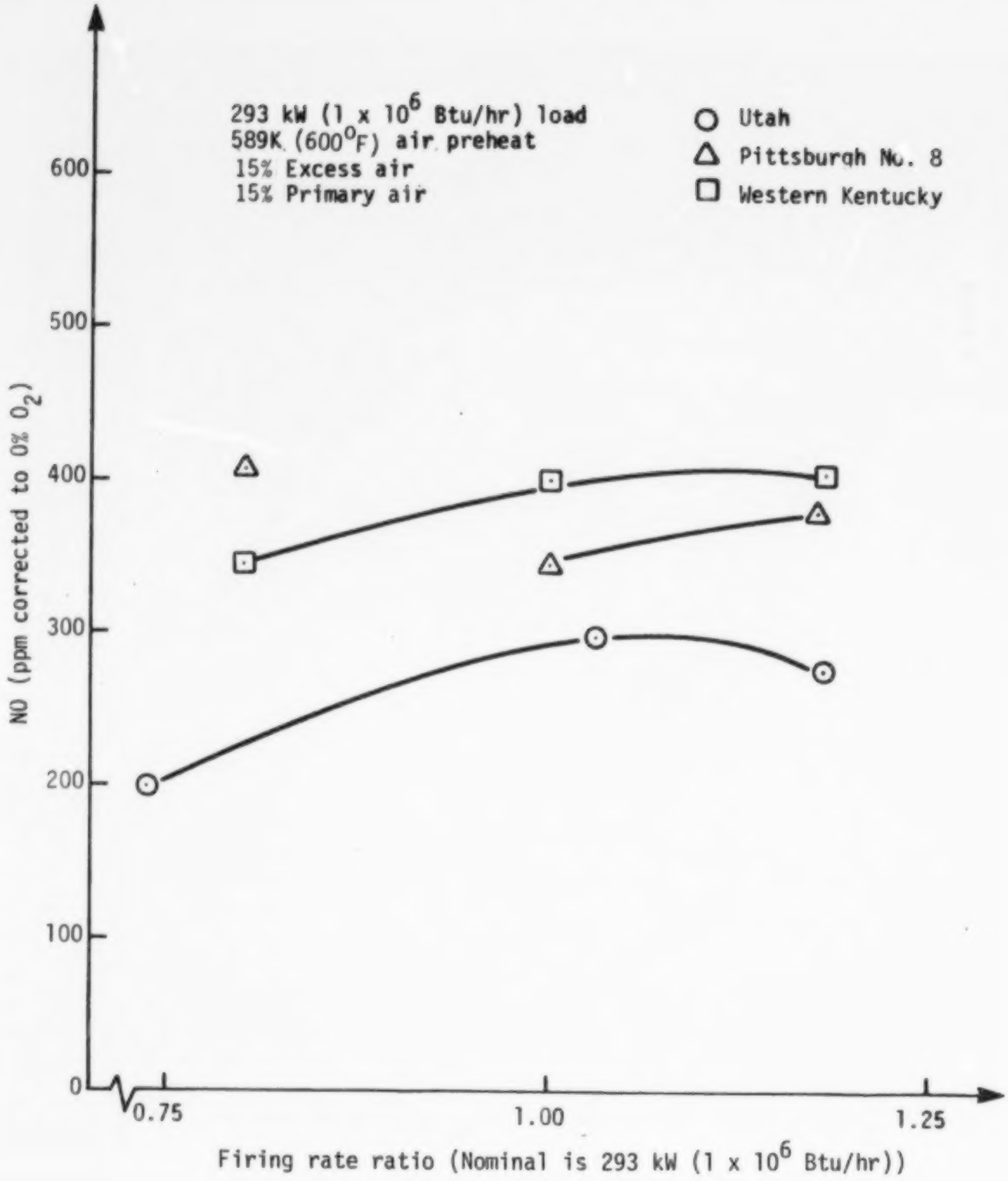

Figure 131. Coal type effects on NO versus load using System 3 burner with inserts.

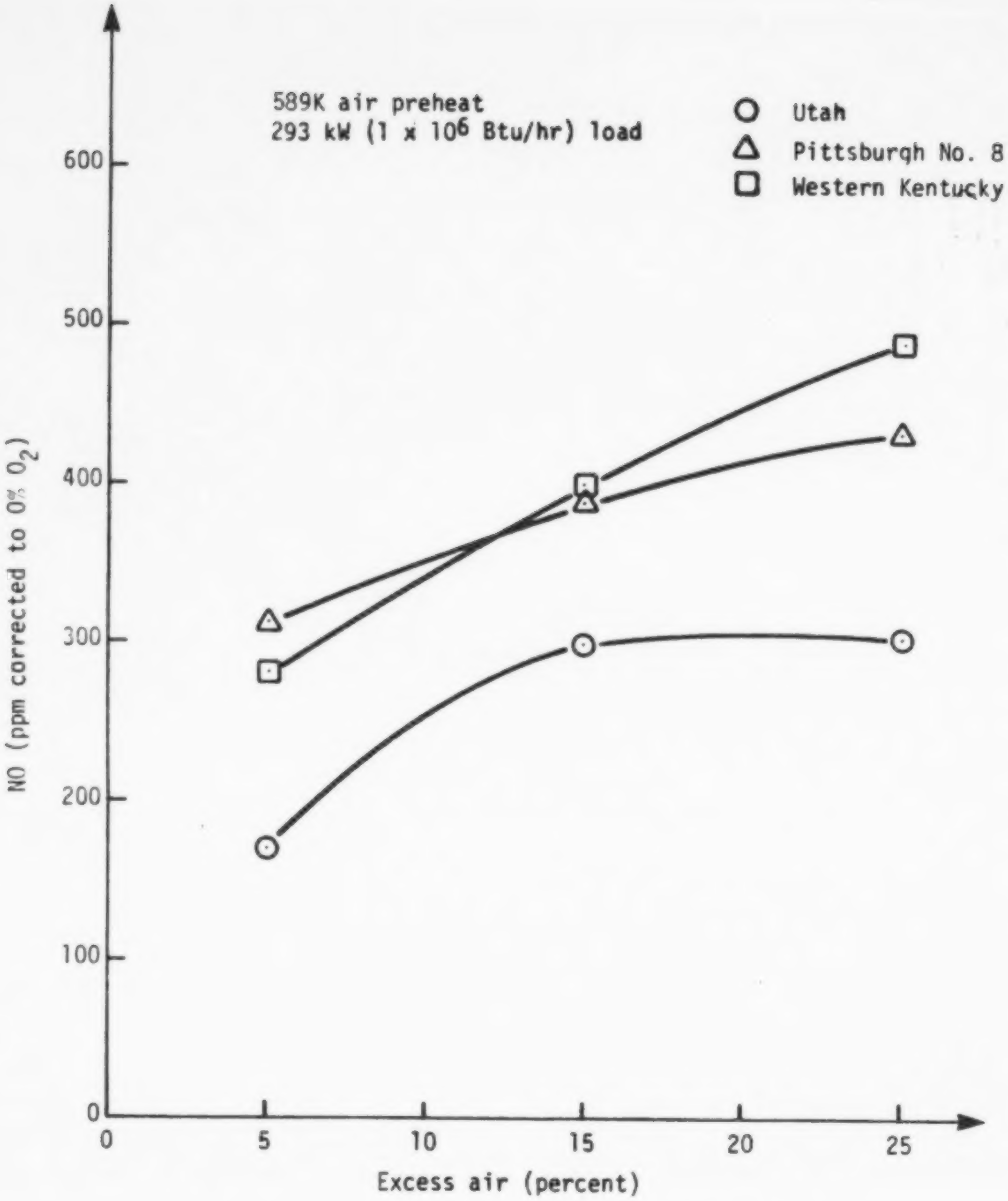

Figure 132. Coal type effects on NO versus excess air using a System 3 burner with inserts.

SECTION 6

CONCLUSIONS AND RECOMMENDATIONS

Through extensive pilot-scale testing, considerable progress has been made in the development of a low-NO_x coal-fired tangential system. A short term small-scale utility boiler field test has confirmed the potential of the system to reduce NO_x in full-scale boilers. In preparation and in parallel to a demonstration of the low-NO_x system in a modern coal-fired tangential boiler, additional pilot-scale testing is required. This section briefly presents the main conclusions derived from the pilot-scale test program and recommends further pilot-scale testing in support of the large-scale demonstration program.

6.1 CONCLUSIONS

Based on coal-fired pilot-scale tangential system burner and vortex characterization tests, the requirements for a low-NO_x tangential system were identified. These are: (1) intiate burning sooner to minimize O_2 availability at the ignition point, (2) operate the fuel/jet vortex interaction zone fuel-rich, (3) protect the fuel jet from dispersion by vortex flow, (4) lower firebox mixing with the constraint of positive ignition, and (5) operate a portion of the char burnout zone oxygen-deficient to get NO decay. In addition to these low-NO_x requirements, constraints must be applied on the system relative to boiler size and efficiency, wall corrosion and slagging, and heat transfer. These constraints dictate that to minimize corrosion and slagging problems, oxygen-deficient combustion gases should not contact the walls. Also, sufficient time and oxygen must be available to fully burn out the fuel and minimize carbon loss, CO, and UHC emissions. Finally, furnace volume and exit gas temperatures must be constrained to those typical of currently operating units.

Given the above requirements, a low-NO_x system was defined. The major system feature is the dividing of the secondary combustion air between injection into the center of the furnace and injection along the furnace walls. The delayed mixing of wall air into the vortex causes a rich combustion zone to develop in the furnace, minimizing fuel and atmospheric NO_x formation. Primary, secondary, and wall jet configurations and flowrates strongly influence the effectiveness of the system to lower NO_x emissions. Testing showed that the best results are achieved with (1) wall air directed horizontally and along the wall (2) wall air flow equal to or greater than 80 percent of secondary combustion air flow (3) primary/secondary air coannular configuration (4) wall air vertically distributed at and above the fuel entry location. At optimal parameter settings, NO reductions of

65 percent from conventional tangential system levels can be achieved at comparable combustion efficiency. In addition, wall oxygen concentration at the burner level is significantly increased over conventional tangential firing. This increase is beneficial from wall corrosion and slagging points of view. Also, in some configurations, the system shows a decrease in NO_x emissions as temperature is increased. This characteristic could be beneficially applied to reduce furnace volume for a given heat release.

6.2 RECOMMENDATIONS

In support of the large-scale utility boiler low-NO_x system demonstration program, further pilot-scale testing is needed to (1) help define burner design and test conditions to be explored in full-scale testing, (2) define emissions and efficiency performance for a range of burner design parameters, as well as the demonstration burner design conditions, (3) define emissions and efficiency performance for a range of charcteristic boiler coal and alternate fuels, as well as the demonstration boiler fuel type, and (4) define additional concepts which have a high potential to further reduce NO_x under good combustion conditions.

These pilot-scale results will significantly broaden the full-scale low-NO_x data base obtained in the demonstration tests. The pilot-scale results will provide information on how the system will perform for other boiler designs and different fuels, which is useful in assessing the retrofit potential of the system to a range of boilers. It will also aid full-scale demonstration program burner design and test condition selection, thus maximizing the value of the demonstration test data. Lastly, it will provide additional low-NO_x concepts and understanding of the low-NO_x system. This information will be useful in upgrading the low-NO_x system for future applications to full-scale boilers.

To maximize the usefulness of the pilot-scale data, testing conditions must closely simulate combustion conditions in the large-scale demonstration boiler. Parameters such as firing intensity, gas temperatures, residence time, and burner and firebox mixing must be properly scaled between the pilot- and full-scale facilities for proper simulation of full-scale performance. Presently, the pilot-scale facility simulates these parameters with a single burner level firebox arrangement. However, modern large-scale boilers have multiple burner levels, depending on unit rating. The interaction of the burner levels influences emission and combustion performance. To properly simulate large-scale boiler performance in the pilot-scale facility, the system must be modified to incorporate at least two burner levels. With the two burner levels, the effect of multiburner level interactions could be simulated and its impact on emission and combustion performance assessed. In addition, the multiple burner level interactions could be optimized to yield minimum NO_x under good combustion conditions. Therefore, to ensure proper full-scale boiler simulation and to increase the flexibility of the pilot-scale facility, two burner levels must be incorporated into the facility for the recommended pilot-scale test program.

REFERENCES

1. Lim, K. J., L. R. Waterland, C. Castaldini, Z. Chiba, and E. B. Higginbotham. Environmental Assessment of Utility Boiler Combustion Modification NO_x Control. U.S. Environmental Protection Agency Report EPA-600/7-80-075a, April 1980.

2. Heap, M. P. et al., "Burner Criteria for NO_x Control, Volume 1 - Influence of Burner Variables on NO_x in Pulverized Coal Flames," Evironmental Protection Technology Series Report No. EPA-600/2-76-061a, March 1976.

3. Pershing, D. W., and J. O. L. Wendt, "Pulverized Coal Combustion: The Influence of Flame Temperature and Coal Composition on Thermal and Fuel NO_x," Proceedings of the 16th Combustion Symposium, The Combustion Institute, Pittsburgh, Penn., 1976.

4. Takagi, T., et al., "NO_x Formation From Nitrogen in Fuel and Air During Turbulent Diffusion Combustion," Proceedings of the 16th Combustion Symposium, The Combustion Institute, Pittsburgh, Penn., 1976.

5. Habelt, W. W., "The Influence of the Coal Oxygen to Nitrogen Ratio on NO_x Formation," presented at 70th Annual AIChE Meeting, November 1977, New York, New York.

6. Macek, A., Seventeenth Symposium (International) on Combustion, The Combustion Institute, 1978, p. 65.

7. Wendt, J. O. L., C. V. Sternling, and M.A. Matovich. Fourteenth Symposium (International) on Combustion, The Combustion Institute, 1973, p. 897.

8. Gibbs, B. M., F. J. Pereira, and J. M. Beer. Sixteenth Symposium (International) on Combustion, The Combustion Institute, 1976, p. 461.

9. Brown, R. A., J. T. Kelly, and P. Neubauer. "Pilot Scale Evaluation of NO_x Combustion Control for Pulverized Coal: Phase II Final Report," EPA-600/7-79-132, June 1978.

10. Breen, B. P. Sixteenth Symposium (International) on Combustion, The Combustion Institute, 1976, p. 19.

11. Crawford, A. R., et al., "The Effect of Combustion Modification on Pollutants and Equipment Performance of Power Generation Equipment," Exxon Research and Engineering Co., EPA-600/2-76-152c, prepared for the Stationary Source Combustion Symposium, September 24-26, 1975.

12. Selkar, A. P., "Program for Reduction of NO_x from Tangential Coal-Fired Boilers, Phase II and IIa," EPA-650/2-73-005a and b, June 1975.

13. Beer, J. M., and K. B. Lee, "The Effect of the Residence Time Distribution on the Performance and Efficiency of Combustors," Tenth Symposium (International) on Combustion. The Combustion Institute, Pittsburgh, 1965, p. 1187.

14. Clarke, A. E., A. J. Gerrard, and L. A. Holliday, "Some Experiences in Gas Turbine Combustion Chamber Practice Using Water Flow Visualization Techniques," Ninth Symposium (International) on Combustion. Academic Press, New York, 1963, p. 878.

15. Beer, J. M., N. A. Chigier, and K. B. Lee, "Modeling of Double Concentric Burning Jets," Ninth Symposium (International) on Combustion, Academic Press, New York, 1963, p. 892.

16. Beer, J. M., "The Significance of Modelling." Third Symposium on Flames and Industry, 'The Use of Models,'" Institute of Fuel, October 1966.

17. Evans, D. G., and M. A. Patrick, "The Use of Modelling Studies in Boiler Furnace Investigations," Journal of the Institute of Fuel, October 1966, p. 414.

18. "Pulverizing Lignite, Valmont Power Station," Combustion Engineering supplied film.

19. Beer, J. M., and N. A. Chigier, Combustion Aerodynamics. Applied Science Publishers, 1972.

20. Wendt, J. O. L., T. L. Corley, J. T. Morcomb, "Interactions Between Sulfur Oxides and Nitrogen Oxides in Combustion Processes," Proceedings of the Second Stationary Source Combustion Symposium, Vol. IV, Fundamental Combustion Research, EPA-600/7-77/-73d, July 1977.

21. Blair, D. W., J. O. L. Wendt, W. Bartok, "Evolution of Nitrogen and Other Species During Controlled Pyrolysis of Coal," Sixteenth Syposium (International) on Combustion, The Combustion Institute, 1976, p. 475.

22. Levy, J. M., et al., "NO_x Abatement in Fossil Fuel Combustion, Chemical Kinetic Considerations," Proceedings of the Third Stationary Source Combustion Symposium, Volume IV, Fundamental Combustion Research and Environmental Assessment, U.S. Environmental Protection Agency Report EPA-600/7-79-050d, February 1979.

23. Sarofim, A. F., et al., "Conversion of Fuel Nitrogen to Nitric Oxide in Premixed and Diffusion Flames," AIChE Symposium Series, Vol. 71, No. 148.

24. Johnson, S. A., et al., "The Primary Combustion Furnace System -- An Advanced Low No_x Concept for Pulverized Coal Combustion," Proceedings: Second NO_x Control Technology Seminar, Electric Power Research Institute Report EPRI FP-1109-SR, July 1979.

25. Myerson, A., "Reduction of NO_x by Hdrocarbons," Fifteenth Symposium (International) on Combustion, The Combustion Institute, Pittsburgh, 1975.

26. Muzio, L. J., et al., "Gas Phase Decomposition of Nitric Oxide in Combustion Products," Sixteenth Symposium (International) on Combustion; The Combustion Institute, Pennsylvania, 1976, p. 199.

27. Gibbs, B. M., et al., "The Influence of Air Staging on the NO Emission from a Fluidized Bed Coal Combustor," Sixteenth Symposium (International) on Combustion; The Combustion Institute, Pennsylvania, 1976.

28. DeSoete, G. G., "Heterogeneous Reduction of NO on Surfaces," presented at EPA Fundamental Combustion Research Contractors Meeting, Newport Beach, June 1978.

29. Field, M. A., et al., Combustion of Pulverized Coal, BCURA publication 1967.

30. Kawamure, T. and D. J. Frey, "Current Developments in Low NO_x Firing Systems," Mitsubishi Industries and CE Powers System, presented at EPA/EPRI Joint Symposium on Stationary Combustion NO_x Control, 1980.

31. "Advanced Low NO_x Concept Tested For Tangentially Fired Boilers," In NO_x Conrtol Review, Industrial Environmental Research Laboratory, U.S. Environmental Protection Agency, Research Triangle Park, N. C., Vol. S, No. 3, Summer 1980.